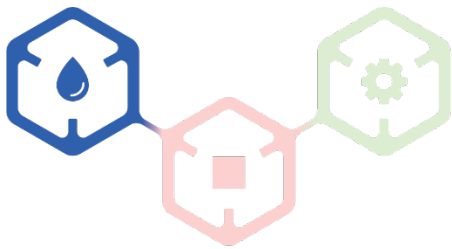




BRINES ACROSS THE SOLAR SYSTEM:
MODERN BRINES

Program and Abstracts
LPI Contribution No. 2614



MODERN BRINES

October 25–28, 2021



BRINES ACROSS THE SOLAR SYSTEM: MODERN BRINES

October 25–28, 2021

Virtual

Institutional Support

Lunar and Planetary Institute

Universities Space Research Association

University of Puerto Rico at Arecibo's Planetary Habitability Laboratory

Convener

Edgard G. Rivera-Valentín (lead)

USRA/Lunar and Planetary Institute

Sean O'Hara

USRA/Lunar and Planetary Institute

Science Organizing Committee

Mohit Melwani Daswani

Jet Propulsion Laboratory, California Institute of Technology

Raina Gough

University of Colorado, Boulder

Cyril Grima

University of Texas Institute for Geophysics

John Hallsworth

Queen's University Belfast

D'Arcy Meyer-Dombard

University of Illinois at Chicago

Lynnae Quick

NASA Goddard Space Flight Center

Josephine Rapp

University of Washington

Mark Schneegurt

Wichita State University

Compiled in 2021 by

Meeting and Publication Services
Lunar and Planetary Institute
USRA Houston
3600 Bay Area Boulevard, Houston TX 77058-1113

This material is based upon work supported by NASA under Award No. 80NSSC20M0173. Any opinions, findings, and conclusions or recommendations expressed in this volume are those of the author(s) and do not necessarily reflect the views of the National Aeronautics and Space Administration.

The Lunar and Planetary Institute is operated by the Universities Space Research Association under a cooperative agreement with the Science Mission Directorate of the National Aeronautics and Space Administration.

Material in this volume may be copied without restraint for library, abstract service, education, or personal research purposes; however, republication of any paper or portion thereof requires the written permission of the authors as well as the appropriate acknowledgment of this publication.

ISSN No. 0161-5297

Abstracts for this conference are available via the conference website at

<https://www.hou.usra.edu/meetings/modernbrines2021/>

Abstracts can be cited as

Author A. B. and Author C. D. (2021) Title of abstract. In *Brines Across the Solar System: Modern Brines*, Abstract #XXXX. LPI Contribution No. 2614, Lunar and Planetary Institute, Houston.



BRINES ACROSS THE SOLAR SYSTEM: MODERN BRINES

Agenda

ALL TIMES LISTED ARE U.S. CENTRAL STANDARD TIME.

Monday, October 25, 2021

- 9:30 a.m. Speaker Check-in
- 9:45 a.m. Virtual Coffee Social
- 10:00 a.m. Keynote Speaker: Brines
- 11:00 a.m. Finding Brines: Spectroscopy is Friend!
- 1:30 p.m. Deliquescence and Brine Stability: Just Add Salt
- 3:00 p.m. Terrestrial Analogs: ET Brines Phone Home
- 4:00 p.m. Poster Session: Brines Across the Solar System

Tuesday, October 26, 2021

- 9:30 a.m. Speaker Check-in
- 9:45 a.m. Virtual Coffee Social
- 10:00 a.m. Keynote Speaker: Geology
- 11:00 a.m. Regolith-Brine Systems: It's Complicated
- 1:30 p.m. Brine Composition: We're All Made of Salt Stuff
- 3:00 p.m. Brine Discovery: Explore Your Worlds!
- 4:00 p.m. Poster Session: Brine Facilitated Geology

Wednesday, October 27, 2021

- 9:30 a.m. Speaker Check-in
- 9:45 a.m. Virtual Coffee Social
- 10:00 a.m. Invited Talks: Mission Debriefs
- 11:00 a.m. Brine Distribution: Pass the Salt, Please!
- 1:30 p.m. Brine Geochemistry: Brines, on the Rocks
- 3:00 p.m. I Saw the Sign: Biosignatures in Brines
- 4:00 p.m. Poster Session: Living with Brines

Thursday, October 28, 2021

- 9:30 a.m. Speaker Check-in
- 9:45 a.m. Virtual Coffee Social
- 10:00 a.m. Keynote Speaker: Astrobiology
- 11:00 a.m. Brine Analogs: You Live Where?!
- 1:30 p.m. Life in the Lab: You Live Here Now
- 3:00 p.m. Habitability: Brines are Juuust Right!
- 4:15 p.m. Invited Talk: Meeting Wrap Up

BRINES ACROSS THE SOLAR SYSTEM: MODERN BRINES

Program

Monday, October 25, 2021

KEYNOTE SPEAKER: BRINES

10:00 a.m.

Chair: Ed Rivera-Valentín

Times	Authors (*Denotes Presenter)	Abstract Title and Summary
10:00 a.m.	Rivera-Valentín E. G. *	<i>Welcome and Introduction</i>
10:05 a.m.	Hanley J. *	<i>Fantastic Brines and Where to Find Them</i>
10:40 a.m.		DISCUSSION
10:50 a.m.		Break

Monday, October 25, 2021

FINDING BRINES: SPECTROSCOPY IS FRIEND!

11:00 a.m.

Chairs: Raina Gough and David Stillman

Times	Authors (*Denotes Presenter)	Abstract Title and Summary
11:00 a.m.	Primm K. M. * Stillman D. E.	<u><i>Macroscopic Deliquescence as Monitored by Dielectric Spectroscopy</i></u> [#6033] Measurements of permittivity and conductivity show that macroscopic sample of 1 wt% magnesium perchlorate with quartz sand deliquesces at a much lower relative humidity (~19%) than previously found (~48%) at -21C.
11:15 a.m.	Fischer E. * Martinez G. M. Renno N. O.	<u><i>Raman Spectroscopy as a Tool to Identify Brine Formation</i></u> [#6051] Here, we quantify the changes in the Raman spectrum of a sample under martian conditions as it changes from crystalline salt to brine and back. Our results show that Raman spectroscopy is a useful tool for liquid water detection on Mars.
11:30 a.m.	Mason D. P. Elwood Madden M. E. *	<u><i>Using Raman Spectroscopy to Detect and Monitor Freezing and Melting Processes in Near-Saturated Water-Salt Mixtures at Mars-Analogue Temperatures</i></u> [#6013] Raman spectroscopy is an ideal tool for studying modern brines in situ on other planets. Melting/freezing processes, as well as brine composition can be readily observed without touching the sample, maintaining planetary protection protocols.
11:45 a.m.	Hanley J. * Bandelier Z. Murphy C. Carmack R. Horgan B.	<u><i>Strategies for Remotely Detecting Chlorine Salts on Mars</i></u> [#6058] Salty liquids form / Across Mars still very tough / Please don't drink these brines.

12:00 p.m.		DISCUSSION
12:10 p.m.		Lunch Break

Monday, October 25, 2021

DELIQUESCENCE AND BRINE STABILITY: JUST ADD SALT

1:30 p.m.

Chairs: Megan Elwood Madden and Rachel Slank

Times	Authors (*Denotes Presenter)	Abstract Title and Summary
1:30 p.m.	Tu S. * Parise J. B. Lars E. Rogers A. D.	<u>Stability Diagrams of Aqueous Chlorate Solutions Under Martian Relevant Temperatures and Relative Humidities</u> [#6043] To better understand the water cycle on Mars, we constructed the T-RH phase diagram of chlorate-H ₂ O binary system based on the water activity of their solutions derived from measured heat capacity at varying m and T.
1:45 p.m.	Fitting A. * Chevrier V. F. Rivera-Valentín E. G. Soto A.	<u>Modeling the Deliquescence of Complex Salt Mixtures at the Phoenix Landing Site</u> [#6042] Summary of our work to determine the deliquescence relative humidity of salt mixtures at the Phoenix landing site as a function of temperature, using Geochemist's Workbench to model the evaporation of individual brine solutions at fixed temperatures.
2:00 p.m.	Rivera-Valentín E. G. * Chevrier V. F. Soto A. Martínez G.	<u>Formation of (Meta)Stable Brines on Present-Day Mars: Implications for Habitability</u> [#6040] Brines all over Mars / Metastable but still rare / Drink responsibly.
2:15 p.m.	Soto A. * Rivera-Valentín E. G. Chevrier V.	<u>Stability of Surficial Brines on Mars During Recent Orbital Cycles</u> [#6015] We investigate how the martian climate response to varying orbital configurations may have controlled the distribution and habitability of brines in Mars' modern history.
2:30 p.m.		DISCUSSION
2:40 p.m.		Break

Monday, October 25, 2021

TERRESTRIAL ANALOGS: ET BRINES PHONE HOME

3:00 p.m.

Chairs: Larry Anovitz and Jennifer Scully

Times	Authors (*Denotes Presenter)	Abstract Title and Summary
3:00 p.m.	Buffo J. J. * Brown E. K. Pontefract A. Schmidt B. E. Klempay B. Lawrence J. Bowman J. Grantham M. Glass J. B. Plattner T. Chivers C. Doran P. Meyer C. R. Barklage M. E. Fluegel B.	<u>British Columbia's Unassuming Planetary Laboratory: How a Handful of Frozen Saline Lakes can Help Us Understand Brines Across the Solar System</u> [#6020] The physicochemical properties of compositionally diverse ice-brine analog systems — constraining their habitability, their essential role in validating numerical models, and implications for the geophysics and astrobiology of planetary ice-brine environments.

3:15 p.m.	Pontefract A. * Carr C. E. Doran P. T. Ratliff L. McNulty K. E. Odenheimer A. B. Bowman J. Som S. Plattner T. Lawrence J. D. Schmidt B. E.	<i>A New Approach to Inferring Habitability Metrics in Hypersaline Environments</i> [#6041] The OAST team presents data revealing a strong relationship between total dissolved solids (TDS), density (ρ), chlorinity (Cl ⁻), and water activity (a_w), which we use to provide guidelines towards standard sampling metrics in hypersaline systems.
3:30 p.m.	Bose M. * Reynoso L. R. Castillo-Rogez J.	<i>Carbon Preservation within Ceres Regolith Minerals: A Need for Analog Work to aid in Successful Sample Return.</i> [#6036] Laboratory work on Ceres analog minerals needs to be undertaken for a safe, viable sample collection from the cerean surface. We will discuss potential and ongoing laboratory measurements to assess trace amounts of carbonaceous matter in salts.
3:45 p.m.		DISCUSSION

Monday, October 25, 2021

POSTER SESSION: BRINES ACROSS THE SOLAR SYSTEM

4:00 p.m.

Chair: Sean O'Hara

Times	Authors (*Denotes Presenter)	Abstract Title and Summary
4:00 p.m.	Bowman J. S. Bastuba A. Som S. Plattner T. Pontefract A. Doran P. Buffo J. Lawrence J. Schmidt B. Team O. A. S. T.	<i>An Objective Definition of Habitable Space and Application to Modeling Water Activity from Geochemistry</i> [#6047] We developed an approach based on a self-organizing map to objectively characterize habitability. We extended this approach to develop a model for predicting water activity from physico-chemical parameters.
4:05 p.m.	Fries M. Steele A. Zolensky M.	<i>Martian Brines in Ancient Salt Lake Beds — A High Priority Target for Mars Sample Return</i> [#6054] Mars has over 600 chloride deposits including those resembling dry lake beds. Mars sample return here may sample present-day brines from ancient martian surface fluids for study of fluids, atmosphere, and prebiological state of the ancient surface.
4:10 p.m.	Rodriguez A. J. Elwood Madden M. E. Mason D. P.	<i>Raman Spectroscopy: Quantitative Analyses of Modern Brines on Mars</i> [#6038] The Raman spectrometer is able to identify polyatomic ion salts in a near saturated solution of another salt. The relative peak height and area of the ions can be used to calculate the concentration of the salt in question relative to water peak.

4:15 p.m.	Hopkins R. J. Rogers A. D. Ehm L. Sklute E. C.	<u>FTIR-ATR Spectra and XRD Analysis of Amorphous Sulfate-Chloride Brine Desiccation Products after Multiple Consecutive Deliquescence-Desiccation Cycles</u> [#6031] This study mixed ferric sulfate with various chlorides and put the mixtures through multiple deliquescence-desiccation cycles. The desiccation products at the end of each cycle were analyzed with FTIR spectroscopy and XRD.
4:20 p.m.	Bryson F. E. Ingall E. D. Hanna A. M. Cardelino M. Plattner T. Meister M. R. Lawrence J. D. Mullen A. Dichek D. Schmidt B. E.	<u>Development and Testing of a Miniature Robotic Electrodialysis (MR ED) System to Remove Salts for Ocean World Sampling</u> [#6032] Astrobiological missions that investigate ocean worlds could encounter high salinity brines. To address complications with salts, we are developing a miniature robotic electrodialysis system to desalt samples with dissolved organic carbon recovery.
4:25 p.m.	Castillo-Rogez J. C. Melwani Daswani M. Glein C. Vance S. Cochrane C.	<u>Role of Non-Water Ices in Driving Salinity and Electrical Conductivity in Ocean Worlds</u> [#6035] Oceans expected in icy moons and dwarf planets could have high electrical conductivities due to abundant non-water ices, even if rock leaching during differentiation was limited and chlorine and sulfur were at CI carbonaceous chondritic levels.
4:30 p.m.		POSTER AND SCIENCE DISCUSSION

Tuesday, October 26, 2021

KEYNOTE SPEAKER: GEOLOGY

10:00 a.m.

Chair: Ed Rivera-Valentín

Times	Authors (*Denotes Presenter)	Abstract Title and Summary
10:00 a.m.	Rivera-Valentín E. G. *	<i>Introduction and Welcome</i>
10:05 a.m.	Castillo-Rogez J. *	<i>Role of Brines in the Geological Evolution of Icy Bodies: Observations and Predictions</i>
10:40 a.m.		DISCUSSION
10:50 a.m.		Break

Tuesday, October 26, 2021

REGOLITH-BRINE SYSTEMS: IT'S COMPLICATED

11:00 a.m.

Chairs: Erik Fischer and Katie Primm

Times	Authors (*Denotes Presenter)	Abstract Title and Summary
11:00 a.m.	Shumway A. O. * Catling D. C. Toner J. D.	<u>Soils Increase the Stability of Magnesium Perchlorate Brines on Mars</u> [#6005] On Mars, liquid water could exist in thin films of adsorbed brine in soil. We study the formation and stability of magnesium perchlorate brines in Mars soil simulants and find that soils reduce the availability of water and freezing point in brines.

11:15 a.m.	Hughes E. B. * Gilmore M. S. Eleazer M.	<i>Experimental Evaporation of Multicomponent Brines Demonstrates Variability in Salt Identification</i> [#6030] We experimentally evaporated multicomponent brines under martian and terrestrial conditions and characterized the results using spectroscopy. For mixed salt assemblages, instrumental analysis technique has a large bearing on identifiable salt.
11:30 a.m.	Anovitz L. M. * Treiman A. H. Mamontov E. Kolesnikov A. I. Stack A. G. Cole D. R. Wesolowski D. J.	<i>Cryogeochemistry: Liquid Water in Unexpected Places</i> [#6060] Nanoscale confinement can increase the stability of liquids such that liquid water is present in extraterrestrial systems under conditions where it would otherwise be frozen, leading to the possibility of cryochemical reactions.
11:45 a.m.	Slank R. A. * Rivera-Valentín E. G. Chevrier V. F.	<i>Experimental Investigation of the Near-Surface Martian Water Cycle with a Salty Regolith: Implications for Brine Formation</i> [#6026] Experiments under Mars-relevant combinations of temperature and humidity with different concentrations of calcium perchlorate mixed with JSC Mars-1 regolith to better constrain our understanding of brines and deliquescence.
12:00 p.m.		DISCUSSION
12:10 p.m.		Break

Tuesday, October 26, 2021

BRINE COMPOSITION: WE'RE ALL MADE OF SALT STUFF

1:30 p.m.

Chairs: Jennifer Hanley and Maitrayee Bose

Times	Authors (*Denotes Presenter)	Abstract Title and Summary
1:30 p.m.	Wang A. *	<i>Salts and Brines: Active Intergradient in Modern-Day Martian Geochemistry</i> [#6016] We report a systematic study using mission observations and the results from analog site studies and from laboratory simulations, to address five big questions about the modern-day salts and brines on Mars.
1:45 p.m.	Baccolo G. * Niles P. B. Delmonte B. Cibin G. Di Stefano E. Hampai D. Keller L. Maggi V. Marcelli A. Michalski J. Snead C. Frezzotti M.	<i>Acidic Brines in Deep Antarctic Ice Promote the Englacial Precipitation of Jarosite and Support the Ice Weathering Model for Jarosite Formation on Mars</i> [#6011] Jarosite can form in deep ice. This implies that deep ice hosts acidic brines where dust interact with liquid water and acids, changing our perspective on the geochemical role of the englacial environment, both on Earth and in the solar system.
2:00 p.m.	Melwani Daswani M. * Castillo-Rogez J. C.	<i>Timing and Metamorphic Temperature Yield Different Brine Compositions at Dwarf Planet Ceres</i> [#6034] Brines generated / In metamorphic Ceres / Evolving in time.

2:15 p.m.	Stillman D. E. * Pettinelli E. Primm K. M. Caprarelli G. Mattei E. Lauro S. E. Cosciotti B.	<i>Perchlorate and Chloride Brines as the Cause of the MARSIS Bright Basal Reflections: Laboratory Measurements</i> [#6028] The apparent permittivity of brines is much larger than other materials; Metastable brines can exist for long periods of time below their eutectic temperature; Brines are the likely cause of the MARSIS bright basal reflections.
2:30 p.m.		DISCUSSION
2:40 p.m.		Break

Tuesday, October 26, 2021

BRINE DISCOVERY: EXPLORE YOUR WORLDS!

3:00 p.m.

Chairs: Carol Raymond and Jacob Buffo

Times	Authors (*Denotes Presenter)	Abstract Title and Summary
3:00 p.m.	De Sanctis M. C. * Ammannito E. Ciarniello M. Raponi A. Carrozzo G. F. Frigeri A. Formisano M. Rousseau B. Ferrari M. De Angelis S. Fonte S. Giardino M. Ehlmann B. L. Marchi S. Raymond C. A. Russell C. T.	<i>Modern Brines at Ceres: Hints from VIR Imaging Spectrometer on Dawn Mission</i> [#6002] Dawn mission indicates that Ceres has been an ocean-world and here we will review the indicators for the presence of modern brines inferred primarily by the VIR spectrometer onboard the mission.
3:15 p.m.	Scully J. E. C. * Baker S. R. Poston M. J. Carey E. M. Castillo-Rogez J. C. Raymond C. A.	<i>Initial Results Suggest that Short-Lived Flows Mobilized by Brines, Immediately Following an Impact, Formed Curvilinear Gullies, Lobate Deposits and Pitted Terrain on Vesta and Ceres</i> [#6004] We use lab experiments (the behavior of brine/liquid water under low transient atmospheric pressures) and geomorphologic analyses to investigate if specific geomorphologic features on Vesta/Ceres were formed by short-lived debris-flow-like processes.
3:30 p.m.	Bishop J. L. * Seelos K. D. Murchie S. L. Arvidson R. E.	<i>Anomalous Terrains West of Olympus Mons may be Result of Cold Spring Flows Percolating Through Near-Surface Permafrost</i> [#6001] Goethite-bearing anomalous terrains observed at the Amazonian-aged bright-toned maculae near Olympus Mons could result from near-surface acid brines percolating through permafrost to produce transient cold spring flows at the surface.
3:45 p.m.		DISCUSSION

Tuesday, October 26, 2021

POSTER SESSION: BRINE FACILITATED GEOLOGY

4:00 p.m.

Chair: Sean O'Hara

Times	Authors (*Denotes Presenter)	Abstract Title and Summary
4:00 p.m.	Geyer C. Elwood Madden M. E. Mason D. P. Rodriguez A. J. Elwood Madden A. S.	<u>Investigating Clay-Brine Interactions to Inform Interpretations of Mineral Assemblages on Mars</u> [#6049] A series of short-term experiments mixing montmorillonite or kaolinite with near-saturated Mars analog brines and analyzing the reaction products with Raman spectroscopy and powder XRD to study the effects of brines on clay minerals.
4:06 p.m.	Pedone M. Ammannito E. Plainaki C. De Sanctis M. C. Raponi A. De Angelis S. Ciarniello M. Ferrari M. Frigeri A. Carrozzo F. G.	<u>Chemical Processes Occurring in Brines Freezing Under Ceres Surface: The Case of Juling and Kupalo Craters</u> [#6010] We constrained the physiochemical properties of initial brines, characterizing potential reservoirs on Ceres, under two craters: Kupalo and Juling. Their distinct mineralogy at surface may be the result of freezing at different T-P initial conditions.
4:12 p.m.	Tu V. M. Ming D. W. Sletten R. S.	<u>The Mineralogy and Cation Exchange of Sediments in Don Juan Pond, Antarctica Dry Valley: Implications for Mars</u> [#6021] The mineralogy of sediments from the CaCl ₂ -rich brine Don Juan Pond, one of the saltiest bodies of water on Earth located in the Dry Valleys of Antarctica, reveals that cation exchange with smectites may have delivered ions to Don Juan Pond brines.
4:18 p.m.	Shi E. B.	<u>Gamma-CaSO₄ with Abnormally High Stability from Hyperarid Region on Earth and from Mars</u> [#6023] γ-CaSO ₄ from Atacama desert and in MIL 03346 were studied using the multiple micro-analysis techniques. The infilling of Si, P, and methyl into their tunnel structure was found to be the reason causing their abnormal stability.
4:24 p.m.	Sklute E. C. Geist A. E. Koretke B. King J. F. Hopkins R. J. Rogers A. D. Clark R. Dyar M. D.	<u>Alteration of Common Regolith Analogues and Precipitation Products from Rapidly Dehydrated Ferric Sulfate Saturated Brines in the Presence and Absence of NaCl — A Story of Amorphous Mars</u> [#6039] Understanding how brines not common to Earth interact with regolith components is an important first step in understanding salt weathering. Ferric sulfate-regolith-(NaCl) dehydration products are monitored by VNIR, MIR, XRD, and Raman over 641 days.
4:30 p.m.		POSTER AND SCIENCE DISCUSSION

Wednesday, October 27, 2021

INVITED TALKS: MISSION DEBRIEFS

10:00 a.m.

Chair: Ed Rivera-Valentín

Times	Authors (*Denotes Presenter)	Abstract Title and Summary
10:00 a.m.	Martínez G. *	<i>Brine Studies Enabled Through Surface-Based Measurements on Mars</i>
10:20 a.m.	Grima C. *	<i>The Europa Clipper Mission and the Search for Brines</i>
10:40 a.m.		DISCUSSION
10:50 a.m.		Break

Wednesday, October 27, 2021

BRINE DISTRIBUTION: PASS THE SALT, PLEASE!

11:00 a.m.

Chairs: Mohit Melwani Daswani and Julie Castell-Rogez

Times	Authors (*Denotes Presenter)	Abstract Title and Summary
11:00 a.m.	Naseem M. * Neveu M.	<i>Salt Distributions in Icy Shells of Ocean Worlds</i> [#6003] Investigation of ice shell compositions and how these affect transport processes, by determining possible spatial distributions of impurities in ice shells resulting from freezing of liquid intrusions by leveraging improvements in geochemical models.
11:15 a.m.	Wolfenbarger N. S. * Fox-Powell M. G. Buffo J. J. Soderlund K. M. Blankenship D. D.	<i>A Framework for Modeling the Distribution of Brine and Salt in an Ice Shell</i> [#6029] We present a framework for modeling the volume fraction of ice, brine, and solid salts in an ice shell inspired by models developed for terrestrial sea ice. We apply the framework to Europa's ice shell to evaluate potential habitats.
11:30 a.m.	Hesse M. A. * Wolfenbarger N. S. McCarthy C.	<i>To Percolate or Not to Percolate? When are Brines in Planetary Ice Shells Mobile?</i> [#6044] We discuss the evidence for an against brine mobility in ice.
11:45 a.m.	Raymond C. A. * Castillo-Rogez J. C. Ermakov A. I. Scully J. E. C. Park R. S. Fu R. R. Quick L. C. Ruesch O.	<i>Brines on Ceres: Origins and Transport Processes</i> [#6057] Data from the Dawn mission at Ceres show evidence for extensive aqueous alteration of Ceres resulting in a global subsurface brine layer in its past. The data also document the presence of modern effusion of residual brines.
12:00 p.m.		DISCUSSION
12:10 p.m.		Lunch Break

Wednesday, October 27, 2021

BRINE GEOCHEMISTRY: BRINES, ON THE ROCKS

1:30 p.m.

Chairs: Alian Wang and Natalie Wolfenbarger

Times	Authors (*Denotes Presenter)	Abstract Title and Summary
1:30 p.m.	Baharier B. * Semprich J. Filiberto J. Potter-McIntyre S. L. Olsson-Francis K. Perl S. Crandall J. R. Schwenzer S. P.	<u><i>Sulphate-Rich Sediments in Direct Contact with a Magmatic Intrusion Potential to Form a Habitable Geothermal Brine on Earth and Mars</i></u> [#6027] The formation of sulphate rich geothermal brines (SRGB) by a magmatic intrusion into sulfate-rich sediments from the San Raphael Swell was reconstructed to understand SRGB habitability constraints.
1:45 p.m.	Filiberto J. * Cogliati S. Crandall J. R. Schwenzer S. P.	<u><i>Geochemical Modeling of Magma-Sediment Interaction Induced Hydrothermal Systems</i></u> [#6014] Here we use temperature, fluid:rock ratio, and oxidation state constraints from a Mars analog as inputs to model how differences in bulk dike composition affect brine chemistry and subsequent alteration mineralogy.
2:00 p.m.	Sevgen S. * Suttle A. Som S. M.	<u><i>Brines Reacting with Rock: How Brine Composition Affects Hydrogen Generation During Serpentinization</i></u> [#6022] We computationally investigated how brine composition affects hydrogen generation during serpentinization by using EQ3/6. We found salts provides a sink for ferrous iron, thus limiting high-temperature hydrogen generation available for biology.
2:15 p.m.	Nellessen M. A. * Crossey L. Gasda P. J. Peterson E. Lanza N. Reyes-Newell A. Delapp D. Yeager C. Labouriau A. Wiens R. C. Clegg S. Legett S. Das D.	<u><i>Geochemical Modeling and Experimental Results of Boron Adsorption onto Martian Clay Minerals from Martian Brines</i></u> [#6055] Boron adsorption onto martian clay minerals and their implications for prebiotic chemistry and the effect of brines on martian clay chemistry.
2:30 p.m.		DISCUSSION
2:40 p.m.		Break

Wednesday, October 27, 2021

I SAW THE SIGN: BIOSIGNATURES IN BRINES

3:00 p.m.

Chairs: Alex Pontefract and Jie Xu

Times	Authors (*Denotes Presenter)	Abstract Title and Summary
3:00 p.m.	Birmingham M. A. * Lockamy D. Goldstein R. H. Olcott A. N. Oceans Across Space and Time Science Team	<u><i>Exploration of Biosignature Preservation Potential of Ancient and Modern Evaporites</i></u> [#6053] Here, we use multiple microscopy techniques and GC/MS to characterize evaporite samples of various ages precipitated in various depositional environments. These approaches reveal chemical and physical signs of life preserved within the minerals.

3:15 p.m.	Perl S. M. * Celestian A. J. Cockell C. S. Basu C. Filiberto J. Potter-McIntyre S. Olsson-Francis K. Schwenzer S. P. Crandall J. R. Baxter B. K. Onstott T. C. Bowman J. Bywaters K. Winzler M. Valera J. Cooper Z. Nisson D. Garner M. Baharier B. Tasoff P.	<u>Preservation of Dynamic Biological Processes from Extant Halophilic Life: In-Situ Lessons Learned from Planetary Analogue Brines and Evaporites</u> [#6048] The purpose of this paper is three-fold. First, we will discuss the modern preservation of halophilic microorganisms. Secondly, we review methodologies for in-situ and laboratory measurements and we conclude with an assessment of brine ecologies.
3:30 p.m.	Cogliati S. * Curtis-Harper E. Schwenzer S. P. Pearson V. K. Olsson-Francis K.	<u>Identification of Fluids Accompanying Bio-Signature Formation in Martian Analogue Experiments</u> [#6018] We investigate chemical variations of brines under biotic and abiotic conditions. We combine laboratory experiments and thermochemical modeling in order to identify bio-signature forming in analogue martian environments.
3:45 p.m.		DISCUSSION

Wednesday, October 27, 2021

POSTER SESSION: LIVING WITH BRINES

4:00 p.m.

Chair: Sean O'Hara

Times	Authors (*Denotes Presenter)	Abstract Title and Summary
4:00 p.m.	Tarasashvili M. V. Aleksidze N. G. Doborjginidze N. G. Gharibashvili N. G.	<u>Iron-Sulfur Brines as Hypothetical Ecosystem Analogues of Early Mars and Icy Worlds</u> [#6059] The problem of the habitability of brines remains disputable, which underlines an importance of the further scientific discussions regarding brines as biomarkers and/or biosignatures.
4:06 p.m.	Rivera-Valentín E. G. Méndez A. Lynch K. L. Soto A.	<u>Special Regions Based Habitat Suitability Index Model for Brine Environments on Mars</u> [#6025] Brine habitats / From ecology let's learn / Compare across Mars.
4:12 p.m.	Mitchell S. Sklute E. C. Boles B. Holbrook K. Jarratt A. Shaffer J. Smith L. Lee P. A. Dyar M. D. Mikucki J. A.	<u>Biosignatures at the Surface Interface Deposited by Subglacial Brine</u> [#6046] We use the Blood Falls ecosystem to study how microorganisms may interact with subterranean liquid environments, alter mineralogy, and produce metabolic biosignatures that may be detectable as subsurface brines emerge.
4:18 p.m.	Fisher L. A. Bovee A. R. Klempay B. Weng M. M. Som S. M. Doran P. T. Carr C. E. Glass J. B. Pontefract A. Schmidt B. E. Bowman J. S. Bartlett D. H.	<u>Comprehensive Analysis of DNA Degradation and Cell Viability of Model Microbes in Magnesium Chloride Brine</u> [#6019] 16S sequencing from a saltern in Southern California shows that DNA in MgCl ₂ brines are dominated by Haloquadratum. We seek to better understand this finding by studying the preservative effects of MgCl ₂ on purified DNA and cells of model halophiles.

4:24 p.m.	Xu J. Baxter B.	<i>Environmental Functions of Purple Sulfur Bacteria in the Great Salt Lake, Utah Under Changing Climatic Conditions</i> [#6008] We study the mechanisms of interaction among anoxygenic photosynthetic sulfur-oxidizers (especially purple sulfur bacteria), sulfate-reducers, dissolved metal species, and metal sulfide precipitates within GSL under various salinities.
4:30 p.m.		POSTER AND SCIENCE DISCUSSION

Thursday, October 28, 2021

KEYNOTE SPEAKER: ASTROBIOLOGY

10:00 a.m.

Chair: Ed Rivera-Valentín

Times	Authors (*Denotes Presenter)	Abstract Title and Summary
10:00 a.m.	Rivera-Valentín E. G. *	<i>Introduction and Welcome</i>
10:05 a.m.	Voytek M. *	<i>Halophiles as Models for Extraterrestrial Life</i>
10:40 a.m.		DISCUSSION
10:50 a.m.		Break

Thursday, October 28, 2021

BRINE ANALOGS: YOU LIVE WHERE?!

11:00 a.m.

Chairs: Michael Werner and Andrew Shumway

Times	Authors (*Denotes Presenter)	Abstract Title and Summary
11:00 a.m.	Evilia C. * Cahoon T. Guerrero A. Rosentreter J.	<i>It Takes a (Halophilic) Community: How to Survive in the Great Salt Lake</i> [#6052] An analysis of the microbial community of the Great Salt Lake was performed to understand this poly-extreme environment. Correlating this with water and computational analyses, we determined that life needs a minimal “survival toolkit” to survive.
11:15 a.m.	Jung J. Loschko T. Werner M. S. *	<i>Multicellular Life in Brine: Nematodes in the Great Salt Lake</i> [#6012] It was previously thought that only halophilic microbes, brine shrimp and brine flies can tolerate hypersaline lakes (>50 ppt). Here, we describe the presence, ecology and evolution of new species of nematode in the Great Salt Lake, UT (150–300 ppt).
11:30 a.m.	Klempay B. * Dutta A. Weng M. M. Doran P. T. Fisher L. A. Rundell S. M. Bartlett D. H. Carr C. E. Elbon C. E. Glass J. B. Pontefract A. Schmidt B. E. Bowman J. S.	<i>Patterns of Horizontal Gene Transfer Within Microbial Community Succession in Evaporative Brine Systems</i> [#6037] Evaporative hypersaline brines are characterized by an explosion of archaeal diversity before they eventually become uninhabitable. The initial stages of this surge of diversity are likely driven by rampant horizontal gene transfer.

11:45 a.m.	Winzler M. L. * Perl S. M. Cockell C. S. Pailing S.	<u>Evaluation of Brine Concentration Efficacies for Nucleic Acid Preservation</u> [#6050] The purpose of this paper is to establish the efficacy of concentrating brine for nucleic acid extraction within three planetary analogue field sites. This research will guide parameters to optimize sample concentration onboard landed missions.
12:00 p.m.		DISCUSSION
12:10 p.m.		Lunch Break

Thursday, October 28, 2021

LIFE IN THE LAB: YOU LIVE HERE NOW

1:30 p.m.

Chairs: Kennda Lynch and Scott Perl

Times	Authors (*Denotes Presenter)	Abstract Title and Summary
1:30 p.m.	Xu J. * Lajoie B. N. Brunner B. Afrin H. Langford R. Fernandez Delgado O. Cantando E. Arnold G.	<u>Potential Bioavailability of Crystallization Water in Sulfate Minerals Under Water-Restricted Conditions — A Case Study of Gypsum Interdunes in the Tularosa Basin, New Mexico</u> [#6007] We conducted systematic field work at five sites of gypsum interdunes in the Tularosa Basin, NM. Through this work, we aim to understand if microbial life may capitalize on the structural water in gypsum under water-restricted conditions.
1:45 p.m.	Smith S. M. * Poulson S. R.	<u>Searching for Life in Salts: Freezing/Geochemical Modeling to Investigate Stability and Microbial Habitability of Modern Martian Brines</u> [#6045] This study evaluated water chemistries in equilibrium with a number of possible martian mineral assemblages using the program FREZCHEM to help determine geochemical constraints on microbial life in a cold, hyperarid martian environment.
2:00 p.m.	Schneegurt M. A. * Zbeeb H. Z. Cesur R. M. Joad Md. Zayed H. H. Ansari I. M. Mahdi A. Luhring T. M. Chen F. Clark B. C.	<u>Bacterial Survival and Growth in Dense Brines, Deliquescent Liquids, and Crystal Fluid Inclusions</u> [#6006] Growth of desiccated salinotolerant microbes, entrapped in salt evaporites, after rehydration to brine by deliquescence and their tolerances to diverse dense brines, identifying significant interactions with the physical qualities of ions and salts.
2:15 p.m.	Smith S. M. Poulson S. R. *	<u>Agar Gelation Spectrophotometric Assay of Chao- and Kosmo-Tropicity of Inorganic Salts, and Implications for Life in Terrestrial and Martian Brines</u> [#6017] Agar gelation spectrophotometric assays of the chaotropicity/kosmotropicity of various pure inorganic salts (inc. nitrates, perchlorates and bicarbonates), as well as binary, ternary and quaternary mixtures of inorganic salts have been performed.
2:30 p.m.		DISCUSSION
2:40 p.m.		Break

Thursday, October 28, 2021

HABITABILITY: BRINES ARE JUUUST RIGHT!

3:00 p.m.

Chairs: Sara Smith and Mark Schneegurt

Times	Authors (*Denotes Presenter)	Abstract Title and Summary
3:00 p.m.	Lynch K. L. * Simpson A. Machineni S. Santiago-Vazquez L. Goodale C. Lopez J.	<u>Guess Who's Coming to Dinner: Investigating the Potential of (Per)Chlorate Supported Ecosystems on Mars</u> [#6024] Extensive studies of terrestrial subsurface life's adaptability to brines and alternative energy spectrums are necessary to understand the habitability of potential of martian brines. This talk will cover efforts to understand such ecosystems.
3:15 p.m.	Méndez A. * Rivera-Valentín E. G.	<u>Implementing Habitat Suitability Models: Habitability of the Martian Surface</u> [#6056] The habitability of the martian surface, with respect to temperature and humidity, is two to four orders of magnitude less habitable than anything on Earth.
3:30 p.m.	Fifer L. M. * Catling D. C. Toner J. D.	<u>A Moderately Alkaline and Volatile-Rich Enceladus Ocean from Plume Modeling</u> [#6009] We model fractionation effects that create compositional differences between Enceladus' subsurface ocean and the gas phase of the erupting plumes. Using this model to derive ocean chemistry, we predict a gas-rich ocean with pH ~7.9–8.5.
3:45 p.m.	Hallsworth J. E. *	<u>Biology of Water Activity in Terrestrial Brines</u> [#6061] NaCl brines permit halophile growth, but MgCl ₂ -brine water activity is below the limit for active life (<0.585) and chaotropicity is the life-limiting parameter. Acid brines are ≥0.714 water activity (pH 2.5) yet microbes may be inactive there.
4:00 p.m.		DISCUSSION

Thursday, October 28, 2021

INVITED TALK: MEETING WRAP UP

4:15 p.m.

Chair: Ed Rivera-Valentín

Times	Authors (*Denotes Presenter)	Abstract Title and Summary
4:15 p.m.	Murray A. *	<i>Charting the Course to Ocean Worlds</i>
4:45 p.m.		DISCUSSION
4:50 p.m.	Rivera-Valentín E. G. *	<i>Farewell Address</i>



BRINES ACROSS THE SOLAR SYSTEM: MODERN BRINES

Table of Contents

Cryogeochemistry: Liquid Water in Unexpected Places <i>L. M. Anovitz, A. H. Treiman, E. Mamontov, A. I. Kolesnikov, A. G. Stack, D. R. Cole, and D. J. Wesolowski</i>	6060
Acidic Brines in Deep Antarctic Ice Promote the Englacial Precipitation of Jarosite and Support the Ice Weathering Model for Jarosite Formation on Mars <i>G. Baccolo, P. B. Niles, B. Delmonte, G. Cibir, E. Di Stefano, D. Hampai, L. Keller, V. Maggi, A. Marcelli, J. Michalski, C. Snead, and M. Frezzotti</i>	6011
Sulphate-Rich Sediments in Direct Contact with a Magmatic Intrusion Potential to Form a Habitable Geothermal Brine on Earth and Mars <i>B. Baharier, J. Semprich, J. Filiberto, S. L. Potter-McIntyre, K. Olsson-Francis, S. Perl, J. R. Crandall, and S. P. Schwenzer</i>	6027
Exploration of Biosignature Preservation Potential of Ancient and Modern Evaporites <i>M. A. Birmingham, D. Lockamy, R. H. Goldstein, A. N. Olcott, and Oceans Across Space and Time Science Team</i>	6053
Anomalous Terrains West of Olympus Mons may be Result of Cold Spring Flows Percolating Through Near-Surface Permafrost <i>J. L. Bishop, K. D. Seelos, S. L. Murchie, and R. E. Arvidson</i>	6001
Carbon Preservation Within Ceres Regolith Minerals: A Need for Analog Work to Aid in Successful Sample Return <i>M. Bose, L. R. Reynoso, and J. Castillo-Rogez</i>	6036
An Objective Definition of Habitable Space and Application to Modeling Water Activity from Geochemistry <i>J. S. Bowman, A. Bastuba, S. Som, T. Plattner, A. Pontefract, P. Doran, J. Buffo, J. Lawrence, B. Schmidt, and O. A. S. T. Team</i>	6047
Development and Testing of a Miniature Robotic Electrodialysis (MR ED) System to Remove Salts for Ocean World Sampling <i>F. E. Bryson, E. D. Ingall, A. M. Hanna, M. Cardelino, T. Plattner, M. R. Meister, J. D. Lawrence, A. Mullen, D. Dichek, and B. E. Schmidt</i>	6032
British Columbia's Unassuming Planetary Laboratory: How a Handful of Frozen Saline Lakes can Help Us Understand Brines Across the Solar System <i>J. J. Buffo, E. K. Brown, A. Pontefract, B. E. Schmidt, B. Klempay, J. Lawrence, J. Bowman, M. Grantham, J. B. Glass, T. Plattner, C. Chivers, P. Doran, C. R. Meyer, M. E. Barklage, and B. Fluegel</i>	6020
Role of Non-Water Ices in Driving Salinity and Electrical Conductivity in Ocean Worlds <i>J. C. Castillo-Rogez, M. Melwani Daswani, C. Glein, S. Vance, and C. Cochrane</i>	6035

Identification of Fluids Accompanying Bio-Signature Formation in Martian Analogue Experiments <i>S. Cogliati, E. Curtis-Harper, S. P. Schwenzer, V. K. Pearson, and K. Olsson-Francis</i>	6018
Modern Brines at Ceres: Hints from VIR Imaging Spectrometer on Dawn Mission <i>M. C. De Sanctis, E. Ammannito, M. Ciarniello, A. Raponi, G. F. Carrozzo, A. Frigeri, M. Formisano, B. Rousseau, M. Ferrari, S. De Angelis, S. Fonte, M. Giardino, B. L. Ehlmann, S. Marchi, C. A. Raymond, and C. T. Russell</i>	6002
It Takes a (Halophilic) Community: How to Survive in the Great Salt Lake <i>C. Evilia, T. Cahoon, A. Guerrero, and J. Rosentreter</i>	6052
A Moderately Alkaline and Volatile-Rich Enceladus Ocean from Plume Modeling <i>L. M. Fifer, D. C. Catling, and J. D. Toner</i>	6009
Geochemical Modeling of Magma-Sediment Interaction Induced Hydrothermal Systems <i>J. Filiberto, S. Cogliati, J. R. Crandall, and S. P. Schwenzer</i>	6014
Raman Spectroscopy as a Tool to Identify Brine Formation <i>E. Fischer, G. M. Martinez, and N. O. Renno</i>	6051
Comprehensive Analysis of DNA Degradation and Cell Viability of Model Microbes in Magnesium Chloride Brine <i>L. A. Fisher, A. R. Bovee, B. Klempay, M. M. Weng, S. M. Som, P. T. Doran, C. E. Carr, J. B. Glass, A. Pontefract, B. E. Schmidt, J. S. Bowman, and D. H. Bartlett</i>	6019
Modeling the Deliquescence of Complex Salt Mixtures at the Phoenix Landing Site <i>A. Fitting, V. F. Chevrier, E. G. Rivera-Valentín, and A. Soto</i>	6042
Martian Brines in Ancient Salt Lake Beds — A High Priority Target for Mars Sample Return <i>M. Fries, A. Steele, and M. Zolensky</i>	6054
Investigating Clay-Brine Interactions to Inform Interpretations of Mineral Assemblages on Mars <i>C. Geyer, M. E. Elwood Madden, D. P. Mason, A. J. Rodriguez, and A. S. Elwood Madden</i>	6049
Water-Activity Limit for Life as We Know It <i>J. E. Hallsworth</i>	6061
Strategies for Remotely Detecting Chlorine Salts on Mars <i>J. Hanley, Z. Bandelier, C. Murphy, R. Carmack, and B. Horgan</i>	6058
To Percolate or Not to Percolate? When are Brines in Planetary Ice Shells Mobile? <i>M. A. Hesse, N. S. Wolfenbarger, and C. McCarthy</i>	6044
FTIR-ATR Spectra and XRD Analysis of Amorphous Sulfate-Chloride Brine Desiccation Products after Multiple Consecutive Deliquescence-Desiccation Cycles <i>R. J. Hopkins, A. D. Rogers, L. Ehm, and E. C. Sklute</i>	6031
Experimental Evaporation of Multicomponent Brines Demonstrates Variability in Salt Identification <i>E. B. Hughes, M. S. Gilmore, and M. Eleazer</i>	6030
Multicellular Life in Brine: Nematodes in the Great Salt Lake <i>J. Jung, T. Loschko, and M. S. Werner</i>	6012

Patterns of Horizontal Gene Transfer Within Microbial Community Succession in Evaporative Brine Systems <i>B. Klempay, A. Dutta, M. M. Weng, P. T. Doran, L. A. Fisher, S. M. Rundell, D. H. Bartlett, C. E. Carr, C. E. Elbon, J. B. Glass, A. Pontefract, B. E. Schmidt, and J. S. Bowman</i>	6037
Guess Who's Coming to Dinner: Investigating the Potential of (Per)Chlorate Supported Ecosystems on Mars <i>K. L. Lynch, A. Simpson, S. Machineni, L. Santiago-Vazquez, C. Goodale, and J. Lopez</i>	6024
Using Raman Spectroscopy to Detect and Monitor Freezing and Melting Processes in Near-Saturated Water-Salt Mixtures at Mars-Analogue Temperatures <i>D. P. Mason and M. E. Elwood Madden</i>	6013
Timing and Metamorphic Temperature Yield Different Brine Compositions at Dwarf Planet Ceres <i>M. Melwani Daswani and J. C. Castillo-Rogez</i>	6034
Implementing Habitat Suitability Models: Habitability of the Martian Surface <i>A. Méndez and E. G. Rivera-Valentín</i>	6056
Biosignatures at the Surface Interface Deposited by Subglacial Brine <i>S. Mitchell, E. C. Sklute, B. Boles, K. Holbrook, A. Jarratt, J. Shaffer, L. Smith, P. A. Lee, M. D. Dyr, and J. A. Mikucki</i>	6046
Salt Distributions in Icy Shells of Ocean Worlds <i>M. Naseem and M. Neveu</i>	6003
Geochemical Modeling and Experimental Results of Boron Adsorption onto Martian Clay Minerals from Martian Brines <i>M. A. Nellesen, L. Crossey, P. J. Gasda, E. Peterson, N. Lanza, A. Reyes-Newell, D. Delapp, C. Yeager, A. Labouriau, R. C. Wiens, S. Clegg, S. Legett, and D. Das</i>	6055
Chemical Processes Occurring in Brines Freezing Under Ceres Surface: The Case of Juling and Kupalo Craters <i>M. Pedone, E. Ammannito, C. Plainaki, M. C. De Sanctis, A. Raponi, S. De Angelis, M. Ciarniello, M. Ferrari, A. Frigeri, and F. G. Carrozzo</i>	6010
Preservation of Dynamic Biological Processes from Extant Halophilic Life: In-Situ Lessons Learned from Planetary Analogue Brines and Evaporites <i>S. M. Perl, A. J. Celestian, C. S. Cockell, C. Basu, J. Filiberto, S. Potter-McIntyre, K. Olsson-Francis, S. P. Schwenzer, J. R. Crandall, B. K. Baxter, T. C. Onstott, J. Bowman, K. Bywaters, M. Winzler, J. Valera, Z. Cooper, D. Nisson, M. Garner, B. Baharier, and P. Tasoff</i>	6048
A New Approach to Inferring Habitability Metrics in Hypersaline Environments <i>A. Pontefract, C. E. Carr, P. T. Doran, L. Ratliff, K. E. McNulty, A. B. Odenheimer, J. Bowman, S. Som, T. Plattner, J. D. Lawrence, and B. E. Schmidt</i>	6041
Macroscopic Deliquescence as Monitored by Dielectric Spectroscopy <i>K. M. Primm and D. E. Stillman</i>	6033
Brines on Ceres: Origins and Transport Processes <i>C. A. Raymond, J. C. Castillo-Rogez, A. I. Ermakov, J. E. C. Scully, R. S. Park, R. R. Fu, L. C. Quick, and O. Ruesch</i>	6057

Formation of (Meta)Stable Brines on Present-Day Mars: Implications for Habitability <i>E. G. Rivera-Valentín, V. F. Chevrier, A. Soto, and G. Martínez</i>	6040
Special Regions Based Habitat Suitability Index Model for Brine Environments on Mars <i>E. G. Rivera-Valentín, A. Méndez, K. L. Lynch, and A. Soto</i>	6025
Raman Spectroscopy: Quantitative Analyses of Modern Brines on Mars <i>A. J. Rodriguez, M. E. Elwood Madden, and D. P. Mason</i>	6038
Bacterial Survival and Growth in Dense Brines, Deliquescent Liquids, and Crystal Fluid Inclusions <i>M. A. Schneegurt, H. Z. Zbeeb, R. M. Cesur, Md. Joad, H. H. Zayed, I. M. Ansari, A. Mahdi, T. M. Luhning, F. Chen, and B. C. Clark</i>	6006
Initial Results Suggest that Short-Lived Flows Mobilized by Brines, Immediately Following an Impact, Formed Curvilinear Gullies, Lobate Deposits and Pitted Terrain on Vesta and Ceres <i>J. E. C. Scully, S. R. Baker, M. J. Poston, E. M. Carey, J. C. Castillo-Rogez, and C. A. Raymond</i>	6004
Brines Reacting with Rock: How Brine Composition Affects Hydrogen Generation During Serpentinization <i>S. Sevgen, A. Suttle, and S. M. Som</i>	6022
Gamma-CaSO ₄ with Abnormally High Stability from Hyperarid Region on Earth and from Mars <i>E. B. Shi</i>	6023
Soils Increase the Stability of Magnesium Perchlorate Brines on Mars <i>A. O. Shumway, D. C. Catling, and J. D. Toner</i>	6005
Alteration of Common Regolith Analogues and Precipitation Products from Rapidly Dehydrated Ferric Sulfate Saturated Brines in the Presence and Absence of NaCl — A Story of Amorphous Mars <i>E. C. Sklute, A. E. Geist, B. Koretke, J. F. King, R. J. Hopkins, A. D. Rogers, R. Clark, and M. D. Dyar</i>	6039
Experimental Investigation of the Near-Surface Martian Water Cycle with a Salty Regolith: Implications for Brine Formation <i>R. A. Slank, E. G. Rivera-Valentín, and V. F. Chevrier</i>	6026
Agar Gelation Spectrophotometric Assay of Chao- and Kosmo-Tropicity of Inorganic Salts, and Implications for Life in Terrestrial and Martian Brines <i>S. M. Smith and S. R. Poulson</i>	6017
Searching for Life in Salts: Freezing/Geochemical Modeling to Investigate Stability and Microbial Habitability of Modern Martian Brines <i>S. M. Smith and S. R. Poulson</i>	6045
Stability of Surficial Brines on Mars During Recent Orbital Cycles <i>A. Soto, E. G. Rivera-Valentín, and V. Chevrier</i>	6015
Perchlorate and Chloride Brines as the Cause of the MARSIS Bright Basal Reflections: Laboratory Measurements <i>D. E. Stillman, E. Pettinelli, K. M. Primm, G. Caprarelli, E. Mattei, S. E. Lauro, and B. Cosciotti</i>	6028

Iron-Sulfur Brines as Hypothetical Ecosystem Analogues of Early Mars and Icy Worlds <i>M. V. Tarasashvili, N. G. Aleksidze, N. G. Doborjginidze, and N. G. Gharibashvili</i>	6059
Stability Diagrams of Aqueous Chlorate Solutions Under Martian Relevant Temperatures and Relative Humidities <i>S. Tu, J. B. Parise, E. Lars, and A. D. Rogers</i>	6043
The Mineralogy and Cation Exchange of Sediments in Don Juan Pond, Antarctica Dry Valley: Implications for Mars <i>V. M. Tu, D. W. Ming, and R. S. Sletten</i>	6021
Salts and Brines: Active Intergradient in Modern-Day Martian Geochemistry <i>A. Wang</i>	6016
Evaluation of Brine Concentration Efficacies for Nucleic Acid Preservation <i>M. L. Winzler, S. M. Perl, C. S. Cockell, and S. Pailing</i>	6050
A Framework for Modeling the Distribution of Brine and Salt in an Ice Shell <i>N. S. Wolfenbarger, M. G. Fox-Powell, J. J. Buffo, K. M. Soderlund, and D. D. Blankenship</i>	6029
Environmental Functions of Purple Sulfur Bacteria in the Great Salt Lake, Utah Under Changing Climatic Conditions <i>J. Xu and B. Baxter</i>	6008
Potential Bioavailability of Crystallization Water in Sulfate Minerals Under Water-Restricted Conditions — A Case Study of Gypsum Interdunes in the Tularosa Basin, New Mexico <i>J. Xu, B. N. Lajoie, B. Brunner, H. Afrin, R. Langford, O. Fernandez Delgado, E. Cantando, and G. Arnold</i>	6007



BRINES ACROSS THE SOLAR SYSTEM: MODERN BRINES

Abstracts

CRYOGEOCHEMISTRY: LIQUID WATER IN UNEXPECTED PLACES. L. M. Anovitz¹, A. H. Treiman², E. Mamontov³, A. I. Kolesnikov³, A.G. Stack¹, D. R. Cole⁴ and D. J. Wesolowski¹, ¹Chemical Sciences Division, MS 6110, Oak Ridge National Laboratory, Oak Ridge, TN 37831-6110, United States, anovitzlm@ornl.gov, ²Lunar and Planetary Institute 3600 Bay Area Boulevard, Houston, TX 77058 treiman@lpi.usra.edu, ³Neutron Scattering Division, Oak Ridge National Laboratory, Oak Ridge, TN 37831-6473, United States mamontove@ornl.gov kolesnikovai@ornl.gov, ⁴School of Earth Sciences, The Ohio State University, Columbus, OH, USA

Introduction: To a reasonable approximation, reactions in aqueous systems stop at temperatures where water is frozen. The slow diffusion or other transport rates possible in the solid state dramatically retard ionic or mineral/fluid reactions. While it is well known that saline brines freeze at temperatures well below those of liquid water (e.g. -21.1°C for 23.3 wt % NaCl in H_2O). The magnitude of such freezing point depression depends on the nature and concentration of the salts involved.

However, it has also been shown by several authors¹⁻⁸ that the freezing point of a confined liquid is also a function of the size and composition of the pore within which it is located. In part this is due to the Gibbs-Thompson effect, and will be true for any small droplet, but it is also a function of the confinement of the fluid within the pore which alters the physical-chemical

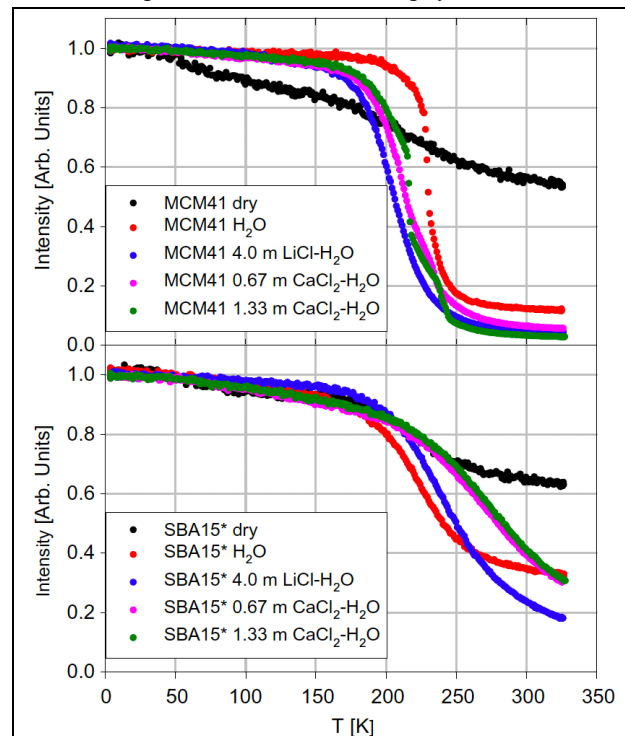


Figure 1: The results of the neutron elastic scattering intensity scans summed for $0.62 \text{ \AA}^{-1} < Q < 1.68 \text{ \AA}^{-1}$ for water and solutions confined in MCM41 and SBA15*. The spectra have been normalized to the intensities measured at 5 K. ²

nature of the fluid compared to the bulk solution (e.g., the electrical double layer, density, phase behavior).

This property of nanoconfined fluids has significant implications for aqueous chemistry in extraterrestrial

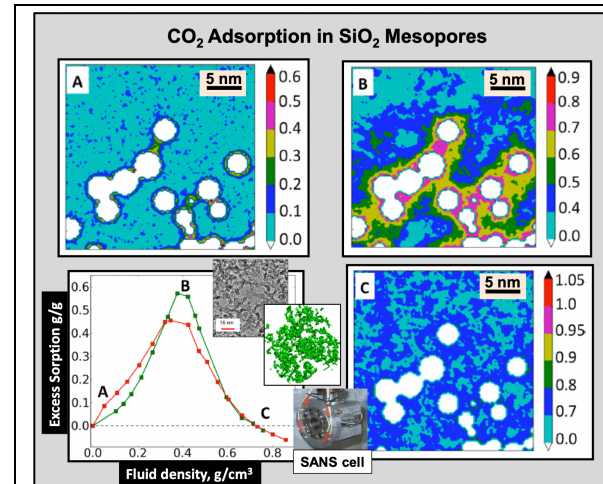


Figure 2: 2D density profiles (g/cm^3) of CO_2 confined in a silica aerogel matrix (average pore size $\sim 14 \text{ nm}$) corresponding to different stages of pore filling at 35°C calculated from Grand Canonical Lattice Gas simulations. The white areas represent thin strands of the silica matrix. The letters indicate corresponding states in the 2D profiles and in a plot of excess sorption as a function of bulk CO_2 density (bottom left) obtained from experiment (red) and modeling (green) for CO_2 in silica aerogel with a density of $0.1 \text{ g}/\text{cm}^3$. Excess adsorption is the difference between the amount of fluid in the system and the amount that would be present at the same T and P in the absence of adsorption. Inserts include a TEM image of the silica (scale bar = 16 nm), a mathematical rendering of this material (green) generated from diffusion-limited cluster-cluster aggregation based on TEM images, and the high P-T experimental SANS cell used. The results demonstrate that density changes in concert with pore size and pore throats are critical in driving pore fluid condensation. ^{9,10}

bodies. As the freezing point of an aqueous fluid can be depressed significantly in small pores, liquid water or brines can, therefore, exist in rocks in such bodies under conditions where bulk water would freeze. Thus, aqueous chemical reactions can also proceed, however

slowly. Furthermore, as the density of fluids under confinement can also be significantly higher than under the same pressure and temperature conditions for bulk water,^{9,11} and as solubility is usually a positive function of fluid density¹² these changes may enhance reactivity and transport (Figure 2). Conversely, some studies also show that the density of confined water may be less than that of the bulk (Figure 3).¹³ While the pore scales involved are generally too small for earth-like organisms, the potential effects of this chemical environment on extraterrestrial life are unknown.

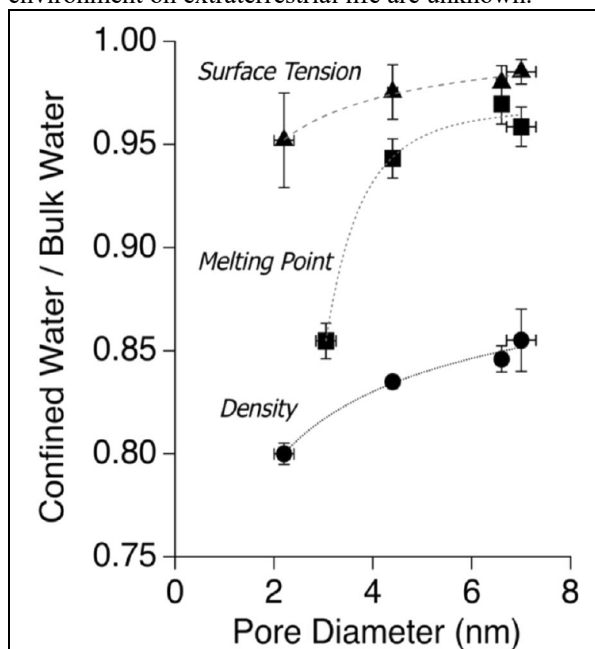


Figure 3: The calculated relative surface tension and density, determined by BET N₂ and water adsorption studies, along with the relative melting point, determined by differential scanning calorimetry, versus silica pore radius (Knight et al., 2019).

Discussion: An example of the effects of confinement of freezing is shown in Figure 1, which displays the results of elastic scans for a series of brines and pure water confined in two synthetic zeolites (MCM-41 and SBA-15) performed on the HFBS Quasi-elastic neutron spectrometer (QENS) at the NIST Center for Neutron Research (NCNR, Mamontov et al., 2008). The synthetic zeolites were used because of their well-defined pore sizes (2.7 nm in MCM-4, and 1.4 nm in SBA-15). In QENS measurements all the intensity is expected to occur in the elastic part of the spectrum below freezing. The onset of diffusion dynamics, that is, of melting, transfers intensity away from the elastic line. As neutrons are both very penetrating through most solids, and very sensitive to motions of hydrogen, and

thus water, the elastic intensity can be used to determine the onset of melting in nanopores.

As can be seen in Figure 1, the nature of confinement-induced freezing point depression is a function of the size and composition of the pore. Anovitz et al.¹⁴ showed, for instance, that when the pores are very small, such as the ~0.5 nm diameter channels in beryl, freezing does not occur at all. The scale at which confinement affect becomes significant may also depend on the size of the confined molecule, being greater for large organic complexes.

To date, the implications of fluid confinement of the chemistry of extraterrestrial systems remain unexplored. However, it seems likely that they imply the potential presence of liquids under conditions that would otherwise not have been considered possible. By extension, water and brine present in nanopores may suggest an alternative strategy of where to search for water on Mars.

Acknowledgments: This material is based upon work supported by the U.S. Department of Energy, Office of Science, Office of Basic Energy Sciences, Chemical Sciences, Geosciences, and Biosciences Division.

References: [1] Christenson (2001) *J. Phys.: Condens. Matter* 13 R95–R133. [2] Mamontov et al. (2008) *Chemical Physics* 352, 117–124. [3] Chathoth et al. (2011) *EPL*, 95, 56001. [4] Kolesnikov et al. (2014) *J. Phys. Chem. B* 118, 13414–13419. [5] Kolesnikov et al. (2016) *PRL* 116, 167802. [6] Kolesnikov et al. (2018) *J. Physics: Conf. Series* 1055, 012002. [7] Kolesnikov et al. (2019) *J. Chemical Physics* 150, 204706. [8] Agarwal et al. (2016) *Nature Nanotechnology* 12, 267–273. [9] Rother et al. (2014) *J. Phys. Chem C* 118, 15525–15533. [10] Stack et al. (2021) *Elements*, 17, 169–174. [11] Gruszkiewicz et al. (2012) *Langmuir* 2012, 28, 5070–5078. [12] Wesolowski et al. (2004) *Aqueous Systems at Elevated Temperatures and Pressures* Ch. 14, 493–595. [13] Knight et al. (2019) *Sci. Rep* 9, 8246. [14] Anovitz et al. (2013) *Physical Review E* 88, 052306.

ACIDIC BRINES IN DEEP ANTARCTIC ICE PROMOTE THE ENGLACIAL PRECIPITATION OF JAROSITE AND SUPPORT THE ICE WEATHERING MODEL FOR JAROSITE FORMATION ON MARS. G. Bacco^{1,2}, P.B. Niles³, B. Delmonte¹, G. Cibir⁴, E. di Stefano^{1,2}, D. Hampai⁵, L. Keller³, V. Maggi^{1,2}, A. Marcelli^{5,6}, J. Michalski⁷, C. Snead⁸ and M. Frezzotti⁹, ¹Department of Environmental and Earth Sciences, University of Milano-Bicocca, Milano, Italy (giovanni.baccolo@unimib.it); ²INFN section of Milano-Bicocca, Milano, Italy; ³NASA Johnson Space Center, Houston, TX 77058, USA (paul.b.niles@nasa.gov); ⁴Diamond Light Source, Harwell Science and Innovation Campus, Didcot OX11 0DE, UK; ⁵Laboratori Nazionali di Frascati, INFN, 00044 Frascati, Italy; ⁶Rome International Center for Materials Science - Superstripes, 00185 Rome, Italy; ⁷Department of Earth Sciences, University of Hong Kong, Hong Kong, Hong Kong; ⁸Jacobs, NASA Johnson Space Center, Houston, TX 77058, USA; ⁹Department of Science, University Roma Tre, Rome, Italy.

Introduction: Once believed stable and immobile from the geochemical point of view, Antarctic deep ice is now receiving growing consideration as a matrix capable of favoring complex reactions that involve the soluble and insoluble impurities trapped within the same ice.

One of the reactions that have been recognized to occur in deep ice is the precipitation of jarosite, a hydrated potassium-iron(III) sulphate [1].

The englacial precipitation of jarosite requires the weathering of iron-bearing minerals through interaction with acidic brines [2]. Our evidence shows that jarosite is the dominant iron-bearing mineral in the deepest part of the Talos Dome ice core (East Antarctica), suggesting that deep ice is a favorable environment for the occurrence of acidic brines. Moreover, this implies that deep Antarctic ice is a geochemically dynamic environment, capable of promoting the dissolution of some minerals and the precipitation of others [3].

But the implications are not limited to Antarctica or Earth. They extend to Mars where jarosite is a common mineral found in surficial layered sediments [4-6]. Since its early prediction on Mars [7], many models have been proposed to describe its genetic environment.

Among them, one has strong similarities with what we have observed in deep Antarctic ice: the ice weathering model [8]. According to it, Martian jarosite formed in past glacial epochs inside massive ice- and dust-rich deposits that were spread on the planet during high obliquity periods [9]. Weathering reactions occurred in depth of such deposits, thanks to the presence of acidic brines [10].

The englacial precipitation of jarosite in Antarctic ice resembles the scenario described by the ice-weathering model. This paradigm changes our interpretation of aqueous geochemistry on Mars. Ice could be much more important than previously thought.

A renewed interest in deep Antarctic ice: After ice coring projects carried out in the last decades, the consideration for deep Antarctic ice is growing again and future deep ice cores are expected in the near future. This is because scientists want to extend ice core-based climatic records to 1.5 million years before present [11]. This interest is paving the way for studies focused on englacial geochemical reactions [2].

The identification of jarosite in the Talos Dome ice core: We have analyzed 54 samples consisting of insoluble particles extracted from ice sections of the Talos Dome ice core, drilled at a peripheral ice dome of East Antarctica. Our results show that below 1000 m deep, jarosite appears as one of the main iron-bearing phases that define the mineral assemblage of the micrometric insoluble particles trapped into ice. Moving down along the core its concentration increases and in the last sections (between 1500 and 1620 m deep) it is the dominant Fe-mineral.

This is the first time that jarosite is observed in ice cores; our evidence suggests that it is not a mineral originally present in the dust deposited at the considered Antarctic site, but it is formed directly into the ice, as a consequence of englacial geochemical reactions. Along with the increase of jarosite we observe a decrease in ferrous minerals, such as hornblende, pyrite, muscovite, and a general increase in iron oxidation state. This agrees with the occurrence of acidic/oxidative weathering in deep ice; jarosite is a common product of such an alteration pathway [12].

Deep ice as a geochemical reactor: To address deep englacial reactions it is necessary to consider the complex dynamics affecting deep ice. The latter is subject to several physico/chemical transformations driven by thermodynamics. Deep ancient ice recrystallizes, progressively increasing the average size of ice crystals [13]. During this process the impurities not compatible with the ice molecular lattice are expelled and accumulated at grain junctions or within intra-grain micro-inclusions [14].

The accumulation of impurities in confined environments determines a local lowering of the pressure melting point, allowing for the occurrence of limited amounts of liquid water. High solute concentrations, liquid waters, confined environments: these are the ingredients for brines and depict a highly reactive environment. The pH of such brines is low because of the concentration of atmospheric acidic species, such as sulfuric and nitric acids, which are highly incompatible with the ice lattice and are rapidly remobilized and concentrated [15-17].

This scenario is confirmed by the same observation of englacial precipitation of jarosite since it requires a

low pH, a limited activity of liquid water and Fe-minerals [12].

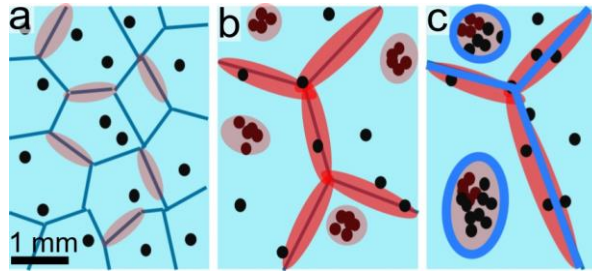


Figure 1 A model of deep ice metamorphism and acidic brines development. a) surficial ice: ice grains are millimetric, only highly incompatible atmospheric acids are accumulated at junctions. b) moderately deep ice (500-1000 m deep): grains increase their size, insoluble impurities aggregate within intra-grain micro-inclusions and acids are strongly segregated at junctions and inclusions. c) deep ice (>1000 m deep): grains are centimetric, both soluble and insoluble impurities are concentrated in small-scale acidic environments where because of high solute concentration, films of liquid water exist, favoring englacial reactions, such as jarosite precipitation.

Paleoclimatic implications: Traditionally mineral dust is considered a stable proxy in deep ice and its records have been used to synchronize and compare deep ice cores when other proxies were deteriorated. With this study we show that dust is also affected by such alterations.

To correctly interpret future deep ice core records, it will be essential to address englacial geochemical reactions, so as to disentangle the original climatic signals embedded into ice, from the ones depending on successive transformations.

Antarctic implications: From the geochemical point of view ice is not considered to be an important factor. Attention has already been given to the subglacial environment [19], but not the englacial one because it is considered stable and not favorable for reactions. Our results show that this is not true, and we need to change our perception of deep ice. From an immobile matrix to an environment whose characteristics can promote complex reactions still largely unknown.

The Antarctic significance of this study could extend to other contexts than deep ice cores. For example, the investigation of weathering processes affecting meteorites collected at the surface of blue ice areas [20]. They are traditionally interpreted as processes that occurred once meteorites were exposed to the atmosphere, but it is likely that they partly took place while meteorites were buried deep into ice.

Brines across the solar system: Our work demonstrates the power of large ice deposits as generators of brines on Earth. There is no reason that

this process should be limited to Earth, and we expect that we should find evidence for brines associated with large ice deposits all across the solar system. As observed in Earth's polar areas, the metamorphism of deep ice leads to the formation of small scale environments where acidic fluids interact with concentrated impurities. On bodies such as Mars, Earth, or elsewhere, the isolation from the planetary crust also prevents the moderation of pH and maintains acidic conditions consistent with jarosite formation.

Our study also demonstrates that brines are reactive even at cryogenic temperatures which could also have broad implications across the solar system. The finding of jarosite in deep ice certainly supports the ice weathering model proposed for Mars and suggests that ice could have been an important player not only with respect to Martian surficial morphology, but also its geochemistry.

Methods: insoluble impurities have been extracted from ice sections through the filtration of meltwater in a clean room. Impurities were retained on polycarbonate filters and inspected through SEM-EDX for morphology and elemental composition and through X-ray synchrotron absorption spectroscopy to determine the mineralogy and oxidation state of iron present in the insoluble particles. Further confirmation about the presence of jarosite came from XRD microscopy. Full details are found in Baccolo et al. [1].

References: [1] Baccolo et al. (2020) *Nat. Comm.* 12, 436. [2] Papike et al. (2005) *Geochim. Cosmochim. Ac.* 70, 1309–1321. [3] Baccolo et al. (2021) *preprint in Cryosphere Discussion*, DOI: [10.5194/tc-2021-162](https://doi.org/10.5194/tc-2021-162). [4] Squyres et al. (2004) *Science* 306, 1698–1703. [5] Farrand et al. (2009) *Icarus* 204, 478–488. [6] Cull et al. (2014) *Geology* 42, 959–962. [7] Burns (1987) *JGR* 92, E570–E574. [8] Niles & Michalski (2009) *Nat. Geosci.* 2, 215–220. [9] Head et al. (2006) *Earth Planet. Sci. Lett.* 241, 663–671. [10] Michalski & Niles (2009) *Geology* 40, 419–422. [11] Jouzel, J. and Masson-Delmotte, V. (2010) *Quat. Sci. Rev.* 29, 3683–3689. [12] Long et al. (1992) *Chem. Geol.* 96, 183–202. [13] De La Chapelle et al. (1998) *JGR* 103, 5091–5105. [14] Wolff (1996) in *Chemical exchange between the atmosphere and polar snow*, 541–560. [15] Ohno, H. et al. (2006) *GRL* 33, L08501. [16] Bohleber, P. et al. (2020) *JAAS* 35, 2204–2212. [17] Eichler, J. et al. (2019) *Front. Earth Sci.* 7, 20. [18] Mulvaney et al. (1988) *Nature* 331, 247–249. [19] Lyons et al. (2019) *JGR* 124, 633–648. [20] Hallis (2013) *Meteorit. Planet. Sci.* 48, 165–179.

SULPHATE-RICH SEDIMENTS IN DIRECT CONTACT WITH A MAGMATIC INTRUSION — POTENTIAL TO FORM A HABITABLE GEOTHERMAL BRINE ON EARTH AND MARS. B. Baharier¹, J. Semprich¹, K. Olsson-Francis¹, J. R. Crandall^{2,3}, J. Filiberto⁴, S. L. Potter-McIntyre², S. Perl⁵, S. P. Schwenzer¹, ¹AstrobiologyOU, School of Environment, Earth, and Ecosystems Sciences, The Open University, Walton Hall, Milton Keynes MK7 6AA, UK (bea.baharier@open.ac.uk) ²Southern Illinois University, School of Earth Systems and Sustainability, Department of Geology, 1259 Lincoln Drive, Carbondale, IL 62901, USA. ³Eastern Illinois University, Department of Geology & Geography, 600 Lincoln Ave., Charleston, IL 61920, USA, ⁴Lunar and Planetary Institute, USRA, 3600 Bay Area Blvd., Houston, TX 77058, USA, ⁵Jet Propulsion Laboratory, California Institute of Technology, 4800 Oak Grove Dr, Pasadena, CA, 91109, USA

Introduction: Magma intruding the crust of a terrestrial body can form geothermal brines, a potentially habitable environment, by liberating fluids bound in minerals and different elemental species within the host rock [1-3]. Sulphate rich geothermal brines (SRGB) are known to support life on Earth [4]. Moreover, potential SRGB relics have been detected on the surface of Mars, a potential habitat for sulphate-based metabolisms [5-12]. Hence, constraining the habitability potential of magma-sediment produced SRGB is essential to understand habitats on Earth and beyond. Within the scope of this research an Earth analogue to Mars is studied to understand SRGB habitability constraints.

Sulphates on Mars occur as $\text{CaSO}_4 \cdot n\text{H}_2\text{O}$ veins, cross-cutting sediments as detected by MSL Curiosity rover in Gale crater [13-14] and in Endeavour Crater by the MER rover as antitaxial veins, indicative of hydraulic fracturing [15-18]. Additionally, sulphates are found within soils [6], as well as from orbit at Jezero Crater, the landing site of the NASA Perseverance Rover, which is capped by a volcanic unit [16].

We have chosen the San Rafael Swell, Utah, US, as an analogue site to study those sulphate forming brines. We have shown that the SRS is a good candidate as a Mars analogue site based on the morphological, mineralogical and chemical similarities of the sites [19-20]. Sulphate in Jurassic sediments of the Carmel Formation also occur as $\text{CaSO}_4 \cdot n\text{H}_2\text{O}$ antitaxial veins and are intruded by a swarm of magmatic bodies [17,21], similar to some Martian settings [15-18]. Here, the interaction between the Jurassic sulphate-rich sediments and a magmatic intrusion is investigated to understand the potential interaction of brines in such scenarios and place constraints on putative habitability of analogous systems on Mars

Geologic Setting: The Carmel Formation was deposited around 166 Ma, under coastal desert conditions as the Sundance sea coastal line interchanged between inundation and regression it left behind red oxidised silt beds interbedded with sabkha sequences made of alabaster gypsum ($\text{CaSO}_4 \cdot 2\text{H}_2\text{O}$) [22].

During the Laramide orogenic event (~ 40 Ma) the gypsum remobilised and formed cross-cutting sulphate veins within the silts [23-24]. Around 4.6 Ma, a swarm of dykes intruded into the Carmel formation [21], potentially forming a sulphur-rich hydrothermal environment. Such a magma-sediment system has previously been shown to produce a habitable (and possibly inhabited) hydrothermal system in the Entrada Sandstone [19-20].

Methods: Rock samples were collected from Aweesome dyke (AD; N3834.252 W11108.351) along a traverse across the alteration flow halo – i.e., samples in direct contact with the dyke to the unaltered host rock. This was done to assess the fluid evolution along a cooling traverse away from the magmatic heat source. The samples were polished and their chemical and morphologically parameters were mapped using Scanning electron microscopy (SEM), energy-dispersive X-ray spectroscopy (EDS) and an electron microprobe (Cameca SX100). The geochemical data and morphology were used to identify an alteration reaction sequence and fluid composition was reconstructed via thermodynamics modelling using the Geochemist's Workbench®.

Results: Mineralogy: The dyke predominantly consists of diopside phenocryst with minor amounts of albite, apatite, labradorite and magnetite within the groundmass. Additionally, the dyke has around seven percent calcite crystals surrounded by $\text{CaSO}_4 \cdot n\text{H}_2\text{O}$ (H_2O amount is below the detection limit by EMPA) veinlets replacing the calcite rims (Fig. 1). Calcite surrounded by sulphate crystals suggests that there were two metasomatic alteration events: the first forming calcite pseudomorphs by intrinsic dyke fluids followed the veinlets precipitation by remobilisation of the Jurassic fluids and sulphates.

Model Results: The fluid composition was reconstructed for each event separately using the React command on Geochemist's Workbench [25]. Three titration models were run for each reaction at temperatures of 100, 200, 300 °C. The first model used a low-salinity $\text{H}_2\text{O}-\text{CO}_2$ fluid with varying amounts of CO_2 . Calcite precipitated by titrating local amphibole

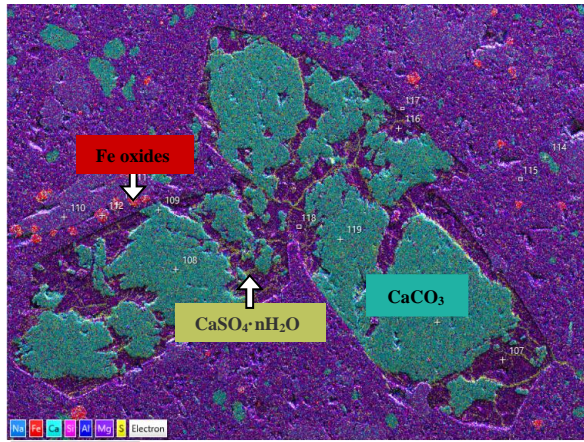


Figure 1. SEM image of Awesome dike with a central calcite pseudomorph with $\text{CaSO}_4 \cdot n\text{H}_2\text{O}$ veinlets.

composition (which is absent in AD) from a nearby magmatic intrusion [26] into a low-salinity $\text{H}_2\text{O}-\text{CO}_2$ fluid of 0.3 mol/kg of CO_2 at high water to rock ratios ($\text{W/R} = 0.003-0.01$ reacted mass). The results were the same in all three temperatures. The second model used fluid representing the Sundance Sea, containing less Mg (30 mmol/kg) and more Ca (22 mmol/kg) than modern oceans [27]. A relatively unaltered local magmatic bulk rock composition [28] was titrated into the Sundance Sea fluids with the addition of CaSO_4 (representing the veins). Anhydrite (CaSO_4) precipitated with 5 wt% CaSO_4 at high W/R ratios (0.001-0.01 reacted mass) at all temperatures.

The fluids formed in the first reaction have a pH of ~ 8.4 dominated by Al^{+3} (40.7 mg/kg), HCO_3^- (895 mg/kg), SiO_2 (119 mg/kg) and Na^+ (283 mg/kg). The second fluid is mildly acidic with a pH of ~ 5.7 with the major composition of SO_4^{-2} (6.2 g/kg), Cl^- (15.3 g/kg), Na^+ (11 g/kg) and Mg^{+2} (690 mg/kg).

Discussion and Conclusion: Calcite was assumed to be a secondary replacement mineral based on morphology. The precursor mineral to calcite is unknown, however, the morphology resembles amphibole crystal habit. Moreover, cogenetic magmatic bodies contain amphiboles [26], which are absent in these Awesome Dyke samples.

These preliminary results suggest that there was an initial influx of low-salinity $\text{H}_2\text{O}-\text{CO}_2$ fluid from the intrusion altering the amphibole phenocryst into the calcite pseudomorph, which formed an initial moderate alkaline fluid. As the dyke cooled it reached a brittle stage that allowed sediment-bound fluid and CaSO_4 to remobilise and precipitate within the dyke. The second fluid was mildly acidic sulphate rich brine with the potential of supporting S metabolic reactions. Both of these reactions have water activities (a_w) of ≥ 0.98 and were short-lived low-grade metasomatic alteration (due

to the high W/R ratio). Reactions with such high a_w values bodes well for habitable settings since nutrient cycling can occur nearly unhindered [29].

The model fluids are substantially distinct from one another, however, as they are both short-lived, they likely would have mixed and continued evolving as they encounter more of the country rock. The mixing of fluids and fluid evolution would potentially form ecological niches with different limiting factors to microbial growth such as chemistry, physiochemistry and potentially other members of the community. High salinity in itself can potentially host an abundant and diverse microbial community as in terrestrial hypersaline Lakes such as Spotted Lake, in Canada (containing 2.8 M of SO_4^{-2}) [30]. Ongoing work will narrow the temperature constraint, detail the fluid evolution path, and constrain habitability potential based on fluid-fluid mixing, reaction with the host rock, and further cooling.

References: [1] Pirajno F. (1992) *Geol. Mag.*, 130, 409- 409. [2] Van Kranendonk M. et al. (2018) *LPSC* 49 abstr. #2535 [3] Farmer J. D. (2000) *GSA Today*, 10, 1-9. [4] Shen Y. and Buick R. (2004) *Earth Sci Rev*, 64, 243–272 [5] Carr M.H. and Head J.W. (2010) *EPSL*, 294, 185-203 [6] Gellert R. et al. (2006) *JGR*, 111, E02S05 [7] Gaillard F. and Scaillet B. (2009) *EPSL*, 279, 34-43 [8] Gendrin A. et al. (2005) *Science*, 307, 1587-1591. [9] Franz, H.B. et al. (2019) *Sulfur on Mars from the Atmosphere to the Core*, in *Volatiles in the Martian Crust*, 119–183, Elsevier. [10] Ehlmann B.L. and Mustard J.F. (2012) *GRL*, 39, L11202 [11] Nixon S.L. et al. (2013) [11] Morris R.V. et al. (2008) *JGR*, 113, E12S42 [12] Bishop J.L. et al. (2009). *JGR*, 114, E00D09. [13] Grotzinger J.P. et al. (2014). *Science*, 343, 6169 [14] Vaniman D. T. et al. (2014). *Science*, 343, 6169 [15] Ehlmann B.L. and Mustard J.F. (2012) *GRL*, 39, L11202 [16] Goudge T. et al. (2015) https://marsnext.jpl.nasa.gov/workshops/2015_08/20Goudge_Jezero_Mars_2020_2nd_Workshop_for_Web.pdf [17] Young B. W. and M. A. Chan (2017), *JGR*, 122, 150–171 [18] Squyres S. W. et al. (2012), *Science*, 336, 570–576 [19] Costello L.J. et al. (2020) *Geochim.*, 80, 1256132 [(20) Crandall J.R. et al. (2018) *LPSC abstr.* #2083, 2220 [21] Delaney P.T. and Gartner A.E. (1997) *Geol. Soc. Am. Bull.*, 109, 1177-1192. [22] Richards H.G. (1958) *J Sed. Res.*, 28, 40-45 [23] Dockrill B. (2006). Ph.D thesis, TCD [24] Chen F. et al. (2016) *Chem. Geol.*, 436, 72–83 [25] Bethke C. (2008), *CUP*, 13-14. [26] Williams J. D. (1983) M.S. thesis Tempe, ASU, 123 [27] Horita J. et al. (2002) *GCA*, 66, 3733-3756 [28] Díez M. (2009) *Lithosphere*, 6, 328-336. [29] Desai, P. et al. 105132 (2020) *Planet. Space Sci.* [30] Pontefract A. (2017) *Front. Microbiol*, 8, 1819.

EXPLORATION OF BIOSIGNATURE PRESERVATION POTENTIAL OF ANCIENT AND MODERN EVAPORITES. M. A. Birmingham¹, D. Lockamy¹, R.H. Goldstein¹, and A. N. Olcott¹ & Oceans Across Space and Time Science Team ¹Department of Geology, University of Kansas (Slawson Hall, Rm 270, 1420 Naismith Dr., Lawrence, KS 66045, mbirmingham@ku.edu).

Introduction: Understanding the modes of preservation of life in evaporites is an essential component in determining habitability on other planets [1]. Previous research has shown the presence of primary microorganisms, such as prokaryotes, algae, and diatoms, preserved within gypsum crystals [1, 2], while halite has been reported to contain enigmatic “hairy blobs,” thought by some to be preserved microorganisms [3, 4] and it has even been suggested that halite can preserve viable bacterial spores [5, 6]. However, less work has been done on the chemical biosignatures preserved within evaporite samples. This study pairs petrographic examination of modern and ancient evaporite samples with biomarker extraction analysis, the better to understand the chemical record of preserved life that can be locked in these minerals.

Methods: Two different classes of evaporative minerals have been examined in this study: halite and gypsum. Samples were collected throughout the North American Midcontinent and range in age from Permian to modern. Additionally, some of the evaporites are primary, preserving an original record of deposition, and some are secondary, preserving the dissolution and reprecipitation of evaporites. The primary environments of deposition vary from transitory lakes to back reef to deep basin, while the secondary precipitants represent vein-filling environments as well as subsurface precipitation. The variable ages and environments of deposition allows for three important components to be considered: (1) how diagenesis can alter both the gypsum and organic material, (2) which environment is optimal for life preservation, (3) whether weathering inclusions play a role in preserving modern signs of life.

These samples were examined using three different microscopic techniques: transmitted light, polarized light, and excitation by UV light. The transmitted and polarized light microscopy allows an exploration of the mineral textures and cross-cutting relationships, while the fluorescent microscopy allows a determination of whether these evaporites contain auto-fluorescent material. Although there are multiple ways to induce auto-fluorescence in geological samples, given the depositional history of these samples, any autofluorescence is likely due to the presence of organic carbon compounds.

Once the microscopy is completed, samples were crushed in a clean stainless steel ball mill then solvent

extracted. These extracts were then analyzed via gas chromatography/mass spectrometry to identify any organic compounds preserved within the evaporites.

Results: Preliminary microscopic analysis of gypsum has revealed the presence of organic carbon compounds within the evaporite minerals. Features suggestive of weathering inclusions, individual crystals filled with organics, and microorganisms have all been observed as modes of life preservation. Additionally, in samples where the matrix is composed of multiple generations of gypsum, only certain crystal morphologies contain autofluorescent compounds.

Another component seen within the gypsum crystals are fluid inclusions. At this point, no organics have been observed in the inclusions. However, they could prove useful in future research to determine the chemical signatures of the original brine [7].

Organic extractions of Permian-aged Blaine Formation gypsum revealed the presence of microbial biomarkers, including hopanes, suggesting that it should be possible to correlate a record of autofluorescent organic compounds with a record of extractable biomarkers. Taken together these data indicate that evaporite minerals could contain a rich record of chemical fossils as well as physical fossils, making them an excellent prospect in the search for life on Earth and beyond.

Acknowledgments: This research is part of the collaborative Oceans Across Space and Time project, funded by NASA’s Astrobiology Program Award 80NSSC18K1301 (PI B.E. Schmidt).

References: [1] Benison K. C. and Karmanocky III F. J. (2014) *Geology*, 42, 615-618. [2] Schopf, J. W. et al. (2012) *Astrobiology*, 12, 619-633. [3] Benison K. C. et al. (2008) *Astrobiology*, 8, 807-812. [4] Benison K. C., et al. (2007), *Journal of Sedimentary Research*, 77, 366-388. [5] Vreeland R. H. et al. (2000) *Nature*, 407, 897-900. [6] Vreeland R. H. et al. (2006) *Extremophiles: Life under Extreme Conditions*, 10, 71-78. [7] Ayllón-Quevedo F. et al. (2007) *Sedimentary Geology*, 201, 212-230.

ANOMALOUS TERRAINS WEST OF OLYMPUS MONS MAY BE RESULT OF COLD SPRING FLOWS PERCOLATING THROUGH NEAR-SURFACE PERMAFROST. J. L. Bishop¹, K. D. Seelos², S. L. Murchie², and R. E. Arvidson³, ¹SETI Institute (Mountain View, CA; jbishop@seti.org), ²JHU/APL (Laurel, MD), ³Washington University (Saint Louis, MO).

Summary: Analysis of CRISM images reveals the presence of the iron hydroxide mineral goethite in anomalous terrains on the western flank of Olympus Mons reveals. These terrains are particularly intriguing because of their late Amazonian age [1]. This goethite could have resulted from surface liquid water, transported ancient sediments, or seeps from near-surface permafrost. Similar to cold spring flows in polar regions on Earth, near-surface acid brine percolating through the permafrost could explain these features.

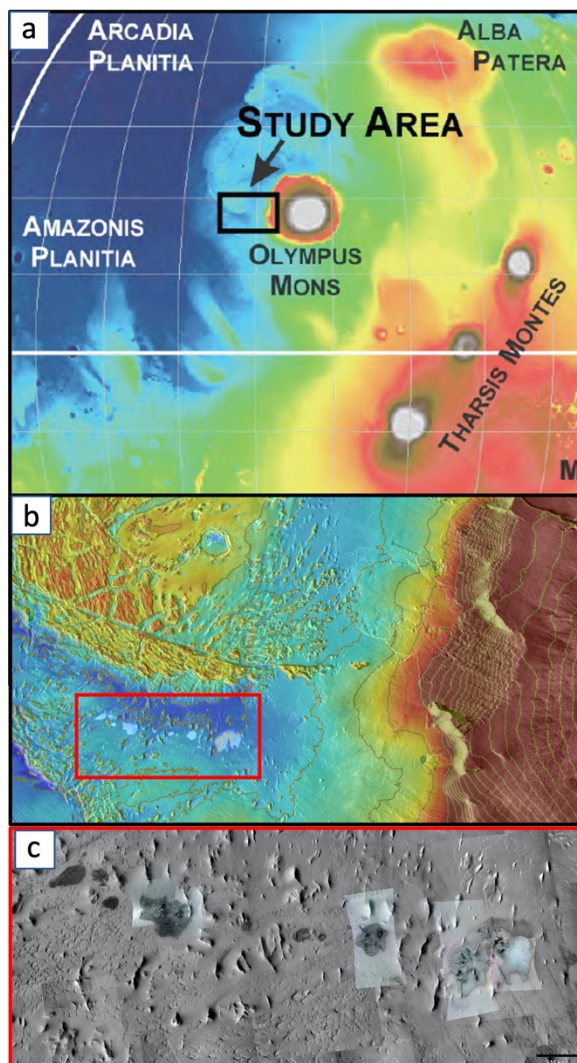


Fig. 1. a) Olympus Maculae study site over MOLA topography. b) Bright maculae shown in MOLA topography over THEMIS daytime IR [2] c) False color CRISM IR view of anomalous terrains with R=2529 nm, G=1506 nm, B=1080 nm overlain on CTX.

Study Site: The Olympus Maculae (Fig. 1) are anomalous terrains located at 217.2 °E, 17.3 °N in an Amazonian landscape shaped by lava flows, glacial deposits, and ridged aureole terrain [2]. This array of 10 semicircular features generally increase in diameter and albedo eastward along an arc. The maculae appear bright in both THEMIS daytime and nighttime images, consistent with fine-grained, coated, or weakly consolidated materials, and are typically dark in the visible. The study region is heavily influenced by aeolian processes and dust deposition that are modifying the surface [3-4].

Unusual Spectral Properties: CRISM spectra vary considerably across these outcrops (Fig. 2): the brightest terrains exhibit distinctive and unique spectral features, whereas the dark terrains are more typical of basaltic materials observed elsewhere [e.g., 5]. Here we analyzed variations in the conspicuous 3.14-3.16 μm band [2] and associations with other spectral features, in averaged spectra from multiple spots within the brightest, bright, intermediate, and dark regions of multiple maculae (Fig. 2). We compared atmospherically and photometrically corrected I/F and ratioed bright region spectra with spectral libraries and found several OH-bearing minerals with comparable features in the 3.0-3.3 μm region, but only goethite consistently matches the spectral features observed for the maculae (Fig. 3).

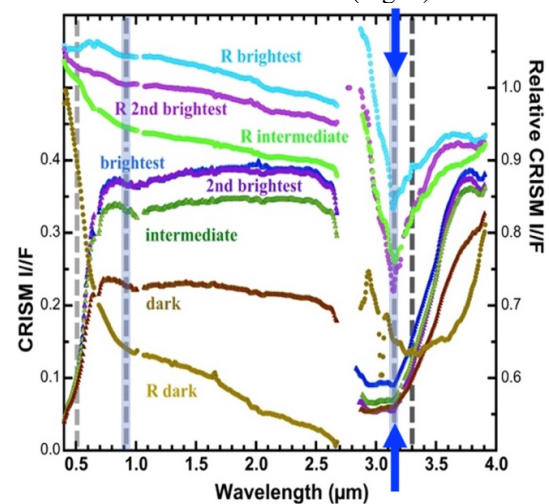


Fig. 2. CRISM corrected I/F and ratio spectra of anomalous terrains from several images. I/F spectra from the brighter regions have a V-shaped band near 3.15 μm that is accentuated in the relative (R) spectra that are ratioed to spectrally neutral, dusty regions. All spectra are averages of multiple spectra collected at regions of interest: brightest, 2nd brightest, intermediate, and dark.

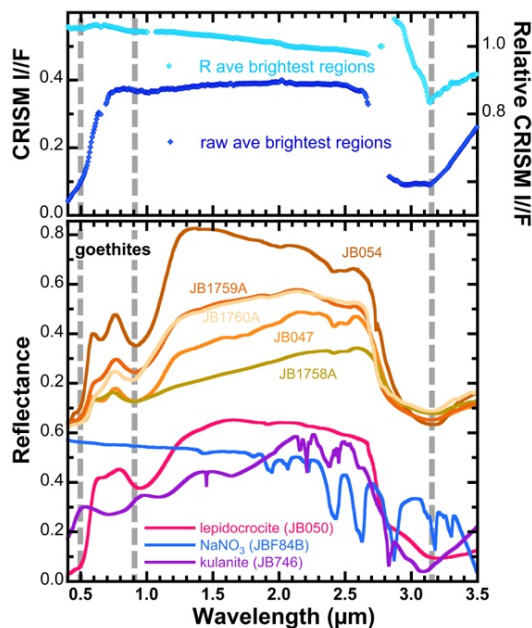


Fig. 3. CRISM spectra of just the brightest regions that exhibit the strongest $\sim 3.15\text{-}\mu\text{m}$ band compared with spectra of several goethite samples and a few other minerals having features near $3.1\text{-}3.2\ \mu\text{m}$.

Goethite Formation: Goethite typically forms on Earth from oxidation of Fe in surface waters [6-7]. Observations from lab and field studies indicate that Fe-sulfates (e.g., jarosite or schwertmannite) occur at lower pH, goethite forms at $\sim\text{pH } 4\text{-}6$, and hematite is favored in near neutral environments [6-9]. Thus, goethite could form in mildly acidic, cold brines below the surface.

Possible Formation Scenarios: The goethite-bearing bright terrains could have resulted from goethite precipitating out of liquid water on the surface in contact with atmospheric oxygen or ancient goethite could have been transported from another region, but neither of these are probable. Another option for formation of goethite in these maculae is via seeps from near-surface flows. Cold springs in the polar desert of the Canadian High Arctic transmit liquid brines at $5\text{-}6\ ^\circ\text{C}$ through permafrost to the surface where the mean annual temperature is $-15\ ^\circ\text{C}$ and lows of $-40\ ^\circ\text{C}$ are common in winter months [10]. Detailed characterization of these cold spring flows suggests that brine flows permeate the permafrost in regions where discharge and lakes are observed on the surface [11].

The current form of the maculae could be the result of surface erosion and dust deposition. At the time of goethite formation the maculae could have been one large deposit or several associated deposits along an arc. Weathering appears to be occurring from west to east and the eastern outcrops could be more recently exposed

to the surface as they are less modified. Winds could be circulating dust and surface grains, resulting in sand-blasting of the surface. The maculae towards the east exhibit the strongest goethite signatures in CRISM spectra. The easternmost maculae is also the largest, which is not yet well explained.

Subsurface brine springs were proposed to explain liquid flows permeating through permafrost and forming lakes and flow features at Axel Heiberg, Canada and Svalbard, Norway [11-12]. A similar process could have been occurring at our study site and is illustrated in Fig. 4. In this model a cold acid brine spring exists underground and forms fluid seeps upwards through the permafrost and regolith in some regions. The cold fluids could be associated with deep geothermal sources.

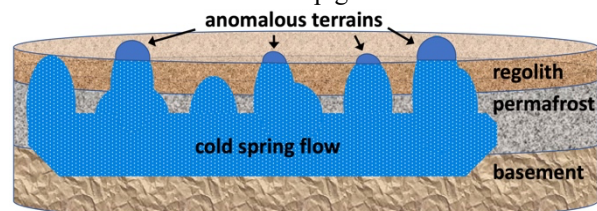


Fig. 4. Diagram of cold spring flow model [after 11,12] that could be responsible for goethite formation at the Olympus Maculae formation.

These acid brines could be circulating and penetrating through the cold ground periodically to feed precipitation of goethite at the surface. Low-temperature investigations of Mars analog salt brines have shown that frozen mineral-salt-ices liquify well below $0\ ^\circ\text{C}$ [13]. Thus, near-surface brines on Mars could be liquid below $0\ ^\circ\text{C}$ as well. Andersen et al. [11] suggest that cold springs could have formed on Mars through melting of glaciers or from relic groundwater forced upward through expansion of permafrost during freezing.

Conclusions: Goethite observed at the Olympus Maculae could have resulted from a near-surface acid brine percolating through the permafrost to produce transient cold spring flows at the surface.

Acknowledgments: Support from MDAP grant 80NSSC17K0451 is much appreciated.

References: [1] Morris E. & Tanaka K. (1994), *Geologic Maps of the Olympus Mons Region of Mars: I-2327*, USGS. [2] Seelos K. et al. (2012) *AGU Fall meeting*. [3] Detelich C. et al. (2019) *LPSC*, #1861. [4] Runyon K. et al. (2019) EPSC-DPS2019-721-1. [5] Murchie S. et al. (2009) *JGR*, 114, 10.1029/2009JE003342. [6] Schwertmann U. & Murad E. (1983) *Clays Clay Miner.*, **31**, 277-284. [7] Cornell R. & Schwertmann U. (2003) *The Iron Oxides...* Wiley. [8] Bigham J. et al. (1996) *Appl. Geochem.*, **11**, 845-849. [9] Battler M. et al. (2013) *Icarus*, **224**, 382-398. [10] Doran P. et al. (1996) *Limnol. Oceanogr.*, **41**, 839-848. [11] Andersen D. et al. (2002) *JGR*, **107**, 10.1029/2000JE001436. [12] Haldorsen S. & Heim M. (1999) *Permafrost Periglacial Proc.*, **10**, 137-149. [13] Yesilbas M. and J. Bishop (2020) *LPSC*, #2788.

CARBON PRESERVATION WITHIN CERES REGOLITH MINERALS: A NEED FOR ANALOG WORK TO AID IN SUCCESSFUL SAMPLE RETURN. M. Bose¹, L. R. Reynoso², and J. Castillo-Rogez³, ¹Arizona State University, Tempe, AZ, ²School for Engineering of Matter, Transport, & Energy, Arizona State University, Tempe, AZ, 85281, ³Jet Propulsion Laboratory, California Institute of Technology. (Maitrayee.Bose@asu.edu)

Introduction: Ceres is a differentiated dwarf planet and is the most water-rich object (~25 wt.%) in the inner solar system. NASA's Dawn spacecraft also revealed many similarities between Ceres and ocean worlds, in particular in terms of composition [1]. Ceres shows localized areas of hydrated carbonates and phyllosilicates due to pervasive aqueous alteration [2–4].

Ceres exhibits compositional links to carbonaceous chondrite-like asteroids. Carbonaceous chondrite parent bodies contain precursors of amino acids, and so likely possess conditions ideal for the formation of complex organics, in addition to the presence of mineral catalytic surfaces and an aqueous environment [5]. In fact, the large veins in the boulders of Cb-type asteroid Bennu require an amount of fluid at least 10^5 the volume of the veins, flowing through its interior [6]. Likewise, Ceres is expected to have hosted liquid throughout its history, first in the form of a global ocean. Later on, aqueous microenvironments, i.e., fluid pools with organic matter and other reactants, could be created through impacts into Ceres' icy surface. Furthermore, local surface deposits of organic matter and high concentrations of carbon possibly aliphatic compounds have been revealed by the Dawn mission [7–8]. Thus, Ceres' environment contains the three prerequisites for life: water, carbon, and a source of energy. For these reasons, Ceres is the focus of a Planetary Mission Concept Study [9] under assessment by the ongoing Planetary Science and Astrobiology Decadal Survey. That study recommends that a sample return from Ceres should be pursued in the next decade. The objective of this study is to get a better understanding of Ceres' surface material, in particular evaporites and organics, in order to inform the design of a future in situ and/or sample return mission at Ceres.

Evaporites on Ceres: Dawn found a pervasive display of salts across Ceres' surface. The vast salt deposits detected in Occator crater (e.g., Cerealia and Vinalia Faculae) likely formed by the extrusion of brine water through fractures created by the impact from depths of >35 km [4]. The bright spots are produced following the effusion of salty liquid transported to the surface by ascending subsurface fluids [10]. Vinalia Faculae contains high concentrations of minerals in a relatively thin, diffuse deposit (~2-3 m thick), most likely sourced from the deep brine reservoir [11-12]. That material is intimately mixed with dark floor material that is likely rich in organic matter. Thus, that region represents the best possible location to sample

both bright material and dark material at Vinalia Faculae.

Spectral analysis shows that Cerealia Facula contains an abundance of carbonates and ammonium salts, as well as hydrated halite toward the center and the presence of liquid water is required for the formation of these minerals [4]. Impact heating melts ice abundant in ions, such as Na^+ , Cl^- , CO_3^{2-} , NH_4^+ , and HCO_3^+ , and a deeper brine component enriched in chlorine also contribute to the faculae. The freezing/sublimation leads to the precipitation of such minerals [13]. Similar compounds have been found at Enceladus [14] and are suspected at Titan [15]. Hence, the investigation of Ceres' salt deposits is expected to provide insights into the compositional evolution of ocean world environments.

Sampling Strategies: Several concepts for the future exploration of Ceres' evaporites sample directly the Vinalia with the goal to return both evaporitic and darker rocky floor material. Because of these missions' interest is in the nature of Ceres' organics, contamination control is a serious concern. Fortunately, a future mission can leverage extensive contamination control strategies developed for previous missions, in particular OSIRIS-REx [16]. To minimize exposure to terrestrial contaminants, collectors could be configured for direct, robotic insertion into analytical instruments. One mission, labeled Calathus, proposes the use of a system to first clean the upper layer of Cerean soil in order to obtain pristine samples [17].

As the sampling of evaporites would be a first, sampling strategies need to be carefully assessed. The main risk in sample collection is sample degradation. We surmise that sodium carbonate and other precipitating salts could have undergone multiple cycles of dissolution, and recrystallization, and could accumulate organic 'fossils' within the salt crystals forming out of the brine solutions. Salts observed on Ceres' surface are highly soluble in water and if the mechanism heats up the sample to the melting point of water, then there is a risk that the salt sample can be altered or destroyed. Therefore, the sample collection mechanisms need to be cooled to below -20°C in order to preserve any organics within the samples [17]. Furthermore, organics are fractionated based on their nature and their relative densities and viscosities [18]. This needs to be considered given organics may be present in trace amounts in the evaporites, which cannot be currently detected by *in situ* techniques. Technological advancements in sample capture and

drilling have allowed for the possibility of exploration of the surfaces of small bodies Bennu and Ryugu. These advancements are highly relevant and applicable to the surface of Ceres. Thus, returning with sufficient material (with a mass of ~100 g from the top 10 cm of the surface) and at ~-20 °C would be sufficient for a complete understanding of the prevalence of organics in the evaporites, and the mechanism of their formation whether in the interior of Ceres or on the surface.

Laboratory Support to a Future Sample Return

Mission: Laboratory work on Ceres analog minerals needs to be undertaken for a safe, viable sample collection from the Cerean surface. This includes physical and mechanical properties of evaporites and carbon incorporation within them. For example, the material in Vinalia Faculae that has been recently emplaced [19] is suggested to have been sprayed or ejected from a vent [20]. Material exposed that way is expected to be in the form of loose grains, which is consistent with the grain size estimated by Raponi et al. [11]. Whether the carbon in the salt crystals and low temperatures result in changing the sticking properties of the sample need to be assessed. The NASA Concept study [9] calls for using a drill bit, derived from the DragonFly mission, to break up surface material as a backup in case the material is stronger than expected. We will discuss potential laboratory measurements that could be done to assess how the presence of carbon changes the optical properties of salts and whether small amounts of carbon-rich material can be traced in salts.

References: [1] Castillo-Rogez J. C. et. al. (2020) *Astrobiology*, 20, No. 2. [2] Schmidt E. B. et. al. (2017) *Nature Geosci.*, 10, 338-343. [3] Bu C. et. al. (2019) *Icarus*, 320, 136-149. [4] De Sanctis M. C. et. al. (2020) *Nature Astronomy*, 4, 786-793. [5] LeBleu-DeBartola A. et. al. (2019) *EPSC-DPS Joint Meeting*, 13. [6] Kaplan H. H. et. al. (2020) *Science*, 370, Issue 6517. [7] De Sanctis M. C. et. al. (2017) *Science*, 355, 719-722. [8] Prettyman T. H. et. al. (2017) *Science*, 355, 55-59. [9] Castillo-Rogez J. C. et. al. (2020) *Ceres: Exploration of Ceres Habitability*, White Paper submitted to the Planetary Science Decadal Survey 2023-2032. [10] Ruesch O. et. al. (2016) *Science*, 353, Issue 6303. [11] Raponi M. C. et. al. (2019) *Icarus*, 320, 83-96. [12] Scully J. E. C. et. al. (2020) *Nature Communications*. [13] Carrozzo F. G. et. al. (2018) *Science Advances*, 4, No. 3. [14] Postberg F. et. al. (2011) *Nature*, 474, 620-622. [15] Schoenfield A. M. et. al. (2021) *Icarus*, 366. [16] Dworkin J. P. et. al. (2018) *Space Sci. Rev.*, 214, 19. [17] Gassot O. et. al. (2021) *Acta Astronautica*, 181, 112-129. [18] Castillo-Rogez J. C. et. al. (2019) *50th Lunar and Planetary Science Conference*, No. 2132. [19] Nathues A. et. al. (2020) *Nature Astronomy*, 4, 794-801. [20] Ruesch O. et. al. (2019b) *Icarus*, 320, 79-48.

AN OBJECTIVE DEFINITION OF HABITABLE SPACE AND APPLICATION TO MODELING WATER ACTIVITY FROM GEOCHEMISTRY. J. S. Bowman^{1*}, A. Bastuba^{1*}, S. Som², T. Plattner³, A. Pontefract⁴, Doran, P.⁵, Buffo, J.⁶, Lawrence, J.⁷, Schmidt, B.⁸, The Oceans Across Space and Time Team. ¹Scripps Institution of Oceanography, UC San Diego (9500 Gilman Dr., La Jolla, CA 92093-0218, jsbowman@ucsd.edu), ²Scripps Institution of Oceanography, UC San Diego, ³Georgia Institute of Technology, ⁴Georgetown University, ⁵Louisiana State University, ⁶Dartmouth University, ⁷Georgia Institute of Technology, ⁸Georgia Institute of Technology. *Co-first authors.

Introduction: Brine composition and concentration is a key determinant of habitability in aqueous environments. These features interact with each other [1] and with temperature and pH in complex ways [2], with assumed non-linear effects on the potential biomass or biological activity present in a given environment. To facilitate the objective mapping of potential habitats across landscapes we designed a classification system for habitable space based on a self-organizing map (SOM) [3].

Methods: Artificial datasets for temperature, pH, Na⁺, Cl⁻, Mg²⁺, SO₄²⁻ were developed for biologically meaningful ranges. These data were scaled, then used for unsupervised training of the SOM on a toroidal grid space consisting of 40,000 map units.

Each map unit in a SOM is described by a vector of values selected from the training data. During training, the vectors associated with each map unit and its neighbors are iteratively updated as new data is presented to the SOM. The trained SOM thus reflects the structure of the underlying data despite consisting of far fewer map units than there are vectors in the training data.

We applied several clustering algorithms to identify regions of similar habitability within the map space. Although clusters are somewhat arbitrary for continuous data, defining regions produces a taxonomy that can be used to provide context for biological or other observed phenomena. Hierarchical clustering with 16 clusters provided the most coherent partitioning of the SOM. Each of the clusters reflects a unique range of values for the considered parameters, and can be used to describe real-world data classified into the SOM. This operation is computationally lightweight, requiring only the identification of the map unit with the minimum distance to the real-world data.

Application to Modeling Water Activity (a_w): A key feature of SOMs is that they provide a means to associate values that are known for the training data with new data for which the values are unknown. To illustrate this feature, we calculated a_w for the training data using the EQ3 model (Fig. 1b). We compared the predicted values with reported values for several concentrator and crystallizer ponds at the South Bay

Salt Works, a solar-salt harvesting facility in San Diego, CA, USA [4], and three deep hypersaline anoxic basins (DHABs) in the Mediterranean Sea ($R^2 = 0.937$, $n = 12$) (Fig. 2). Although the model tended to overestimate a_w , it nonetheless captured the general trends suggesting that with further development a_w can be modeled effectively from a limited number of physico-chemical parameters. Future work will focus on a more complete evaluation of model efficacy using laboratory brines and from diverse natural environments.

Acknowledgments: This work was supported by the Oceans Across Space and Time project (NASA 80NSSC18K1301) to B.S.

References:

- [1] Stevens A.H., Cockell C.S. (2020) *Front. Microbiol.*, 11. [2] Neill W.K.O., Blain D., Hallsworth J.E., Benison K.C. (2021) *Astrobiology*, 21:1–12. [3] Kohonen T. (2013) *Neural Networks*, 37, 52–65. [4] Klempay B., Arandia N., Dekas A., Bartlett D., Carr C., Doran P., et al. (2021) *Environ. Microbiol.*, 23:7, 3825-3839.

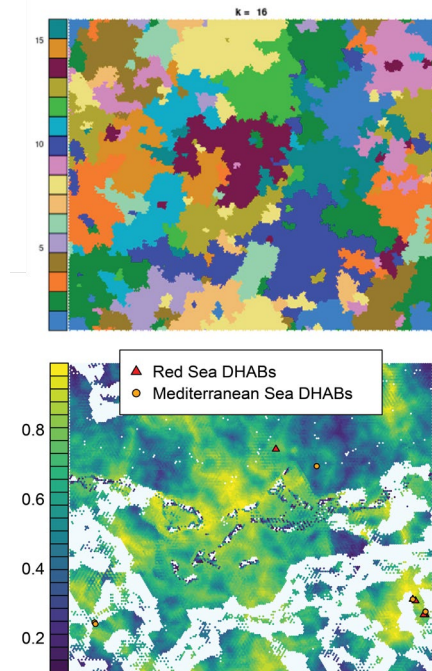


Fig. 1. A self-organizing map (SOM) was created from a synthetic dataset of temperature, pH, Na^+ , Cl^- , Mg^{2+} , SO_4^{2-} . Top) The final values associated with each map unit were clustered using hierarchical clustering. Bottom) Water activity was calculated using the EQ3 model for each map unit. Grey map units indicate input values that were outside of the bounds of the EQ3 model.

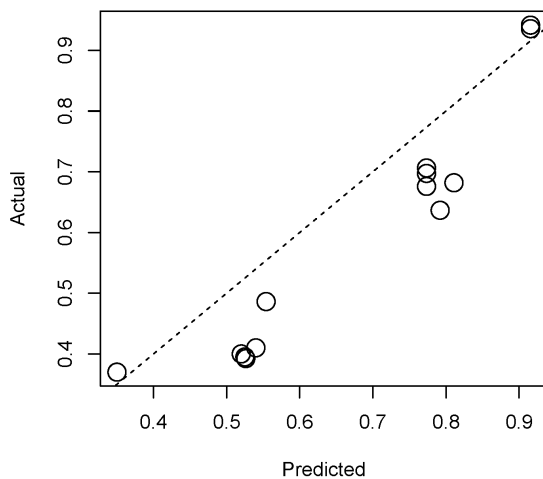


Fig. 2. The SOM was used to predict water activity for data from solar salterns and deep sea hypersaline anoxic basins. There was generally good agreement between predictions and measured values ($R^2 = 0.937$) though some brines deviated from model predictions.

DEVELOPMENT AND TESTING OF A MINIATURE ROBOTIC ELECTRODIALYSIS (MR ED) SYSTEM TO REMOVE SALTS FOR OCEAN WORLD SAMPLING. F. E. Bryson¹, E. D. Ingall¹, A. M. Hanna¹, M. Cardelino¹, T. Plattner¹, M. R. Meister¹, J. D. Lawrence¹, A. Mullen¹, D. Dichek¹ and B. E. Schmidt^{1,2}, ¹Georgia Institute of Technology (fbryson7@gatech.edu), ²Cornell University

Introduction: Jupiter’s moon Europa is believed to have a subsurface ocean beneath its ice shell, making it a compelling astrobiological target. In support of the search for life, the Vertical Entry Robot for Navigating Europa (VERNE) project recommended a system of instruments for characterization and life detection with sample processing for high salinity environments [1] [2]. A primary challenge this system would face on Europa is the unknown range of sample composition and salinity in the ocean, as well as the potential for encountering highly saline brines within the ice shell. Although these brines are biologically interesting as they could preferentially preserve organics [3] [4], the salts can clog small fluidic systems and alter and inhibit measurement capabilities in instruments, e.g. mass spectrometers and DNA or other biomolecule sequencers, requiring samples to be desalted before analysis [2]. Therefore, a key technology development for liquid sampling on ocean worlds is a robust system to desalt highly saline fluids.

Electrodialysis (ED) systems remove salt from aqueous solutions by applying an electric potential across a series of ion-selective membranes that separate the sample solution from another solution that receives ionic species, called the concentrate. The electric potential causes ions to move from the sample into the concentrate, which creates a low salinity sample. ED is proven to retain a significant percentage of dissolved organic carbon (DOC) [5], and thus it is a promising technology to desalt samples to permit analysis of

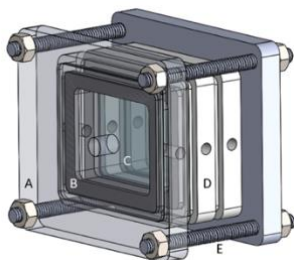


Figure 2 MR ED apparatus: Endcaps (A) seal the outer chambers, between which gasket material (B) seals the chambers and the ion-exchange membranes (C) between the three Delrin chambers (D). Nylon threaded rods and nuts (E) are used to connect the endcaps.

biomolecules on ocean worlds. However, current electro dialysis systems used for DOC recovery are too large for deployment on instruments sent to ocean worlds. Here we present results from the testing of a Miniature Robotic Electro dialysis (MR ED) system that is more suitable for deployment on spacecraft.

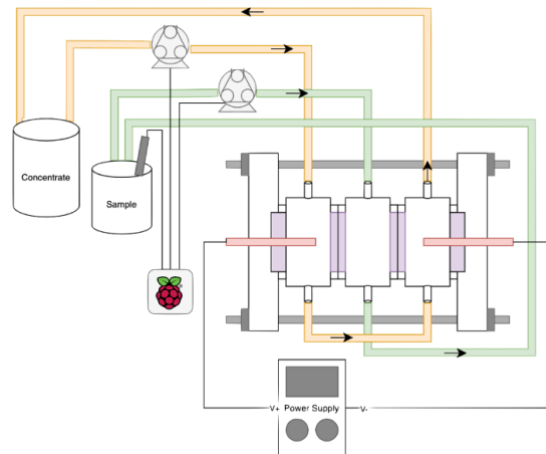


Figure 1 Schematic of the experimental setup: Raw sample is pumped through the central sample chamber, across which an electric potential supplied by the anode and cathode encourages ion transport across membranes. The sample is constantly evaluated for salt concentration via conductivity.

System Design: The MR ED system uses one pair of ion selective membranes with continuous specific conductivity monitoring to achieve a self-contained, autonomous system for desalting samples (Figure 2). The system currently supports as little as 50 mL of sample in circulation, which allows for additional downstream processing and analysis and requires less sample be collected than larger ED systems.

This sample is circulated through the center sample chamber as the electric potential is applied across two custom platinized titanium electrodes, while a separate solution is circulated through the outer chambers separated by the ion-selective membranes (1). To minimize system size and the need for electrode rinse solutions, the electrodes reside within the concentrate chambers. A solution of Na₃PO₄ is used for the concentrate in most desalting experiments to avoid unwanted reactions with the electrodes, although tests that use a separate volume of the initial sample solution for the concentrate have been completed in order to mimic *in situ* operations. An external power source that applies up to 30 V at up to 1.5 A is used to supply the electric potential; a low power comparative to other ED systems is useful to prove desalting for ocean world operations where power is limited.

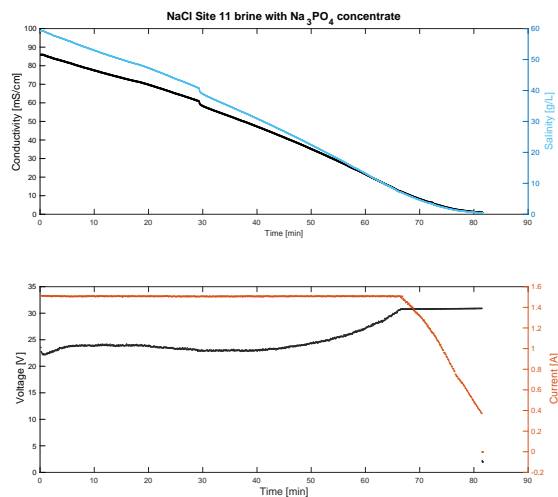


Figure 3 Conductivity, salinity and power results from NaCl brine desalting test: A NaCl brine taken from South Bay Saltworks in San Diego, CA was desalted to 7.7 mM salinity within 82 minutes, using a Na₃PO₄ concentrate. Salinity is calculated from the specific conductivity, which is continuously measured throughout the test using conductivity and temperature sensors.

Results: Initial results show an average 70% DOC recovery in tests of laboratory NaCl solutions with added glucose, as well as in field samples taken from the Skidaway River (Savannah, GA), and NaCl brines from South Bay Saltworks (San Diego, CA). Furthermore, tests with field samples from the Skidaway River that mimic mission operations, in which a separate volume of the sample solution is used for the concentrate (at the same initial ionic strengths), have additionally achieved successful desalting and DOC recovery.

Future Work: We intend to further develop the benchtop system into an autonomous miniature ED system self-contained with its power and sensing systems. This contained, portable unit would allow for allows for easy transport to field testing locations and allow in situ processing on Earth.

Additionally, more work is needed to better characterize MR ED's effectiveness on brines, as well as on salts other than NaCl that might exist on Europa, such as MgCl₂.

Acknowledgements: This work is supported by the VERNE collaborative research project primarily completed at Georgia Tech with collaborators from other institutions such as UW-APL, UCSD, WHOI etc. This work has been supported by NASA Grant No. 80NSSC19K0615, PI B. E. Schmidt.

References: [1] B. E. Schmidt *et al.* (2021) [Manuscript submitted for publication]. [2] J. Lawrence and A.D. Mullen *et al.* (2021) [Manuscript

submitted for publication], 2021. [3] L. A. Fisher *et al.* (2021) *Environmental Microbiology*, 23(7), 3360–3369. [4] G. Merlino, A. Barozzi, G. Michoud, D. K. Ngugi, and D. Daffonchio (2018) *FEMS Microbiology Ecology*, 94(7). [5] L. R. Chambers *et al.* (2016) *Aquat Geochem*, 22(5), 555–572.

BRITISH COLUMBIA'S UNASSUMING PLANETARY LABORATORY: HOW A HANDFUL OF FROZEN SALINE LAKES CAN HELP US UNDERSTAND BRINES ACROSS THE SOLAR SYSTEM. J. J. Buffo¹, E. K. Brown², A. Pontefract³, B. E. Schmidt⁴, B. Klempay⁵, J. Lawrence², J. Bowman⁵, M. Grantham², J. B. Glass², T. Plattner², C. Chivers², P. Doran⁶, C. R. Meyer¹, M. E. Barklage⁷, and B. Fluegel⁸, ¹Dartmouth College (jacob.j.buffo@dartmouth.edu), ²Georgia Institute of Technology, ³Georgetown University, ⁴Cornell University, ⁵Scripps Institution of Oceanography, ⁶Louisiana State University, ⁷Illinois State Geological Survey, ⁸Northwestern University.

Introduction: Mounting observational and theoretical evidence supports the ubiquity of brines across the solar system (e.g., ice-ocean worlds, Mars). This fact, combined with their indelible link to astrobiology, has led to the prioritization of improving our understanding of brine-rich systems in the lens of planetary exploration, planetary protection, resource identification, and the search for life beyond Earth.

A fundamental challenge in expanding our knowledge of solar system brines is the fact that all the proposed brine-bearing worlds (less Earth) reside beyond the frost line. As such, stable/metastable brines are buried beneath/within icy shells, caps, or regolith, complicating their direct measurement unless active plume or effusive processes are occurring, and placing any near surface brines in a perpetual battle against impending solidification. Until direct *in situ* missions (e.g., penetrators [1]) become consistently tenable, we will continue to rely upon our ability to relate remote sensing measurements of icy world surfaces to their subterranean brine properties and processes [2, 3].

While this has been our principal strategy thus far (e.g., predictions of interior ocean compositions from surface ice or plume particle chemistry), uncertainties in this inversion method, namely quantitatively linking ice and brine properties, continue to leave the compositions and concentrations of planetary brines significantly underconstrained [2, 3]. Compounding these challenges is the putative chemical diversity of planetary brines across the solar system (e.g., [4-6]). Concomitantly, given the likely importance of brines in governing both the geophysics and habitability of icy worlds, constraining the dynamics, longevity, habitability, and, crucially, the *observable signatures* of compositionally diverse and potentially habitable ice-brine environments are foundational goals of the planetary science community, as evidenced by the science priorities of upcoming spacecraft missions (e.g., Europa Clipper, JUICE, Dragonfly) [2, 3, 7].

Two primary strategies for improving our understanding of planetary ice-brine systems are the use of polar terrestrial analogs (e.g., sea ice, Antarctic Dry Valley lakes) and predictive theoretical models (e.g., [2, 3]). While terrestrial analog ice-brine systems provide exceptional compositional endmembers for understanding the relationship between ice

characteristics and parent brine properties, they represent a small subset of potential planetary brine chemistries. Furthermore, the successful extension of terrestrial analog dynamics to the spatiotemporal scales and chemical diversity of planetary environments relies on the accuracy and applicability of numerical models – which in turn require benchmark data, such as measurements of analog environments, to validate.

Reactive transport models (which track the thermochemistry and multiphase processes of multicomponent systems) have been shown to succinctly capture the NaCl-dominated dynamics and evolution of our most well-studied terrestrial analog ice-brine system – sea ice – but validation against more compositionally diverse ice-brine systems remains lacking. This is in part due to a limited amount of data regarding chemically diverse naturally occurring ice-brine analogs [2, 3]. Expanding our existing catalog of ice-brine analog systems will provide an improved understanding of their dynamics and habitability and produce a test data set to validate reactive transport models designed to simulate planetary ice-brine environments, bolstering confidence in their application to planetary science and mission relevant problems.

Here we introduce the unique planetary analog lakes of south central British Columbia, describe our biogeochemical survey of these lakes and the novel data set we've accrued, discuss a two-dimensional reactive transport model we've adapted to accommodate diverse planetary ice-brine environments, validate the model against empirical lake data, and discuss the implications for the future of forecasting planetary brine properties and dynamics in the lens of planetary exploration and planetary protection.

Field Site/Work: The Cariboo Plateau of south-central British Columbia houses an array of compositionally diverse hypersaline lakes. Many of the chemistries represented in these systems are unique to the area (e.g., MgSO₄ and NaCO₃ dominated ice-brine systems) and may more closely represent the compositions of oceans and brines of icy worlds across the solar system than does our NaCl dominated ocean or the brines of other terrestrial analog ice-brine environments (e.g., Dry Valley lakes) [8].

The lakes form perennial ice covers, offering a unique opportunity to investigate the thermal and

physicochemical properties of ices derived from unique planetary relevant brines as well as the characteristics of their parent fluid, their formation history, and thus the quantitative relation between ice observational properties and their underlying parent brines. We will present thermal, physical, and biogeochemical profiles of these unique ices (e.g., Figure 1) and discuss their relevance to the identification and characterization of planetary brines.

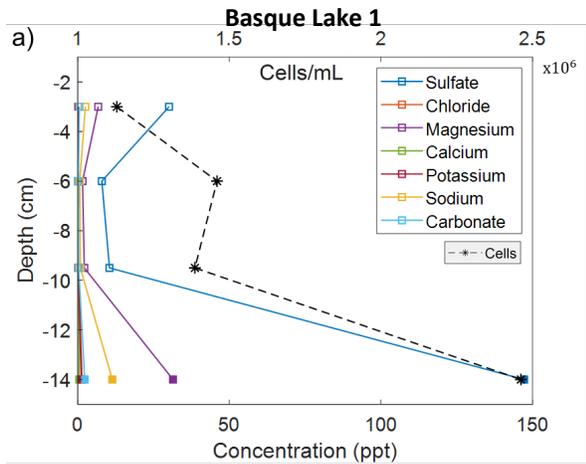


Figure 1 – Biogeochemical profiles of unique ice-brine systems. Ionic composition and cell density of the ice and brine (solid squares) in a hypersaline lake system [8].

2D Model of Planetary Ice-Brine Systems: To extend the knowledge garnered from these unique analog environments to planetary systems we have modified the two-dimensional multiphase reactive transport model SOFTBALL [9] to accommodate diverse brine chemistries and planetary environmental conditions [3]. The model tracks several habitability relevant parameters including water content and ice/brine compositions (e.g., Figure 2). Here we validate the numerical model against the physicochemical profiles of the hypersaline lakes, bolstering confidence in its application to a diverse array of planetary chemistries/environments, and discuss the significant implications the model’s use will have in our ability to forecast the dynamics, evolution, and properties of ice-brine systems throughout the solar system.

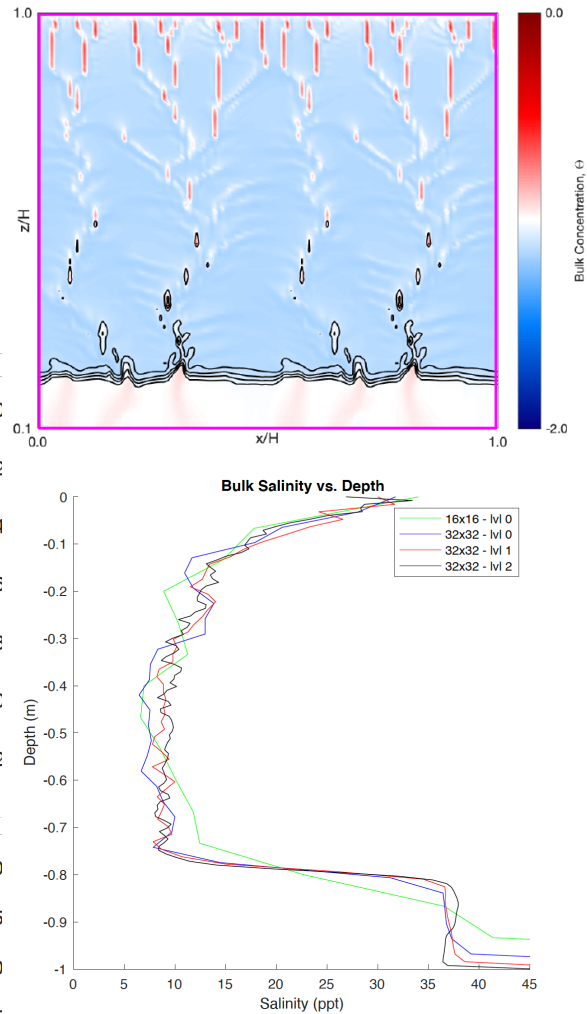


Figure 2 – **Top)** Two-dimensional profile of nondimensional bulk concentration (salinity) in sea ice simulated using the multiphase reactive transport model SOFTBALL – porosity contours in black [3]. **Bottom)** Horizontally averaged salinity profile of the 2D profile using different resolutions. Note the similarity of the ‘c-shaped’ profile produced by the model to that of the ionic concentration profiles of Figure 1.

References: [1] Bryson F. E. et al. (2020) *ASCENCD 2020*. [2] Buffo J. et al. (2020) *JGR: Planets*. [3] Buffo J. J. et al. (2021) *JGR: Planets*. [4] Postberg F. et al. (2009) 459, 1098-101. [5] Trumbo S. K. et al. (2019) *Sci. Adv.* 5, 7123. [6] Zolotov M.Y. and Shock E. L. (2001) *JGR: Planets*. 106, 32815-32827. [7] Vance S. D. et al. (2020) *JGR: Planets*. 6736. [8] Buffo J. et al. (in review) *Astrobiology*. [9] Parkinson J. G. R. et al. (2020) *JCP: X*. 5, 100043.

ROLE OF NON-WATER ICES IN DRIVING SALINITY AND ELECTRICAL CONDUCTIVITY IN OCEAN WORLDS. J. C. Castillo-Rogez¹, M. Melwani Daswani¹, C. R. Glein², S. D. Vance¹, C. Cochrane¹, ¹Jet Propulsion Laboratory, California Institute of Technology, Pasadena, CA, ²Southwest Research Institute, San Antonio, TX. (Point of Contact: Julie.C.Castillo@jpl.nasa.gov)

Introduction: Forward modeling of the electrical conductivity of icy moon oceans has assumed that chlorides, sulfates, and other ions released from rock leaching are the main solutes and generators of electrical conductivity (EC). We show that accreted volatiles, such as CO₂, and NH₃, can also contribute a significant fraction of solutes for bodies whose volatile content was in part supplied from cometary materials. These volatiles make a major contribution to the EC of aqueous solutions in icy bodies, which is an important consideration for future observations making use of electromagnetic sounding in searching for deep oceans.

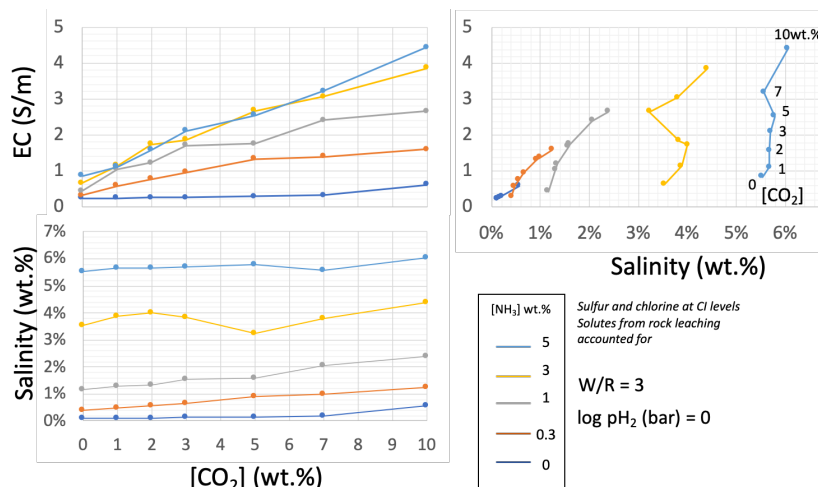
Motivations: In recent formation models of giant planet systems, icy moons could acquire part of their materials from pebbles scattered from regions farther in the outer solar system. For the Galilean satellites, this implies a greater content in cometary volatiles than assumed in previous models. Recent evolution models also show that early oceans could be enriched in CO₂ and NH₃ following the breakdown of carbonates and organic compounds as a result of the thermal metamorphism of accreted carbonaceous chondritic materials. Carbonates have been found at Enceladus and Ceres; the latter also displays evidence for ammonium in multiple forms on its surface. Lastly, this study is responsive to the ongoing interest in future missions to the Galilean moons, Enceladus, Titan, Triton and the moons of Uranus, Pluto's system, and Ceres, many of which would include magnetometers.

Summary of Approach: We assess the fate of accreted volatiles using the Geochemist's Workbench

(GWB) [1] at 1 atm. GWB computes EC using the approach of [2] which is suitable for ionic strengths up to 1 mol/kg over the range 0°C–95 °C, pH (1–10), and conductivity (30–70,000 10⁻⁶ S cm⁻¹). The EC estimates presented below assume that the hydrosphere is all liquid, i.e., not accounting for what occurs to solute concentrations in liquids upon freezing of an ice shell.

Key Results: If ocean salinity is a sole function of fluid-rock reaction under equilibrium conditions, then the salinity is on the order of 0.1–0.2wt. %, yielding an EC ~0.2 S/m. If CO₂ (and no NH₃) is added to the solution in small amount (<2 wt.%), it is consumed to form dolomite and magnesite with little contribution to salinity (less than [Na⁺] and [Cl⁻]). The fraction of bi/carbonate ions in solution increases with increasing [NH₃] (Figure 1). For [CO₂]=5 wt.% and [NH₃] \sim 1% (as lower bounds on cometary abundances), the salinity is ~2wt.% and EC~2 S/m. Increasing temperature, pressure, and concentration following freezing of the ocean can increase the EC above 10 S/m.

Summary: Oceans expected in icy moons and dwarf planets, including Europa, some of the Uranian satellites, and Neptune's satellite Triton, could have high electrical conductivities due to abundant non-water ices, even if the extent of rock leaching during differentiation was limited and chlorine and sulfur abundances were at low, CI carbonaceous chondritic levels. The effects of non-H₂O ices require thorough quantification to aid the planning and future interpretation of magnetic induction experiments at candidate ocean worlds.



References: [1] Bethke, C.M. (2007) *Geochemical and Biogeochemical Reaction Modeling*, 2nd ed., CUP. [2] McCleskey, R. B., et al. (2012) *GCA* 77, 369-382.

Acknowledgments: Part of this research was carried out at the Jet Propulsion Laboratory, California Institute of Technology, under a contract with the National Aeronautics and Space Administration.

← Figure 1: Salinity and EC as a function of accreted CO₂ and NH₃ abundances (wt.% of volatile phase), calculated at 0 °C, 1 atm, W/R = 3, and log pH₂ (bar) = 0.

IDENTIFICATION OF FLUIDS ACCOMPANYING BIO-SIGNATURE FORMATION IN MARTIAN ANALOGUE EXPERIMENTS. S. Cogliati¹, E. Curtis-Harper¹, S. P. Schwenzer¹, V. K. Pearson¹ and K. Olsson-Francis¹.
¹AstrobiologyOU, EEES, The Open University, Milton Keynes MK7 6AA, UK. simone.cogliati@open.ac.uk

Introduction: Geological, geochemical and geomorphological evidence collected by orbiting spacecrafts and rovers (e.g. Curiosity, Opportunity) on Mars suggests the presence of impact-generated hydrothermal systems and fluvio-lacustrine environments that may have been habitable in the Noachian - early Hesperian [1-2]. However, finding evidence that life has existed on Mars is dependent on the identification of bio-signatures that testify biological processes have occurred in martian aqueous environments. Owing to the detrimental effect that the conditions at the surface of Mars have on organic molecules [3, 4], inorganic biosignatures, such as secondary alteration minerals associated with microbial activity, may be more appropriate for assessing whether life existed on early Mars. Clay minerals, carbonates and sulfates found at Gale and Jezero craters are considered to have formed in extinct aqueous systems following basalt weathering and / or brine evaporation [5, 6]. At present, it is not possible to determine unambiguously whether the formation of these alteration minerals is the result of biotic weathering or solely related to the interaction of martian brines with rocks of basaltic composition. Laboratory experiments and field studies can only study basalt weathering under abiotic and biotic conditions over short timeframes (days to months). By contrast, thermochemical modelling can be used to study alteration processes that can occur over geological time scales, owing to its capability to predict secondary mineral assemblages and variations in fluid chemistries through the assessment of reaction pathways during water-rock interaction [7-9]. By combining laboratory experiments and thermochemical modelling it is possible to investigate alteration mineral and brine chemistries that may form biotically and abiotically during basalt weathering over a range of different time scales [10].

Experimental and modeling approach: We investigated the microbial weathering of a martian analogue basalt using a combination of laboratory-based experiments and thermochemical modelling, in order to characterize changes in fluid chemistry and resultant mineral formation. In doing so, we aimed to identify, unambiguously, inorganic bio-signatures formed by biotic weathering processes that may be used to assess the presence of life on Mars.

To experimentally study basalt dissolution under abiotic conditions, a martian regolith analogue was

combined with a brine that has previously been shown to support bacterial growth [11]. The regolith analogue has a chemistry similar to the composition of the Rocknest basalts [12] and was composed of terrestrial basalt supplemented with aegirine, a pyroxene, to ensure that the iron concentration was similar to that measured on Mars [13].

Biotic weathering experiments were performed using an anaerobic community. This community consisted of chemolithotrophic, heterotrophic and fermentative microorganisms from an anoxic inter-tidal zone (the River Dee, UK (53°21'15,40N, 3°10'24,95 W) [11]). For both biotic and abiotic dissolution experiments, the regolith was placed in an acid-washed Wheaton bottle and autoclaved at 121 °C for 15 min, then 100 mL of brine (see composition in Table 1) was added and the pH adjusted up to 7.0 with filtered, sterilized 10 mM NaOH. The experiments were conducted with an experimental water/rock ratio of 100/33. Abiotic and biotic experiments were performed for 28 days, in parallel. The variations in pH and brine composition were measured using an Orion 3-Star Thermo Scientific bench top meter and an Inductively Coupled Plasma Atomic Emission Spectrometer (ICP-AES), respectively.

Ion	Concentration (Moles)
H ⁺	2.36E-01
O ₂	4.80E-01
Cl ⁻	6.52E-01
S ²⁻	8.76E-03
C	2.30E-01
Na ⁺	9.10E-01
N ⁺	1.87E-02

Thermochemical modelling was performed using the code CHIM-XPT [14, 15], which has already been used to study water-rock interactions in martian environments [e.g., 5, 9]. The input data for the models included the Mars analogue regolith composition and the chemical composition of the brine. Rock dissolution was modelled from an initial water//rock ratio of 10⁶ to a final water/rock ratio of 1 in order to simulate different environmental conditions and degrees of interaction between rock and water. The modeling was carried out at 2 bar and 14 °C, which was used to simulate the pressure and temperature of the growth experiment. Three models were conducted: in the first model the pH was treated as a free parameter to simulate rock

weathering in an abiotic environment; in the other two models the pH was set at 6.0 and 6.5 to reproduce the pH conditions observed during microbial weathering.

Results: The results in Figure 1 A and B show the variations of the brine chemistry over time during the biotic and abiotic laboratory experiments. It is evident that the action of the microbes favors the release of some elements into the aqueous environment. The differences in the fluid compositions are even more pronounced in the thermochemical models where the analogue dissolution is simulated for a longer period of time (Figure 2A-B), indicating a long-term biotic influence on fluid chemistry.

Conclusion: These results highlight the differences in brine chemistries that may have evolved in abiotic and biotic martian aqueous environments and reinforce the necessity to combine laboratory experiments with thermochemical modelling when investigating bio-signatures.

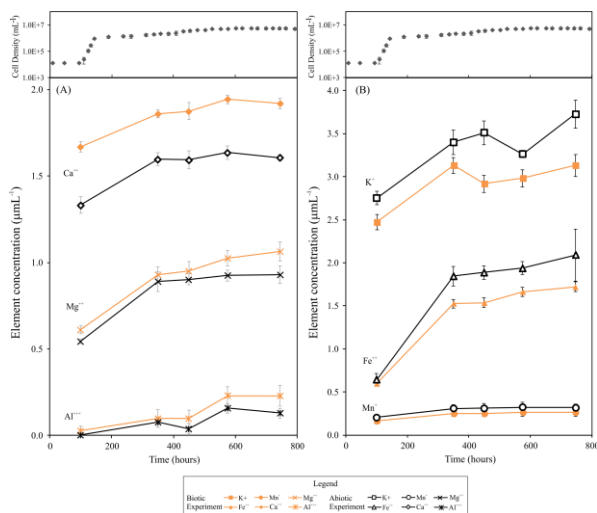


Figure 1. Variation over time of some key elements within the brine during abiotic and biotic weathering experiments. In (A) variations of Mg, Al and Ca; in (B) variation of K, Fe and Mn. Open symbols denote data from the abiotic experiment whereas full symbols represent data from the biotic experiment. The values reported are the means of five independent experiments, and the standard deviation of the mean associated with these measurements is shown. Mean values of cell density measured for each time period is reported in the graphs above each figure.

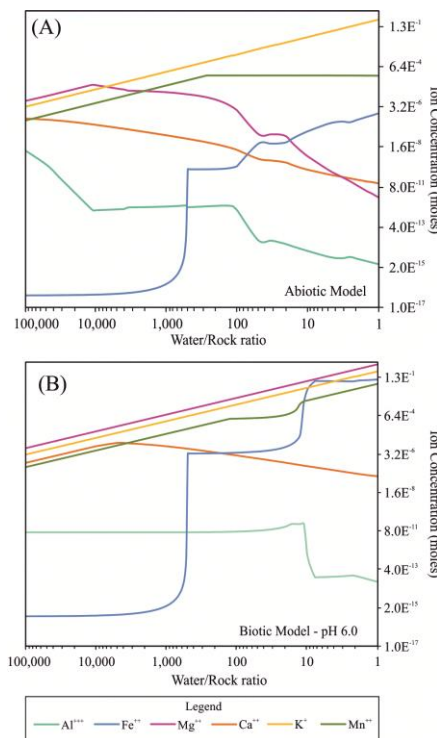


Figure 2. Variation of some key elements in abiotic model (A) where the pH is a free parameter and in the biotic model (B) where the pH is set at 6.0 to simulate an environment where the pH is controlled by the action of microbes.

Acknowledgments: We acknowledge funding from STFC Doctoral Training Grant 2012 (UKRI grant reference ST/K502212/1) and from Research England Expanding Excellence in England (E3) fund (grant code 124.18).

References: [1] Abramov O. and Kring, D. A. (2005) *JGR*, 110, E12SE09. [2] Grotzinger J. P. et al. (2014) *Science*, 343, 1242777-13. [3] Dartnell L. R. et al. (2007) *GRL*, 34, 4–9. [4] Dartnell L. R. et al. (2011) *Astrobiology*, 11, 997-1016. [5] Bridges J. C. et al. (2015) *JGR*, 120, 1–19. [6] Poulet F. et al. (2005) *Nature*, 438, 623–627. [7] Filiberto J. and Schwenzer S. (2013) *Meteor. Planet. Sci.*, 48, 1937–1957. [8] Kühn M. (2004) *Lecture Notes in Earth Sciences* (Berlin:Springer). [9] Bridges, J. C. and Schwenzer S. P. (2012) *EPSL*, 359–360, 117–123. [10] Olsson-Francis K. et al. (2017) *Front. Microbiol.*, 8, 1668. [11] Curtis-Harper, E. et al. (2018) *Microorganisms*, 6, 1–19. [12] Blake D.F. et al. (2013) *Science*, 341, 1–8. [13] Ramkissoon N. K. et al. (2019) *Planet. Space Sci.*, 179, 1–18. [14] Reed M. H. et al. (2010) *Chem. Inf. Model.* 53, 1689–1699. [15] Reed M. H. and Spycher N. F. (2006) in *Aqueous-Mineral-Gas Systems and Minplot Guide*. Eugene, OR: University of Oregon.

Modern brines at Ceres: hints from VIR imaging spectrometer on Dawn mission, M.C. De Sanctis¹, E. Ammannito², M. Ciarniello¹, A. Raponi¹, F.G. Carrozzo¹, A. Frigeri¹, M. Formisano¹, B. Rousseau¹, M. Ferrari¹, S. De Angelis¹, S. Fonte¹, M. Giardino¹, B.L. Ehlmann^{3,4}, S. Marchi^{1,5}, C.A. Raymond^{3,4}, C.T. Russell⁶

¹Istituto di Astrofisica e Planetologia Spaziali, INAF, Via del Fosso del Cavaliere 100, 00133 Roma, Italy; ²Agenzia Spaziale Italiana, ASI, via del Politecnico, 00133 Roma, Italy; ³Jet Propulsion Laboratory, California Institute of Technology, Pasadena, CA, USA; ⁴Division of Geological and Planetary Sciences, California Institute of Technology, Pasadena, CA, USA; ⁵SWRI, 1050 Walnut Street, Boulder, CO 80302, USA; ⁶Earth Planetary and Space Sciences, University of California, Los Angeles, CA, USA.

Introduction: Ceres, the largest body in the main belt and the closest dwarf planet to the Sun has been the subject of extensive observation by the Dawn mission [1]. Since telescopic observation was known that Ceres is constituted by a large amount of water. The Dawn data show that Ceres overall density is 2.16 g/cm³ but the crust is composed of an intimate mixture of rock and ice, with a much lower density of ~1.25 g/cm³, implying a great quantity of water in the crust ([1,2]).

The surface is cratered but very large craters are absent, indicating efficient relaxation [3]. Ceres has mountains, like the geologically recent Ahuna Mons, that are likely of cryovolcanic origin [4]. The crater distribution [3] and morphological features [5] support the inference that Ceres' crust is a mixture of ice, rock and salt hydrates that is periodically mobilized to produce extrusive features such as Ahuna Mons, as well as flow features and bright deposits.

After Dawn mission results, it became clear that Ceres is an ocean-world, but the physical status of the water (ice vs liquid) has been extensively debated [6]. Here we will review the indicators for the presence of modern brines inferred primarily by the VIR spectrometer on board of Dawn.

VIR/Dawn Discoveries: VIR spectrometer [7] extensively observed the surface of Ceres. The surface mineralogy indicates that Ceres experienced extensive water-related processes and chemical differentiation. The surface is mainly composed of a dark and spectrally neutral material (carbon, magnetite), Mg-phyllosilicates, ammoniated clays, carbonates and salts [8,9]. The observed species suggest endogenous, global-scale aqueous alteration [8,9] indicating the presence of a global ocean in the past of dwarf planet history [6].

Water ice has been identified in several small locations [10] and ice abundance variation over a short timescale (few months) has been observed in one crater (Juling crater [11]). It must be recalled that water ice is not stable at Ceres surface and most of these water ice exposures have been found in shadowed areas, where

the temperatures are much lower with respect to the average surface as suggested by numerical models (e.g. [15]). Nevertheless, the reason for the observed variation in the ice abundance in Juling is still to be understood and suggest a sort of "water cycle" at Ceres.

The surface shows important variations in the abundance and presence of different species, including the presence of salts. Sodium carbonates have been identified in several bright areas on the surface, notably in Occator crater's bright material (faculae) (Fig. 1) [12,13]. Also hydrous sodium carbonate has been identified in the vicinity of the water ice deposits [13] indicating close relationship between water and salts.

In the Occator faculae, sodium carbonate constitutes most of the bright material but it is not the only component. Recently, by investigating the IR spectra of the central part of Occator large facula (fig. 1), brines constituted by NaCl·2H₂O (hydrohalite), NH₄Cl (ammonium chloride), and Na₂CO₃ (natrite) have been identified [14].



Fig. 1 The dome of Cerealia facula in Occator crater. The bright material is mainly sodium carbonate. Image Credit: NASA, JPL-Caltech, UCLA, MPS/DLR/IDA

The formation of the Occator central pit and tholus, and the emplacement of the bright material, has been

extensively debated. Among the different hypothesis, there are two major scenarios: the first one involves the formation and extrusion of liquid salty water induced by the heat released by the Occator impact without pre-existing circulation of fluids at depth; the second considers the presence of pre-existing fluids that extrude onto the surface, facilitated by the fractures and conduits formed consequently to the impact.

Both the hypothesis require circulation of fluids at depth, able to extrude onto the surface, but the origins of those fluids (induced by external factors or by endogenic processes) and consequent implications, are different.

The facula shows concentric and radial fractures within the Cerealia tholus, which are the expression of the uplift stress. These extensional fractures represent the preferable conduits where fluids can escape towards the surface. The VIR data acquired on Occator bright material indicate that the hydrous salt is mainly on top of the Cerealia tholus in proximity of the fractures. Moreover, the presence of hydroalite, being very unstable at the Ceres surface and dehydrating in halite (NaCl) in a very short time (tens of years), suggests a very recent or continuous emplacement, implying that brines would still be able to extrude onto the surface [14].

The extremely recent emplacement is mainly consistent with the scenario of an endogenic process of circulation of salty aqueous solutions able to extrude onto the surface if the conditions are favorable (as the presence of fractures). The distribution of different species present on the faculae suggests that this material was produced inside Ceres, in modern brine-fed hydrothermal systems that recently brought this material to the surface.

Moreover, a long-term preservation of deep brines is possible if the crust is rich in clathrate hydrates as suggested by the model of Castillo-Rogez et al. 2019 [16] and by the lack of convection modes in the subsurface of Ceres [17].

Conclusions: Together with other observations by Dawn mission, such as the presence of cryo-volcanos, fluid landslides, geomorphological features, the VIR/Dawn discoveries suggest the presence of modern brines circulating inside Ceres and able to extrude onto the surface.

Many of the minerals observed on Ceres have been also detected in the plumes originating from the subsurface ocean of Enceladus (e.g. [18]), supporting the fascinating hypothesis of a residual ocean also in Ceres. Ceres is very appealing in terms of habitability,

given also the discovery of aliphatic organics [15] and the likely existence of carbon globally present on the surface [16]. As such, the dwarf planet is a privileged target for the search of life in the solar system, showing clear signs of fluids circulation in the recent past or even at present, and the presence of aqueous alteration products, water ice and organic material.

Acknowledgments: We thank the Italian Space Agency (ASI) (grant I/004/12/0) and NASA for supporting this work. We also thank the Dawn Mission Operations team and the Framing Camera team. The Visible and Infrared Mapping Spectrometer (VIR) was funded and coordinated by the Italian Space Agency and built by Leonardo (Italy), with the scientific leadership of the Institute for Space Astrophysics and Planetology, Italian National Institute for Astrophysics, Italy, and is operated by the Institute for Space Astrophysics and Planetology, Rome, Italy.

Dawn data are archived in NASA's Planetary Data System; VIR spectral data may be obtained at <http://sbn.psi.edu/pds/resource/dwncvir.html>

References: [1] Russell, C.T. et al, (2016), *Science*, 353, 6303, 1008-1010; [2] Ermakov, A. I., et al., (2017) *J. Geophys. Res: Planets*, 122, 2267–2293. [3] Marchi, S. et al (2016) *Nat Commun* 7, 12257 <https://doi.org/10.1038/ncomms12257>; [4] Ruesch O. et al. (2016), *Science*, 353, 6303, DOI: 10.1126/science.aaf4286; [5] Sizemore H. et al. (2018), *JGR*, DOI: 10.1029/2018JE005699 [6] De Sanctis, M.C. et al (2020), *Space Sci Rev*. DOI: /10.1007/s11214-020-00683-w [7] De Sanctis, M.C. et al., (2011) *Space Sci Rev* 163:329–369 DOI 10.1007/s11214-010-9668-5 [8] De Sanctis, M.C. et al. (2015), *Nature* 528, 241–244; [9] Ammannito, E. et al. (2016), *Science*, 353 aaf4279; [10] Combe J.-P. et al. (2016), *Science*, 353 [11] Raponi, A. et al. (2018), *Science Adv.*, 4:eaa03757; [12] De Sanctis M.C. et al., (2016) *Nature*, 536; [13] Carrozzo G.F. et al. (2018), *Science Adv.*, 4: e1701645; [14] De Sanctis, M.C. et al. (2020), *Nature Astronomy*, DOI: 10.1038/s41550-020-1138-8; [15] Formisano M. et al., (2018). *JGR* 123, 9, [16] Castillo-Rogez, J. et al., (2019), *GRL*, 46, 4; [17] Formisano M. et al., (2020) *MNRAS*, 494, 4, [18] Waite J.H. et al, (2017) *Science*, 356, 155–159

It takes a (halophilic) community: how to survive in the Great Salt Lake. T. Cahoon¹, A. Guerrero¹, J. Rosentreter¹ and C. Evilia^{1*}, ¹Department of Chemistry, Idaho State University, Pocatello, ID 83209, evilcary@isu.edu

Abstract: The Great Salt Lake, Utah, is one of the world's most recognized hypersaline environments. It is a beautiful dual-color system with two environments in one lake: a hypersaline, pink northern arm and moderately saline, blue-green southern arm separated by a railroad bridge that spans the lake. The salinity is due to high concentrations of metals from the local geochemistry and, due to this chemistry and UV exposure, is likely high in chemical radicals. This makes the environment poly-extreme, potentially mimicking extreme environments on other planets.

The Great Salt Lake has been studied for many years [1-4]. While most studies have looked at the diversity and population of microbial halophiles in the lake, a more extensive analysis of the microbial population in the lake needs to be done to better understand how microbes survive. We have undertaken a metagenomic analysis using next-generation sequencing and computational analysis, of three sampling sites in the lake: the Spiral Jetty (Rozel Point) in the northern arm, as well as one northern and southern point off the railroad causeway. We cross-correlated our metagenomic analysis with water analyses at these sites to observe trends in microbial and salt content. The northern arm exhibits high diversity in the extreme archaeal halophiles, and this corresponds to its extreme metal ion content. The southern arm is ~2.5x lower in metal ion content and has a much more diverse bacterial population. To explore how these microbes survive and thrive, we computationally surveyed representatives of our top microbial hits from the NCBI genome database for the presence of a minimal genetic "survival toolkit", including superoxide dismutase, perchlorate reductase, antioxidant pathway genes, and other genes. We found that microbes from the northern arm are enriched in these genes compared to inhabitants of the southern arm. Because not all genes are present in all organisms and some of these survival enzymes are secreted, it is likely that the collective community of microbes are what support life here.

We hypothesize that survival in this toxic, hypersaline environment requires a gene-encoded survival toolkit, which includes enzymes that tolerate high concentrations of metal cations in order to reduce radicals and neutralize anions, such as perchlorate and other oxoacids. Because not all microbes have all of these genes, they must form a community to survive under these conditions. Because variations of these

terrestrial hypersaline environments might be found elsewhere in the solar system, halophilic microbes could provide clues to survival tactics, should life be found in these poly-extreme environments.

Acknowledgements: For help with the bioinformatics, we would like to acknowledge Mike Lee, Blue Marble Space Institute of Science, NASA Ames Research Center. Access to the sampling sites on the Great Salt Lake railroad causeway was granted by Andrew Rupke P.G., Geologist, Utah Geological Survey. All water analyses were done by Tyson Pattie at IAS Environmental Chem, Inc. Funding was provided by a faculty research grant from Idaho State University.

References: [1] Post F.J. (1977) *Microb Ecol.*, 3, 143–165. [2] Meuser J.E., Baxter B.K., Spear J.R., Peters J.W., Posewitz M.C. and Boyd E.S. (2013) *Microb Ecol.*, 66, 268–280. [3] Tazi L., Breakwell D.P., Harker A.R. and Crandall K.A. (2014) *Extrem Life Extreme Cond.*, 18, 525–535. [4] Almeida-Dalmet S., Sikaroodi M., Gillevet P.M., Litchfield C.D. & Baxter B.K. (2015) *Microorganisms*, 3, 310–326.

A MODERATELY ALKALINE AND VOLATILE-RICH ENCELADUS OCEAN FROM PLUME MODELING. L. M. Fifer¹, D. C. Catling¹ and J. D. Toner¹, ¹Earth and Space Sciences, University of Washington, Seattle, WA 98195 (lufifer@uw.edu)

Introduction: Plumes erupting from Enceladus' tiger stripe fissures deliver water vapor and gases from a subsurface ocean to the surface and space. The plume composition measured by the Cassini spacecraft informs our knowledge of Enceladus' ocean chemistry. In particular, the abundances of various gases measured by the Ion and Neutral Mass Spectrometer (INMS) are crucial to understanding the dissolved gases, ions and pH in the ocean, and the ocean's capacity to sustain life. The gases observed in the plume include hydrogen (H₂), carbon dioxide (CO₂), methane (CH₄) and ammonia (NH₃) [1].

However, the relative abundances of gases in the plumes may not perfectly reflect the abundances in the ocean. Two fractionation processes occur during eruption: 1) exsolution of gases at species-specific rates, and 2) condensation of water vapor onto the icy walls of the plume conduit. Gas exsolution tends to enrich the plume in rapidly exsolving gases (in particular, water vapor), while condensation depletes the plume in water vapor because other gases (e.g. CO₂, H₂) do not condense out significantly [2].

In this work, we present a model of chemical fractionation in the gas phase of Enceladus' erupting plumes to estimate dissolved gas concentrations in the ocean. In addition, we use a model of equilibrium aqueous chemistry to estimate the ocean pH and concentrations of ammonium, carbonate and bicarbonate ions. We also consider the ocean's capacity to sustain life in the form of hydrogenotrophic methanogens.

How Plume Gases Determine Ocean Chemistry and Activity: The gases measured in the plume by the INMS instrument (and crucially, their inferred concentrations in the ocean) provide a wealth of information about Enceladus' chemistry, ongoing internal processes, and even the moon's origin. Abundant CO₂ would lower the pH of the ocean, due to the formation of carbonic acid (CO₂ + H₂O → H₂CO₃), which dissociates to provide free protons (H⁺). In turn, pH affects the dominant form of inorganic carbon in the ocean: at pH <~9.4, HCO₃⁻ dominates; at higher pH, CO₃²⁻ dominates [3]. Conversely to CO₂, abundant NH₃ would tend to raise the pH because it acts as a weak base, i.e. a proton acceptor. Ocean pH will also determine whether NH₃ dominates (pH > 9.25) or NH₄⁺ dominates (pH < 9.25), and the abundance of NH₄⁺ (a key ion in terrestrial metabolism).

Other gases provide insight into geochemical and potential biological processes within the ocean. The presence of both H₂ and CH₄ has been taken as evidence for hydrothermal activity at the ocean floor [1]. H₂ and CO₂ together could provide a source of chemical energy as a redox pair that methanogens, if present, could use.

Finally, better estimates for oceanic gas concentrations can help to constrain Enceladus' formation history. The deuterium/hydrogen (D/H) ratio of water measured in the plume suggests that Enceladus formed from similar materials to comets [1]. Abundances of other volatiles (e.g. CO₂, CH₄, NH₃) may therefore be present at cometary levels too.

Condensation of Water Vapor onto Ice Walls: As the plume travels upwards through the tiger stripe fissures, it will experience colder temperatures towards the surface. As a result, water vapor will tend to condense out of the plume, primarily onto the walls of the icy fissures, and secondarily onto ice grains carried by the plume gas [2]. However, other gases (CO₂, CH₄, NH₃, H₂) are unlikely to condense significantly given their volatility, so water vapor becomes depleted in the plume relative to other gases during its journey through the plume conduit. Glein et al. [2] estimated the amount of condensation onto the ice walls by assuming that the plume water vapor remains in equilibrium with the ice wall. The wall temperature is defined by thermal equilibrium with the ocean at the bottom of the fissure (~273 K), and by the observed temperature of the tiger stripes at the fissure outlet (197 ± 20 K) [4].

In our work, we adopt a model of plume dynamics (including both evaporation at the surface of the ocean, and condensation of vapor in the plume conduit) developed by Nakajima and Ingersoll [5]. In this model, mass, energy and momentum are conserved in the ocean-plume-fissure system as the plume accelerates upward through the plume conduit and partially condenses onto the fissure walls. The upper boundary condition is set by the plume velocity at the outlet, which we set to either the escape velocity (a lower limit) or the speed of sound (an upper limit). The lower boundary condition is defined by an evaporation flux driven by a pressure difference between the saturation vapor pressure of the ocean and the partial pressure of water vapor directly above the ocean surface. We iteratively pick this pressure difference using the 'shooting method' until one of the velocity conditions at the outlet is matched. We also vary the diameter and depth of the plume conduit across different models. As

in Nakajima and Ingersoll [5], we use the mass output of the eruption to constrain the fissure geometry, and only select those fissure geometries that accurately reproduce observed eruption rates.

Gas Exsolution from the Ocean Surface: Just as a pressure difference across the ocean-plume boundary drives water evaporation, low partial pressures directly above the ocean drive exsolution of other dissolved gases (CO_2 , CH_4 , NH_3 , H_2). We use a thin-film model of gas exsolution, where mass transfer is modeled via diffusion across a stagnant (non-convecting) thin film, with typical thickness of 0.1 mm for gases in water [6]. The exsolution flux is determined by the pressure difference between a hypothetical partial pressure in equilibrium with the dissolved concentration, and the actual partial pressure directly above the ocean surface. There is also a mass transfer coefficient, which is a function of the solubility and diffusion rate of the gas in water. We assume that the ratios of molar fluxes for each species across the ocean-plume boundary are equal to the ratios of their partial pressures in the plume, which allows us to derive each species' concentration in the ocean.

Equilibrium Aqueous Chemistry: To calculate the ocean pH and concentrations of HCO_3^- , CO_3^{2-} and NH_4^+ ions in the ocean, we use charge balance, the dissociation constants associated with these ions, and appropriate activity coefficients. We also include the measured concentrations of NaCl (0.05 - 0.2 mol kg^{-1}) and NaHCO_3 or Na_2CO_3 (0.01 - 0.1 mol kg^{-1}) [7] in this calculation.

Affinity for Methanogenesis: Finally, we use the same method as Waite et al. [1] to determine the available energy for methanogenesis in the H_2 - CO_2 redox pair. We calculate this affinity via:

$$A = 2.3026RT(\log K - \log Q)$$

where R is the universal gas constant, T is the temperature, K is the equilibrium constant and Q is the reaction quotient, which depends on the concentrations of all species in the reaction ($\text{CO}_2 + 4\text{H}_2 \rightleftharpoons \text{CH}_4 + 2\text{H}_2\text{O}$). If $Q = K$, then the system is at equilibrium, the affinity is zero, and methanogens would have no energetic incentive to perform the reaction.

Results: In our modeling, we find that wider and/or shallower fissures tend to produce oceans with higher concentrations of gases because these models produce relatively smaller amounts of vapor condensation during eruption so the relative abundances in the plume more closely reflect the concentrations in the ocean. When limiting our results to models that reproduce observed plume eruption rates, we find relatively high concentrations of all dissolved gases, around 10^{-4} - 10^{-2} mol kg^{-1} (Fig. 1) [10]. From equilibrium aqueous

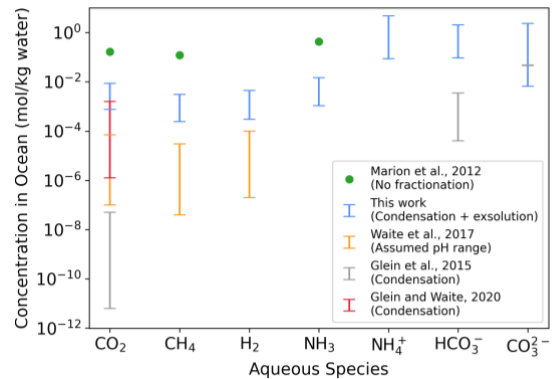


Figure 1: Calculated ranges for dissolved gas and ion concentrations from this work and previous studies [1], [2], [8], [9].

chemistry, we predict an ocean pH of ~ 7.9 - 8.5 , which is less alkaline than recent estimates that range from 8.5-13.5. This pH is also closer to terrestrial ocean pH than previous estimates, which may be encouraging in the search for Earth-like life on Enceladus, and for Enceladus-analog environments on Earth.

We also predict high concentrations of ammonium ions (10^{-1} - 10^0 mol kg^{-1}) and up to ~ 2 mol kg^{-1} of HCO_3^- or CO_3^{2-} . Consequently the total ammonium ($\sum \text{NH}_3 = [\text{NH}_3] + [\text{NH}_3^+]$) and total inorganic carbon ($\sum \text{CO}_2 = [\text{CO}_2] + [\text{HCO}_3^-] + [\text{CO}_3^{2-}]$) abundances that we predict for the bulk moon overlap with cometary abundances of these volatiles.

Finally, we find ample energy in the H_2 - CO_2 redox pair to support hydrogenotrophic methanogens, corresponding to ~ 120 - 140 kJ per mole of reaction. The presence of available energy could suggest that no life is present to harness it, but could also point to a small biosphere that only partially uses the available energy due to other nutrient limitations.

Acknowledgments: Supported by NASA Habitable Worlds Program grant #80NSSC19K0311.

References: [1] Waite, J. H. et al. (2017). *Science*, 356, 155–159. [2] Glein, C. R. et al. (2015). *Geochim. Cosmochim. Acta*, 162, 202–219. [3] F.J. Millero et al. (2002). *Deep-Sea Research I*, 49, 1705–1723. [4] Goguen, J. D. et al. (2013). [5] Nakajima, M., & Ingersoll, A. P. (2016). *Icarus*, 272, 309–318. [6] Cussler, E. L. (2009). [7] Postberg, F. et al. (2009). *Nature*, 459, 1098–1101. [8] Marion, G. M. et al. (2012). [9] Glein, C. R. and Waite, J. H. (2020). *Geophys. Res. Lett.*, 47, 1689-1699. [10] Fifer et al. (2021) *Planet. Sci. J.*, submitted.

GEOCHEMICAL MODELING OF MAGMA-SEDIMENT INTERACTION INDUCED HYDROTHERMAL SYSTEMS: CONSTRAINTS ON THE EFFECT OF MAGMA COMPOSITION.

J. Filiberto¹, S. Cogliati², J.R. Crandall³, and S.P. Schwenzer², ¹Lunar and Planetary Institute, USRA, Houston, TX 77058. jfiliberto@lpi.usra.edu ²AstrobiologyOU, EEES, The Open University, Milton Keynes MK7 6AA, UK, ³Eastern Illinois University, Department of Geology & Geography, 600 Lincoln Ave., Charleston, IL 61920, USA.

Introduction: Magmatism is one of the key processes, along with impacts, that provides both volatile species and energy to the surface throughout Martian history [1]. Magmatism on Mars may produce habitable environments through degassing and/or interaction with sedimentary systems [2-6]. Magma intruding sedimentary rocks will metamorphose the country rock liberating any bound water (in minerals, ice, pore space, etc) [6, 7]. Costello et al. [5] and Crandall et al. [3] (**Fig. 1**) have previously investigated a magmatic dike intruding the Entrada Sandstone on the Colorado Plateau, UT, which produced a habitable (and possibly inhabited) Cl-rich brine system. However, the dike has a significantly different composition than typical magmas on Mars, which complicates a direct one to one application. Therefore, here we use the temperature, fluid:rock ratio, and oxidation state constraints from the Mars analog as inputs to model how differences in bulk dike composition will affect brine chemistry and subsequent alteration mineralogy.



Figure 1. From [3] showing the contact between the dike and the Entrada Sandstone. Dike is approximately 30 cm across. The contact zone is yellow in color compared with the less altered Entrada Sandstone being red in color.

Mars Analog Hydrothermal System: Costello et al. [5] and Crandall et al. [3] previously showed that when the magmatic dike (**Fig. 1**) intruded the Entrada Sandstone it produced a high temperature hydrothermal system. Based on the mineralogy and bulk compositional changes of the altered dike, [5] showed that the system reached $> 200\text{ }^{\circ}\text{C}$ and was altered by a near-neutral pH CO_2 -bearing fluid. Extending this work to the contact zone, bleached features perpendicular to the dike, and sandstone xenolithic material within the dike itself, [3] showed that the hydrothermal system actually reached $> 700\text{ }^{\circ}\text{C}$ and was altered by a Cl- CO_2 -rich brine, which mobilized S, P, Fe, Ca, Si, and K in the system (**Fig. 2**). Further, there is evidence in the xenolithic material that the system reached even higher temperatures [3]. The high temperature of the system is outside the range of terrestrial microbes, likely initially sterilizing the system [8-10], but upon cooling would have been a habitable environment. Further, based on combined mineralogy and C-O-S isotopes, the contact zone around the dike may have been inhabited [3]. While these results are intriguing for creating a habitable and potentially inhabited environment on Earth, there are compositional differences between the terrestrial dike and Martian basaltic compositions [11, 12], which were not previously considered but would affect brine chemistry and alteration mineralogy.

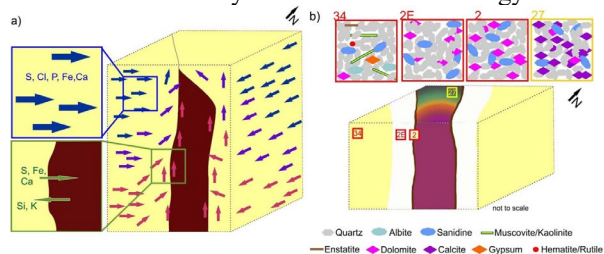


Figure 2. From [3] and modified from [5] summarizing the hydrothermal system during (A) and after (B) dike emplacement within the Entrada Sandstone. Figure not to scale. (A) Intrusion of the dike into the sandstone producing a hydrothermal system mobilizing S, Cl, P, Fe, Ca, Si, and K. Green arrows indicate element mobility. Red arrows represent hot fluids, while blue arrows represent cold fluids. (B) The system how it appears today. Orange boxes show the representative mineralogy for samples that experienced hydrothermal alteration, while the yellow box shows the mineralogy for the xenolithic material.

Modeling Approach: Here, we are modeling how bulk composition of the mafic dike affects both brine chemistry and alteration mineralogy following a similar approach from impact-induced systems [13]. For this work, we use the code CHIM-XPT, which has been used for modeling terrestrial basaltic systems, e.g., mid-ocean ridge systems [14, 15], and has been successfully applied to many Martian systems [e.g., 13, 16, 17]. For this work, we are modeling the alteration of four basaltic compositions (Table 1) providing a range in bulk compositions. Further, results of the terrestrial dike can be directly compared with the observed alteration mineralogy [3, 5] and the modeling of Humphrey can be directly compared with previous modeling results [13]. Finally, as our system showed significant Cl-mobility we have included halogens in our model. We use average halogen contents for terrestrial lamproites for the dike system [18], which is similar to the calculated halogen contents for some Martian parental magmas [19]. Future work will vary the basaltic Cl content to see the effect on brine chemistry.

Table 1. Bulk Composition of terrestrial dike and Martian basalts as modeled.				
Wt%	Dike	Jake_M	Humphrey	Clast in NWA7034
SiO ₂	34.8	51.6	45.9	54.0
TiO ₂	5.7	0.65	0.58	1.0
Al ₂ O ₃	14.7	15.7	10.7	11.5
FeO	7.4	10.8	18.60	12.0
MgO	3.8	4.4	10.41	7.0
CaO	11.6	6.7	7.84	6.00
Na ₂ O	1.0	7.0	2.5	3.10
K ₂ O	4.4	2.12	0.1	1.20
P ₂ O ₅	2.6	0.68	0.56	1.20
Cl	0.2	0.2	0.2	0.2
F	0.2	0.2	0.2	0.2
References and details: Dike composition modified from: [3, 20]; Mars basalts as summarized in: [12]; Halogens from: [18, 19]				

Acknowledgments: JF, JRC, and SPS acknowledge funding from NASA PSTAR grant No. 80NSSC18K1686. SPS and SC acknowledge funding from Research England Expanding Excellence in England (E3) fund (grant code 124.18).

References: [1] Carr M.H. and Head J.W. (1997) *EPSL*, 294, 185-203. [2] Shock E.L. (1996) *Evolution of hydrothermal ecosystems on Earth (and Mars?)*, 202, 40-60. [3] Crandall J.R. et al. (2021) *PSJ*, 2, 138. [4] Farmer J.D. (1996) in *Ciba Foundation Symposium*. [5] Costello L. et al. (2020) *Geochemistry*, 10.1016/j.chemer.2020.125613. [6] Hochstein M. and

Browne P. (2000) *Encyclopedia of volcanoes*, 835-855. [7] Griffiths R.W. (2000) *Annual Review of Fluid Mechanics*, 32, 477-518. [8] Cowan D.A. (2004) *Trends in microbiology*, 12, 58-60. [9] Rothschild L.J. and Mancinelli R.L. (2001) *Nature*, 409, 1092-1101. [10] Kashefi K. and Lovley D.R. (2003) *Science*, 301, 934-934. [11] McSween H.Y. et al. (2003) *JGR-P*, 108, (E12). [12] Filiberto J. (2017) *ChemGeo*, 466, 1-14. [13] Schwenzer S.P. and Kring D.A. (2013) *Icarus*, 226, 487-496. [14] Reed M. et al. (2010) *Users Guide for CHIM-XPT*. [15] Reed M.H. and Spycher N.F. (2006) *User Guide for CHILLER*. [16] Filiberto J. and Schwenzer S.P. (2013) *MaPS*, 48, 1937-1957. [17] Melwani Daswani M. et al. (2016) *MaPS*, 51, 2154-2174. [18] Webster J.D. et al. (2019) *The Role of Halogens in Terrestrial and Extraterrestrial Geochemical Processes*, 307-430. [19] Filiberto J. et al. (2019) in *Volatiles in the Martian Crust*, Elsevier, 13-33. [20] Wannamaker P.E. (2000) *JVGR*, 96, 175-190.

RAMAN SPECTROSCOPY AS A TOOL TO IDENTIFY BRINE FORMATION. E. Fischer¹, G. M. Martínez^{1,2} and N. O. Rennó¹, ¹Department of Climate and Space Sciences and Engineering, University of Michigan, Ann Arbor, MI, USA, ²Lunar and Planetary Institute/USRA, Houston, TX, USA.

Introduction: Pure liquid water is not stable at present-day Mars conditions. It would rapidly evaporate in the extremely dry Martian atmosphere and freeze at most times of the Martian day due to the low temperature. Brines, highly saline solutions of salts in water, on the other hand, can have a much reduced freezing point and evaporation rate and are therefore the most likely form of temporarily stable bulk liquid water on the surface or in the shallow subsurface of Mars. Perchlorate salts are among the most promising candidates for Martian brine formation. These salts have been detected in the Martian regolith in polar latitudes by the Phoenix lander [1], in mid-latitudes by the Mars Reconnaissance Orbiter [2], as well as in equatorial latitudes by the Curiosity rover [3].

Two methods of brine formation on Mars have been suggested. The first is brine formation by deliquescence, where the hygroscopic salt absorbs atmospheric water vapor when the humidity passes a threshold, the deliquescence relative humidity [4-7]. The second method is brine formation by lowering the melting point of water ice through contact with salts in the regolith [6,8]. Since perchlorate salts are suggested to be distributed globally [9], this would happen wherever water ice such as frost or subsurface ice is in contact with the regolith and the temperature is above the eutectic temperature of the brine.

Here, we show experimentally obtained Raman spectra of the above mentioned materials involved in brine formation on Mars and analyze their characteristics that can aide in their identification in more complex in-situ measurement campaigns on Mars. As an example of a perchlorate salt we use $\text{Ca}(\text{ClO}_4)_2 \cdot 4\text{H}_2\text{O}$ due to its low eutectic temperature of 199 K [11] and its ubiquity on Mars [1-3].

Methodology: All our Raman spectra, except the reference spectrum of pure liquid water, were obtained under Martian pressure, temperature and relative humidity conditions in the Michigan Mars Environmental Chamber (MMEC). The MMEC can simulate the full range of Martian surface conditions. The chamber and full experimental setup are described in detail in [6,8,10]. The Raman spectrometer used in this study is a Kaiser Optical Systems Inc. RamanRXN1 with a 532 nm laser. Our study focuses on two Raman band regions with the strongest signal of the materials studied: the perchlorate symmetric stretching band between ~ 900 and 1000 cm^{-1} and the O-H stretching band between ~ 3000 and 3800 cm^{-1} [10]. We further

used Gaussian decomposition with baseline subtraction to determine individual peak positions, full widths at half maximum and relative amplitudes to quantitatively analyze the obtained spectra.

Results: We obtained Raman spectra of pure liquid water at ambient conditions, water ice and calcium perchlorate tetrahydrate at 190 K and 800 Pa (to prevent deliquescence or hydration state changes), calcium perchlorate brine at 255 K and 800 Pa, and calcium perchlorate salt recrystallized out of a brine at 190 K and 800 Pa [10].

Table 1 lists the observed peaks of the decomposed spectra obtained from the samples. These values, obtained under idealized laboratory conditions, can be used to identify perchlorate brines in in situ measurements on Mars.

	ClO_4 band	O-H band
H_2O (l)		3230(217), 3420(218), 3540(206), 3620(109)
H_2O (s)		3046(99), 3115(57), 3227(206), 3336(56), 3399(140)
$\text{Ca}(\text{ClO}_4)_2 \cdot 4\text{H}_2\text{O}$	939(16)*, 952(9)	3115(81)*, 3249(113)*, 3437(147)*, 3437(27), 3467(23), 3487(15), 3509(25), 3536 (23), 3560(155)*, 3602(13), 3630(18)
$\text{Ca}(\text{ClO}_4)_2$ saturated in H_2O	936(17)	3256(219)*, 3495(249), 3555(106)
$\text{Ca}(\text{ClO}_4)_2 \cdot x\text{H}_2\text{O}$ recrystallized	934 (13)	3311(271), 3389(66), 3456(38), 3496(31), 3520(19), 3543(17), 3546(132)

Table 1: Decomposed peak positions and widths (in parentheses) of the Raman spectra shown in this study. Asterisks indicate weak peaks with low intensities. [10]

Pure Liquid Water and Ice. Fig. 1 shows the Raman spectra of pure water at ambient conditions (top) and water ice at 190 K and 800 Pa (bottom). The four observed wide Gaussian peaks for liquid water are similar to those reported in [12]. The first two are ice-like components whereas the other two are unique for liquid water. In our experiments the 3230 cm^{-1} peak increased in wavenumber with decreasing temperature, while the 3420 cm^{-1} peak decreased in wavenumber with decreasing temperature. Both show a rate of change of $\sim 0.2\text{--}0.5 \text{ cm}^{-1}/\text{K}$. We also observed an

increase of the 3230 cm^{-1} peak's relative intensity compared to the 3420 cm^{-1} peak with decreasing temperature [10,13]. Of the five Gaussian peaks for water ice, the two with the highest wavenumber coincide with the ice-like peaks in the liquid water spectrum. The prominent 3115 cm^{-1} peak has the strongest intensity and can be used as an indicator of the presence of water ice in a sample. Similar to liquid water, the ice wavenumbers decrease by $\sim 0.3\text{--}0.5\text{ cm}^{-1}/\text{K}$ with decreasing temperature.

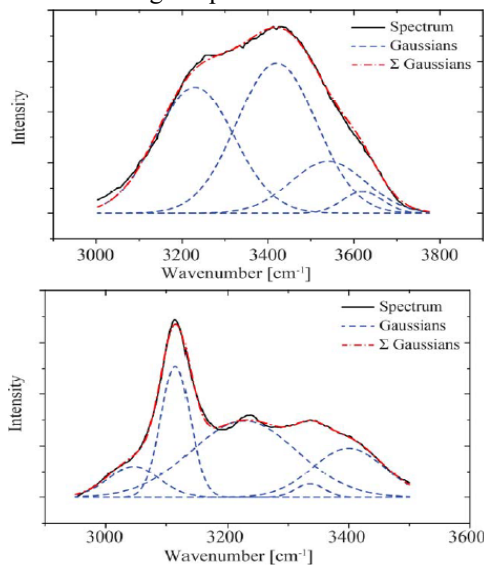


Fig. 1: Decomposition of the Raman spectrum of liquid water (top) and water ice (bottom) in the O-H stretching band. [10]

Crystalline Calcium Perchlorate Tetrahydrate. Fig. 2 shows the Raman spectrum of this salt in the O-H stretching band. It shows a number of very narrow peaks, typical for crystalline hydrated perchlorates [6]. The prominent peak at 952 cm^{-1} in Table 1 is representative of the tetrahydrate. Impurities of higher hydration states result in the weak 939 cm^{-1} peak.

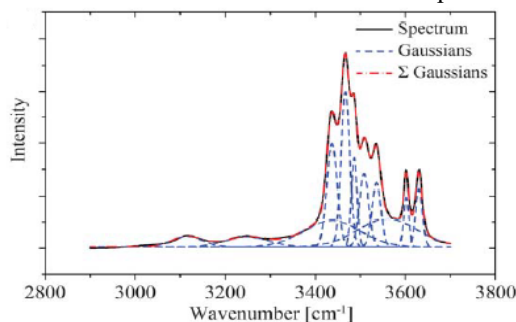


Fig. 2: Decomposition of the Raman spectrum of hydrated perchlorate salt in the O-H stretching band. [10]

Calcium Perchlorate Brine. Fig. 3 shows the Raman spectrum of the saturated brine in the O-H stretching band. The perchlorate band shows that the tetrahydrate peak of the crystalline salt has completely shifted to 934 cm^{-1} , typical for perchlorate solutions.

The O-H band shows three wide peaks at similar positions to those of the pure liquid water sample, but shifted to higher wavenumbers. Additionally the highest wavenumber peak is much more intense in the solution compared to pure water and its relative intensity increases with the saturation level.

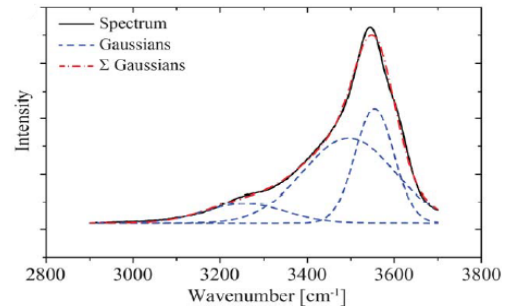


Fig. 3: Decomposition of the Raman spectrum of saturated perchlorate solution in the O-H stretching band. [10]

Recrystallized Calcium Perchlorate. Table 1 shows that the perchlorate band of the recrystallized salt shows a single peak at 934 cm^{-1} , indicating that it is not the tetrahydrate but a higher hydration state. In the O-H band we see a return to the narrow peaks indicative of the crystalline hydrated perchlorate salt.

Discussion and Conclusions: Our spectra provide a reference for the detection of perchlorate salt hydrates and liquid brine of perchlorate salts in the Martian soil. While the perchlorate band can be used to distinguish different hydration states of salts, the O-H band can help identify and distinguish liquid brine and crystalline hydrated salts. A change in the O-H spectrum from the numerous narrow peaks to the wider water-like peaks are a clear indication of brine formation. Furthermore, our reference spectra of water ice at Martian conditions can aid in the identification of thin ice layers such as surface frost by Raman spectrometer onboard landers and rovers. These results show that Raman spectroscopy is a useful tool for liquid water detection on Mars.

References: [1] Hecht, M. H. et al. (2009) *Science*, 325, 64–67. [2] Ojha, L. et al. (2015) *Nat. Geosci.*, 8(11), 829–832. [3] Glavin D. P. et al. (2013) *JGR: Planets*, 118(10), 1955–1973. [4] Chevrier, V. F. et al. (2009) *GRL*, 36(10). [5] Gough, R. V. et al. (2011) *EPSL*, 312(3), 371–377. [6] Fischer, E. et al. (2014) *GRL*, 41(13), 4456–4462. [7] Nuding, D. L. et al. (2015) *JGR: Planets*, 120(3), 588–598. [8] Fischer, E. et al. (2016) *Astrobiology*, 16(12). [9] Osterloo, M. M. et al. (2010) *JGR*, 115, E10012. [10] Fischer, E. (2016) *Fisica de la Tierra*, 28, 181–195. [11] Marion, G. M. et al. (2010) *Icarus*, 207(2), 675–685. [12] Zhang, Y. H. and Chan, C. K. (2003) *J. Phys. Chem. A*, 107(31), 5956–5962. [13] Dolenko, T. A. et al. (2000) *J. Raman Spectrosc.*, 31(8-9), 863–870.

Comprehensive analysis of DNA degradation and cell viability of model microbes in magnesium chloride brine L. A. Fisher¹, A. R. Bovee², B. Klempay¹, M. M. Weng³, S. M. Som⁴, P. T. Doran⁵, C. E. Carr⁶, J. B. Glass⁶, A. Pontefract⁶, B. E. Schmidt⁷, J. S. Bowman¹, and D. H. Bartlett¹ ¹University of California San Diego, ²University of California Los Angeles, ³Georgetown University, ⁴Blue Marble Space Institute of Science, ⁵Louisiana State University, ⁶Georgia Institute of Technology, ⁷Cornell University.

Introduction: MgCl₂ dominated hypersaline environments severely impact microbial life by exerting chaotropic stress and greatly depressing water activity. Chaotropes disorder biological macromolecules, resulting in protein denaturation and membrane solubilization, eventually leading to cell death. Chaotropic brines include terrestrial salterns, and athalassohaline (AT) deep-sea hypersaline anoxic basins (DHABs). The latter are strongly stratified polyextreme MgCl₂ saturated brine pools that accumulate in benthic depressions within enclosed seas. There is strong evidence of active microbial life up to 2.27-3.03M MgCl₂ in AT DHABs, while the brine endmembers at >4M MgCl₂ and water activity (a_w) equal to ~0.4 are largely considered sterile. The currently accepted a_w limit of life is ~0.6 [1]. Sulfate reduction rate measurements in some AT DHAB brines combined with Next Generation Sequencing (NGS) methods suggest the presence of active, highly specialized microbial life [2]. However, the preservative effects of MgCl₂ on biomolecules make life detection approaches difficult. High concentrations of this salt preserves DNA for months with little degradation [3]. Recent environmental 16S amplicon sequencing from a saltern in Southern California shows that DNA in sterile ~4M MgCl₂ brines are dominated by *Haloquadratum walsbyi* [4]. Here, we seek to better understand these findings by studying the preservative effects of MgCl₂ on purified DNA and cells of model microorganisms.

Experimental design: We plan to expose actively growing cultures of the haloarchaea *Halobacterium salinarum* NRC-1, *Haloquadratum walsbyi*, and the bacterium *Escherichia coli* MG1655, along with their respective purified DNA, to 4M MgCl₂. DNA will be extracted and desalted throughout the incubation period for downstream analysis via PCR, Qubit, TapeStation™, and Nanopore sequencing. These assays will assess the DNA quality, concentration, size, and methylation events respectively. Cell viability will be determined with Live/Dead™ staining, flow cytometry (FCM), colony forming units (CFUs), and cell population levels will be followed using optical density readings. Raman analysis will be conducted throughout the incubation to better understand the effects of MgCl₂ on tractable biomolecules such as haloarchaeal pigments.

Preliminary results: The first phase of this experiment was conducted using *Escherichia coli* MG1655. After freshly grown *E. coli* cells were exposed to 4M MgCl₂ for three weeks, DNA did not degrade based on

gel electrophoresis and successful PCR amplification of extracted DNA. CFUs decreased by four orders of magnitude within two hours of exposure while optical density evaluated at 600nm (OD600) remained constant, suggesting that the cells maintained their integrity rather than lysing (Duda et al., 2004). CFUs agreed with FCM results suggesting rapid cell death.

Future work: Work with *E. coli* will guide the next phase of experiments using the model halophiles *Halobacterium salinarum* NRC-1 and *Haloquadratum walsbyi*. Exposing whole cell and purified DNA separately in 4M MgCl₂ will determine if there are differential DNA degradation rates between microbes and if the cell acts as a ‘shelter’ for DNA. Furthermore, we hope to provide a comprehensive analysis of cell survivorship and develop fluorescent labelling and Raman techniques that can be applied to other hypersaline environments for the purposes of life detection.

Significance: Bitterns and AT DHABs contain physical properties analogous to environments within other ocean worlds. The icy moons of Saturn (Enceladus and Titan) and Jupiter (Europa, Callisto, and Ganymede) likely harbor oceans underneath thick surface ice. The ice shells and oceans of these moons could be conducive to life and favor the preservation of organic material. Furthermore, the presence of surface salts, especially on Europa and Mars, including magnesium and chaotropic perchlorate compounds in high concentrations, respectively, points to a need to understand microbial habitability and preservation in MgCl₂ brines.

Acknowledgments: This work is supported by the Oceans Across Space and Time (OAST) collaborative research project funded by NASA’s Astrobiology Program award 80NSSC18K1301 (PI: B. E. Schmidt). We thank the entire OAST team for their time and thought provoking discussions.

References:

- [1] Yakimov M. M. *et al.* (2015) *Environ. Microbiol.*, 17(2), 364-382. [2] Steinle L. *et al.* (2018) *ISME*, 12, 1414-1426. [3] Hallsworth J. E. *et al.* (2007) *Environ. Microbiol.*, 9(3) 801-813. [4] Klempay B. *et al.* (2021) *Environ. Microbiol.*, 23(7), 3825–3839

MODELING THE DELIQUESCENT OF COMPLEX SALT MIXTURES AT THE PHOENIX LANDING SITE. A. Fitting¹, V. F. Chevrier¹, E. G. Rivera-Valentín², A. Soto³: ¹Arkansas Center for Space and Planetary Sciences, University of Arkansas, Fayetteville, AR, 72701 (abfittin@uark.edu), ²Lunar and Planetary Institute (USRA), Houston, TX, ³Southwest Research Institute, Boulder, CO.

Introduction: The habitability of the surface of Mars depends on multiple factors, including, but not limited to, temperature, relative humidity, UV, and nutrients [1]. Of these parameters, temperature and relative humidity control the stability of liquid water, which is of primary astrobiological importance and has driven the exploration of Mars for the past two decades. Pure water is generally unstable on the surface of Mars, being subjected to freezing, evaporation and boiling, but these processes are highly variable depending on the location and intrinsic properties of the liquid [2]. Indeed, the presence of abundant hydrated salts on the surface of Mars suggests the possible presence of brines [3,4], which present the advantage of stabilizing liquid water at lower temperatures [2,5]. Previous works on mapping the stability of brines on the surface and subsurface of Mars have focused on single brines, such as, for example, calcium or magnesium perchlorates [6]. However, it is possible that mixtures of salts could significantly reduce the freezing or deliquescence points for brines [7,8]. However, no comprehensive model has been undertaken to simulate the behavior of complex brines at the surface of Mars. Here, we present the first results on deliquescence of mixtures of salts, constrained by the composition determined by the Phoenix lander [9,10].

Methods: The objective of this work is first to determine the deliquescence relative humidity (DRH) of the salt mixtures at the Phoenix landing site as a function of temperature, for a realistic ionic composition as measured by the Wet Chemistry Laboratory (WCL) onboard the Phoenix lander. In a second step we will apply these results through a diurnal and seasonal model of relative humidity and temperature at the surface of Mars to determine the locations and times of day where deliquescence occurs on the surface and in the shallow subsurface. This abstract focuses on the first part of this process. Unfortunately, of the widely used thermodynamic codes for thermodynamic simulations, such as FREZCHEM or Geochemist's Workbench, none of them directly simulates water activity (or deliquescence) as a function of temperature. Therefore, we used an indirect method [8], in which we modelled the evaporation of individual brine solutions at fixed temperatures (Fig. 1). We then determined the water activity at each salt that precipitated, until evaporation was complete. For each evaporation run, we also graphed water activity as a function of water mass (Fig. 2). Because in thermodynamic modeling, deli-

quescence and efflorescence occur at the same point, measuring the evaporation directly gave us the deliquescence water activity values for each temperature and salt composition. The first salt to precipitate is equivalent to the point of complete deliquescence and the last salt to precipitate gives the minimum deliquescence relative humidity (or eutonic point). We ran the simulations in 5 K increments between 198 K and 283 K.

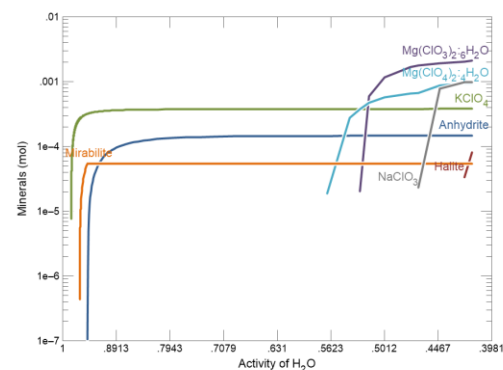


Figure 1: Evaporation of brines using model 1 (chlorate-rich) at 273 K. The process was repeated at each temperature between 198 K and 283 K by 5 K increments.

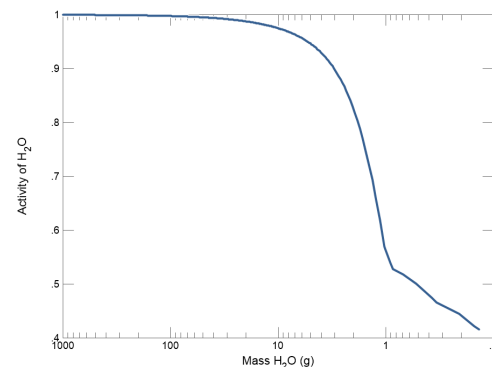


Figure 2: Activity of water as a function of residual mass of liquid water during the evaporation of model 1 brine (chlorate-rich) at 273 K.

We used three different models depending on assumption on the initial ionic composition measured by the WCL [9] with various methods to balance the ionic charge [8]. Model 1 is rich in chlorate ion, model 2 is balanced between chlorate and sulfate, and model 3 is

rich in sulfate and magnesium (see [8] for detailed discussion on the model descriptions). This abstract focuses on model 1, which has the highest chlorate composition (and thus lowest sulfate). Each composition measured by the WCL was evaporated starting from 1000 g of liquid brine, and the activity of water was recorded at each precipitating salt. This water activity corresponds to the deliquescence relative humidity for the salt mixture.

Results and discussion:

An interesting observation relating to the deliquescence diagrams of the multi-salt assemblages is that the DRH always increases with decreasing temperature. This is mostly because of the higher hydrates forming at lower temperatures. We created a combined graph from our data showing the water activity of each precipitating mineral as a function of temperature (Fig. 3). Across all temperatures, sulfates tended to have high water activity values. At higher temperatures (>258 K), chlorides exhibit the lowest water activity values, whereas between 208 K and 253 K, chlorates were lowest. At the lowest temperatures (<208 K), chlorides once again showed the lowest water activity values, with chlorates close behind. Combining the lowest water activity values at each temperature for model 1, creating a solidus line, with an ice stability line, we can see a zone (below the ice line and above the solidus line) where liquid may be stable. We added data from the Phoenix lander to test for potential brine formation (Fig. 4). Data points from PHX that are associated with potential evidence for liquid brines, through melting or adsorption as inferred from the regolith's dielectric signatures [11], have been highlighted in yellow, blue, and green. Most of these colored points do not land in the liquid stability zone, but some do, indicating that there may be a possibility of liquid brine formation.

Conclusions: In all simulated brines of Phoenix-type composition, we observed that the deliquescence relative humidity is essentially controlled by chlorine bearing salts (chlorides, chlorates or perchlorates) and sometimes even by a single species. Deliquescence occurs at DRH as low as 0.37 at temperatures around 273 K, so lower than for single salts (0.52 for Ca-perchlorate but at much lower temperature, 198 K). Despite this slightly increased stability field for multibrines, it is unlikely this will provide improved habitable environment at the surface of Mars. In addition, while the water activity of the solidus line does drop close to 0.4, this is at higher temperatures. In the temperature range where Phoenix data points fall in the liquid stability zone, the water activity is not lower than about 0.5, showing again that it is unlikely that

the multibrines will increase the likelihood of stable liquids at the surface of Mars.

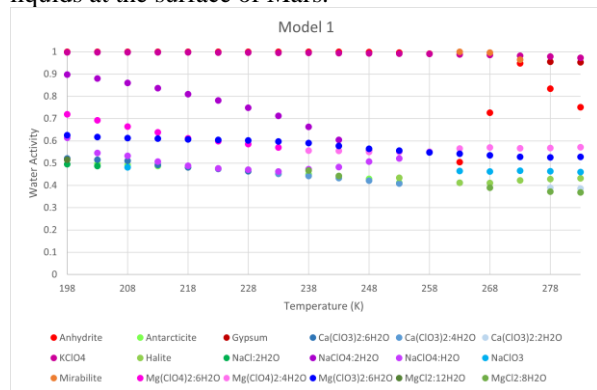


Figure 3: Water activity or deliquescence relative humidity as a function of temperature for model 1.

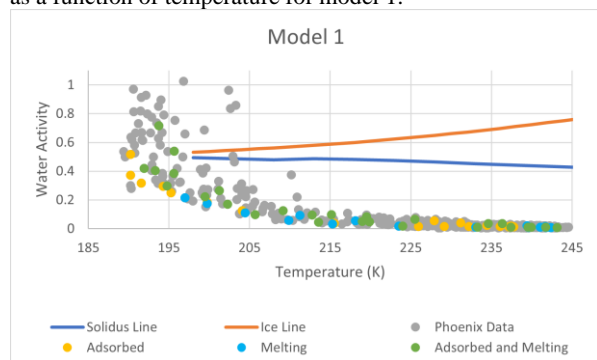


Figure 4: Lowest water activity or deliquescence relative humidity as a function of temperature for model 1, with an ice stability line and data from the Phoenix lander.

Acknowledgements: This work is funded by the NASA Habitable Worlds grant # 80NSSC17K0742.

References: [1] Rummel J. D. et al. (2014) *Astrobiology* 14 (11), 887-968. [2] Chevrier V., T. S. Altheide (2008) *Geophysical Research Letters* 35 (L22101). [3] Chevrier V. F., E. G. Rivera-Valentin (2012) *Geophysical Research Letters* 39 (L21202). [4] Gough R. et al. (2019) *Icarus* 321, 1-13. [5] Chevrier V. et al. (2009) *Geophysical Research Letters* 36 (L10202). [6] Chevrier V. F. et al. (2019) *Lunar and Planetary Science Conference L* (2019). [7] Gough R. V. et al. (2012) *Lunar and Planetary Science Conference XLIII* (1706). [8] Elsenousy A., V. F. Chevrier, paper presented at the 45th Lunar and Planetary Science Conference, The Woodlands, Texas, March 17-21, 2014. [9] Hecht M. H. et al. (2009) *Science* 325, 64-67. [10] Kounaves S. P. et al. (2010) *Geophysical Research Letters* 37 (9), L09201. [11] Stillman, D. E., and R. E. Grimm (2011), Dielectric signatures of adsorbed and salty liquid water at the Phoenix landing site, Mars, *J. Geophys. Res.*, 116, E09005, doi:10.1029/2011JE003838.

MARTIAN BRINES IN ANCIENT SALT LAKE BEDS – A HIGH PRIORITY TARGET FOR MARS SAMPLE RETURN. M. Fries¹, A. Steele², and M. Zolensky¹, ¹NASA Astromaterials Research and Exploration Science (ARES), Johnson Space Center, Houston, TX. ²Earth and Planets Laboratory, Carnegie Institution for Science, Washington D.C. Email: marc.d.fries@nasa.gov

Introduction: Mars hosts over 600 chloride deposits as identified from orbital imagery [1-3], including deposits in settings resembling dry, evaporite lacustrine bedforms on Earth. A Mars sample return mission to one of these salt lake beds has a strong potential to directly sample present-day brines originating from ancient martian surface fluids, allowing direct laboratory investigation into fluids, atmosphere, and either potential biology or prebiological conditions on the martian surface at the Noachian through the Hesperian epochs. These sites are extraordinarily well suited for sample return missions because they are favorable for landing and for drill-based sampling, and preserve samples of parent water bodies, including dissolved atmosphere and potential well-preserved biological remains. Such a mission would provide a foundational set of reference samples for understanding Mars' physiochemical and pre-/biological history, likely to be investigated in depth for generations to come.

Science Return from Chloride Lacustrine Settings: Evaporite salt deposits are noted for their extremely favorable preservation of ancient organics [4,5]. The parent fluid from which they precipitated can also be preserved. For example, halite grains discovered in the Zag and Monahans meteorites contain 4.5 Ga-old organics and parent brine [6]. The strong possibility exists that samples of the ancient martian atmosphere may be present in fluid inclusions as well, allowing direct analysis [7]. It is reasonable to expect that chloride salts at or very near the surface of martian lake bed deposits retain samples of their parent fluid and any organics present from the time when the lakes evaporated, which has been dated to the Noachian and Hesperian [2]. In terrestrial examples, halite has been shown to preserve ancient microbes as well, although the age of these microbes most reliably extends into the 100 ka range [8] and may not reliably preserve potential martian microbes dating from Hesperian ages. If a modern-day microbiome exists in the martian salt flat settings, however, it may be directly sampled. Samples collected from martian lake bed(s) would directly address the hypothesis of martian life present in the end stages of purported surface water. It would also collect material with some of the best preservation potential available (salts and other evaporites), which is present at or very near the surface.

Landing and Sampling: Lake bed settings can be especially well suited for spacecraft landing sites. On

Earth, lake beds in the American west have been favored sites for automotive high speed testing (e.g. Bonneville Salt Flats, UT) and airfields (e.g. Edwards AFB, CA) because of their broad expanses of level, compacted ground. Lacustrine evaporite flats also feature relatively homogenous mineralogy across broad areas. This simplifies the task of sampling because small, precise landing ellipses are not strictly necessary, and landed mobility is probably not necessary either. Martian lacustrine settings are favorable for relatively straightforward "grab and go" sampling with a high likelihood that a prescribed set of evaporite and sediment samples can be reliably collected. The mineralogy of these settings also tends to favor drilling, as relatively friable evaporite and sedimentary minerals dominate. Overall, risks involved in both landing and sampling are reduced.

Summary: Martian chloride deposits should be considered a prime science target for future sample return mission(s). Evaporite lake beds are known from terrestrial examples to feature broad, flat expanses of nearly homogenous mineralogy. That mineralogy is composed of materials with superb organic and microbiological preservation potential which are exposed at the surface. Sampling risks are reduced because high science value target materials are widespread, reducing the need for landing accuracy and obviating the need for mobility. The samples collected date from the period when martian surface fluids evaporated from the surface, which has been identified as a science priority [e.g. 5,9,10,11,12].

References: [1] Osterloo, M.M., et al, 2008. *Science*, 319(5870), pp.1651-1654. [2] Osterloo, M.M., et al., 2010. *JGR: Planets*, 115(E10). [3] Hynek, B.M., et al, 2015. *Geology*, 43(9), pp.787-790. [4] Johnson, S.S., et al., 2020. *Astrobiology*, 20(2), pp.167-178. [5] Cockell, C.S., et al. 2020. *Astrobiology*, 20(7), pp.864-877. [6] Chan Q. H. S., et al. 2018. *Science Advances* 4, eaao3521. [7] Blamey, N.J. and Brand, U., 2019. *Gondwana Research*, 69, pp.163-176. [8] Lowenstein, T.K., et al., 2011. *GSA Today*, 21(1), pp.4-9. [9] Shkolyar, S. and Farmer, J.D., 2018. *Astrobiology*, 18(11), pp.1460-1478. [10] Wray, J.J., et al., 2009, In *AGU Fall Meeting Abstracts* (Vol. 2009, pp. P41B-06). [11] McCleese, D., Greeley, R. and MacPherson, G., 2001. *JPL Publication*, 1, pp.1-47. [12] Beaty, D.W., et al., 2019. *Meteoritics & Planetary Science*, 54, pp.S3-S152.

Investigating clay-brine interactions to inform interpretations of mineral assemblages on Mars C. Geyer¹, M.E. Elwood Madden¹, D. P. Mason^{1,2}, A.J. Rodriguez¹, and A.S. Elwood Madden¹, ¹University of Oklahoma (melwood@ou.edu), ²University of New Mexico.

Introduction: Despite the presence of both salts and clays on Mars, the effects of near-saturated brines on clay diagenesis and weathering remain poorly understood. Indeed, deposits with alternating clay- and sulfate-rich layers suggest briny solutions [1] have interacted with clay-rich layers in the past [2, 3]. In addition, if modern brines are active in the subsurface [4] or at the surface in areas with seasonal melting or deliquescence [5], they may continue to alter clay chemistry and mineralogy.

Here we report a series of short-term experiments mixing montmorillonite or kaolinite with near-saturated Mars analog brines and analyzing the reaction products with Raman spectroscopy and powder XRD to study the effects of brines on clay minerals. Two sets of experiments were conducted, the first were observations of immediate reactions between brines and clays at 295 K. The second set of experiments focused on simulating hydrothermal clay-brine reactions.

Methods: We mixed Clay Mineral Society Source clay standards, either SAz-1 montmorillonite, STx-1 montmorillonite, or KGa-1 kaolinite with near-saturated and serially diluted brines at 295K, then immediately analyzed the reaction products with Raman spectroscopy or XRD. Raman spectra were collected using a Renishaw InVia Raman Spectrometer with both 532 nm (green) and 785 nm (red) lasers and analyzed with Wire 4.1 software. XRD patterns were collected from smear slides using a Rigaku Ultima IV (Cu tube at 40 kV and 44mA) and data interpreted using MDI Jade 2010 with the ICDD PDF4+ database. All of the 295K experiments were analyzed within 10 hours of combining brines with clay.

We also mixed kaolinite (KGa-2) with a subset of the brines to simulate hydrothermal reactions. After 50 days the brines and clay were separated and powder XRD analysis was performed on the clays. Further hydrothermal experiments and Raman analyses are underway.

Results: Montmorillonite + Brine: Raman peaks indicative of each polyatomic anion (e.g. SO_4 , ClO_4) present in the brine were observed in the clay-brine mixtures. The montmorillonite starting material produces distinct Raman peaks at 201 cm^{-1} , 432 cm^{-1} , and 709 cm^{-1} [6], as well as at $\sim 1260\text{ cm}^{-1}$. These peaks indicative of montmorillonite are clearly visible both when the clay is dry and when it is mixed with UPW or brine (Figure 1a).

When the montmorillonite was mixed with sulfate-bearing brines, a new Raman peak appeared around 1010 cm^{-1} that is consistent with gypsum (Figure 1). This peak is not present in the unreacted clay, nor is it present in the spectra of the brines on their own. This suggests that gypsum precipitated almost immediately when the sulfate brines were mixed with the montmorillonite. This was confirmed in the XRD analyses as can be seen in Figure 2. From the XRD analysis we can see two additional mineral phases which are not observed in the original starting material: gypsum ($\sim 11.5\text{ }2\text{-}\theta$) and epsomite ($\sim 20.88\text{ }2\text{-}\theta$) [7, 8]. When epsomite is normalized out of the near-saturated MgSO_4 pattern it is clear that gypsum precipitation increases with increasing salt concentration. Similarly, gypsum abundance is highest in the near-saturated Na_2SO_4 brine and decreases in lower concentration brine experiments.

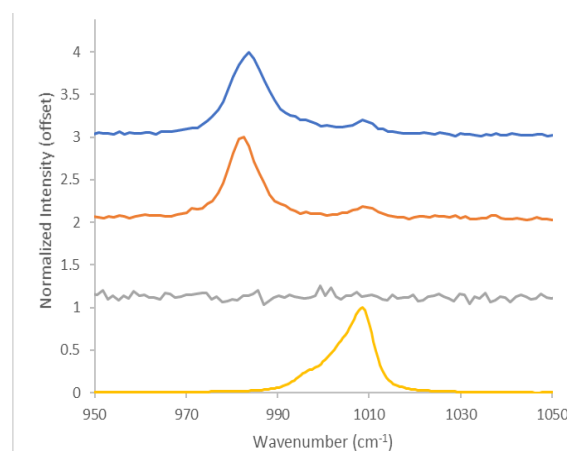


Figure 1 – Raman Spectra of Immediate Reactions. Top spectra (blue) was collected from montmorillonite mixed with near-saturated MgSO_4 brine, second (red) with NaSO_4 brine, and third (grey) with ultrapure water. The bottom (yellow) spectra is gypsum from the RUFF database.

Kaolinite + Brine: Kaolinite shows several distinct Raman peaks readily observable using the 532 nm green laser at approximately 3620 cm^{-1} and 3700 cm^{-1} . There is also an intense Raman peak around 140 cm^{-1} , similar to Raman bands observed in previous studies [9]. Sulfate and perchlorate peaks associated with ions in the brine were apparent in the kaolinite-brine mixtures. However, no significant changes were observed in the kaolinite or brine Raman spectra as a

result of mixing at 295K. Similarly, no new mineral phases were observed in XRD analyses observed in the 373 hydrothermal experiments.

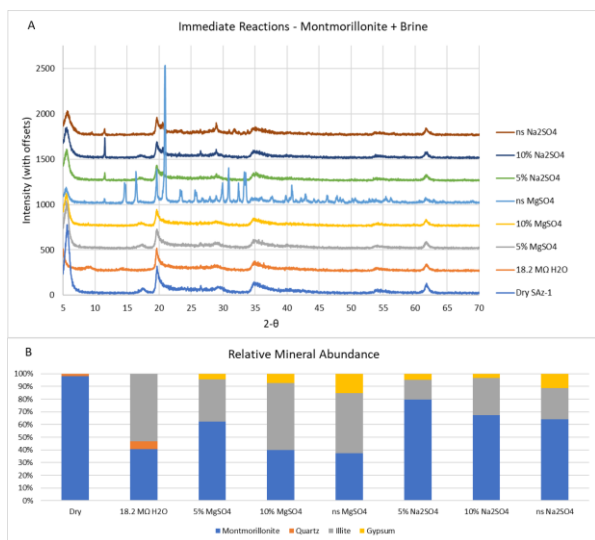


Figure 2 – XRD Analyses- Montmorillonite + Brine.

Cation exchange as a pathway to gypsum formation: The rapid gypsum precipitation observed in the montmorillonite-sulfate brine experiments was most likely a result of cation exchange reactions, where ions within the aqueous solution replace cations loosely bound within the clay interlayer. We hypothesize that the Mg^{2+} and Na^+ ions abundant in the sulfate brines exchanged with Ca^{2+} in the montmorillonite interlayer. Once the Ca^{2+} ions were released, they quickly reacted with the abundant SO_4^{2-} ions also present in the brine to precipitate gypsum.

Montmorillonite has a relatively high cation exchange capacity- 89 meq/100g- compared to kaolinite (3 meq/100g) [10]. Gypsum has also been observed forming in montmorillonites mixed with magnesium sulfate salts as they change hydration states, also likely due to cation exchange reactions [11].

Implications for Modern Brines on Mars: Widespread observations of sulfate minerals across the surface of Mars as well as in SNC meteorites demonstrate that sulfate-rich fluids have played a significant role in near-surface processes on Mars [12-16]. While the hydration state of the various calcium sulfate minerals found in veins on Mars is still being investigated [14, 17], it seems clear that a potential origin for these minerals may be cation exchange reactions that occur over very short time periods due to the mixing of clays and sulfate brines.

Observations of sulfate minerals in chondritic meteorites [18-20], as well as possible sulfate salts on icy moons [21, 22] further expand the range of sulfate-

fluid activity throughout the solar system. Indeed, sulfate-rich fluids have left their mark over much of Mars' surface, suggesting sulfate-water-rock interactions may be key to understanding volatile cycling and potential habitability on Mars and other planetary bodies [23-26]. The lack of apparent interactions between brines and kaolinite in contrast to the rapid precipitation of calcium and magnesium sulfate minerals, as seen in the results of this and other studies, is also important for interpretations of clay-bearing sediments on Mars. Compared to smectite, kaolinite appears to be robust in the presence of brines.

Acknowledgments: This project was partially funded by NASA PDART grant 80NSSC18K0512 and the University of Oklahoma.

References: [1] Rapin, W., et al., *Nature geoscience* (2019). [2] Michalski, J. and P.B. Niles, *Geology* (2012). [3] Bishop, J.L., et al., *Icarus* (2020). [4] Orosei, R., et al., *Science* (2018). [5] Heinz, J., et al., *Geophysical research letters* (2016). [6] Bishop, J.L. and E. Murad, *J. Raman Spectrosc.* (2004). [7] Tien, P. and T.C. Waugh, *Kansas Geological Survey* (1970). [8] Vaniman, D.T. and S.J. Chipera, *American Mineralogist* (2006). [9] Frost, R.L., *Clays and Clay Minerals* (1995). [10] Borden, D. and R. Giese, *Clays and Clay Minerals* (2001). [11] Wilson, S.A. and D.L. Bish, *J. Geophys. Res: Planets* (2011). [12] Squyres, S.W., et al., *Science* (2012). [13] Vaniman, D., et al., *Science* (2014). [14] Nachon, M., et al., *J. Geophys. Res: Planets* (2014). [15] Massé, M., et al., *Earth Planet. Sci. Lett* (2012). [16] Bridges, J.C., et al., *Space Science Reviews* (2001). [17] Rapin, W., et al., *Earth Planet. Sci. Lett* (2016). [18] Harries, D. and F. Langenhorst, *Meteorit Planet Sci.* (2013). [19] Izawa, M., et al., *Earth Planet. Sci. Lett* (2010). [20] Lauretta, D.S., X. Hua, and P.R. Buseck, *Geochim. Cosmochim. Acta* (2000). [21] McCord, T.B., G.B. Hansen, and C.A. Hibbitts, *Science* (2001). [22] Kargel, J.S., et al., *Icarus* (2000). [23] King, P., D. Lescinsky, and H. Nesbitt, *Geochim. Cosmochim. Acta* (2004). [24] Bibring, J.-P., et al., *Science* (2006). [25] Grotzinger, J.P., et al., *Science* (2014). [26] Michalski, J.R., et al., *Icarus* (2013).

Water-Activity Limit for Life As We Know It. J. E. Hallsworth¹. ¹Institute for Global Food Security, School of Biological Sciences, Queen's University Belfast, Northern Ireland, UK. E-mail: johnhallsworth@yahoo.com

Introduction: Life as we know it requires sufficient water to enable cellular hydration and function. This is dependent on the effective water concentration; the thermodynamic parameter 'water activity' which is based on Raoult's Law allocated a scale from 0 to 1 (and is dependent on temperature and pressure). Each individual cell, enzyme, biological process, etc has its own water-activity window for functionality and its own water-activity optimum. These values can be plastic to some degree because they depend on factors such as physiological condition and temperature. However, water activity imposes potent limits on active life even under conditions that are otherwise optimal.

Some terrestrial microbes – termed xerophiles – grow optimally at reduced water activity, and some of these – termed halophiles – are adapted to life in brines. Xerophiles have been described as those microbes able to grow below a water activity of 0.850 (under at least two sets of environmental conditions) and must also grow optimally below 0.950 [1]. Remarkably, species such as the ascomycete *Aspergillus penicillioides* are able to flourish at low water-activity in brines, at low relative humidity, or at high concentrations of other solutes including sugars. For such organisms, high-glycerol milieux are the most-permissive for growth and metabolism at low water-activity [2,3], whereas brines are more challenging [4].

Terrestrial brines are typically complex in their chemical composition and can fluctuate in their temperature, concentration, composition, water activity, pH, etc on timescales from seconds or minutes up to 1000s years or more. Furthermore, brines can exhibit numerous parameters that can cause cellular stress: low water activity, high osmolarity, chaotropicity, extremes of temperature or pH, exposure to ultra-violet radiation, lack of nutrients, etc [5]. Indeed, individual salts can impose multiple parameters that cause concomitant mechanistically diverse stresses to the cell [6]. Nevertheless, even within this complexity water activity remains a major determinant for terrestrial biology; and for the limitations of terrestrial biology.

Water Activity Limits for Active Life on Earth: Water-activity values, expressed as a fraction of 1, can seem small and insignificant yet cells are sensitive to changes of about ± 0.001 [7]. The past 100 years or so of culture-based growth studies has not yielded any verifiable evidence of microbial division below 0.585 water activity (= 58.5% relative humidity) [2,3,8-10]. Furthermore, differentiation and cell division have only been observed at 0.585 water activity for one species, *A. penicillioides*, and only at 24°C (297 K) [3]. According to reliable studies which yield empirical

data for microbial proliferation, the lowest water activity at which growth has been observed in brines is 0.635 (for halophilic archaea), at 37°C (310 K) [9]. No data indicate that any life-form can function at ≤ 0.585 water activity at temperatures far from 24°C (e.g., sub-zero, or temperatures over 50°C) or at other extremes (e.g., below pH 4 or above 9). Furthermore, there are no empirical data which show cellular metabolism at any water-activity values below 0.585, for any type of xerophile and regardless of the domain of life.

Bosch et al. [11] recently reassessed the metabolism of microbes during entry into and out of a desiccated (anhydrobiotic) state, including taxa living in high-salt desert soil crusts. The authors (of which I was one) present circumstantial evidence that DNA repair and other enzyme-mediated processes occur during anhydrobiosis, when the cytosol is < 0.250 water activity. It is already known that some enzymes can function well below the 0.585 water-activity limit for cell division [10]. The question is whether we regard these processes as cellular metabolism *per se*; for a discussion of this distinction, see Section 3.1 of Rummel et al. [12]. We know that some halophiles can survive desiccation–rehydration cycles; their long-term survival in an anhydrobiotic state can enable the colonisation of liquids-of-salt deliquescence here on Earth and, potentially, on Mars and other planetary bodies [13-15].

Saturated NaCl is Not so Extreme: The most-abundant salt in Earth's biosphere is NaCl, so this salt has in large part governed the evolutionary trajectory of terrestrial halophiles [16]. In relation to the scale of water activity over which some microbial cells can survive (0 to 1) and the window over which we know they can grow (0.585 to 1), the water activity of NaCl-saturated solutions is moderate [16]. For a temperature range of 0 to 50°C (1 atm), for example, a pure NaCl-saturated brine has water-activity values ranging from a modest 0.745 to 0.765 [17]. Brines with water-activity values lower than this (see below) are typically so chaotropic or acidic (and/or exhibit other extremes) that their water activity is not the life-limiting parameter; with very few exceptions [9]. As discussed by Lee et al. [16], natural selection to favour the evolution of halophiles that are more-xerophilic than those we currently know [9] has therefore been limited.

Testament to the thermodynamically moderate nature of NaCl-saturated brines, they host biodiverse and biomass-rich ecosystems consisting of all domains of life (see Table 1 of [16]). These ecosystems are capable of complete biogeochemical cycling, with complex ecologies which include predatory amoebae [16] and vampire bacteria [18, 19], as well as symbiotic nano-

haloarchaea [20] and halophilic viruses. Furthermore, there are higher organisms that can inhabit NaCl brines including nematodes [21], brine shrimps, and even fish (the Death Valley pupfish) [16]. By contrast, other types of terrestrial brines (as well as those elsewhere in the Solar System) are typically more-complex and more-hostile to life. These include low water-activity brines that are chaotropic or acidic.

Water Activity of Chaotropic Brines and Acidic Brines: Saturated solutions of salts such as MgCl₂, CaCl₂, and LiCl reduce water activity to levels way below that for pure NaCl. For example, at 5°C (278 K) saturated solutions of these salts have values of 0.345, 0.400, and 0.140, and at 25°C (298 K) 0.325, 0.295, and 0.012, respectively [17]. Unsurprisingly, there are no biological data to demonstrate active life in such brines either *in vitro* or in nature. Studies of mRNA in deep-sea, MgCl₂-dominated brines in the sub-saturated concentration range revealed that active microbial life is prevented at water-activity values above the limit for halophile activity in NaCl brines [22–24]. Furthermore, these and other studies [e.g., ref. 6] demonstrate conclusively that the limiting parameter is chaotropicity; the entropic disordering of cellular macromolecules [25, 26]. Addition of NaCl to these MgCl₂-rich brines can enable active life to resume because (even though the water activity is further reduced), the kosmotropicity of NaCl mitigates the chaotropicity of MgCl₂ [22]. MgCl₂ also reduces water activity, causes osmotic stress, and reduces pH but its chaotropicity is the most-potent cellular stress parameter, regardless of the domain of life [6, 9, 22]. Chaotropic substances (including salts) enable the flexibility of cellular macromolecules and thereby enhance biological activity at low temperatures [27, 28], as confirmed by recent studies of enzyme activity at 5°C in the presence of perchlorate salts [29].

Alkaline brines are not known to exhibit water-activity values lower than those for saturated NaCl. By contrast, the values for some acid brines can be extremely low. For example, the brine of Gneiss Lake (Western Australia) was measured to be 0.714 water activity (at the *in-situ* temperature of 34°C [307 K] and pH 1.4) [30]. This water-activity value is within the known window for cellular function of some halophiles; see above. However, we have no data to suggest that any microbe is able to function at this combination of extreme pH and low water-activity [31]. Whereas Gneiss Lake contains DNA and 16S rRNA of microbial communities, these are likely active only when the brine is diluted by rainwater; i.e., when the water activity is higher than 0.714. The most-acidophilic microorganism known is the archaeon *Picrophilus torridus*, which grows down to a pH of -0.06 (at 60°C, 333 K) [32]. However, this species is not halophilic. Furthermore, a recent analysis suggests that

its limited xerotolerance (there is no evidence that it can grow below 0.900 water activity), rather than its tolerance to acidity *per se*, is what constrains its ability to grow at even higher concentrations of acid [31].

Conclusions: Water activity, a cellular stress parameter independent of turgor [6] limits life in different types of habitat, not only brines [7–10, 31, 33, 34]. Whereas terrestrial life requires salts, it also requires sufficient water [7, 35] and whilst supra- or sub-optimal water activity can be highly stressful for cellular systems, stress is an inextricable and continuous aspect of life [36]. Terrestrial brine systems do not always emulate those found elsewhere in the Solar System, but do help us to understand the biophysical limits of microbial life. What may be less-well appreciated is that astrobiological approaches to scientific enquiry also help us understand the biology of present-day life here, on Earth [37].

References: [1] Pitt J. I. (1975) In: *Water Relations of Foods*, 273–307, Duckworth R. B. (Ed.). London: Academic Press. [2] Stevenson A. et al. (2017) *Environ. Microbiol.* 19, 947–967. [3] Stevenson A. et al. (2017) *Environ. Microbiol.* 19, 687–697. [4] Nazareth S. W. & Gonsalves V. (2014) *Front. Microbiol.* 5, 412. [5] Hallsworth J. E. (2019) *Nature Ecol. Evol.* 3, 1503–1504. [6] Alves F. L. (2019) *Curr. Genet.* 61, 457–477. [7] Stevenson A. et al. (2015) *ISME J.* 9, 1333–1351. [8] Pitt J. I. & Christian J. H. B. (1968) *Appl. Environ. Microbiol.* 16, 1853–1858. [9] Hallsworth J. E. (2019) *Environ. Microbiol.* 21, 2202–2211. [10] Stevenson A. et al. (2015) *Environ. Microbiol.* 2, 257–277. [11] Bosch A. et al. (2021) *Environ. Microbiol.* In press. doi.org/10.1111/1462-2920.15699. [12] Rummel J. D. et al. (2014) *Astrobiology* 14, 887–968. [13] Crits-Christoph A. et al. (2016) *Environ. Microbiol.* 18, 2064–2077. [14] Hallsworth J. E. (2020) *Nature Astron.* 4, 739–740. [15] Rivera-Valentín E. G. et al. (2021) *Nature Astron.* 4, 756–761. [16] Lee C. J. et al. (2018) *FEMS Microbiol. Rev.* 42, 672–693. [17] Winston P. W. & Bates D. H. (1960) *Ecology* 41, 232–237. [18] Moreira D. et al. (2021) *Nature Commun.* 12, 2454. [19] Yakimov M. M. et al. (2021) *Environ. Microbiol.* Submitted. [20] La Cono V. et al. (2020) *PNAS* 117, 20223–20234. [21] Jung J. et al. (2021) *BAS: Modern Brines 2021*, Abstract# 6012. [22] Hallsworth J. E. et al. (2007) *Environ. Microbiol.* 9, 801–813. [23] Yakimov M. M. et al. (2015) *Environ. Microbiol.* 17, 364–382. [24] La Cono V. et al. (2019) *Sci. Rep.* 9, 1679. [25] Cray J. A. et al. (2013) *Environ. Microbiol.* 15, 287–296. [26] Ball P. & Hallsworth J. E. (2015) *Phys. Chem. Chem. Phys.* 17, 8297–8305. [27] Chin J. P. et al. (2010) *PNAS* 107, 7835–7840. [28] Cray J. A. et al. (2015) *Curr. Opin. Biotechnol.* 33, 228–259. [29] Gault S. et al. (2021) *Sci. Rep.* 11, 16523. [30] Benison K. et al. (2021) *Astrobiology* 21, 729–740. [31] Hallsworth J. E. et al. (2021) *Nature Astron.* 5, 665–675. [32] Schleper C. et al. (1995) *J. Bacteriol. Res.* 177, 7050–7059. [33] Lievens et al. (2015) *Environ. Microbiol.* 17, 278–298. [34] Williams J. P. & Hallsworth J. E. (2009) *Environ. Microbiol.* 11, 3292–3308. [35] Ball, P. (2017) *PNAS* 114, 13327–13335. [36] Hallsworth J. E. (2018) *Fung. Biol.* 122, 379–385. [37] Hallsworth J. E. et al. (2021) *Environ. Microbiol.* 23, 3335–3344.

STRATEGIES FOR REMOTELY DETECTING CHLORINE SALTS ON MARS. J. Hanley^{1,2}, Z. Bandelier², S. Mittal^{3,2}, C. Murphy^{4,2}, R. Carmack², B. Horgan⁵. ¹Lowell Observatory, Flagstaff, AZ (jhanley@lowell.edu); ²Northern Arizona University, Flagstaff, AZ; ³Northeastern University, Boston, MA; ⁴Amherst College, Amherst, MA; ⁵Purdue University, West Lafayette, IN.

Introduction: The presence of chlorine salts on Mars is important for understanding the geological and chemical history of the planet, as the presence of chlorine salts can help us infer the chemistry and evaporation history of surface lakes and playas. Furthermore, the spectral similarity between perchlorates and sulfates raises the possibility that previous sulfate detections may actually be perchlorates (Fig. 1). This has major implications for habitability, as perchlorates indicate much lower water activity brines, which are less favorable for habitability than sulfates. This is because chloride, perchlorate, and chlorate salts can all suppress the freezing temperature of water significantly, in some cases with a eutectic temperature down to 204 K [1, 2]. They also slow down the evaporation rate, extending the lifetime of the liquid water solution.

Chlorine salts may also play a role in the mechanical properties of the regolith, as well as the stability of subsurface water. High soil cohesion was encountered at the Phoenix landing site making sample analysis challenging; such cohesion may result from hydrated salts and eutectic brines bonding grains together at their contacts by wetting, or from dehydrated salts crystallizing at grain contacts. Changes in hydration state with time (such as diurnally or seasonally) may then result in correlated changes in cohesive properties with time [3].

Although we know that chlorine salts exist on the surface at the Phoenix landing site, we do not know what their original hydration state or cation-anion pair was (e.g. Ca(ClO₄)₂·4H₂O vs NaClO₄ anhydrous vs Mg(ClO₃)₂·6H₂O vs NaCl, etc.). The biggest challenge to positively identifying and distinguishing these salts through remote sensing is that many hydrated salts look very similar in the near-infrared, even when comparing to sulfate salts [4, 5]. We have developed

new parameters specifically for identification and mapping of variations in the wavelength locations of absorption band minima in CRISM spectra [6]. Here we present strategies and discuss limitations for detecting chlorine salts through VNIR remote sensing spectroscopy.

Methods: The majority of CRISM analyses use spectral indices, however, these indices are not able to differentiate between spectrally similar minerals. For example, the SINDEXTM measures the convexity at 2.3 μm due to sulfate absorptions at 1.9/2.1 μm (poly/mono-hydrated sulfates) and 2.4 μm. This index, though, will also be positive for any hydrated mineral with a fall off toward 2.5 μm, like kaolinite. Likewise, hydrated minerals are often identified using the CRISM BD1900R parameter, which finds the average depth of absorption between 1.91-1.94 μm relative to ~1.86/2.12 μm; yet, this parameter is non-specific to a particular hydrated mineral.

New parameters indicative of hydrated perchlorates and oxychlorine salts (Table 1) [7], were created and utilized along with other common parameters [7]. Interesting features were then extracted and compared to known spectra to identify minerals present.

We have analyzed a variety of locations across Mars, including a likely paleolake in Columbus Crater, the north polar regions where Phoenix detected perchlorate, and Curiosity’s landing site at Gale Crater.

Results: High values displayed by these parameters allowed us to find the best spectra with absorptions unique to chlorine salts. These parameters often overlap with other spectral features of minerals commonly found on Mars, and care must be taken to look at the whole spectrum, rather than a single feature for identification, as well as mineralogical and geological context.

Table 1. Newly created spectral parameters. Formulation is based on Viviano-Beck et al. [7]. R#### is the reflectance at a given wavelength, kernel width is the number of channels over which the median of the reflectance was taken in order to reduce residual noise when applied to CRISM data. From [6].

Name	Parameter	Formulation	Kernel Width	Rationale	Caveats
BD2130	2.14 μm ClO ₄ -H ₂ O feature band depth*	$.5 * \left[1 - \frac{R2120}{a * R2030 + b * R2190} \right] + .5 * \left[1 - \frac{R2140}{a * R2030 + b * R2190} \right]$	R2030:5 R2120:3 R2140:3 R2190:5	Hydrous perchlorates	Orthopyroxene Alunite Gypsum Kaolinite Margarite
BD2220	2.2 μm Cl-O combination or overtone feature band depth*	$1 - \frac{R2220}{a * R2140 + b * R2320}$	R2140:5 R2220:3 R2320:5	Oxychlorine salts	Nontronite Talc Zeolite

In Columbus Crater, these parameters led to the identification of many spectra that have features suggestive of chlorine salts (Figure 1). However, pixels highlighted by BD2220 were sometimes false-positives caused by the similar wavelength features in phyllosilicates. The close wavelengths between the 2.22 μm feature in several chlorine salts and absorptions in phyllosilicates prevented identification of chlorine salts within the lower phyllosilicate-bearing unit. Spectra from two CRISM images have features unique to chlorine salts. Salts from 13FF5 and 16CFE have an absorption centered near 2.12 μm . $\text{CaCl}_2 \cdot 2\text{H}_2\text{O}$ and $\text{MgCl}_2 \cdot 4\text{H}_2\text{O}$ have similar absorptions at 2.12 μm . The CRISM spectra have a hydration absorption feature centered near 1.43 μm consistent with $\text{MgCl}_2 \cdot 6\text{H}_2\text{O}$, $\text{Mg}(\text{ClO}_3)_2 \cdot 2\text{H}_2\text{O}$, $\text{Mg}(\text{ClO}_3)_2 \cdot 6\text{H}_2\text{O}$, and $\text{CaCl}_2 \cdot 6\text{H}_2\text{O}$.

Within Gale Crater, A091 and 37DF showed strong absorptions at 1.9 μm , and 37DF showed an additional broad absorption at 2.13 μm . The parameter BD2130 used to look for the 2.13 μm absorption was intended to identify hydrated perchlorates. High-calcium pyroxene (HCP) exhibits features that are also highlighted by the BD2130 parameter, having absorption features near 1.03 μm and 2.3 μm [7]. Figure 2 shows the comparison and not perfect overlap of the HCP and oxychlorine parameters.

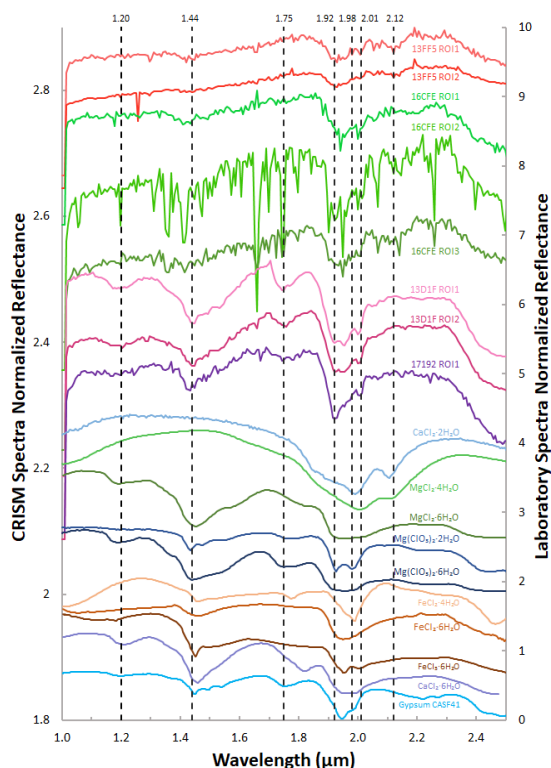


Figure 1. Comparison of CRISM spectra with lab spectra of Cl-salts [5, 6] and gypsum [CAT spectral library] All spectra are normalized and offset.

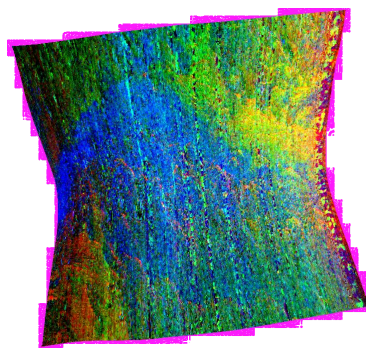


Figure 2. CRISM image 37DF in Gale Crater as a color composite with spectral parameters $R = \text{HCPINDEX2}$, $G = \text{BD2130}$, and $B = 1900_2$. The yellow region in the top-quadrant of the image shows areas of overlap between the HCP and ClO parameters.

The 1.9 μm absorption that was observed in 37DF and A091 is indicative of hydrated salts. After comparing the spectra from these sites to known lab spectra they were seen to most closely resembled $\text{MgSO}_4 \cdot 7\text{H}_2\text{O}$ and hydrated $\text{Ca}(\text{ClO})_2$.

In the north polar regions near the Phoenix landing site, where perchlorates were discovered, our study identified a lot of water ice, even in the summer, presumably buried at shallow depths. We also observed some features that indicate chlorine salts (Figure 3).

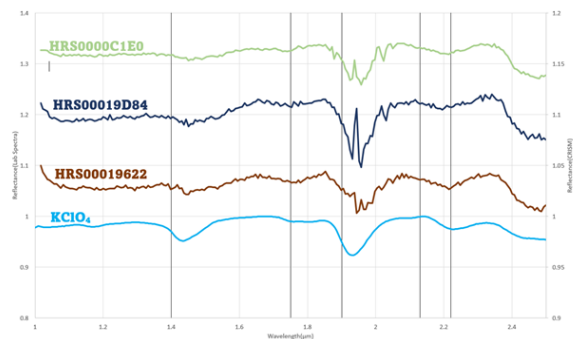


Figure 3. Interesting spectra from HRS0000C1E0, HRS00019D84, and HRS00019622 in the north polar regions plotted against KClO_4 . The plots have been normalized and offset for easier comparison.

Implications: Our new parameters aim to improve our ability to identify chlorine salts and differentiate between hydrated and anhydrous phases. Proper identification of these salts would give insight to the history of brines on Mars.

Acknowledgements: This work is funded by MDAP #NNX16AJ51G and Northern Arizona University's REU Program.

References: [1] Hanley J. et al (2012) *GRL* 39, L08201. [2] Chevrier V.F. et al (2009) *GRL* 36, L10202. [3] Hanley J. et al (2014). #2879. [4] Hanley J. et al (2015) *JGR* 120, 1415–1426. [5] Hanley J. et al (2014) *JGR* 119, 2370–2377. [6] Carmack R. et al (2019). *LPSC* Abstract #1701. [7] Viviano-Beck C.E. et al (2014) *JGR* 119, 2014JE004627. [8] Achilles C.N. et al (2017) *JGR* 122, 2344–2361.

To percolate or not to percolate? When are brines in planetary ice shells mobile? M. A. Hesse¹, N. S. Wolfenbarger², and C. McCarthy³, ¹Department of Geological Science, The University of Texas at Austin, Austin TX 78712, USA (e-mail address: mhesse@jsg.utexas.edu), ²Institute for Geophysics, University of Texas at Austin, J.J. Pickle Research Campus, Austin, TX 78758, USA, ³Lamont-Doherty Earth Observatory of Columbia University, Palisades, NY, 10964.

Introduction: Tidal heating is thought to sustain large subsurface oceans in several Jovian and Saturnian satellites and these icy ocean worlds are prime candidates in the search for extraterrestrial life within our solar system. The habitability of these internal oceans and thus our ability to detect life in them depends crucially on energy and material transport through the surrounding ice layers.

The migration of brines, generated by partial melting, has the potential to significantly affect both energy and material fluxes through these ice shells and hence their habitability. Yet, it is currently not clear under what circumstances brines are mobile within the ice. In particular, it is important to understand if brines are mobile at small porosities or if there is a percolation threshold for brine in ice.

Here we review two strands of evidence that come to opposite conclusions and discuss the implications for the habitability of icy ocean worlds. The first comes from observations of solidification of brines and the second partially melting of ice. Both processes occur during the evolution of the ice shell, suggesting that brine mobility may be process dependent.

Solidification textures: The textures that form during solidification of multi-component systems are highly dependent on freezing rate. At high rates but moderate undercooling, the solidification front experiences an instability that leads to elongated crystal growth and formation of a mushy layer [1]. This is contrasted with slow solidification, which allows formation of eutectic microstructures [2], or rapid solidification with large undercooling, which can form amorphous ice [3].

Brine channels in sea ice. The best example of the pore space resulting from rapid partial solidification is terrestrial sea ice. The formation of sea ice leads to the development of a “mushy layer” where salts entrained in the ice allow for liquid water to remain stable as brine below the pure ice pressure-melting temperature. Figure 1 a&b shows that the brine resides in elongate channels that are perpendicular to the solidification front. The rejection of salts from sea ice as seawater freezes involves a gravity-driven drainage process where brine is convectively overturned within a permeable layer adjacent to the ice-ocean interface.

Percolation threshold in sea ice. Below brine volume fractions of 0.05 the (vertical) permeability of sea ice decreases rapidly to detection levels (Figure 1c). Sea ice is therefore commonly assumed to have a percolation threshold. This has been confirmed

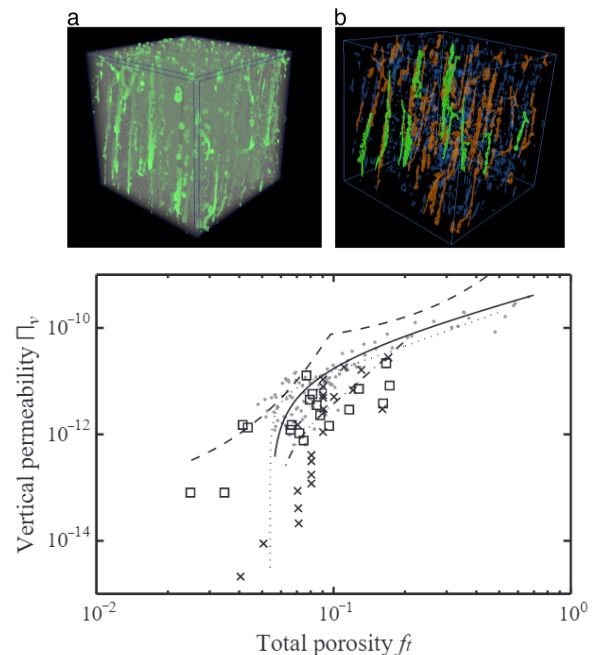


Figure 1. a & b) Brine channels in sea ice visualized with CT-microtomography [6]. c) Sea ice vertical permeability-porosity relationships and data from [7].

experimentally and justified theoretically [4], but is not used in all sea ice models [5]. This percolation threshold is thought to govern the bulk salinity of sea ice as it approaches equilibrium thickness, also referred to as the stable salinity. The brine layer width and spacing has been argued to influence the value of critical porosity, which governs this percolation threshold, suggesting granular marine ice and columnar sea ice may have distinct permeability-porosity relationships.

Low temperature gradient environments. A major criticism of examining sea ice desalination processes for planetary ice shells, is their vastly different formation conditions (temperature and pressure); however a recent work has shown that conditions beneath terrestrial ice shelves could be similar to the ice-ocean interfaces of Europa and Enceladus [8]. Columnar ice samples approaching these conditions showed evidence of strikingly similar stable salinities, demonstrating a percolation threshold likely exists even in low temperature gradient conditions [8]. Notably, one of these samples was from ice between 400 to 600 years old [9].

Partial melting textures: The melt distribution during partial melting is governed by energy minimization, due to the high homologous temperature of partially molten ice. This allows the textures to evolve towards equilibrium geometries that minimize surface energies. Partial melting generally leads to small porosities, so that the existence of a percolation threshold is particularly important

Textural equilibrium. At textural equilibrium the distribution and connectivity of the brine is determined by the ratio of the interfacial energies of solid-solid and the solid-liquid phase boundaries [10, 11]. This ratio can be expressed as the dihedral angle, θ , subtended at the corner of brine-filled pores and given by $\theta = 2 \arccos(\gamma_{ss}/\gamma_{sl})$ where γ_{sl} and γ_{ss} are the solid-liquid and solid-solid interfacial energies (Figure 2). Texturally equilibrated melt networks are connected at any porosity, if $\theta \leq 60$ [11, 12, 13, 14]. Laboratory studies have measured the dihedral angle of ice in contact with water [15], saline brine [16, 17], sulfuric acid [18], ammonia [19]. In all cases, the dihedral angle was between 20 and 60 degrees. This suggests that brines formed by partial melting in ice are mobile.

Further evidence for the connectivity of the brine at very small melt fractions comes from the mechanical and transport properties of ice. An interconnected melt phase allows for fast diffusion along grain boundaries to relieve stress concentrations. Without exception, experimental studies on ice containing a melt phase have shown a decrease in viscosity [20, 21, 22]. In fact, studies of ice doped with only trace amounts of sulfuric acid (1-15 ppm), found reduction in viscosity compared to undoped ice, suggesting that the critical melt fraction may be vanishingly small [23, 24].

Brine migration in ice shells. The evidence for lack of a percolation threshold together with the pronounced melting point depressions due to relevant salts, suggests that planetary ice shells experience partial melting and brine drainage in significant portions of the convecting ice shell.

Implications for habitability of ocean worlds:

Determining under what conditions brines experience a percolation threshold in ice is critical because it determines whether an ice shell starves or nourishes the underlying ocean. Solidification of the brine generally leads to such a percolation threshold as evidenced by sea ice. In contrast, partial melting of impure ice generally leads to a connected brine network. As such brine may be connected in regions of partial melting but disconnected near the base of the ice. Understanding how these two regions interact and how textures from both partial melting and solidification are modified by shearing due to solid state convection in the ice is therefore critical to assess the habitability of icy ocean worlds.

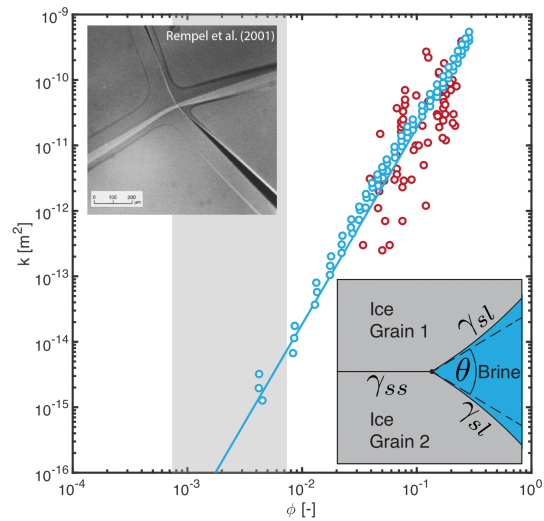


Figure 2. Comparison of porosity-permeability relations measured in sea-ice and computed for texturally equilibrated melt networks [14]. Lower insert shows the definition of the dihedral angle upper insert shows brine network in ice [25].

References: [1] Wells, A.J. et al. (2019) *Phil. Trans. Royal Soc. A* 377, 2146. [2] McCarthy C. et al. (2007) *Amer. Mineral.* 92, 1550-1560. [3] Cao, H.S (2021) *J. Phys. D: Appl. Phys.* 54, 203002. [4] Golden K.M., et al. (1998) *Science* 282(5397), 2238-2241. [5] Buffo, J.J. et al. (2021) *J. Geophys. Res.* 126(5). [6] Lieb-Lappen, R.M. (2017) *Cold Reg. SciTech* 138, 24-35. [7] Petrich, C. et al. (2006) *Cold Reg. SciTech* 44, 131-144. [8] Wolfenbarger N. et al (2021) *ESSOAr.10507059*. [9] Zotikov, I.A. et al, (1980) *Science* 207(4438). [10] Smith C. S. (1941) *Metal. Mater. Trans.*, 175, 15-51. [11] Nye J.F. and Frank F.C. (1973) *Hydrol. Sci. J.*, 95, 157-161. [12] Nye J. F. (1989) *J. Glaciol.*, 35(119) 17-22. [13] Ghanbarzadeh S. et al. (2014) *Phys. Rev. Lett.*, 113, 1-5. [14] Rudge, J.F. (2018) *Proc. Math. Phys. Eng.*, 474, 1-24. [15] Wettlaufer, J.S. (1999) *Proc. Math. Phys. Eng.*, 357, 3403-3425. [16] De La Chapelle S. et al, (1999) *Geophys. Res. Lett.* 26(2), 251-254. [17] Blackford, J.R. et al (2007) *Proc. Inst. Mech. Eng.*, 221(3), 151-156. [18] McCarthy, C. et al. (2013) *J. Micro.*, 249(2), 150-197. [19] McCarthy, C. et al. (2019) *Geosciences*, 9(8), 2019. [20] Durham W.B. et al., (1993) *J. Geophys. Res.* 98, 17,667-17,682. [21] Arakawa and Maeno, (1994) *Geophys. Res. Lett.* 21(14), 1515-1518. [22] DeLa Chapelle, S. et al. (1995) *Scripta Metal. Mater.* 33(3), 447-450. [23] Li, X. et al., (2009) *J. Glaciol* 55(191), 481-484; [24] Hammonds, K. et al. (2018). [25] Rempel, A.W. et al (2001) *Nature*, 411, 568-571.

FTIR-ATR SPECTRA AND XRD ANALYSIS OF AMORPHOUS SULFATE-CHLORIDE BRINE DESICCATION PRODUCTS AFTER MULTIPLE CONSECUTIVE DELIQUESCENT-DESICCATION CYCLES. R. J. Hopkins¹, A. D. Rogers¹, L. Ehm¹, and E. C. Sklute² ¹Department of Geosciences, Stony Brook University, 255 Earth and Space Science Building, Stony Brook, NY 11794. ²Planetary Science Institute, 1700 E. Fort Lowell Rd Ste 106, Tucson, AZ 85719. reed.hopkins@stonybrook.edu

Introduction: Amorphous materials represent a significant percentage (~15-70 wt%) of both drilled and scooped sediment samples analyzed by MSL Curiosity at Gale crater [1-6]. Estimates of the composition of the amorphous component in these samples show enrichment in sulfate and iron oxide [7], as well as the possibility of mixed-cation sulfate, phosphate, and chloride-perchlorate-chlorate amorphous salts [8]. This study focuses on mixtures of ferric sulfate and various chlorides. Chlorides have been found at the Phoenix landing site [9], as well as distributed globally on Mars [10]. Both chlorides and ferric sulfates are known to deliquesce at high relative humidity (RH), and rapid dehydration of these materials can lead to the formation of an amorphous solid [11,12]. The RH in the subsurface of Mars can go through large variations on both a diurnal and seasonal cycle, which may be favorable to subsurface brine formation [13-15]. These cycles may lead to repeating deliquescence-desiccation of salts and brines. Due to the possibility of both ferric sulfate and chlorides contributing to a Martian subsurface brine through deliquescence, it is important to consider mixtures of these brines, and the nature of their potential amorphous products after rapid dehydration. When studying these mixtures in a laboratory setting, it may also be important to consider multiple cycles of deliquescence and desiccation.

To this end, this study mixed ferric sulfate with various chlorides and put the mixtures through multiple deliquescence-desiccation cycles. At the end of each cycle, the desiccation products of the brine mixtures were analyzed with x-ray diffraction (XRD) and Fourier Transform Infrared (FTIR) spectroscopy.

Methods: The starting chlorides used in this study include $\text{MgCl}_2 \cdot 6\text{H}_2\text{O}$, $\text{FeCl}_2 \cdot 4\text{H}_2\text{O}$, $\text{FeCl}_3 \cdot 6\text{H}_2\text{O}$, $\text{CaCl}_2 \cdot 2\text{H}_2\text{O}$, and NaCl . Powders of each of these chlorides were mixed with powdered ferric sulfate, $\text{Fe}_2(\text{SO}_4)_3$. The ferric sulfate powder is formed by heating ferric sulfate hydrate at 350 °C for 2 hours. Each starting mixture consisted of 0.5 g of ferric sulfate mixed with 0.5 g of one of the five chlorides. To deliquesce, the mixtures were placed in air-tight containers buffered with deionized water, which stabilizes the RH at ~92%. Samples were desiccated in identical containers buffered with lithium chloride, which stabilizes the RH at ~11%. Instead of cycling between low and high RH with a set timeline, it was

determined that the timing of RH cycles would depend on when the samples were fully deliquesced or desiccated. Full deliquescence was determined qualitatively when the sample was entirely liquid. Full desiccation was determined when the sample returned to a powdered state, became hard and brittle, or a mix of both. Initial tests showed that it took a maximum of 3 days for all the samples to fully deliquesce, and 10 days to fully desiccate. The exception were samples containing magnesium chloride, which took multiple weeks to fully desiccate. Three batches of the five mixtures of ferric sulfate and a chloride were made. Each batch went through one, two, or three full deliquescence-desiccation cycles.

At the end of the last desiccation for each batch, the products were analyzed with FTIR spectroscopy and XRD. The FTIR instrument used was a Nicolet 6700 spectrometer with an attenuated total reflectance (ATR) Smart Orbit diamond attachment (330-4000 cm^{-1} , 2 cm^{-1} resolution, 128 scans). The XRD instrument used was a Rigaku Miniflex ($\text{CuK}\alpha$, 15mA, 40kV), optimized to reduce the fluorescence of iron-bearing samples. Any crystalline phases seen in the XRD patterns were identified using the Match! phase identification software, made by Crystal Impact.

One hypothesis was that that the products of the first desiccation may subsequently deliquesce differently than the initial heterogenous mixture. Additionally, a brine resulting from the deliquescence of an amorphous solid may have a different homogeneity than a brine resulting from a powder mixture, which may affect the morphology or crystallinity of the next desiccation.

Results: Overall, very little change was observed between compositionally equivalent samples through 1, 2, or 3 deliquescence-desiccation cycles, in both FTIR spectra and XRD patterns. In some samples, specific absorptions in the FTIR spectra are slightly shifted to lower wavenumbers with additional cycles. The FTIR spectra of the $\text{Fe}_2(\text{SO}_4)_3 - \text{CaCl}_2 \cdot 2\text{H}_2\text{O}$ mixtures after 1, 2, and 3 cycles are shown in Figure 1, as these samples had the most spectral variation. For this composition, the samples after 1 and 2 cycles are nearly identical, while the sample after 3 cycles has clearer differences in adsorption features. All three spectra show absorptions of gypsum, but the 3-cycle sample is missing a key absorption at ~1680 cm^{-1} (Fig. 1A). Additionally, the 3-cycle sample has an absorption at ~1145 cm^{-1} that is not obvious in the 1 and 2 cycle

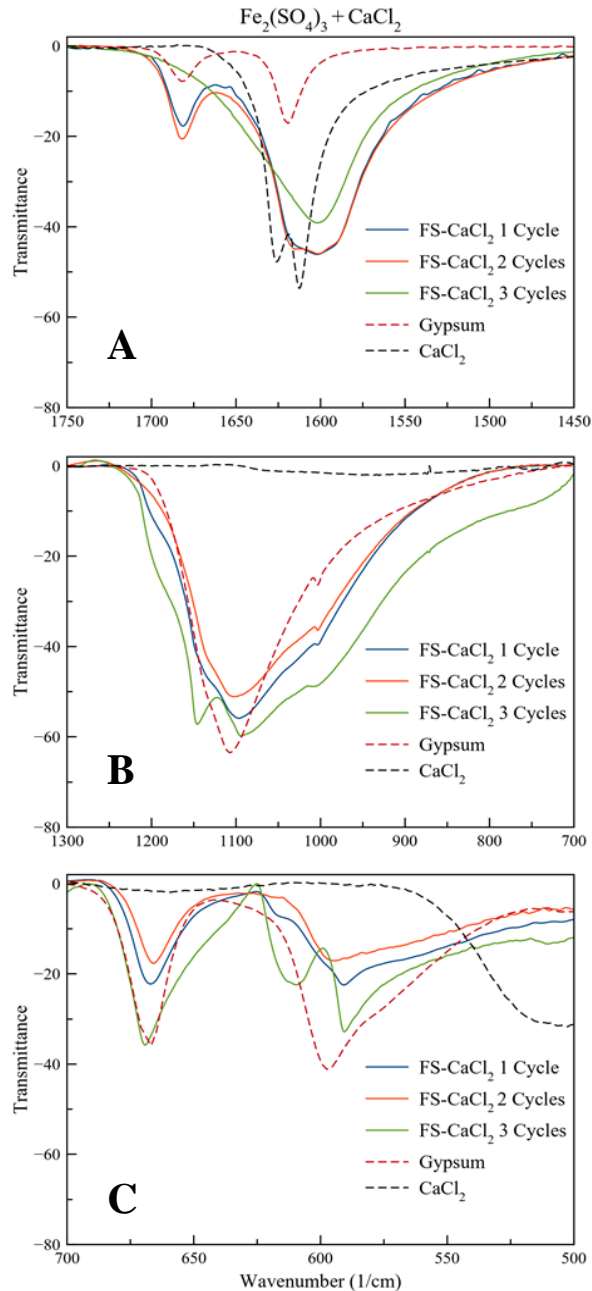


Figure 1. FTIR spectra, in three wavenumber regions, of the ferric sulfate (FS) and calcium chloride mixture desiccation products through 1, 2, and 3 cycles.

spectra, but may be present in these spectra as a shoulder (Fig. 1B). The same is true for the absorption at ~610 cm⁻¹, which is also only found in the 3-cycle sample (Fig. 1C).

There is even less variation in the XRD patterns of samples after 1, 2, or 3 cycles. The ferric sulfate control sample, and the mixtures with FeCl₃·6H₂O both resulted in an entirely amorphous material for all experiments, regardless of number of cycles. The other samples

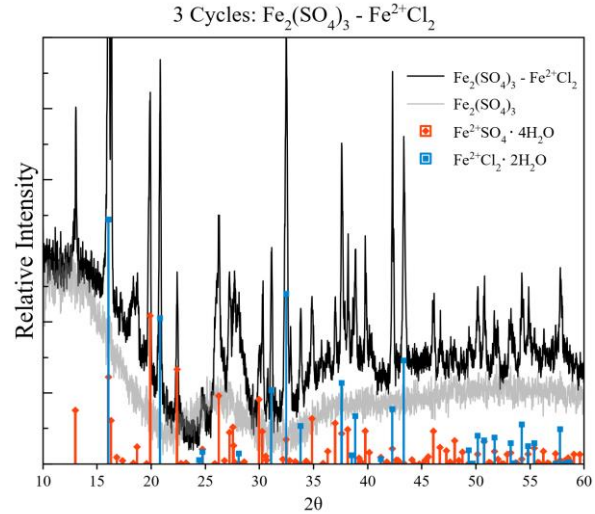


Figure 2. XRD patterns of the ferric sulfate and ferrous chloride mixture (black) and the ferric sulfate control (grey) after 3 cycles. The red and blue peaks are those associated with hydrated ferrous sulfate and hydrated ferrous chloride, respectively

resulted in a mixture of amorphous and crystalline material after each desiccation. For these mixed XRD patterns, the amorphous component can be mostly attributed to amorphous ferric sulfate. An example of this is given in Figure 2, which shows the XRD pattern of the Fe₂(SO₄)₃ - FeCl₂·4H₂O mixture after a 3rd desiccation of 3 cycles. The sample product is a combination of amorphous ferric sulfate, hydrated ferrous sulfate, and hydrated ferrous chloride.

Conclusions: Aside from minor changes in the FTIR spectra of some samples, there is no substantial difference between samples that underwent a different number of full deliquescence-desiccation cycles. While there is more research required on this topic, this study increases the confidence of only performing one deliquescence-desiccation cycle on chloride and ferric sulfate mixtures in future studies.

References: [1] Achilles N. C. et al. (2017) *JGR*, 122, 2344-2361. [2] Achilles N. C. et al. (2017) *GSA Annual*, 49. [3] Bish D. L. (2013) *Science*, 341, 6153. [4] Rampe E. B. et al. (2017) *EPSL*, 471, 172-185. [5] Vaniman D. T. et al. (2014) *Science*, 343, 6169. [6] Yen A. S. et al. (2017) *EPSL*, 471, 186-198. [7] Dehouck E. et al. (2014) *JGR*, 119, 2640-2657. [8] Morris R. V. (2016) *PNAS*, 113, 7071-7076. [9] Hecht H. M. et al. (2009) *Science*, 325, 64-67. [10] Osterloo M. M. et al. (2010) *JGR*, 115, E10. [11] Sklute E. C. et al. (2015) *JGR*, 120, 809-830. [12] Sklute E. C. et al. (2018) *Icarus*, 302, 285-295. [13] Fischer E. et al. (2019) *JGR*, 124, 2780-2792. [14] Fischer E. et al. (2016) *Astrobiology*, 16, 937-948. [15] Rivera-Valentín E. G. et al. (2018) *JGR*, 123, 1156-1167.

EXPERIMENTAL EVAPORATION OF MULTICOMPONENT BRINES DEMONSTRATES VARIABILITY IN SALT IDENTIFICATION. E. B. Hughes^{1,2} M. S. Gilmore², and M. Eleazer³ ¹Dept. of Earth and Atmospheric Sciences, Georgia Institute of Technology, Atlanta, GA, 30332, ²Dept. of Earth and Environmental Sciences, ³Astronomy Dept., Wesleyan University, Middletown, CT, 06459. Email contact: ehughes36@gatech.edu

Introduction: Salts have been identified widely on Mars, demonstrating that brine activity was once relatively pervasive; brines may also be transiently forming on the surface of Mars today [1-3]. Here we perform evaporation experiments at Mars condition to examine the evaporation pathways of Mars-relevant multicomponent brines. We examine the relationship between martian brine chemistry, precipitating salt assemblages and their detection. We characterize precipitates via Visible to Near Infrared (VNIR) spectroscopy and Raman spectroscopy, which are relevant to MRO CRISM data and Mars2020 rover instrumentation.

Brine Development and Creation: Brine recipes were derived from literature describing potential compositions of modern and ancient martian brines. All recipes included mixed anion and cation compositions; described here are two SO₄/Cl mixed brine recipes. Each composition was modeled to higher concentrations using the low-temperature evaporation modeling program FREZCHEM9.2 [4]. This model also provided a prediction of expected precipitates.

Recipes with unbalanced ionic compositions were balanced, and brines were made by dissolving soluble salts in 200 mL solutions to achieve the desired recipe molalities. Once fully dissolved, brines were separated into two beakers containing 100 mL of solution each, one of which was placed in a laboratory hood under ambient terrestrial conditions, and the other was placed in a Martian Analogue Chamber (MAC).

Evaporation Experiment: The MAC is designed to mimic modern martian surface conditions in the equatorial regions during the martian summer. The chamber was kept near 0°C throughout the experiment with a CO₂ atmosphere of 6 millibar. Upon reaching complete evaporation, the samples were analyzed using VNIR spectroscopy, Raman spectroscopy and in the case of terrestrially evaporated brines, X-Ray Diffraction (XRD). The instruments used were a ASD FieldSpecPro, a Bruker Bravo Raman Spectrometer, and a Philips Diffractometer coupled with an Enraf-Nonius X-ray Generator, respectively. Precipitates formed under martian conditions were analyzed in a glove box under ultra-dry N₂ to prevent atmospherically induced spectral absorptions or alteration to the salts.

Results: We observe differences between the model-predicted salt assemblages and the physical assemblages, as well as differences in salts identified

across methods. Here we discuss results from two brines.

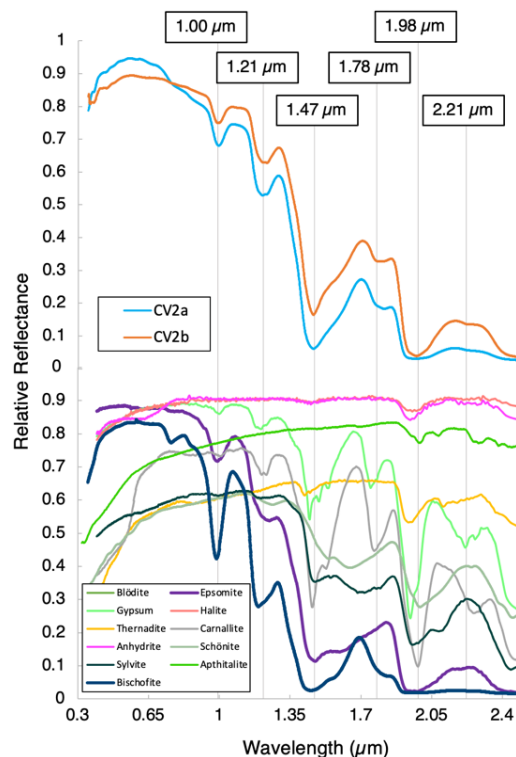


Figure 1. VNIR spectra of CV2a and CV2b; bischofite is present in both samples.

Clark and Van Hart [5] Brine 2: CV2a (evaporated under terrestrial conditions) was modeled to form approx. 43 wt.% carnallite (KMgCl₃•6H₂O), 24 wt.% hexahydrate (MgSO₄•6H₂O), 22 wt.% bischofite (MgCl₂•6H₂O), and 11 wt.% halite (NaCl); CV2b (evaporated under martian conditions) was modeled to precipitate 37 wt.% epsomite (MgSO₄•7H₂O), 27 wt.% bischofite, 17 wt.% carnallite, 14 wt.% halite and 5 wt.% sylvite (KCl). Differences in predicted assemblage are due to the stability of various salts under colder temperatures (e.g., hexahydrate is more stable under higher temperatures than epsomite). Carnallite dominated the predicted assemblage but was not positively identified via any method for either sample. In VNIR analysis, only bischofite, predicted to make up less than a quarter mass of the salt assemblage for both brines, was confirmed for both samples (fig. 1). Raman spectra confirmed the presence of only epsomite for each sample, with all other modeled salts unidentified.

ble (fig. 3). In XRD analysis, only halite was identifiable.

Marion and Kargel [4] Brine: MKCa (evaporated under terrestrial conditions) was modeled to precipitate 55 wt.% halite, 31 wt.% blödite ($\text{Na}_2\text{Mg}(\text{SO}_4)_2 \cdot 4\text{H}_2\text{O}$), 7 wt.% schönite ($\text{K}_2\text{Mg}(\text{SO}_4)_2 \cdot 6\text{H}_2\text{O}$), 4 wt.% aphthitalite ($\text{Na}_2\text{SO}_4 \cdot 3\text{K}_2\text{SO}_4$), and 2 wt.% arcanite (K_2SO_4). MKCb (evaporated under martian conditions) was modeled to precipitate 45 wt.% halite, 26 wt.% mirabilite ($\text{Na}_2\text{SO}_4 \cdot 10\text{H}_2\text{O}$), 16 wt.% schönite, and 12 wt.% epsomite. Differences in modeled assemblages are due primarily to the modeled stability of blödite under Earth conditions, and its instability under martian conditions, where Mg, SO_4 , and Na ions would be partitioned into mirabilite and epsomite rather than blödite. In VNIR analysis, schönite and epsomite were likely identified for MKCa and schönite, blödite and epsomite were likely identified for MKCb (fig. 2). In Raman data, schönite was confirmed and epsomite was probably confirmed for MKCa, and schönite and epsomite were both probably confirmed for MKCb (fig. 3). Only halite was confirmed via XRD analysis.

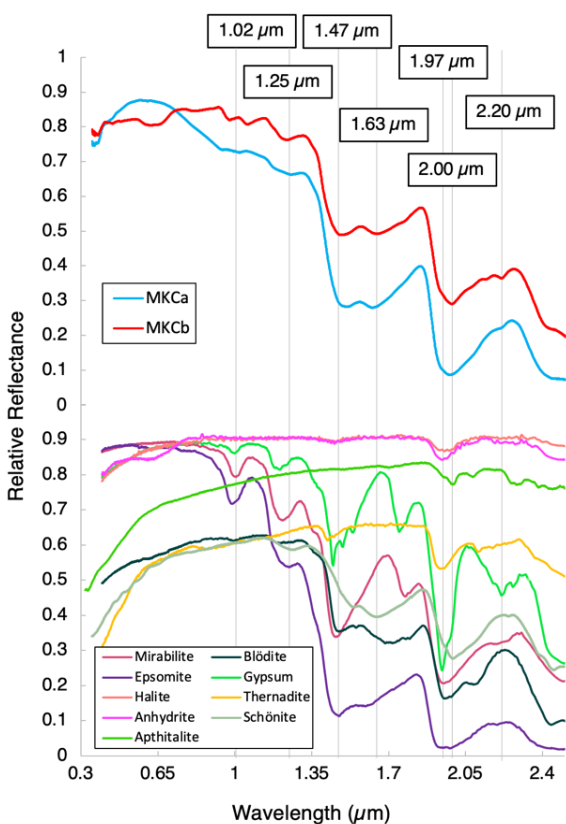


Figure 2. VNIR spectra of MKCa and MKCb; schönite and epsomite are probably present in both samples, and blödite is also probably present in MKCb.

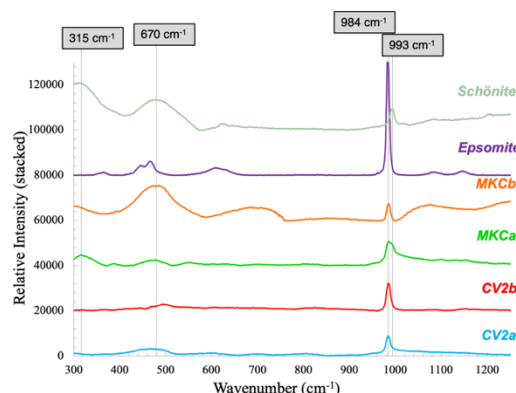


Figure 3. Raman spectra for MKC and CV2.

Discussion: The FREZCHEM model, based on Pitzer thermodynamic equation parameters, predicts that salts with higher hydration states should be more stable under colder conditions, and that mixed cation salts are generally stable under warmer earth conditions but unstable under colder martian conditions. Our experiments indicate that salts formed under Earth conditions are similar to those formed under martian conditions, suggesting that in multicomponent brines, the precipitation pathways do not necessarily follow thermodynamic predictions. It is unclear whether this is due to presence of additional cations, the speed of evaporation or another environmental variable.

Identification method plays a pivotal role in identifiable salt for multicomponent brines. For MKC and CV2, no two methods of identification shared precisely the same IDs. Halite goes unidentified via spectral observation (due to its lack of absorptions in the VNIR and Raman spectral ranges), but other salts are not identifiable via XRD analysis.

Implications for Mars: Based on our experimental work, multicomponent brines evaporating under martian conditions may be more likely to adhere to the modeled predictions than terrestrially evaporated brines. However, utilizing multiple identification methods is key to identifying the full range of potentially present minerals. It is possible significant amounts of halides are present on Mars but go spectrally identifiable when intimately or spectrally mixed with salts with higher hydration states.

Acknowledgments: Thanks to Dr. Darby Dyar and Dr. Peter Martin.

References: [1] Ehlmann and Edwards (2014) *Annu. Rev. Earth Planet. Sci.* 42, 291. [2] Rivera-Valentín et al. (2020) *Nature Astro.* 4, 756-761 [3] Tosca et al. (2005) *EPSL* 240, 122-148 [4] Marion and Kargel (2008) *Adv. in Astrobio. and Biogeophys.* Springer-Verlag Berlin. [5] Clark and Van Hart (1981) *Icarus* 45, 370.

Multicellular life in brine: Nematodes in the Great Salt Lake. J. Jung¹, T. Loschko¹, M. S. Werner¹

¹University of Utah, School of Biological Sciences, 257 South 1400 East, 201, Salt Lake City, UT 84112, michael.werner@utah.edu.

Introduction: Saline lakes (>3 g/L) are formed in terminal drainage basins when evaporation exceeds precipitation [1]. In hypersaline conditions (>50 g/L) the osmotic balance in plant tissue and animal blood or hemolymph is overwhelmed. Thus, geological, climatic, and anthropogenic forces that promote the formation of saline lakes can lead to mass extinctions of flora and fauna [2–4]. Remarkably however, small roundworms (nematodes) were recently found in Mono Lake, an arsenic-rich saline lake in California [5]. Nematodes are a remarkably successful and ancient phylum: they are the most abundant animals on Earth, they have been thawed (alive) from ~30,000-year-old ice, and can be found in the driest and coldest environments on our planet. Yet, the generality of these findings, i.e. the prevalence of nematodes in saline or hypersaline lakes, is currently unknown. More broadly, the adaptive potential of multicellular organisms to survive shifts to saline environments is poorly understood. Revealing these principles may also reveal the resiliency of multicellular organisms to drying lakes on Earth [6], and the possibility of complex life to exist in brines throughout our solar system [7,8].

One key to answering these questions is to identify biotic and chemical interactions between different trophic levels. Chemoautotrophs and photosynthetic bacteria can serve critical functions as primary producers in environments that are too harsh for plants [9]. In turn non-autotrophic bacteria, fungi and nematodes can promote ecosystem health by making nitrogen available to primary producers [10,11]. However, the evolution and stability of lake sediment ecosystems to rapidly changing salinities is unknown. To address these questions, we investigated whether nematodes or other microfauna inhabit the Great Salt Lake in Utah, a saline remnant of a massive ice-age freshwater lake.

Results: To date, only microbes, brine shrimp and brine flies are thought to inhabit the Great Salt Lake. We have acquired the first evidence that nematodes also reside there, including sites in brackish delta from freshwater inflows, to lake sediment approaching 16% salinity (Figure 1A-B). Notably, this is considerably higher than ocean water (3.5%) or recently sampled sediment from Mono Lake (0.01-3.4%)[5]. We also found a dramatic drop off in diversity with increased salinity (Figure 1C), consistent with specific adaptation to an extreme environment. Genotyping reveals that

nematodes from the most saline parts of the lake represent a new species of Monhysteridae – an ancient family of nematodes that is found in brackish waters. Finally, we have also found a strong correlation of nematode abundance with the presence of microbialites, benthic carbonate sediments formed by bacteria. Fossil evidence of microbialites date back to ~3.5 billion years ago and are among the earliest evidence of life on Earth [13]. We are currently genotyping nematode-associated microbes to assess whether they are grazing on the associated archaeal and prokaryotic bacteria that comprise microbialites. Collectively, these results demonstrate that nematodes commonly inhabit brine environments, that we haven't yet reached the limit of their tolerance to salinity, and that their ecology may be similar to that of an early earth ecosystem.

References: [1] Hammer U.T. (1986) *Saline Lake Ecosystems of the World*. [2] Weissflog L. et al. (2009) *Earth Sci.*, 425, 291–295. [3] Beutel M.W., et al. (2001) *Dordrecht*, 91–105. [4] Ermakhanov Z.K., et al. (2012) *Lakes Reserv.*, 17, 3–9. [5] Shih P.Y., et al. (2019) *Curr Biol.*, 29, 3339–3344. [6] Wurtsbaugh W.A., et al. (2017) *Nat Geosci.*, 10, 816–821. [7] Lauro S.E., et al. (2021) *Nature Astronomy*, 63–70. [8] Perl S.M., Baxter B.K. (2020) *Great Salt Lake Biology*, 487–514. [9] Jasser I. (2006) *Ecohydrology & Hydrobiology*, 69–77. [10] Martínez-Espinosa R.M., et al. (2020) *Int J Mol Sci.*, 21. [11] Ekschmitt K., et al. (1999) *Plant Soil*, 212: 45–61. [12] Oviatt C.G., Shroder J.F. (2016) *Lake Bonneville: A Scientific Update*. [13] Noffke, et al. (2013) *Astrobiology*, 12, 1103–1124.

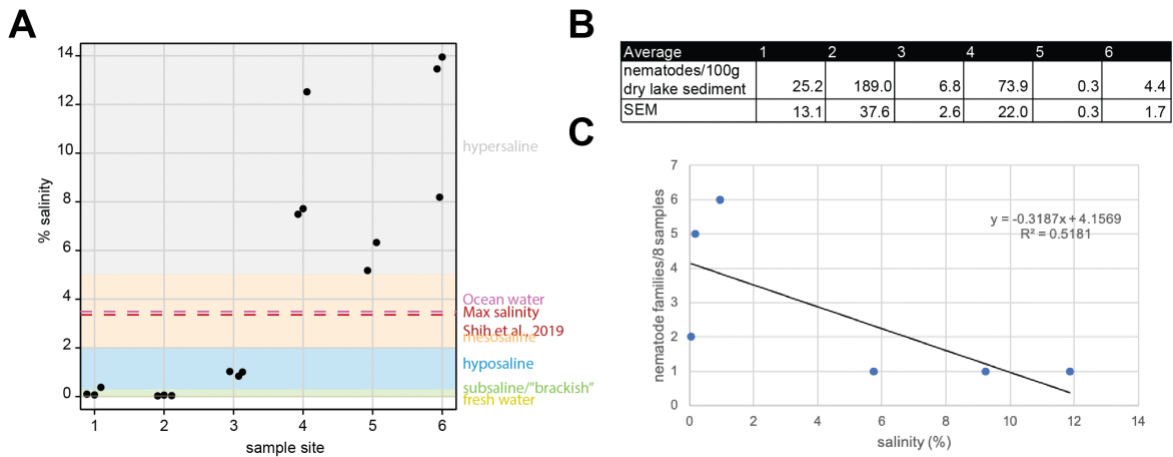


Figure 1: (A) Salinity of sample sites from the Great Salt Lake. (B) Average abundance and standard error mean (SEM) of nematodes from different sample sites per 100g dry sediment. (C) Family diversity of nematodes plotted against salinity. Family taxa were identified by Sanger Sequencing 500 nucleotides of the small subunit ribosomal DNA (SSU).

Patterns of horizontal gene transfer within microbial community succession in evaporative brine systems.

B. Klempay¹, A. Dutta¹, M. M. Weng², P. T. Doran³, L. A. Fisher¹, S. M. Rundell⁴, D. H. Bartlett¹, C. E. Carr⁵, C. E. Elbon⁵, J. B. Glass⁵, A. Pontefract², B. E. Schmidt⁶, and J. S. Bowman¹, ¹University of California San Diego, ²Georgetown University, ³Louisiana State University, ⁴University of Washington, ⁵Georgia Institute of Technology, ⁶Cornell University.

Introduction: As remnant ocean worlds (such as Mars) transition from wet to dry, their residual liquid waters eventually accumulate high concentrations of dissolved salts via evapoconcentration. Life in these evaporative brines must adapt to constantly changing and increasingly stressful environmental conditions; as the various salt species gradually become saturated, they precipitate one-by-one, drastically altering the geochemistry of the remaining brine [1]. We investigated how the microbial community coevolves with this geochemical succession in one terrestrial evaporative brine system: a solar salt harvesting facility in Chula Vista, California, where seawater is evaporated in a series of shallow ponds, forming a broad geochemical gradient from seawater to highly chaotropic, MgCl₂-saturated brines.

Microbial community succession: Using environmental 16S amplicon sequencing, we discovered that the microbial community succession in these salterns was driven primarily by the water activity (a_w) of the brines and took place in three distinct stages. The first stage ($1 \geq a_w \geq 0.7$) was characterized by an explosion of abundance and diversity of closely related haloarchaea, which dominate hypersaline brines globally. The second stage ($0.7 \geq a_w \geq 0.64$) was characterized by progressively more intense selection pressure and dwindling survival as water activity approached limit of life. At the very edge of the habitable window, the microbial community was dominated by a single taxon, *Haloquadratum walsbyi*. Finally, the conditions within the brines became too harsh for active microbial life. This third and final stage ($a_w \leq 0.64$) was characterized by a ‘fossil’ microbial community: preserved cell remnants and exogenous genetic material [2].

Evidence of horizontal gene transfer: We used shotgun metagenomic sequencing to further investigate the surge of haloarchaeal microdiversity observed in stage 1, with particular interest given to the role of horizontal gene transfer (HGT). Haloarchaea—especially *Halorubrum* and *Haloarcula*—are known for frequent recombination and HGT, leading to high intragenus and intraspecific diversity [3, 4]. We therefore hypothesized that evidence of HGT found within the saltern metagenomes would correlate closely with haloarchaeal diversity. However, our preliminary results suggest instead that the surge in

microdiversity described in stage 1 actually lags the peak in HGT. The frequencies of genes annotated as either mobile genetic elements or HGT agents share a pronounced maximum c. $a_w = 0.92$, much earlier within the evaporitic geochemical succession than the peak in haloarchaeal diversity ($a_w \approx 0.7$). This suggests that while HGT might initiate the surge of microdiversity, it is maintained and expanded by other ecological processes (e.g., niche partitioning or viral infection). Further investigation will focus on identifying specific genes that are frequent targets for HGT, and whether certain variants of those genes confer adaptive benefits to their hosts, allowing them to survive better in increasingly harsh, hypersaline brines.

Broader significance: Terrestrial evaporative brine systems are valuable analogues for Mars’s ancient receding oceans. On Mars, and other remnant ocean worlds, hypersaline brines could have been among the last refugia of life, making them promising targets in the search for extinct and extant extraterrestrial life. Understanding how life on Earth adapts to the constantly changing brine chemistries in terrestrial analogue environments is therefore essential to the search for life on Mars and elsewhere.

Acknowledgments: This work was part of the Oceans Across Space and Time (OAST) project, funded by NASA’s Astrobiology Program award 80NSSC18K1301 (PI: B. E. Schmidt). We are grateful to the entire OAST team for their support and expertise. We also thank the South Bay Salt Works and Brian Collins at the San Diego Bay National Wildlife Refuge for facilitating this effort.

References: [1] Tosca N. J., Knoll A. H., and McLennan S. M. (2008) *Science*, 320, 1204–1208. [2] Klempay B. *et al.* (2021) *Environ. Microbiol.*, 23(7), 3825–3839 [3] Ram Mohan N. *et al.* (2014) *Front. Microbiol.*, 5(143), [4] Papke R. T. *et al.* (2004) *Science*, 353, 1928–1930.

GUESS WHO'S COMING TO DINNER: INVESTIGATING THE POTENTIAL OF (PER)CHLORATE SUPPORTED ECOSYSTEMS ON MARS. K. L. Lynch^{1,3}, A. Simpson², S. Machineni³, L. Santiago-Vazquez³, C. Goodale⁴, J. Lopez³; ¹Lunar and Planetary Institute (USRA), Houston, TX 77058, ²Jet Propulsion Laboratory, Pasadena, CA 91109, ³Department of Biology & Biotechnology, University of Houston Clear Lake, Houston TX, 77058, ⁴The Evergreen State College, Olympia, WA 98505

Introduction: One of the main astrobiological goals of the Mars exploration program is to fully understand the extent of habitable environments on the red planet, which includes determining all the potential energy sources that could support microbial ecosystems. Yet, there has been sparse analog study of one of the most abundant and energetic metabolic martian resource: perchlorate. This is because, until recently, there has been no documented evidence of naturally occurring perchlorate (NOP) and perchlorate-reducing microorganisms (PRMs) co-existing in a relevant Mars analog environment. Recent work has now demonstrated the coexistence of PRMs with (NOP) in the Pilot Valley Basin Mars analog environment and more detailed study is underway to understand the characteristics of microbial (per)chlorate reduction in this relevant Mars analog environment as a guide to elucidating the possible influence of chlorine oxyanions on habitability and life on the red planet [1].

Perchlorate was first discovered on Mars during the 2008 Phoenix lander mission [2] and was subsequently inferred to have been present in soils examined by both Viking landers in 1976 [3]. Recent analyses by the Sample Analysis at Mars (SAM) instrument onboard the *Curiosity* rover provided the most detailed information about perchlorate presence on Mars. The SAM analysis detected 0.05-1wt% perchlorate in the samples drilled in Gale crater. The detected perchlorate likely exists as salts physically mixed with minerals and/or adsorbed on mineral surfaces. Beside perchlorate, chloride and chlorate are also present in Gale crater [4]. Laboratory analysis of analog samples run under SAM-like conditions indicated that chlorate salts mixed with Fe(III) oxides and phyllosilicates can exist in Gale crater [5, 6]. The presence of chlorides in Gale crater has been inferred from an observation that chlorine content estimated from the SAM measurements of perchlorate and/or chlorate is always lower than the total chlorine measured by the Alpha Particle X-ray Spectrometer [7]. Collectively, these observations revealed that chlorine in all three oxidation states is present in Gale crater. Further, (per)chlorates have also been identified in both chondritic and Martian meteorites as well as lunar samples, thereby indicating the potential ubiquity of (per)chlorate salts in the solar system [8, 9].

The presence of oxychlorine and chloride species can therefore indicate that a complex chlorine biogeochemical cycle was once active on Mars. In

particular, (per)chlorate may have helped support life during the planet's wet past as a terminal electron acceptor, and possibly could still support life in the shallow subsurface (1m to 10m).

To assess the possibility of perchlorate-supported ecosystems on Mars, it is vital to understand these systems on Earth. Hence, an interdisciplinary study is underway to explore whether and how a (per)chlorate-based microbial chlorine cycle is driven in the basin sediments of Pilot Valley and could serve as a biogeochemical model for Mars.

Geochemical Modeling: The goal of the geochemical modeling portion of the study was to investigate the energetic potential for active biological perchlorate reduction in the Pilot Valley Mars analog and also under Mars environmental conditions using the PHREEQC geochemical modeling software package.

Pilot Valley is a paleolake basin analogous to those found on Mars in terms of aqueous mineral composition, and has special astrobiological relevance because like Mars, it contains naturally occurring perchlorate salts. PV is also home to the first reported instance of perchlorate reducing microbes (PRM) co-occurring with natural sources of perchlorate. Results of modelling in Pilot Valley indicate high favorability for active perchlorate reduction using multiple electron donors (Figure 1).

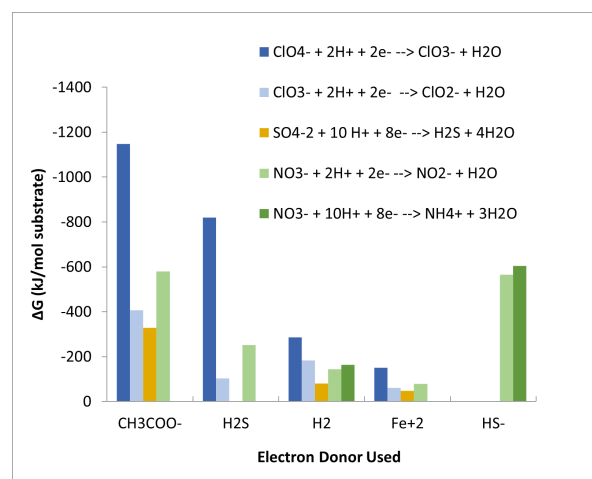


Figure 1: The estimated real-world favorability of microbial respiratory pathways under simulated geochemical conditions of Pilot Valley, Utah using native electron donors.

For a thermodynamic analysis of biological perchlorate reduction feasibility on Mars, Gale Crater was chosen as a study environment for a potentially habitable subsurface aquifer. The Mars Curiosity Rover has traversed and studied 400 m of elevation with stratigraphically distinct rock assemblages that have been characterized using a variety of instruments, making Gale Crater the best-studied depositional environment on Mars. There is strong evidence for perchlorate enrichments in Gale Crater sediments that indicate there could have also been dissolved perchlorate salts in subsurface fluids, much like Pilot Valley brines.

The preliminary work presented here focuses on estimating the thermodynamic favorability of known biological perchlorate reduction pathways within a simulated Gale Crater groundwater environment. Figures 2 & 3 shows initial results of thermodynamic favorability with three different electron donors for perchlorate reduction at the Cumberland sample site in Gale Crater.

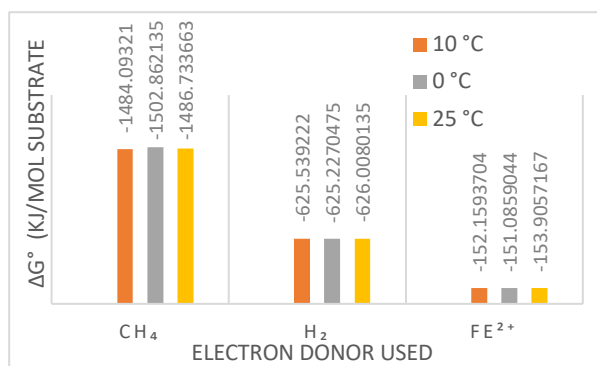


Figure 2: Estimated real-world favorability of dissimilatory perchlorate reduction in simulated Gale Crater groundwater for various temperature conditions, using 0.01 kg of initially dissolved solids and 1 atm pressure.

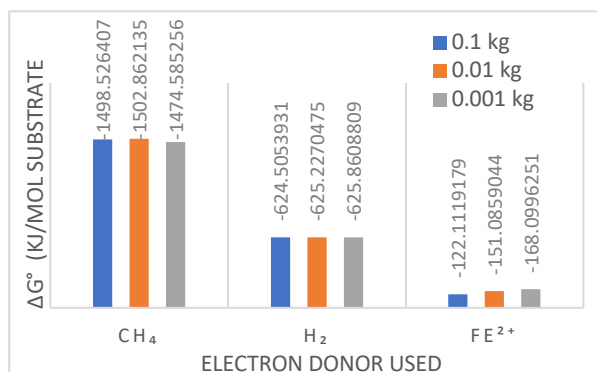


Figure 3: Estimated real-world favorability of dissimilatory perchlorate reduction in simulated Gale Crater groundwater for various masses of initially dissolved solids, using 0 °C and 1 atm pressure conditions.

Microbial Ecology: Our 2019 published experimental results show that perchlorate reducing bacteria co-exist with the naturally occurring perchlorate (NOP) present in the basin. Our results also provide strong evidence of active microbial reduction of the NOP throughout the basin. To understand what pathways are used for microbial (per)chlorate reduction in Pilot Valley, and which microorganisms are the dominant users of (per)chlorates, sediments have been cultured and isolated with (per)chlorates as the sole terminal electron acceptor for use in more detailed molecular and genomic studies which will be discussed further in our presentation.



Figure 4: In Situ perchlorate reduction field experiment.

Acknowledgments: This research has been partially supported by LPI Summer Intern Program, University of Houston Clear Lake, and USRA.

References: [1] Lynch, K.L., et al. (2019) *Astrobiology*, **19**(5). [2] Hecht, M.H., et al. (2009) *Science*, **325**(5936). [3] Navarro-González, R., et al., (2010) *JGR Planets*, **115**(E12). [4] Clark, J., et al. (2021) *Minerals*, **11**(5). [5] Hogancamp, J.V., et al. (2018), *JGR Planets*, **123**(11). [6] Clark, J.V., et al. (2020), *JGR Planets*, **125**(2). [7] Sutter, B., et al. (2017), *Int. Journal of Astrobiology*, **16**(3). [8] Kounaves, S.P., et al. (2014), *Icarus*, **229**. [9] Jackson, W.A., et al. (2015), *Earth and Planetary Science Letters*, **430**.

Using Raman spectroscopy to detect and monitor freezing and melting processes in near-saturated water-salt mixtures at Mars-analogue temperatures. D. P. Mason^{1,2} and M. E. Elwood Madden², ¹University of New Mexico (danmason@unm.edu), ²University of Oklahoma (melwood@ou.edu).

Introduction: Raman spectroscopy is an ideal tool to analyze the geochemistry and mineralogy of heterogeneous mixtures of solids, liquid, and gases in-situ, while maintaining planetary protection protocols. Here we characterize saturated or near-saturated CaCl_2 , MgCl_2 , MgSO_4 , Na_2SO_4 , NaCl , and NaClO_4 brines, as well as ultrapure water, and mixed MgSO_4 - NaCl , MgSO_4 - NaClO_4 , Na_2SO_4 - NaCl , Na_2SO_4 - NaClO_4 , and NaCl - NaClO_4 brines from 200 K to 295 K to determine how changes in temperature affect spectral signatures of planetary analogue brines.

Methods: Raman spectroscopy is a vibrational spectroscopy technique that uses the interaction of laser light with covalently bonded electrons to identify the composition of materials. We used a Renishaw inVia High Resolution Raman microscope and spectrometer to collect Raman spectra from 200 K to 295 K using a Linkam THMS600 temperature-controlled stage. We used both a 785 nm and a 532 nm laser (45 watts each, Renishaw) at 1% laser power in streamline mode to gather data, using a 50x objective along with a 1200 l/cm grating. We collected data from twelve different solutions: ultrapure water, CaCl_2 , MgCl_2 , MgSO_4 , Na_2SO_4 , NaCl , and NaClO_4 endmember brines, and MgSO_4 - NaCl , MgSO_4 - NaClO_4 , Na_2SO_4 - NaCl , and Na_2SO_4 - NaClO_4 , NaCl - NaClO_4 mixed brines. The endmember brines were produced by saturating 18M Ω ultrapure water with each reagent grade salt at 295 K. Mixed brines were composed of a 50/50 volumetric mixture of the respective saturated endmember brines.

A 0.4 mL sample of each solution was placed in a quartz crucible within the Linkam stage with the temperature adjusted as follows-- at each observation point, we focused the laser just below the surface of the liquid brine or on the surface of the ice/solids once the brines froze. First, we collected spectra at 295 K, then lowered the temperature to 200 K at a rate of 100 K/min and proceeded to collect spectra at 10 K increments until the sample was 5 K below the melting point of the solution being tested. We then collected spectra at 1 K increments until the temperature was ~5 K above the melting point of the solution. During these smaller temperature adjustments around the melting point, the temperature changed at a rate of at least 20 K/min. We determined the phases present in the sample (liquid, solid, or a mix of the two) by both visually observing the sample to determine whether it looked more similar to ice or more similar to liquid, as well as spectrally by comparing the resultant spectrum to those taken when the sample was definitively ice (200 K) or

definitively liquid (295 K). Once we collected the spectra, we used the WiRE 4.1 software to process and analyze the spectra, including curve fits.

Results: Sulfate and perchlorate brines produced clear, distinct peaks associated with each anion in both the solid and liquid phase. While chloride brines did not produce distinct anion peaks in the liquid phase, subtle changes were observed in the OH-stretching region, suggesting changes to the molecular water vibration states due to complexation (Figure 1).

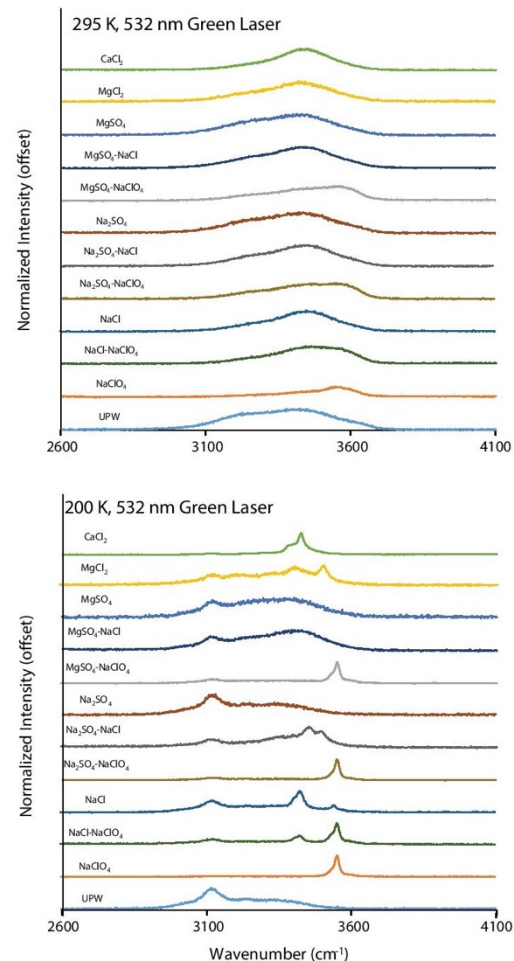


Figure 1. Raman spectra (532 nm laser) of endmember and mixed brines at 295 K and 200 K.

However, the presence of cations did not influence the spectral signature of the liquid brines in any meaning-

ful way when the anions were held constant. Indeed peak positions also match spectra collected for calcium and magnesium perchlorate solutions [1-4].

Peak intensity was variable within the mixed brines. In general, perchlorate peaks are more intense than sulfate peaks. This may lead to signals from perchlorate anions overshadowing the signals from sulfate anions in mixed brines.

Solid-Liquid Transitions: Solid-liquid phase transitions were clearly observed in each of the solutions using both 785 nm (red) and 532 nm (green) excitation lasers, particularly in the OH-stretching region between 3000-4000 cm^{-1} with the 532 nm laser (e.g. NaClO_4 spectra shown in Figure 2).

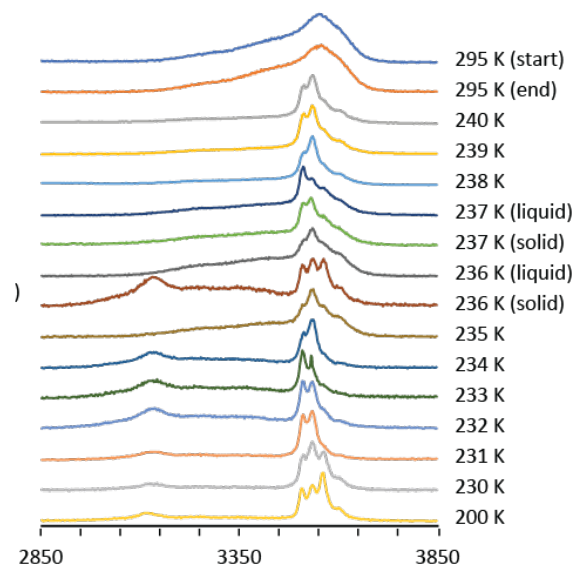


Figure 2. NaClO_4 brine spectra (532 nm laser) show peaks indicative of both solid and liquid over a wide range of temperatures (235 K to 240 K). Therefore, Raman spectroscopy may be used to detect partial melting at Mars-relevant temperatures.

We observed differences in the spectra of frozen sulfate brines when we changed the cooling rates, suggesting that subtle changes in environmental conditions may influence the hydration state and/or crystallinity of the solid magnesium and sodium- sulfate salts. While we noted significant shifts in the sulfate peak position during freezing, we did not observe a similar magnitude of shift in the perchlorate peak position during freezing. Instead, the main perchlorate peak remains relatively fixed at approximately 938 cm^{-1} , regardless of the phase of the sample. This suggests that perchlorate anions do not interact as strongly with surrounding molecules, making them more immune to

phase changes in the surrounding solution. Conversely, the shift in the sulfate peak suggests that sulfate ions are more strongly influenced by the surrounding water molecules in the hydration shell that forms in liquid aqueous solutions, making the sulfate spectra more sensitive to phase changes in the solution, as has also been observed in the Raman spectra of ion hydration shells [5].

Implications: The resulting reference dataset can be used to interpret spectra from future samples analyzed in-situ on planetary bodies. These experiments and the resulting spectral library will allow future researchers to use Raman spectroscopy to look for in-situ melting, freezing, evaporation, and deliquescence as well as identify the composition of high salinity brines and their frozen products in a range of planetary environments, including permafrost and recurring slope lineae on Mars, potential ice and salt-rich regolith on asteroids such as Ceres, and ice shells and possible seeps or geysers on icy moons and other bodies.

Acknowledgments: This project was funded by NASA PDART grant 80NSSC18K0512. A. Rodriguez helped with brine synthesis and development of Raman instrumentation protocols and N. Wood helped with data processing.

References: [1] Fischer, E. (2016). *Física de la Tierra*, 28, 181. [2] Nuding, D. L. *et al.* (2014) *Icarus*. 243, 420–428. [3] Nikolakakos, G. and Whiteway, J. A. (2015) *GRL* 42(19), 7899–7906. [4] Primm, K. M. *et al.* (2018) *JGR-P* 123(8), 2076–2088. [5] Wang, Y. *et al.* (2016) *J Raman Spect.* 47(10), 1231–1238.

TIMING AND METAMORPHIC TEMPERATURE YIELD DIFFERENT BRINE COMPOSITIONS AT DWARF PLANET CERES. M. Melwani Daswani¹ and J. C. Castillo-Rogez¹, ¹Jet Propulsion Laboratory, California Institute of Technology (daswani@jpl.nasa.gov).

Introduction: Several strong lines of evidence point towards dwarf planet Ceres being or having been a habitable world for *life as we know it*. Most notably, NASA's Dawn spacecraft revealed mineral salts and organics expressed at the surface, which are inferred to be the result of deep-seated briny fluids migrating from the mantle to the surface in the recent past [e.g. 1]. Here we describe the results of thermodynamic models used to decipher the precise origin, composition, and subsurface pervasiveness of the brines, which may help resolve whether Ceres was, and continues to be, a habitable world.

Methods, constraints, and assumptions: Dawn's gravity data constrains the present-day mantle density (ρ_{mantle}) to $\sim 2700 \text{ kg/m}^3$ [2] or $\sim 2430 \text{ kg/m}^3$ [3], which is consistent with a partially hydrated rocky interior containing fluid-filled porosity (ϕ_{mantle}) up to $\sim 30 \text{ vol. \%}$. We performed thermodynamic models using programs Perple_X [4] and Rcrust [5] to determine the changing mineralogy and fluids in Ceres' mantle from shortly after accretion until the present day, anchoring the pressure and temperature conditions in the thermodynamic models to the thermal evolution model by [6]; the nominal case is shown in Figure 1.

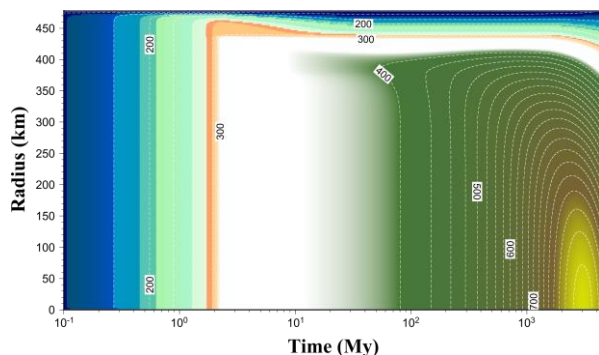


Figure 1. Thermal evolution model of Ceres from [6] used to anchor the pressure and temperature conditions of the thermodynamic model, from the surface to the center of Ceres. Temperature units shown in the figure are Kelvin.

We used appropriate solution models and thermodynamic data implemented in Perple_X, including data for the speciation of solutes in aqueous fluids [7]. We assumed a variety of possible initial compositions for Ceres after accretion, based on whether the building blocks of Ceres were primarily CM-chondrite-like, CI-chondrite-like, cometary, a mixture of cometary and CI-chondrite materials, and

various amounts of additional water (0, 10, 25 wt. %) beyond that already trapped in the minerals and organics present in chondrites and comets. Finally, we also allowed the release and extraction of any fluids in excess of predetermined volumes to reside in the mantle (0, 10, 30 vol. %, or multiple layers of decreasing porosity from surface to core). A total of 40 thermodynamic – thermal evolution models were performed.

Results and discussion: Only eight of the combinations of variables tested in the evolution models resulted in mantle densities consistent with the Dawn spacecraft's observations. Five of these cases resulted from a thermally evolved body of CI chondrite composition ($\pm \text{H}_2\text{O}$) containing $\phi_{\text{mantle}} = 17\text{--}30 \text{ vol. \%}$, yielding $\rho_{\text{mantle}} \approx 2430 \text{ kg/m}^3$. Two other consistent cases developed from the thermal evolution of CI chondrite compositions without additional water, yielding $\rho_{\text{mantle}} \approx 2740 \text{ kg/m}^3$, and $\phi_{\text{mantle}} \approx 21 \text{ vol. \%}$.

Only one body evolved from a CM chondrite composition yielded a mantle density consistent with Dawn data (CM chondrite + 25 wt. % H_2O , with $\phi_{\text{mantle}} \approx 17 \text{ vol. \%}$, and $\rho_{\text{mantle}} \approx 2712 \text{ kg/m}^3$).

None of the thermodynamic – thermal evolution models using cometary building blocks resulted in ρ_{mantle} consistent with Dawn data: they resulted instead in $\rho_{\text{mantle}} < 2100 \text{ kg/m}^3$ or $\rho_{\text{mantle}} > 2900 \text{ kg/m}^3$.

Mineralogy, fluid volumes generated, and timing. During the thermal evolution of the candidate primordial Ceres bodies, the changing density of the mantle is a result of the changing mineralogy, which was tracked by the thermodynamic programs.

Figure 2 illustrates a typical evolution of the phase assemblage as a function of the thermal evolution, shown here only along the 100 MPa isobar for simplicity, for a case where Ceres is initially composed of 90 wt. % CI chondrite material plus 10 wt. % H_2O , and the maximum fluid-bearing capacity of the mantle is fixed at 30 vol. % (fluids in excess are extracted to the surface). At this pressure within the interior of Ceres, free fluids are in excess of the fluid-bearing capacity of the mantle, and are extracted from the interior $< 100 \text{ Myr}$ after accretion. The phases at this depth, at 100 Myr, in order of descending abundance, are: antigorite, magnesite, free fluids (i.e. unbound from minerals), pyrite, talc, clinopyroxene, dolomite, chlorite, stilpnomelane, and minor mounts of graphite. At 100 Myr, a total of $\sim 11 \text{ wt. \%}$ of fluid has been extracted to the surface from this depth.

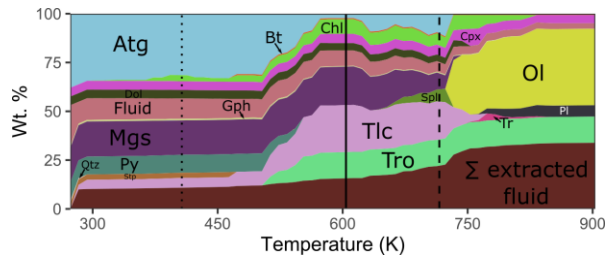


Figure 2. Phase assemblage abundance along the 100 MPa isobar within Ceres, with increasing temperature. Vertical dotted line denotes the temperature at 100 Myr after formation, vertical dashed line denotes the temperature at 3 Gyr after formation, vertical solid line denotes the temperature at 4.5 Gyr. Phase abbreviations are: Atg = antigorite, Bt = biotite, Chl = chlorite, Cpx = clinopyroxene, Dol = dolomite, Fluid = free fluids, Gph = graphite, Mgs = magnesite, Ol = olivine, Pl = plagioclase, Py = pyrite, Spl = spinel, Qtz = quartz, Stpl = stilpnomelane, Tr = tremolite, Tro = troilite, Σ extracted fluid = sum of fluid mass extracted since accretion.

Temperatures within Ceres peak at around 3 Gyr after formation (Fig. 1). At 100 MPa and 3 Gyr, the phases in order of descending abundance consist of: talc, troilite, magnesite, antigorite, chlorite, free fluids, clinopyroxene, spinel, dolomite, and minor biotite and graphite. At this depth, temperatures within Ceres do not reach the stability field of olivine (Fig. 2). By 3 Gyr, an additional ~10 wt. % fluid has been extracted from the interior as a result of the destabilization of volatile-bearing minerals (namely antigorite, magnesite, talc, pyrite), for a cumulative ~21 wt. % fluid extracted to the surface from this depth, since the formation of Ceres.

Temperatures in the interior of Ceres decrease from about 3 Gyr until the present day (Fig. 1), and the equilibrium phase assemblage changes as a result (Fig. 2), with the net effect of replacing antigorite with talc. In order of descending abundance, the equilibrium phase assemblage consists of: talc, magnesite, troilite, free fluids, chlorite, clinopyroxene, dolomite, antigorite, and minor biotite and graphite. The mean $\rho_{\text{mantle}} = 2432 \text{ kg/m}^3$, consistent with Dawn data.

Brine compositions. Following the same representative model, we describe the composition of the fluids generated and extracted from the interior over time. The earliest (i.e. low temperature) fluids released at 100 MPa from the 90 wt. % CI chondrite plus 10 wt. % H_2O Ceres are very dilute, as expected from the additional water. However, as fluids are irreversibly removed and temperatures in the mantle increase during the thermal evolution of Ceres, fluids become progressively more enriched in Na^+ , HS^- , dissolved CO_2 , K^+ and OH^- . Fluids released from this depth within Ceres are reducing and very basic (pH = 11 – 14).

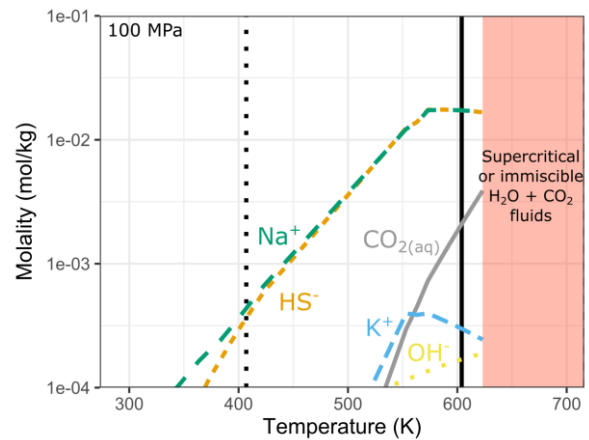
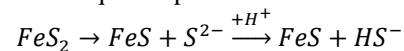


Figure 3. Solute concentration in the aqueous fluids released at 100 MPa within Ceres. Early, low temperature fluids are dilute, whereas later fluids produced with increasing temperature become more Na^+ , HS^- and CO_2 -rich. Vertical dotted line denotes the temperature 100 Myr after formation, and vertical solid line denotes temperature in the present day. For clarity, solutes $<10^{-4} \text{ mol/kg}$ are not shown here.

Conclusions: We have presented a series of models for the generation of different brine compositions within Ceres, that strive for geochemical and geophysical consistency with current spacecraft constraints. Metamorphic phase changes caused by the thermal evolution of Ceres are likely to produce fluids that may be released to the surface, as volatile-rich minerals exsolved volatiles with varying temperature in time. For example, Figures 2–3 show that pyrite transforms to troilite, consuming acidity and releasing dissolved sulfide into the aqueous phase:



Similarly, carbonates destabilize and release CO_3^{2-} , HCO_3^- and $\text{CO}_2(\text{aq})$, and Na-rich clinopyroxene releases Na^+ as it transforms into Na-free clinopyroxene with increasing temperature (Figs. 2–3), which is consistent with NaCO_3 minerals observed by Dawn [1].

Acknowledgments: The research was carried out at the Jet Propulsion Laboratory, California Institute of Technology, under a contract with the National Aeronautics and Space Administration (80NM0018D0004). Government sponsorship acknowledged.

References: [1] Raymond C. A. et al. (2020) *Nature Astron.*, 4, 741–747. [2] Mao X. and McKinnon W. B. (2018) *Icarus*, 299, 430–442. [3] Ermakov A. I. et al. (2017) *JGR:Planets*, 122, 2267–2293. [4] Connolly J. A. D. (2005) *EPSL*, 236, 524–541. [5] Mayne M. J. et al. (2016) *JMG*, 34, 663–682. [6] Castillo-Rogez J. C., et al. (2019) *GRL*, 46, 1963–1972. [7] Connolly J. A. D. and Galvez M. E. (2018) *EPSL*, 501, 90–102.

IMPLEMENTING HABITAT SUITABILITY MODELS: HABITABILITY OF THE MARTIAN SURFACE.

A. Méndez¹, E. G. Rivera-Valentín²; ¹Planetary Habitability Laboratory, University of Puerto Rico at Arecibo, Arecibo, PR 00612 (abel.mendez@upr.edu), ²Lunar and Planetary Institute (USRA), Houston, TX 77058.

Introduction: Habitat Suitability Models (HSM) provide a formal framework for habitability studies [1]. The surface of Mars is the next best object beyond Earth to test HSM. Past and future missions are delivering more information about the martian environments. For example, surface brines may support transient liquids environments suitable for life [2,3]. Here we evaluate the surface habitability of martian brines in equilibrium with the atmosphere as a function of near-surface temperature and relative humidity. We are using data derived from the MarsWRF global circulation model [4], and in situ measurements from the Phoenix (PHX) lander and the Mars Science Laboratory (MSL) rover. For context, we compare our results with two martian analogs, the Atacama Desert in Chile and the Antarctic Dry Valleys, and El Yunque Rain Forest in Puerto Rico.

Development of the HSM: There are six basic steps to construct an HSM: (1) select the space and time of interest, (2) select variables of interest, (3) select the species or communities of interest, (4) identify one or more standards of comparison, (5) parametrize the habitability model, and (6) validate and correct the model. A critical step is a model parametrization with a quantity proportional to the biological carrying capacity of the system. Here we use a general mass-energy model where habitability is defined as $H = qME$, where M and E are the mass and energy available for life, respectively, and q is the quality factor or fraction usable by life.

Temperature, T , and relative humidity, RH, are two well-known factors controlling the viability and growth of microbial populations. Relative humidity is a proxy for the available water (water activity) and temperature for the available energy. After parametrization, we derived an expression for the thermal-humidity, or *thermowet*, habitability $H(T, RH)$ as

$$H(T, RH) = \frac{ME}{[ME]_{\text{ref}}} = \frac{(q_m \bar{p} V)(q_e A t \sigma T^4)}{[(q_m \bar{p} V)(q_e A t \sigma T^4)]_{\text{ref}}} = \frac{RH \rho_e T^4}{[RH \rho_e T^4]_{\text{ref}}}$$

where p_e is the water vapor saturation concentration over liquid water. Our reference environment is the special region point (*i.e.*, 255 K, 0.6 water activity) [5,6]. For simplicity, the quality factors of the environment of interest and the reference are assumed equal, and they cancel out. This model assumes that relative humidity is nearly in equilibrium with surface

brines and is a good proxy for the water activity of the potential habitat.

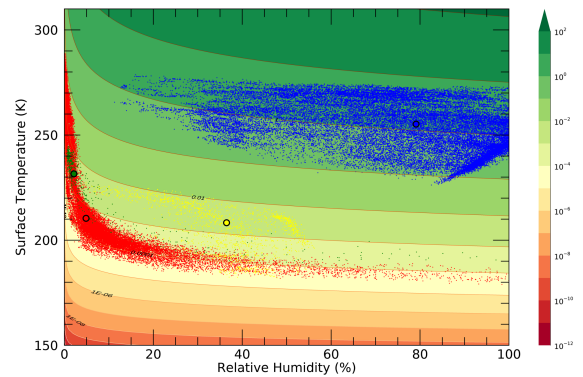


Figure 1. Thermowet habitability phase space (contour legend). The plot includes data for the Atacama Desert (blue dots), MSL lander (red dots), PHX lander (green dots), and the MarsWRF model (yellow dots). The black circles correspond to time-average conditions for each colored location.

Conclusion: Our results show that the habitability of the martian surface, relative to temperature and humidity, is two to four orders of magnitude less habitable than the know limits for life on Earth (Figure 1). A caveat of this analysis are microenvironments where brines may be out of equilibrium with the local atmosphere. It will be necessary for further observations of the Martian surface at improved spatial and temporal resolution, as well as experimental work on the thermodynamics and kinetics of brines under Mars-relevant conditions to better characterize the habitability of Mars at the scale of microbial life.

Acknowledgments: This work was supported by the Planetary Habitability Laboratory (PHL) and the University of Puerto Rico at Arecibo (UPR Arecibo).

References: [1] Méndez, A. *et al.* (2021) *Astrobiology* **21**(8), 1017-1027. [2] Rivera-Valentín, E. G. *et al.* (2020) *Nat. Astro.* **4**, 756 – 761. [3] Chevrier, V. F. *et al.* (2020) *PSJ* **1**, 64. [4] Richardson, M. I. *et al.* (2007) *JGR Planets* **112**, E09001. [5] Kminek, G. *et al.* (2010) *Adv. Space. Res.* **46**, 811 – 829. [6] Rummel, J. D. *et al.* (2014) *Astrobiology* **14**(11), 887 – 968.

BIOSIGNATURES AT THE SURFACE INTERFACE DEPOSITED BY SUBGLACIAL BRINE. S. Mitchell¹, E. C. Sklute², B. Boles¹, K. Holbrook¹, A. Jarratt¹, J. Shaffer¹, L. Smith¹, P.A. Lee³, M.D. Dyar², J. A. Mikucki¹, ¹Dept. of Microbiology, University of Tennessee, M409 Walters Life Sciences, Knoxville, TN, 37996, ²Planetary Science Institute, 1700 East Fort Lowell, Tucson, AZ 85719, ³Hollings Marine Laboratory, College of Charleston, 331 Fort Johnson Rd., Charleston, SC, 29412

Blood Falls, Antarctica is a unique iron and salt deposit feature at the terminus of the Taylor Glacier in the McMurdo Dry Valleys, Antarctica. The dry valleys have long been considered an important Martian analogue due to its unique cold and dry conditions [1]. Blood Falls forms when episodic discharge of sub-oxic, iron-rich brine from an aquifer below the glacier reaches the surface. The microbial community within the subglacial brine that feeds Blood Falls outflow is chemosynthetic and contains phyla known to be involved in iron and sulfur transformations [4,5]. This brine routes through a conduit in the glacier to the surface where it is exposed to changes in pressure, UV radiation, oxygen and other surface stressors. How this impacts the subglacial microbial community is currently unknown. This unique system is also an ideal analog for Ocean Worlds since it provides a rare opportunity to study a subsurface-surface brine network through ice and allows us to ask questions about how brines transform as they move through ice interfaces with drastically different physicochemical properties. We use the Blood Falls ecosystem to study how microorganisms may interact with subterranean liquid environments, alter mineralogy, and produce metabolic biosignatures that may be detectable as subsurface brines emerge.



Figure 1. Blood Falls, Antarctica. Visible mineral transformations occurring at a surface-subsurface interface following an active discharge event through glacier ice.

Subglacial brine episodically discharges to the surface at Blood Falls and contains high concentrations of sulfate (~50 mM), chloride (~1375 mM), and iron (0.47- 3.5 mM) [3,4]. Limited mineralogical analysis, conducted several decades ago, shows surficial brine discharge precipitates are dominated by halite and aragonite [2]. Indications of mineral transformations are visible on surface features coated with brine

outflow and provide evidence of interaction occurring at the subsurface-surface interface (Fig.1). Elucidating biosignatures that arise as subsurface brine interacts with surficial environments is critical towards advancing life detection methods in astrobiology. In this study, we employed advanced mineral analysis of environmental samples from Blood Falls materials. Results of these analyses provide evidence of biotic mineral transformation occurring at the surface. Enrichments of environmental samples from the subsurface-surface interface indicate the presence of a microbial community capable of performing community-driven transformation of iron (Fig. 2).

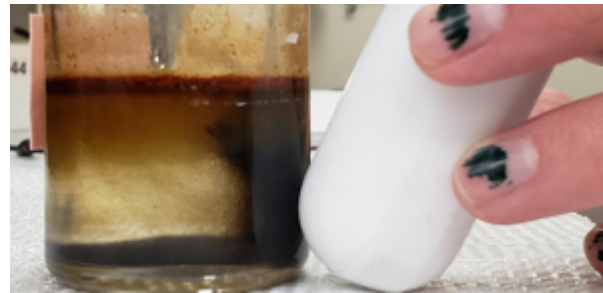


Figure 2. Microbially mediated mineral transformation. Evidence of iron transformation to magnetite by *Shewanella* sp. Strain BF02_Schw (BF02), an isolate collected from the surface discharge at Blood Falls, Antarctica.

Proton Transfer Reaction – Mass Spectrometry (PTR-MS) was used to explore the potential for volatile production from materials collected at Blood Falls. Preliminary analysis of the volatile compounds produced by a natural sample collected from the surface discharge revealed a number of spectral features with masses ranging from m/z 30 to m/z 120. Potential identifications for these features include ketones, alcohols, non-methane hydrocarbons and sulfur-containing VOCs.

Fourier-transform infrared spectroscopy results show that these samples contain primarily carbonate and/or phosphate. Neither phase appears in our spectral libraries, ruling out the more common minerals. Interestingly, the carbonate does not show up in the Mössbauer spectra, indicating that it is not an iron-bearing carbonate. The ferrous distribution in the Mössbauer spectrum could be consistent with a phosphate. XRD and Raman are currently underway to clarify this mystery. Results from this study provide insights into the

application of spectral analysis to detect biosignatures from the subsurface-surface brine network.

Acknowledgments: NASA proposal # 16-EXO16_2-0163 (NASA 80NSSC17K0243)

References: [1] Doran, P.T., Lyons, W.B. and McKnight, D.M. eds., 2010. *Astrobiological analogs* (5). Cambridge University Press. [2] Black, R.F., et al. *J. of Geol* 73(1), pp.175-181.[3] Lyons, W.B., et al., 2019. The geochemistry of englacial brine from Taylor Glacier, Antarctica. *J. Geophys. Res. Biogeophys.*, 124(3), pp.633-648. [4] Mikucki, J.A. and Priscu, J.C., 2007. Bacterial diversity associated with Blood Falls, a sub-glacial outflow from the Taylor Glacier, Antarctica. *Appl. Env. Microbiol.*, 73(12), pp.4029-4039. [5] Mikucki, J.A., et al. *Science*, 324(5925), pp.397-400.

SALT DISTRIBUTIONS IN ICY SHELLS OF OCEAN WORLDS. M. Naseem¹ and M. Neveu², ¹Independent Research Collaborator, NASA Solar Systems Working Project (xmariamnaseemx@gmail.com), ²NASA Goddard Space Flight Center / University of Maryland College Park (marc.f.neveu@nasa.gov).

Introduction: Numerous studies have found evidence of convection and cryovolcanism throughout the outer solar system, suggesting transport processes occur in the ice shells of ocean worlds like Europa. There are multiple science motivations for understanding transport through ice shells, including gaining insight into how material is delivered to the surface and informing the connection between surface expression and subsurface conditions to unveil potential indicators of habitability and signs of life. Transport processes hinge on thermo-mechanical properties of ice shell materials, which depend on the shell's composition. The chemistry and compositional structure of (predominantly water) ice shells remain poorly understood. To pave the way for investigation of ice shell compositions and how these affect transport processes, we sought to determine possible spatial distributions of impurities in ice shells resulting from the freezing of liquid intrusions by leveraging recent improvements in geochemical models for freezing solutions.

Methods: *Freezing routine.* In planetary science, the most widely used code implementing the Pitzer model to compute compositions of salty solutions is FREZCHEM [1]. A broad set of species were added to FREZCHEM over the years, making it versatile but lacking thermodynamic consistency because parameters for previously added species were not re-fitted to the expanded set of species. Revised, consistent fits based on additional experimental data were used to improve the Pitzer-based model for Na-K-Mg-Ca-Cl-SO₄ chemistries and ported to the more modular PHREEQC geochemistry software [2].

A freezing routine was written to compute with PHREEQC the composition of progressively freezing solutions containing dissolved salts. This routine was benchmarked to ice and salt compositions resulting from freezing of a hypothetical Na-Mg-Ca-SO₄-Cl-H₂O system representing a briny European ocean using starting chemistries from [3], resulting in formation of ice, mirabilite (Na₂SO₄•10H₂O), epsomite (MgSO₄•7H₂O), gypsum (CaSO₄•2H₂O), meridianiite (MgSO₄•11H₂O), hydrohalite (NaCl•2H₂O), and leftover solute concentrations during freezing close to those of [3] with slight changes in sulfate species due to model improvements [2].

Spatial distribution of formed salts. In our hypothetical scenario, we considered freezing in a spherical cryomagma chamber within an ice shell. We assumed that

the chamber starts at the temperature at which ice begins to form, because the intruding liquid is sourced from the ice shell-ocean interface which is at the freezing point. It is also assumed that the intruding liquid retains the ocean composition (e.g., fluid velocities within fractures of 1 m/s are postulated for Enceladus [4]) until the onset of freezing. The spatial distribution of solids that form in the chamber depends both on their relative densities (ice < solution < salts) and on the relative time-scales of freezing (governed by the chamber size and temperature contrast with the surrounding shell), salt formation (governed by temperature and chemical disequilibrium), and salt settling (governed by grain size and convective or diffusive mixing). If freezing is faster than salt formation, as may occur initially if the fluid intrusion encounters a much colder surrounding ice shell, the forming salts are incorporated in the thickening chamber wall (**Fig. 1a**). Otherwise, the solid distribution can span the end-members of **Fig. 1b** (no settling) and **1c** (no mixing).

Freezing takes place from the outside in. Initially, the liquid in the chamber undergoes fast freezing. Ice forming along the chamber wall traps the salts that precipitate in the area of ice formation, preventing the formed salts from continuing to equilibrate with the fluids (fractional crystallization). As the liquid temperature decreases, the wall thickens, and the chamber shrinks. Assuming a uniform ice temperature around the chamber, the wall thickness is uniform, the chamber remains spherical, and its dimensions can be described by a single parameter R_2 as shown in **Fig. 1a**. We look at the later equilibrium crystallization stage (in which the formed solids can still participate in chemical reactions, i.e., be subsequently consumed in forming other products more stable at lower temperatures) through two separate end-members. In one end-member, the liquid in the chamber is well mixed (**Fig. 1b**). During slow freezing, all salts are rejected from the thickening pure water ice wall (decreasing R_2). In the second end-member, we assume that the liquid in the chamber is not mixed (**Fig. 1c**). During slow freezing, mixed salts are rejected into the chamber and settle at the bottom, encircled and overlain by a thickening pure H₂O ice wall.

In each case, starting from a PHREEQC freezing simulation output, we distribute volumes of ice and salts formed at each temperature step according to the above assumptions. This allows us to derive possible spatial distributions of salts intruded in ice shells.

Results: For the starting ocean composition of [3], in the case of fast freezing trapping salt in the thickening ice wall, our analysis indicated that when the eutectic is reached at ~ 236 K, the ratio of the chamber radius to its initial radius R_1 (when ice first forms) is $R_2/R_1 = 54\%$. The portion of the chamber inward of R_2 is filled with the eutectic composition of solids. As shown in **Fig. 1a**, bottom pane, once fully frozen, the chamber comprises an outer shell rich in sulfates (70-90 vol.% of ice increasing from the outside in, 2-26 vol.% meridianiite, ≤ 6 vol.% mirabilite, and <0.1 vol.% gypsum) that crystallize at higher temperatures, whereas the chamber core is rich in sodium chloride (80 vol.% ice, 18 vol.% hydrohalite, and 2 vol.% meridianiite).

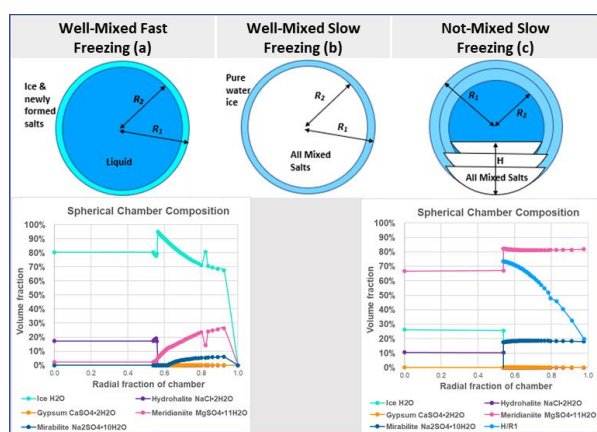


Figure 1. Schematics of freezing spherical intrusion into an ice shell and spatial distribution of forming solids. (a) Fast freezing by fractional crystallization (top) with quantitative solid distribution for a starting fluid composition from [3] (bottom). (b) Slow freezing by equilibrium crystallization with salts excluded from ice and well mixed with chamber fluid. (c) As in (b), but with salts settling by density rather than remaining well-mixed. Bottom pane: composition of the settled salt layer and (for $R_2/R_1 < 0.54$) central salt-ice eutectic mixture.

In the slow freezing case where liquid is well-mixed in the chamber (**Fig. 1b**), when the eutectic temperature is reached at 240 K, $R_2/R_1 = 64\%$. Outside of R_2 , the chamber is pure water ice; inward of R_2 the homogeneous composition, not shown on Fig. 1, is given by eutectic proportions of ice (26 vol.%) and salt (67 vol.% meridianiite, 10 vol.% hydrohalite, 0.2 vol.% gypsum). (The sum exceeds 100% due to volume changes associated with solid formation that, in practice, would be accommodated by strain or fracturing.)

In the end-member of slow freezing with no mixing (**Fig. 1c**), we introduce an additional parameter to describe the cumulative height of settled salt (H). Using

formulae for spherical segments, the incremental sediment heights (h) at each temperature step of a PHREEQC output were calculated and added to obtain H . Given H and the volume of remaining solution at each temperature step, R_2 was calculated using a binary search algorithm coded in *Scilab*. At the eutectic temperature (240 K), $H = 0.93 R_1$ and $R_2/R_1 = 0.54$. Similar to the fast freezing case, the composition switches from sulfate-dominated to mixed sulfate/chloride at $R_2/R_1 = 0.54$. The bottom half of the chamber is sulfate-rich, with 80:20 volumetric proportions of Mg:Na-sulfate. The upper dome of radius $0.54 R_1$ comprises about 2/3 Mg-sulfate, 1/4 ice, and 10% NaCl by volume.

Discussion: Distinction between cases (a), (b), and (c) is not warranted in simpler, binary systems (e.g., NaCl-H₂O or MgSO₄-H₂O). For such systems, salts only begin crystallizing at the eutectic as in case (b) or in case (c) with $H = 0$ (the height of salts settled before the eutectic is reached). However, realistic ocean compositions comprise multiple salts that, upon freezing, can become distributed in a fashion bounded by the end-members simulated here. We are investigating additional salt distributions for up-to-date simulated compositions of Europa's ocean based on devolatilization of accreted rocky material and water-rock interaction [5].

Our simulations can quantify the water activity and micronutrient supply of near-surface liquid water environments. These aspects will be examined next.

Salts tend to be denser, more insulating, and stronger than water ice. This can affect the propensity for fracturing and convection within an ice shell, affecting surface ↔ ocean exchange in ways which will be quantitatively investigated in upcoming work.

Acknowledgments: We thank J. Toner for helping us make the PHREEQC freezing routine easier to use. This work was supported by NASA's Solar System Workings program (#80NSSC20K0139). The PHREEQC routine and a legacy FREZCHEM repository are publicly available at <https://github.com/MarcNeveu/frezchem>.

References: [1] Marion G. M. and Kargel J. S. (2008) Springer-Verlag, 251 pp. [2] Toner J. D. and Catling D. C. (2017) *J Chem. Eng. Data*, 62, 3151-3168. [3] Marion G. M. et al. (2005) *GCA*, 69, 259-274. [4] Spencer J. R. et al. (2018) In *Enceladus and the Icy Moons of Saturn*, U. AZ Press, pp. 163-174. [5] Melwani Daswani et al., in revision.

GEOCHEMICAL MODELING AND EXPERIMENTAL RESULTS OF BORON ADSORPTION ONTO MARTIAN CLAY MINERALS FROM MARTIAN BRINES. M. A. Nellesen¹, L. Crossey¹, P. Gasda², E. Peterson¹, N. Lanza², A. Reyes-Newell², D. Delapp², C. Yeager², A. Labouriau², R. C. Wiens², S. Clegg², S. Legett², D. Das³, ¹University of New Mexico, ²Los Alamos National Laboratory, ³McGill University.

Introduction: It has been hypothesized that the presence of boron may be essential for prebiotic processes to occur [1]. Borate-ribose complexes are relatively stable in water; without borate, ribose quickly breaks down in solution [2]. The formation of boron-ribose complexes [2] may thus be necessary for the formation of RNA. Boron has been detected in calcium sulfate veins by ChemCam on the NASA *Curiosity* rover [1, 3, 4]. This opens the possibility for RNA-based life to have developed independently on Mars [3]. This study hopes to understand borate behavior in the martian groundwater by determining how brines may have emplaced boron into martian clays and how this boron may be able to interact and assist in prebiotic chemistry.

In water, boron appears as either borate or boric acid, and its speciation depends on pH. In alkaline water, boron comes in the form of a borate and will adsorb to 2:1 phyllosilicates [5]; a pH range of 8-9 [6] providing the most adsorption, with variance depending on clay species.

Methods: Expanding on the experiments from [7], this study conducted analysis of clay structure via X-Ray Diffraction (XRD) before and after boron sorption. Further sorption experiments were run in a CaSO_4 system to simulate a martian environment more accurately. These samples were analyzed using Inductively Coupled Plasma – Optical Emission Spectroscopy (ICP-OES) as in previous experiments [7]. Geochemist's Workbench was used to model speciation of boron in a hypothetical martian system rich in CaSO_4 .

Results: XRD analysis included oriented mounts of the clays to determine pre- and post-adsorption structure, which captured the change in structure with the addition of boron to the clays (**Figure 1 & 2**). The majority of the clays displayed a notable rightward shift in the 001 peak position, indicating a decrease in the d-spacing with the addition of the boron. Talc and saponite were the two exceptions, with no significant shift in the 001 peak.

Adsorption analysis compared the previous sorption assays [7] in a CaCl_2 system to our assays in a CaSO_4 system (**Figure 3**). The two sulfate assays demonstrated lower sorption capacity than the chloride counterparts, but still allowed for minor levels of sorption. The sulfate system, at saturation,

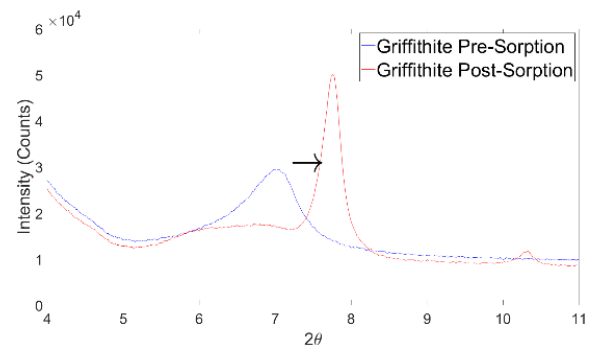


Fig. 1. XRD analysis (oriented mount) of griffithite (Mars analog clay) before and after boron sorption, showing shift in 001 peak position.

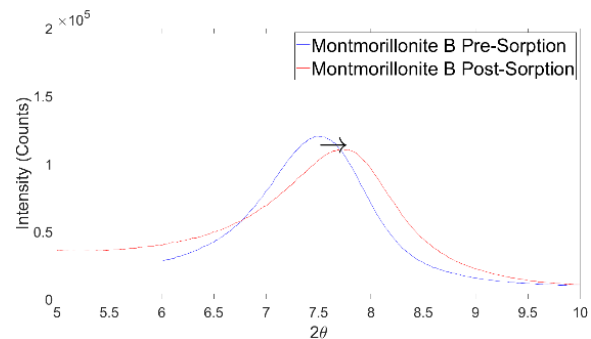


Fig. 2. XRD analysis (oriented mount) of montmorillonite B (terrestrial analog clay) before and after boron sorption, showing shift in 001 peak position.

level exhibited less sorption than when oversaturated. The saturated system also exhibited no change in total sorption within the pH range tested, while the oversaturated system exhibited increased sorption with increased pH, as seen in the previous experiments [7].

Modeling indicated that boron speciation tends towards boric acid at low pH and towards borate ion at higher pH, transitioning at pH ~8-9 (**Figure 4**). Speciation of the borate ion is dependent on the amount of Ca in solution, as low calcium favors the negative $\text{B}(\text{OH})_4^-$ anion, while higher Ca favors the $\text{CaB}(\text{OH})_4^+$ cation.

Discussion: XRD analysis of the clays, before and after sorption, revealed a shift in the 001 peak position in most of the clays. Most of the clays exhibited a rightward shift, indicating a decrease in the d-spacing, indicating that the interlayer thickness

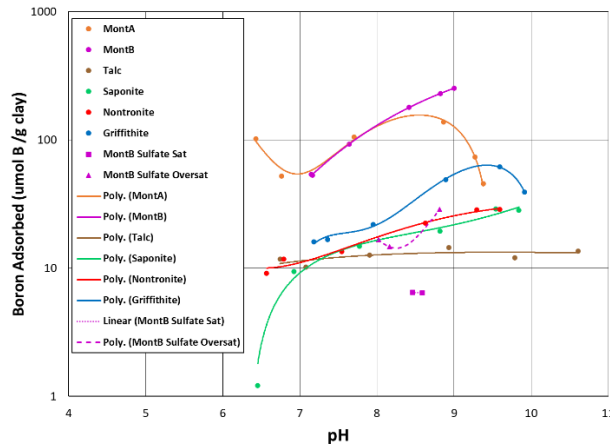


Fig. 3. ICP-OES clay sorption analysis comparing chloride and sulfate systems.

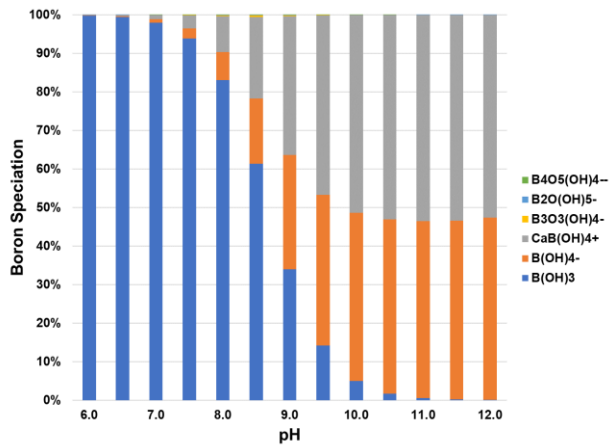


Fig. 4. Speciation model of boron over pH in CaSO₄ system at saturation

between clay sheets became thinner. This may be due to boron sorption into the interlayer positions, whereby increased electrostatic interactions brought the layers tighter together. Talc and saponite did not exhibit this 001 peak shift, likely because talc did not sorb significant levels of boron, whereas saponite may have sorbed boron to a different location.

The adsorption curves for montmorillonite B in the sulfate system were different between the saturated and oversaturated systems. The saturated system exhibited minimal sorption, lower than that of even the talc/chloride system, indicating that at gypsum saturation levels, boron sorption is insignificant. When sulfate was oversaturated, the boron adsorption curve resembled those of the saponite and nontronite, however the rate of increased sorption in relation to pH was steeper than the two martian analogs. This indicates that CaSO₄

needs to exceed saturation in order for borate sorption to be comparable to CaCl₂ systems.

Modeling revealed that Ca concentration strongly affects boron speciation within the pH range (pH 7-10) required for optimal sorption. As the two dominant borate species are oppositely charged, Ca concentrations affect the scope of boron sorption, depending on the charge of available sorption sites. Previous literature indicated that Ca enhanced boron sorption [5, 6]. Increased Ca concentrations result in higher proportions of the borate cation (suggesting the positive species better sorbs to the clay), however the sorption experiments indicated that the CaSO₄ systems (Mars-like) sorbed less readily with boron than in the CaCl₂ system, suggesting that sulfate sequesters Ca under the experimental conditions. Further adsorption modeling is needed to understand the mechanics between borate species and available sorption sites.

Summary: Boron was likely an important component in ancient martian brines and this affected boron emplacement via sorption into Martian lithology. XRD analysis showed a distinct structural change in the clays, indicative of boron sorption. Experimental analysis and modeling revealed that sorption in a CaSO₄ system is less efficient than in CaCl₂-rich brines, but still may allow for significant boron sorption in a Mars-like setting or similar terrestrial setting. As evidenced by boron’s emplacement within calcium-sulfate veins, boron on Mars is linked with brine activity. Thus boron’s potential to support prebiotic chemistry, through sorption to clays and interaction with ribose, is highly dependent on brine composition.

Future Work: Further studies include TEM analysis for finer scale analysis of adsorption mechanisms. Furthermore, these samples will be used for ChemCam analysis and calibrations at a later date.

Acknowledgements: Thank you to LANL LDRD-ER, UNM, NASA Mars Exploration Program, and National Geographic Early Career Grant Program for providing funding, resources, and aide throughout this project and to Rio Tinto US Borax for allowing sample collection.

References: [1] Scorei et al. 2012, Origins of Life and Evolution of Biospheres. [2] T. Georgelin et al. 2014, Carbohydrate Research. [3] Gasda et al. 2017, Geophys. Rev. Lett., 44, 8739-8748 [4] Das et al., 2020, JGR:Planets 125.8. [5] Keren and Mezuman 1981 Clays Clay Min, 29, 198-204 [6] S. Karahan et al. 2006, Journal of Colloid and Interface Science, 293, 36-42. [7] M. Nellesen et al., 2021, LPSC, abstract 2413

CHEMICAL PROCESSES OCCURRING IN BRINES FREEZING UNDER CERES SURFACE: THE CASE OF JULING AND KUPALO CRATERS. M. Pedone¹, E. Ammannito¹, C. Plainaki¹, M. C. De Sanctis², A. Raponi², S. De Angelis², M. Ciarniello², M. Ferrari², A. Frigeri² and F. G. Carrozzo², ¹ASI, Agenzia Spaziale Italiana, via del Politecnico s.n.c., 00133, Rome, Italy, (corresponding author e-mail address: maria.pedone@est.asi.it), ²IAPS, Istituto di Astrofisica e Planetologia Spaziali, INAF, Via del Fosso del Cavaliere, 100, 00133, Rome.

Introduction: In the dwarf planet Ceres, a residual ocean at shallow depth may still exist today in the form of localized reservoirs [1]. We constrained the physiochemical properties of initial aqueous fluids, characterizing potential reservoirs, located under two craters: Kupalo (39.6°S, 173°E) and Juling (36°S, 168.3°E), located in the eastern part of Toharu Quadrangle Ac-H-12 [2, 3]. These two craters are selected because they are close each other but are mineralogical distinct, showing the presence of different carbonates (Kupalo) and water ice (Juling).

This work: We investigate if the distinct mineralogy at surface could be the result of the upwelling of different subsurface aqueous solutions, characterized by different initial conditions (in terms of pressure, temperature, and chemical composition).

At first, our simulations were performed using the FREZCHEM code [4] assuming that the Ceres reservoir is characterized by a mixture of chloride and sodium carbonate and has the same physical properties as the ones summarized in [5]. We used the code to infer the initial speciation of aqueous solutions that possibly were under Kupalo and Juling craters. In the model, for each crater, we selected fractional crystallization pathway by changing temperature value from the initial $T_i=273$ K to the final $T_f=245$ K in which the starting solutions have frozen to precipitate the solid phases characterizing the surface. The given temperatures are relevant since the first value is the melting point of pure ice and the latter is the eutectic temperature of relevant salt-ice mixtures [6]. Moreover, we carried out the freezing simulations by selecting three different values of initial total pressure: 1, 1.5 and 30 bar which correspond to a depth value ranging from 300 m to 10 km. Then, we compared the results deriving from the simulations with chemical equilibria calculations to understand the stability for each precipitated mineral, during the cooling process. In fact, the mineral (solid) equilibrium state is related to the activities of solutes (liquid) and the ionic strength of solutions.

Results and Discussions: Our preliminary study revealed that lower temperature and elevated salinity cause salt precipitation. The formation of water ice occurred at $T < 270$ K and its concentration exponentially decreased for lower temperature affecting the ionic strength of remaining solution. Decreasing temperature caused the precipitations of carbonates (thermodynamically favored since $\Delta G > 0$), followed by

the formation of sulphates and, later, of Cl-bearing salts from more saline brines.

In other words, regarding carbonates, $MgCO_3$, $CaCO_3$ and $CaMg(CO_3)_2$ could have been the first solids to precipitate (before water ice formation) during the freezing of brines.

The formation of hydrated sodium carbonate (natron $Na_2CO_3 \cdot 10H_2O$) is highly favored in Na-enriched solution (anhydrous sodium carbonate has been detected in Kupalo [2]); instead, natron could form only after water ice precipitation in Na-depleted solutions (water ice was detected in Juling [7]).

Natrite (Na_2CO_3) was found in Kupalo's surface layers and not in Juling. We suggest that it could have been directly formed from the hydrated natron and nahcolite ($Na_2CO_3 \cdot 10H_2O$ and $NaHCO_3$ respectively) at 1 bar of total pressure. We can emphasize that, alternatively, at higher pressure ($P > 1$ bar), natrite could only derive from dehydration of natron since nahcolite could not have formed.

Freezing drives chemical and physical changes in the solutions, and these processes change the velocity/density ratios of aqueous solutions from which precipitated minerals would have arrived at surface erupting with a velocity at least of $\sim 8 \cdot 10^{-5}$ m/s.

Our models suggested that Na and Cl-enriched (Kupalo-like) solutions could freeze at a lower temperature with respect to Na and Cl-depleted (Juling-like) solutions. As temperatures are inversely correlated with salinity values, it cannot be excluded that Kupalo brines have frozen, reaching temperatures lower than Juling, becoming more saline.

In a high-salinity and high ionic strength condition, under shallower layers, also gases escaping is more favorable so that the gas-driven transport may be more decisive for bringing high-density solids (as sodium carbonate particles) to the surface.

Moreover, some solids' formation is highly pressure-dependent, as for sodium compounds. Beneath Kupalo, at specific pressure conditions, some kinetics-dependent salts could form, suggesting that aqueous solutions plausibly were affected by cooling processes slower than the nearby Juling.

Acknowledgments: This research was funded by Agenzia Spaziale Italiana and supported by the Dawn VIR team at INAF-IAPS in Rome, Italy.

Data deriving from the mission Dawn are available at repository PDS (Planetary Data System) at url:

<https://sbn.psi.edu/pds/resource/dawn/dwncvirL1.html>
and also <https://sbib.psi.edu/data/PDS-Ceres/about.html>. FREZCHEM code is free and available at url: <https://www.dri.edu/frezchem>.

References: [1] Quick L. C. et al. (2019) *Icarus*, <https://doi.org/10.1016/j.icarus.2018.07.016>.
[2] De Sanctis M. C. et al. (2019) *Icarus*, 318, 230–240.
[3] Frigeri A. et al. (2019) *Icarus*, 318, 14–21.
[4] Marion G. M. et al. (2010) *Computers & Geosciences*, 36, 10–15.
[5] Zolotov M. Yu. (2017) *Icarus*, 296, 289–304.
[6] Castillo-Rogez J. C., et al. (2018) *Meteoritics and Planetary Science*, <https://doi.org/10.1111/maps.13181>.
[7] Raponi A. et al. (2018) *Science Advances*, doi:10.1126/sciadv.aao3757.

PRESERVATION OF DYNAMIC BIOLOGICAL PROCESSES FROM EXTANT HALOPHILIC LIFE: IN-SITU LESSONS LEARNED FROM PLANETARY ANALOGUE BRINES AND EVAPORITES. S.M. Perl¹⁻³, A.J. Celestian², C.S. Cockell⁴, C. Basu⁵, J. Filiberto⁶, S. Potter-McIntyre⁷, K. Olsson-Francis⁸, S.P. Schwenzer⁸, J.R. Crandall⁹, B.K. Baxter¹⁰, T.C. Onstott¹¹, J. Bowman¹², K. Bywaters¹³, M. Winzler¹⁴, J. Valera¹⁵, Z. Cooper¹⁶, D. Nisson¹¹, M. Garner¹⁷, B. Baharier⁸, P. Tasoff¹⁸. ¹NASA Jet Propulsion Laboratory, California Institute of Technology, Pasadena, CA (scott.m.perl@jpl.nasa.gov), ²Mineral Sciences, Los Angeles Natural History Museum, Los Angeles, CA, ³Blue Marble Space Institute of Science (BMSIS), Seattle, WA, ⁴University of Edinburgh, Scotland, UK, ⁵California State University, Northridge, CA, ⁶Lunar and Planetary Institute, Houston, TX, ⁷Southern Illinois University, Carbondale, IL, ⁸The Open University, UK, ⁹Eastern Illinois University, Charleston, IL, ¹⁰Great Salt Lake Institute, Westminster College, Salt Lake City, UT, ¹¹Princeton University, Princeton, NJ, ¹²Scripps Institute of Oceanography, La Jolla, CA, ¹³Honeybee Robotics, Altadena, CA, ¹⁴California State University, Long Beach, Long Beach, CA, ¹⁵University of California, Santa Barbara, Santa Barbara, CA, ¹⁶University of Washington, Seattle, WA, ¹⁷Montana State University, Bozeman, MT, ¹⁸Benioff Center for Microbiome Medicine (UCSF), San Francisco, CA

Introduction: Extant life can thrive in brine environments due to the availability of energy and nutrient sources that halophilic life requires to maintain metabolic processes and nutrient cycling. The dynamic nature of extant life due to consumption of nutrients, cell motility, phototaxis and chemotaxis, can present significant opportunities for preservation of biological processes in modern brine settings. While the robustness of this preservation can indeed occur over geologic timescales, it is the initial/geologically modern timescale that can provide the highest level of biogenicity.

The purpose of this paper is three-fold. First, we will discuss the modern preservation of halophilic microorganisms and how their biochemical products can impact the mineral record. Secondly, we will review methodologies for in-situ and laboratory measurements that complement Martian and Europa mission-relevant studies and sample analyses. We conclude with an assessment of how to decipher between biologically-impacted brine and evaporitic mineralogy and abiotic mineral substrates with the intent to categorize biogenicity in the modern setting with long-term preservation in mind.

Terrestrial and Planetary Closed-basin Lake Systems & Brine Environments: Typically, the salinity of closed-basin lake systems on Earth can be ~10x of their oceanic environment counterparts. Due to a lack of circulation and major non-saline water inputs (taking into account rainfall and snowmelt), these sites are ideal targets for geochemical and geobiological planetary analogues [1] for Mars. Due to the lack of plate tectonics, as well as these sites having deltaic and other aqueous features preserved in the rock and mineral record, this allows for a greater in-situ assessment of local habitability. Brines and saline minerals have been given recent interest due to the search for extant life [2,3] in potential settings such as Martian Recurring Slope Lineae (RSL) where pockets

of potentially free moving brine solutions sublimate [3] during the Martian summers and freeze in place during the colder months.

Modern Biogenic Preservation within Brine and Evaporite Minerals: The kinetic pathways from unsaturated brines into evaporite minerals allow can allow for chemical constraints to be place on potential microenvironments that are generated within fluid inclusions formed from the mineral precipitation process [1,5]. These inclusions allow for both steady-state preservation as well as in-vivo monitoring of halophile cells in these entombed settings (Fig 1). Chemotactic responses can easily be recorded post-preservation with respect to elemental chemistry of the original brine and lithology of the mineral and brine [6].

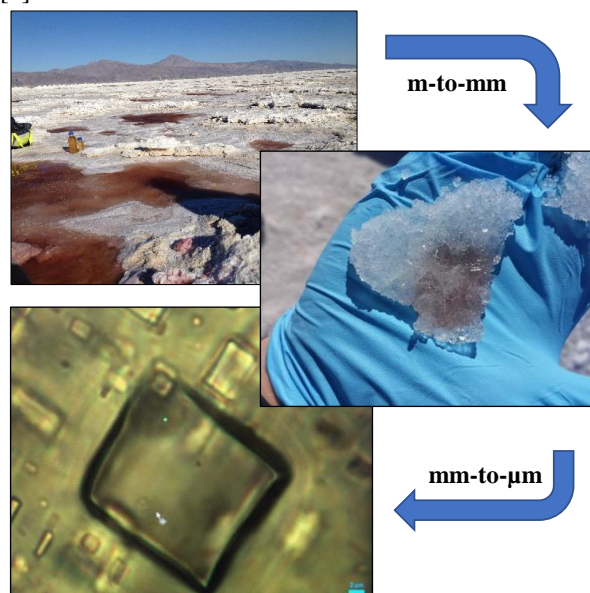


Fig. 1. Typical kinetic pathway from unsaturated brine to evaporite mineral assemblages. Largely constrained by elemental chemistry, these pathways can be used as kinetic endmembers for mineral preservation and potential brine nutrient sources for halophilic microorganisms. Geologically modern brines are the initial biogenic preservation points where in-situ detections of biochemical products can easily be measured. (A) Surface brine pool, (B) Precipitated NaCl. (C) Array of fluid inclusions with entombed halophiles. Scale bar is 2µm.

After solar flux exposure occurs in/on the authigenic evaporite and brine solution, the photobiological responses in the form of pigment generation is typically the first set of adaptation responses to such stresses. Survival strategies for terrestrial halophilic life typically respond to UV-A and UV-B solar flux. The impact without these adaptations can potentially lyse cells and disrupt nutrient cycling within fluid inclusions. Cellular adaptations to combat solar fluxes and high salt [7] on Earth have provided halophiles with the expressed genes to both filter Na as well as produce carotenoids that can be used as positive detections for biology [5]

Mission-relevant Sample Analyses & Biological Validation In-Situ: Current mission payloads do not yet have the ability to spatially resolve micron-scale features within ancient hydrated minerals left behind after late Noachian water-rock interactions on Mars. However, due to the nature of the halophile photobiological response, the generation of carotenoid pigment biomarkers, while occurring on the micron-scale (Fig. 2), can be observed on the meter-scale (Fig. 1a).

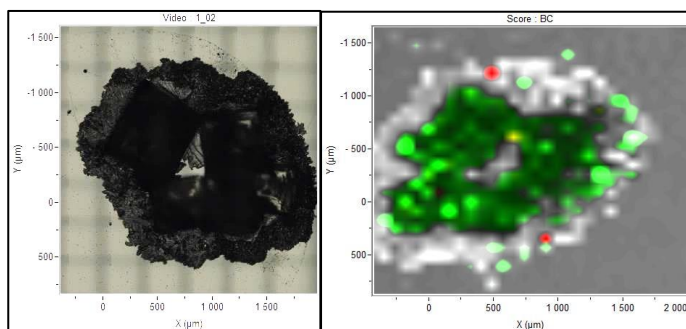


Fig. 2. (L) Optical image of NaCl hooper crystals with superimposed Raman PCA map on (R). The entombment process not only allows for halophilic microorganisms to be preserved but gives a non-permeable sub-crystalline fluid environment where cumulative carotenoid pigment chemistries are also preserved. Green sections in Fig. 2R show Raman wavelengths that correspond to β -carotene ($C_{40}H_{56}$) and Bacterioruberin ($C_{50}H_{76}O_4$) superimposed via PCA map [5,8]

Should these features be observed on surface outcrop by the SHERLOC investigation [9] on the *Perseverance* rover these sample would be ideal for future Mars Sample Return studies. Moreover, these features can be well preserved in partially frozen brine inclusions where psychrophilic microorganisms (that have halo-tolerant genes expressed) that can remain motile [10] at temperatures $\leq -15^{\circ}C$. Needing water to remain in a fluidic state, cell motility in brines would be another ideal biosignature that can be recorded in the form on non-Brownian motion [11] along with potential chemotactic responses. While terrestrial nucleic acids can be preserved in modern settings

[1,5,6] these biomolecules are not robust over geologic time. While these provided the best indications of species-level and taxonomic information [12], lipid biomarkers preserved in salt deposits can yield evidence of ancient life in the mineral record [13].

Modern brines in the Context of Geologic Time: Deciphering between potentially older/ancient biogenic pigment features within modern (liquid) brines and cryobrines presents a challenge with respect to duration of preservation and longevity of evidence. Recent work has shown [14] that even in warmer brine solutions, constraints on habitability and fluid duration can be made. These temperature endmembers can provide insight to the ecological stresses (T, salinity, a_w , others) that halophilic microorganisms need to adapt to in order to survive and create the very biomarker evidence that we are seeking in future in-situ campaigns for extant life [2] and for Mars Sample Return studies [15]

Categorizing Abiotic Brine Substrates and Biotic Features: While modern and ancient brines provide a significant preservation medium for dynamic extant life as well as signs of extinct/ancient microbial life, being able to decipher between abiotic fluids and biogenic features in these preservation mediums [12] is critical for validating biogenicity. For Mars, RSL brines would need to be sampled and concentrated in order to increase the probability of biogenic yield [6] for even the simplest biomolecules. For Europa, ice-melt from the irradiated surface ices would need to be heated slowly in order to reduce the potential for osmotic shock to the cellular membranes and brought onboard for a similar brine concentration. Bulk assessment (non-spatial) of pigment biomarkers as well other complex molecules would still have potential issues of salt inhibition and proper abiotic brine baselines would need to be established to ensure any biogenic peak is both indigenous and repeatable.

References: [1] Perl & Baxter (2020). *Springer*, Cham. pp 487–514. doi:10.1007/978-3-030-40352-2_16. [2] Carrier et al. (2020). *Astrobiology* 20:785-814 [3] Perl et al. (2020) Planetary Science & Astrobiology Decadal Survey 2023-2032. *Nat. Acad. of Sci.* [4] Ohja et al. (2015) *Nature Geosci* 8, 829–832. [5] Perl et al. (in-revision), *Astrobiology* [6] Winzler et al. (this volume), *Mod. Brines*. [7] Basu & Perl (in-revision), *Life Sci. Space. Res.* [8] Perl, Celestian, et al. (in-prep). [9] Eshelman et al. (2019) *Astrobiology* 19 (6) 771-784 [10] Cooper & Perl (in-prep). [11] Bedrossian M. et al. (2017) *Astrobiology* 17:913–925. [12] Perl et al. (2021) *Astrobiology* v21, 8. [13] Cockell et al. (2020) *Astrobiology* Jul 2020.864-877. [14] Crandall et al. (2021). *The Planetary Science Journal*, 2. DOI:10.3847/PSJ/ac053e [15] Muirhead et al. (2020) *Acta Astronautica*, v176, 131-138

A NEW APPROACH TO INFERRING HABITABILITY METRICS IN HYPERSALINE ENVIRONMENTS.

A. Pontefract^{1*}, C. E. Carr^{2*}, P.T. Doran³, L. Ratliff¹, K. E. McNulty³, A. B. Odenheimer³, J. Bowman⁴, S. Som⁵, T. Plattner², J. D. Lawrence², B. E. Schmidt^{2,6} and the Oceans Across Space and Time (OAST) Team. ¹Georgetown University (3700 O St. NW, Washington DC 20057, ap1678@georgetown.edu), ²Georgia Institute of Technology (cecarr@gatech.edu), ³Louisiana State University, ⁴Scripps Institute of Oceanography, ⁵Blue Marble Institute, ⁶Cornell University. *Co-first authors.

Introduction: Hypersaline systems are highly prevalent in our solar system, and are exemplary environments in which to explore habitability beyond Earth [1-8]. As such, there is increasing interest in hypersaline (> 35 ppt) system habitability metrics such as salinity and water activity (a_w). Determination of salinity has been well studied, and the majority of instrumentation for work in saline systems is based on NaCl dominated chemistry, with salinities < 40 ppt [9, 10]. Standard measurements of salinity for these environments are achieved via conductivity (measured in *e.g.*, mS/cm), and converted using well-established relationships to PSU (practical salinity units) [11, 12]. While a gold standard for Earth-ocean (thalassohaline) chemistry, these metrics begin to fail when utilized in high salinity environments, or in systems with non-standard chemistry [13], where meters for *in situ* measurements top out ~ 200 mS/cm and 70 PSU, corresponding to ~3-4 M NaCl [14]. In addition, non-marine (athalassohaline) brines do not increase in conductivity monotonically, and thus can only be empirically determined. In contrast to salinity, a_w , an important habitability metric in saline systems, has received comparatively little attention and only recently has begun to be measured *in situ*. Historically, the most accurate determinations of a_w have been from empirical measurements using a chilled dew-point meter, as ionic concentrations > 100 mM result in complex ion-ion interactions that become increasingly difficult to model, especially in athalassohaline environments [15, 16].

Given the above-mentioned difficulties in determining these metrics within hypersaline systems, we as a community need to adopt common methodologies in order to effectively interrogate these systems, producing studies that are cross-comparable. Moreover, there is a wealth of geochemical information from previously studied hypersaline environments, where a_w was not measured, which places limitations on the utility of this data to define habitable phase space in aqueous systems on Earth and beyond.

Here, the Oceans Across Space and Time (OAST) team presents data revealing a strong relationship between total dissolved solids (TDS), density (ρ), chlorinity (Cl⁻), and water activity (a_w), which we use to provide community guidelines towards standard sampling metrics in hypersaline systems.

Methods: Brine geochemical data from lab-generated (*i.e.*, ideal) binary salt solutions of NaCl, MgCl₂, Na₂SO₄ and MgSO₄ from 0.1 M to saturation for each salt solution respectively, were used to develop a detailed model from which to begin to interrogate environmental solutions. For the lab-generated brines, ρ , pH, conductivity, and a_w were measured, and TDS and ionic strength were calculated from the known concentrations, at standard temperature and pressure. A stepwise linear regression approach was used to fit these data, with the goal of determining the effect of standard physicochemical parameters on a_w , and to determine which variables could be used to predict a_w . The regression was performed using the `stepwiselm()` function in MATLAB using a constant model as the starting point. The criterion for adding or removing a model term is the p-value of an F-test of the change in the sum of squared error (p-value < 0.05).

Predicting Water Activity: The resulting model (12 terms in 6 predictors) showed that TDS, Cl⁻, Mg²⁺, SO₄²⁻, and conductivity had significant effects with multiple interactions, achieving a root mean squared error (RMSE) of 0.00367 and adjusted (adj.) R² of 0.9997. However, this result likely reflects overfitting with respect to the goal of determining patterns that are likely in environmental conditions, which will differ from the ideal brines and have more noise (unmeasured ions). Thus, we sought to discover a simpler model.

Conductivity and Water Activity: Noting that conductivity was highly non-linear and saturated (**Figure 1**), we repeated the analysis without conductivity data. This yielded a much simpler model, $1 + \rho + \text{Cl}^-\text{Mg}^{2+}$ (Wilkinson Notation, coefficients omitted, X*Y indicates X+Y+X:Y interaction term), but with worse performance (RMSE 0.02110, Adj.R² 0.9890), indicating that conductivity captures important information about a_w .

Simplifying the Model: To gain additional insight, we performed the same regression process on data obtained from acid brine lakes by Benison et al. [7]. This revealed a simple model ($1 + \text{TDS} + \text{Cl}^-$) with low RMSE (0.00742) and intermediate goodness of fit (Adj.R² 0.9905). Caveats here are the limited a_w range represented by these data (0.714-0.944), the limited brine types, and that these are ideal brines without the influence from mixes and unknown/unmeasured ions.

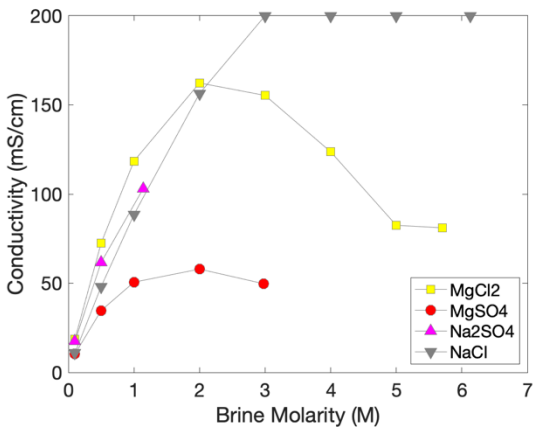


Figure 1. Conductivity is non-linear in high salinity, ideal brines and showed evidence of saturation (measurement artifact) for NaCl brines $\geq 3M$.

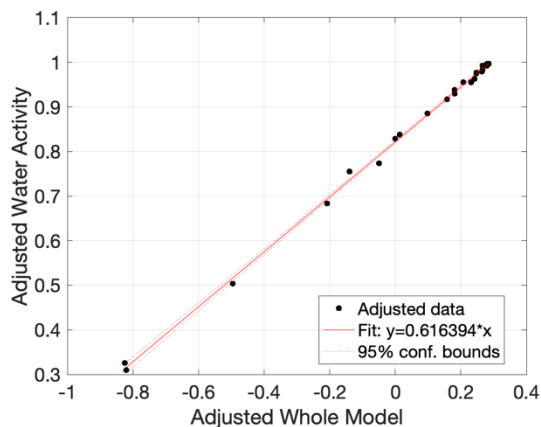


Figure 2. Simplified model fit for ideal brines, showing high correlation between TDS, density, Cl⁻, and predicted (red line) vs. measured a_w .

Benison et al. [7] did not report ρ , preventing direct comparison to our lab data. However, we used our “Benison” regression model as the starting model for stepwise regression on our lab data. This resulted in discovery of a new simplified model, $1 + \text{TDS} \cdot \text{Cl}^- + \rho \cdot \text{Cl}^-$, nearly as good (RMSE 0.00937, adj. R^2 0.9979) as the original full model. The stepwise process revealed that while conductivity was the most significant factor in the first term addition, it was insignificant, and was removed, after addition of ρ , $\rho \cdot \text{Cl}^-$, and TDS:Cl⁻.

Discussion: Our initial model revealed that conductivity is important in predicting a_w . It is possible that this is due to the non-linear nature of conductivity with ion concentration (and therefore a_w), which may be a result of charge shielding, where “non-conductive ion pairs are formed by ion association” [17]. In contrast, our simplified model involved far fewer terms, and is thus more measurable in an environmental context. In addition, our simplified model does not involve

conductivity, and could therefore overcome issues with non-linearity and saturation of conductivity measurements that may occur in hypersaline systems.

TDS was identified as significant in all in all models of the ideal brines, where conductivity was included, in which case ρ was substituted. For the ideal brines, it is likely that TDS provided smoothing of ion measurement errors. In a complex system where the exact ionic composition is not known, TDS will be highly relevant.

Conclusions: This work reveals that for lab and *in situ* determinations of water activity (a_w), regression can achieve accurate results to two decimal places with a simple model driven by chlorinity (Cl⁻), total dissolved solids (TDS), and density (ρ).

As next steps, we will incorporate geochemical data collected at the South Bay Salt Works, Chula Vista, CA, from a range of NaCl and MgCl₂ evaporative ponds, and from the Basque Lakes, representing MgSO₄-dominated brines (*i.e.*, [18]), as well as from archival sources. A major challenge will be the ability to predict a_w to 3 decimal places, a requirement that has been previously identified [7, 19] as thought necessary for understanding microbial activity in these extreme environments.

Acknowledgments: OAST is supported by the NASA Astrobiology Program award 80NSSC18K1301 (PI: B. E. Schmidt). We thank the entire OAST team for their time and thought-provoking discussions.

References: [1] Preston, L. J. and Dartnell, L. R. (2014) *Int J Astrobiology*, 13, 1, 81-98. [2] Antunes, A., et al. (2020) *Curr. Issues Mol. Biol.* [3] Fisher, L. A., et al. (2021) *Environ Microbiol.* [4] Jebbar, M., et al. (2020) *Space Sci Rev*, 216, 1, 10. [5] Merino, N., et al. (2019) *Front in Microbiol*, 10, 780. [6] Saccò, M., et al. (2021) *Biol Rev.* [7] Benison, K. C., et al. (2021) *Astrobiol.*, 21, 6, 729-740. [8] Klempay, B., et al. (2021) *Environ Microbiol*, 23, 7, 3825-3839. [9] Le Menn, M., *Instrument. and Metrology in Oceanog.*. 2012: John Wiley & Sons. [10] UNESCO, I. (1981) *10th Report Joint Panel on Oceanographic Tables and Standards (JPOTS)*, 25. [11] Pawlowicz, R., et al. (2012) *Ocean Science*, 8, 2. [12] IOC, S. (2010) *UNESCO, Manuals and Guides*, 56, 1-196. [13] Anati, D. A. (1999) *Int J Salt Lake Research*, 8, 1, 55-70. [14] Haynes, W. M., *CRC handbook of chemistry and physics*. 2014: CRC press. [15] Stevens, A. H. and Cockell, C. S. (2020) *Frontiers in Microbiology*, 11, 1478. [16] Pitzer, K. S. and Kim, J. J., *Thermodynamics of electrolytes.: IV. Activity and osmotic coefficients for mixed electrolytes*, in *Molecular Structures and statistical thermodynamics*. 1993, World Scientific. p. 413-419. [17] Zhang, W., et al. (2020) *ACS Omega*, 5, 35, 22465-22474. [18] Pontefract, A., et al. (2019) *AbSciCon 2019*. [19] Stevenson, A., et al. (2015) *The ISME journal*, 9, 6, 1333-1351.

MACROSCOPIC DELIQUESCENT AS MONITORED BY DIELECTRIC SPECTROSCOPY. K. M. Primm¹ and D. E. Stillman², ¹ Planetary Science Institute, Tucson, AZ (kprimm@psi.edu). ² Dept. of Space Studies, Southwest Research Institute, Boulder, CO 80302 (dstillman@boulder.swri.edu).

Introduction: Perchlorate (ClO_4^-) and chloride (Cl^-), salts are globally ubiquitous within the martian regolith, significantly reduce the freezing point of water and can absorb water vapor to form an aqueous solution – a process known as deliquescence. While research has been conducted on deliquescent salts, two questions remain. (1) What is the rate of deliquescence under martian conditions and (2) what RH_r does deliquescence occur when the salt is mixed with regolith in a more representative sample size? Here, we measure the electrical properties (dielectric permittivity and conductivity) of multiple salt and simulated martian regolith mixtures using a large grain-supported sample ($\sim 8 \text{ cm}^3$), under temperature and RH_r conditions at martian pressures.

Background: Deliquescence occurs when RH_r exceeds the salt hydrate specific deliquescence relative humidity (DRH). Although some experimental studies are consistent with thermodynamic models, there are many salts that diverge from models (e.g., MgCl_2 [1-3]) and phenomena that cannot be modeled such as efflorescence. Efflorescence occurs when RH_r is less than the salt specific efflorescence relative humidity (ERH). Most salts exhibit a hysteric behavior when the ERH occurs at a lower RH_r than DRH, leading to metastable brine. Note, the metastability of brine occurs when brine exists outside of its thermodynamically-predicted bounds.

The rate at which deliquescence can occur is also an important factor to determine when trying to constrain the possibility of brine on other planetary bodies. The amount of salt and its size may kinetically inhibit deliquescence as a greater amount of water must be absorbed from the atmosphere to fully saturate and dissolve the salt. Previous experiments demonstrated that deliquescence took >3.5 hours to begin [4], implying that deliquescence could not currently take place near Mars' surface. This is in contrast to the rapid kinetics measured in minutes by others [2,5-9]. We hypothesize that the differences in kinetics may be caused by the salt grain size, since *Fischer et al.* [4] used a grain size of $<300 \mu\text{m}$ compared to a smaller particle size ($1\text{--}30 \mu\text{m}$) used by the other researchers. Additionally, *Fischer et al.* [4] appeared to use a very concentrated amount of salt whereas the others used a much smaller volume of salt.

DRH and ERH values did not appear to change when $\text{Mg}(\text{ClO}_4)_2$ was mixed with Mars-relevant minerals [10-11]. Both studies measured very small (sub-mm thickness and $\sim 10 \text{ mm}$ in diameter) amounts of salt-regolith mixtures since they used Raman

spectroscopy that can only detect changes on the surface.

Methodology: We mixed a 1 wt% dry anhydrous $\text{Mg}(\text{ClO}_4)_2$ with quartz sand with 36% porosity. It was loaded into a three-electrode parallel-plate sample holder within a custom-built Mars chamber. The bottom-guarded, guard, and top electrode will have diameters of 20, 55, 30 mm. The guard electrode is grounded to null fringing field, ensuring that the electric field lines above the guarded electrode (which it surrounds) are parallel up to the top electrode. A teflon cup/annulus cap is screwed onto the threaded guard electrode so that the sample can be poured into the sample holder. The top opening has a diameter of 45 mm, of which the top electrode will cover 30 mm. The thickness of the sample will be $\sim 5 \text{ mm}$ and is measured with a micrometer attached to the top.

Briefly, the fully-loaded sample holder is secured on a liquid nitrogen (LN2) cold plate inside our Mars chamber with resistive heaters, and temperature sensors to control the temperature. A vacuum pump will lower the pressure below that of Mars and we will then pump in CO_2 to simulate the atmospheric composition of Mars. We will then add water vapor to the chamber by passing CO_2 gas through a glass frit bubbler to humidify the CO_2 gas and measure the water vapor pressure with a Vaisala DMT152 humidity sensor.

The downside of measuring a larger sample is that gas and heat will take many minutes to diffuse into the sample, compared to the sub-mm samples measured previously where the temperature and RH_r of the environment could be assumed to be that of the sample. However, this sample size will be more representative of the surface layer, meaning that the gas diffusion time could replicate conditions on Mars.

Electrical properties of salt-regolith mixtures will be measured using a Solartron 1260A Impedance Analyzer and a Solartron 1296A Dielectric Interface, connected to a three-electrode sample holder [12-14]. The frequency of injected current is swept from high to low (1 MHz–100 mHz). Complex impedance is converted into complex permittivity using the electrode geometry. We will measure continuously to monitor the deliquescent behavior of the sample and determine when equilibrium has been reached.

Results: Figure 1 shows how the sample changed throughout the temperature and RH_r space. Our first measurement (blue lines) of the sample, showed that it was mostly dry, with a small low-frequency dispersion (LFD) [10,15]. As the sample was lowered in temperature and RH_r (cyan lines), the LFD shifted to

lower frequencies and was reduced in strength. Water vapor was then added to the sample starting 4.5 hours, and was absorbed quickly (not shown), which increased the permittivity of the sample as well as its DC conductivity (green lines). Note the DC conductivity is the limit of the conductivity at low frequency as shown in Fig 1D. The RH_v was held around the ERH for ~21 hours, this allowed the sample to absorb more water, which resulted in a larger DC conductivity (yellow lines). Water vapor was then removed from the chamber and the conductivity responded by reducing in magnitude as water was lost (orange lines). We then removed almost all water vapor to dry out the sample (red lines).

Discussion: By measuring the dielectric permittivity and conductivity of the sample as the temperature and RH_v are changing, we can detect small amounts of brine and relative amounts of brine while the sample is absorbing more water vapor (i.e., green to yellow line in Fig. 1C and D).

Here the sample is absorbing water vapor at the green line which happens to be at the ERH line instead of the DRH line. The sample continues to absorb more water vapor and deliquesces around the yellow line where the permittivity and conductivity drastically increases. The sample is then dried out resulting in a lower permittivity and conductivity (orange and red lines).

Here we see that water absorption happens quickly, but deliquescence doesn't occur until 8 hours later. Furthermore, this sample also deliquesced at a much lower RH_v (~19%) than expected (~48%) at this temperature (-21°C).

Conclusion: These results show that deliquescence can take up to 8 hours to fully saturate a 1wt% dry anhydrous Mg(ClO₄)₂ with quartz sand with 36% porosity sample at 19% RH_v at -21°C under martian pressures. From this study because the sample deliquesced at a much lower RH_v, it seems as if the martian surface has the possibility of absorbing water vapor quickly and deliquescing. However, these studies need to be done at different temperatures and samples. We will continue to measure this rate of deliquescence of the sample at different temperatures and move to Ca(ClO₄)₂.

Acknowledgments: NASA SSW #80NSSC20K0858.

References: [1] Greenspan (1977) *JRNBS A:Phys. and Chem.*, 81A. [2] Gough et al. (2011) *EPSL*, 312. [3] Primm et al. (2017) *GCA*, 212. [4] Fischer et al. (2014) *GRL*, 41. [5] Nikolakakos and Whiteway (2015) *GRL*, 42.[6] Gough et al. (2014) *EPSL*, 393. [7] Gough et al. (2016) *PSS*, 131. [8] Nuding et al. (2014) *Icarus*, 243. [9] Nuding et al. (2015) *JGR: Planets*, 120. [10] Nikolakakos & Whiteway (2018) *Icarus*,

308. [11] Primm et al. (2018) *JGR:Planets*, 123. [12] Stillman et al. (2010) *JPCB*, 114. [13] Stillman et al. (2013a) *JGR*, 116, E03001 [14] Stillman et al. (2013b) *Ann. Glac.*, 54(64). [15] Shahidi et al. (1975) *Nature*, 258.

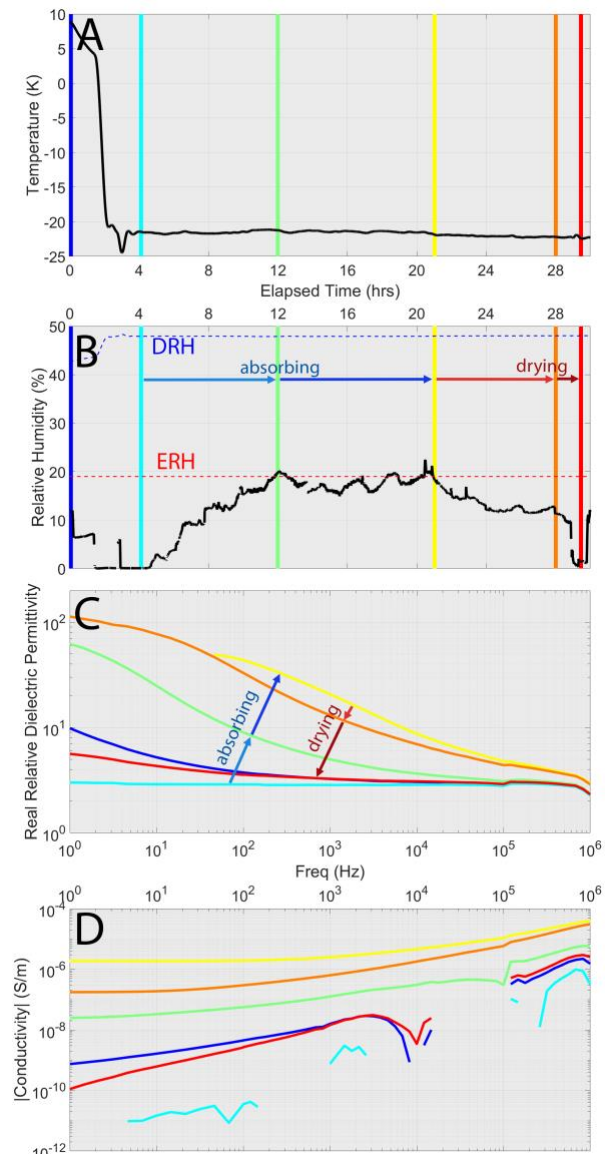


Figure 1. Experimental trajectory for 1wt% dry anhydrous Mg(ClO₄)₂ with quartz sand with 36% porosity (A) temperature (°C) (B) relative humidity. Each colored line represents the same point from (A) and (B) in all four plots. (C) shows the specific points for dielectric permittivity of the sample and (D) shows the same points, but for conductivity of the sample. As the permittivity at low frequency increases with the amount of bound water or bound charges in the sample. The conductivity represents the amount of free charge (i.e., ions) that can migrate freely through the sample.

BRINES ON CERES: ORIGINS AND TRANSPORT PROCESSES. ¹C. A. Raymond, ¹J. C. Castillo-Rogez, ²A. I. Ermakov, ¹J. E. C. Scully, ¹R. S. Park, ³R. R. Fu, ⁴L. C. Quick, ⁵O. Ruesch, ¹Jet Propulsion Laboratory, California Institute of Technology, Pasadena, California, USA, ²University of California, Berkeley, CA, USA, ³Harvard University, Cambridge, MA, USA, ⁴Goddard Space Flight Center, Greenbelt, MD, USA, ⁵WWU, Munster, DE

Introduction: Data collected by NASA's Dawn spacecraft provide evidence that global aqueous alteration of dwarf planet Ceres resulted in a chemically evolved body that remains volatile rich [1], while recent emplacement of bright deposits sourced from brines attests to Ceres being a persistently geologically-active world [2, 3, 4]. Modeling of Ceres' relaxed shape at long wavelength, constrained by density estimates from gravity modeling are consistent with a crust rich in ice, possible clathrates, and <20 vol.% silicates and salts; a mantle of hydrated rock with some porosity; and a global muddy layer at the crust-mantle interface (Figure 1). Results obtained during the last phase of the Dawn mission (XM2) show evidence of this deep brine in the relative youth and composition of bright salt deposits, most notably within Occator crater. The geologically-young Ahuna Mons, a 4-km high mountain also appears to be sourced from a deep muddy layer [5].

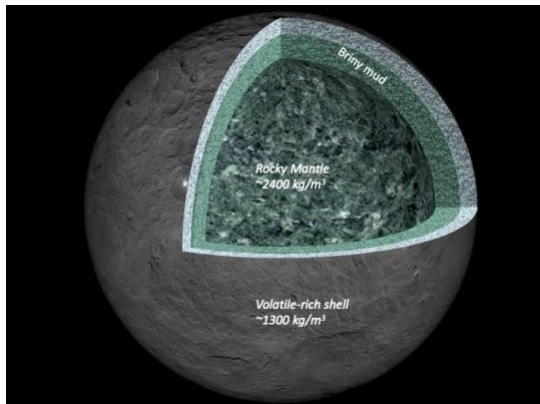


Figure 1. Ceres' interior structure derived from gravity and topography data from the Dawn mission. Credit: PIA22660 (<https://photojournal.jpl.nasa.gov/catalog/PIA22660>).

Origin of Brines: All permissible internal evolution models consistent with Dawn data lead to the presence of a global liquid layer early in Ceres' evolution [6], while the inferred presence of clathrates supports the persistence of brines to the present day [7]. Although Ceres' ~40-km-thick crust appears strong ($\sim 10^{25}$ Pa-s), its global shape at wavelengths >150 km indicates that viscosity decays at a rate of one order of magnitude per 10 to 15 km to $<10^{21}$ Pa-s by about 40 km depth [8]. The influence of this layer on the global shape suggests a saturated mud layer below the crust, consistent with slow freezing of a global ocean. Although, a mostly

liquid brine layer is not ruled out [8], admittance analysis suggests the density of material below the crust (~ 2430 kg/m³, [9]) is consistent with a mixture of silicates and brines.

Lateral heterogeneity in brine distribution was investigated using XM2 data of Occator crater and the surrounding Hanami Planum (HP) region [10]. HP is a discrete highland of ~555 km diameter with elevation reaching 6 km with respect to Ceres' reference ellipsoid. It displays a broad-scale negative isostatic gravity anomaly (indicating excess light material) that is anti-correlated to topography [9, 11], indicating significant heterogeneity relative to surrounding areas [10]. Markov Chain Monte Carlo (MCMC) modeling of the isostatic gravity field in the region was performed to investigate the sources of both the broad HP anomaly and the deep low anomaly near Occator Crater (Figure 2). The inferred mass deficits are interpreted as areas of brine enrichment, which may reflect modulation of the depth and thickness of deep brines resulting from heterogeneity in the clathrate distribution between HP and the lowlands (as a result of the depth and extent of impact gardening). The inferred brine-rich region beneath the Occator region likely contributed to and prolonged eruptions within Occator crater.

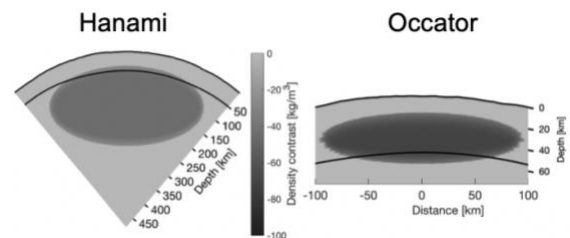


Figure 2. Cross-sections of median values of density contrast derived from high-likelihood MCMC solutions [10]. Top surface is observed topography; Black line shows crust/mantle boundary at ~55 km. Hanami's total mass deficit is found to be ~0.1% of Ceres' mass ($-89.1^{+1.5}_{-1.6} \times 10^{16}$ kg/m³). The Occator region's residual mass deficit is $-6.2^{+0.5}_{-0.6} \times 10^{16}$ kg/m³.

Impact heating of the crust can also drive brine production. Thermal evolution modeling of the temperature field at Occator crater, following the impact ~20 My ago is shown in Figure 3. The impact created a liquid pool beneath the center of the crater that collected salt impurities trapped in the crust and potentially captured impactor material that could be subject to aqueous alteration [12]. That pool persisted for ~5 My

and could have contributed to a first stage of evaporite emplacement [4]. However, the youth of the Occator salt deposits and the evidence for hydrohalite which rapidly dehydrates in vacuum [13], indicates ongoing brine effusion within the crater. Hence the source of that recent activity is likely the persistent brine layer inferred beneath Hanami Planum at ~ 35 km depth [10].

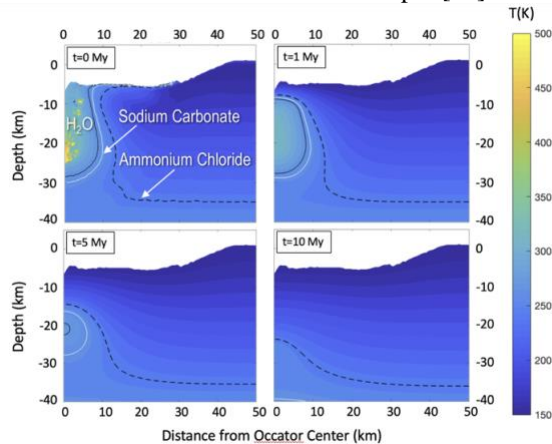


Figure 3. Occator crater post-impact temperature field, calculated by rescaling the hydrocode modeling of [12] for lower thermal conductivity using the methods of [14]. Contours for the eutectic temperatures of sodium carbonate and ammonium chloride are annotated, showing where these salts are in solution beneath the crater. From [10].

Brine Transport. The widespread presence of bright deposits across Ceres' surface (e.g., [15]), that occur in central peaks of craters and in the lone Ahuna Mons cryovolcano [16, 17] are rich in sodium carbonate. These deposits indicate widespread migration of subsurface brines to the surface over its geologic history.

Brine activity in the 20 My old Occator Crater is long-lived, and the youngest material (<4 My) occurs in the central pit of the Cerealia Dome [2, 18]. The distribution and geologic setting of the deposits, suggest that brines exploited fractures and porosity to form the faculae deposits [19, 20, 4, 10]. While the impact melt was initially water-rich, later magmas were rich in sodium carbonate, chlorides and other salts [20, 21]. The probable mechanisms that transport brines to the surface include pressure-driven flow through fractures as brines freeze at depth [22], and/or as a result of gas release [21]. Quick et al. [21] predict cycles of brine effusion modulated by the freezing and pressure-driven opening of fractures that penetrate to a deep brine reservoir.

The only major deposit of sodium carbonate not associated with an impact crater is Ahuna Mons, a youthful constructional feature attributed to brine effusion [23]. It is at the center of a large positive isostatic gravity anomaly; its high density argues for a

source rich in silicates, consistent with a muddy plume originating in the deep brine layer at the crust-mantle boundary [5]. The presence of Ahuna Mons is additional evidence for transport of deep brines to the surface, as impact heating can be ruled out in this case.

Implications: Dawn's comprehensive gravity, topography, morphology and surface composition data sets collected during the prime mission have demonstrated that large icy planetesimals can experience extensive, global aqueous alteration resulting in early subsurface oceans. The high-resolution data collected at Occator crater during the XM2 phase document ongoing brine activity showing that such large initially icy bodies can retain subsurface brines even in the absence of tidal heating. Ceres' relaxed global shape and globally-distributed salt deposits, as well as recent activity at multiple locations argue for an extended brine layer, although its thickness and composition remain murky. The presence of subsurface brines on Ceres throughout its history, evidence of organic materials, and active transport processes make Ceres a rich target for understanding habitability and astrobiological potential on ocean worlds [24].

Acknowledgments: Part of this work was carried out at the Jet Propulsion Laboratory, California Institute of Technology, under contract to NASA. Government sponsorship acknowledged.

References: [1] Ammannito E. et al. (2016) *Science*, 353, aaf4279. [2] Nathues A. et al. (2020) *Nature Astron.*, 4, 749-801. [3] De Sanctis M.C. et al. (2016) *Nature*, 536, 54-57. [4] Scully J.E.C. et al. (2020) *Nature Comm.*, 11, 3680. [5] Ruesch, O. et al. (2019) *Nat. Geosci.*, 12, 505-509. [6] Castillo-Rogez, J.C. et al. (2018) *MAPS*, 53, 1820-1843. [7] Castillo-Rogez J.C. et al. (2019) *GRL*, 46, 1963-1972. [8] Fu R.R. et al. (2017) *EPSL*, 476, 153-164. [9] Ermakov A.I. et al. (2017) *JGR*, 122, 2267-2293. [10] Raymond C.A. et al. (2020) *Nature Astron.*, 4, 741-747. [11] Park, R. et al. (2016) *Nature*, 537, 515-517. [12] Bowling T. J. (2019) *Icarus*, 320, 110-118. [13] DeSanctis, M.C. et al., *Nature Astron.*, 4, 786-793. [14] Hesse M. & Castillo-Rogez, J.C. (2018) *GRL*, 46, 1213-1221. [15] Carrozzo, F.G. et al. (2017) *Science Adv.*, 4, e1701645. [16] Stein, N. et al. (2017) *Icarus*, 320, 188-201. [17] Zambon, F. et al. (2017) *Icarus*, 318, 212-229. [18] Neesemann, A. et al. (2019) *Icarus*, 320, 60-82 [19] Schmidt, B.E. et al. (2020) *Nat. Geosci.*, 13, 605-610. [20] Schenk, P.M. et al. (2020) *Nature Comm.*, 11, 3679. [21] Quick, L.C. et al. (2019) *Icarus*, 320, 119-135. [22] Neveu, M. & Desch, S. J. (2015) *GRL*, 42, 10,197-10,206. [23] Ruesch, O. et al. (2016) *Science*, 353, aaf4286. [24] Castillo-Rogez, J.C. et al. (2020) *Astrobio.*, 20, 269-291.

FORMATION OF (META)STABLE BRINES ON PRESENT-DAY MARS: IMPLICATIONS FOR HABITABILITY. E. G. Rivera-Valentín¹, V. F. Chevrier², A. Soto³, G. Martínez¹; ¹Lunar and Planetary Institute (USRA), Houston, TX 77058. ²Arkansas Center for Space and Planetary Sciences, University of Arkansas, Fayetteville, AR 72701, ³Southwest Research Institute, Boulder, CO 80302.

Introduction: Whether present-day Mars can support terrestrial-like life depends on multiple factors, such as temperature, radiation, and availability of nutrients, and, importantly, liquid water. Pure liquid water, though, is unstable on the Martian surface due to rapid phase changes. With an average surface pressure of 600 Pa, the boiling point on Mars is ~ 273 K, and with an average surface temperature of ~ 220 K pure liquid water rapidly freezes. Additionally, in-situ meteorological measurements have indicated that, at most, the near-surface water vapor pressure reaches some $e \approx 2$ Pa [1]. Thus to avoid rapid evaporation, pure liquid water would need to be stable at ~ 215 K, well below its freezing point. Even in the shallow subsurface where evaporation is slowed due to diffusion through a porous overburden [2] the large concentration gradient can quickly drive mass loss.

Brines, though, are proposed to form and persist as they have increased stability against the cold and hyper-arid surface conditions. Salty aqueous solutions have reduced water vapor pressures above the liquid because their water activity $a_w < 1$, where $a_w = e_b/p_{sat,l}$, e_b is the water vapor pressure above the brine, and $p_{sat,l}$ is the temperature (T) dependent saturation vapor pressure above pure liquid water. This results in a brine boiling at a higher temperature and evaporating slower. Dissolved salts also lead to reduced freezing temperatures. As such, brines are stable under a broader range of Mars-relevant environmental conditions. Brines may be forming on Mars through melting via salt-ice interactions, such as at the regolith-ice table interface [3], or via salt deliquescence [4-6]. Furthermore, experimental work under Mars-relevant conditions have shown that brines may persist beyond their predicted stable region, leading to metastable liquids [5,7].

To date, though, the only potential direct observation of liquid on Mars were droplets on the struts of the Phoenix lander [8]. Phoenix (PHX) also provided indirect evidence of brine formation in the subsurface by way of variations in the measured dielectric properties of the regolith [9] and the heterogeneous distribution of salts [10]. In-situ meteorological measurements by PHX further support brine formation through both melting [3] and deliquescence [11], while measurements by the Mars Science Laboratory (MSL) support the potential formation of brines by deliquescence at the near-surface of low thermal inertia terrains [6].

Here we explore the stability of brines on Mars, by reviewing recent work [12,13] that has used in-situ measurements and general circulation models to predict where, when, and for how long brines may be stable on the near-surface. We particularly focus on calcium perchlorate due to its low freezing-point ($T = 198$ K) at $a_w = 0.52$. The Mars Special Regions criteria (water activity $a_w \geq 0.6$ and temperature $T \geq 255$ K) [14] is adopted to assess the habitability of such brines.

Methods: For this study, we used the Mars Weather Research and Forecasting (MarsWRF) general circulation model (GCM). For surface temperature calculations, a multilayer subsurface thermal diffusion and surface energy balance model uses surface albedo and thermal inertia maps derived from orbital observations. For the water cycle, MarsWRF employs the microphysics scheme implemented by [15]. For this work, simulations were run at 5° by 5° horizontal resolution with 52 vertical levels. Simulated hourly surface temperature, pressure, and water mixing ratio, which we then translated to relative humidity w.r.t. liquid (RH_l), were then used to test for brine formation and stability. Additionally, we used temperature and humidity measurements by PHX and MSL.

Results: In Fig. 1, we plot the simulated combinations of temperature and relative humidity w.r.t. liquid experienced on the martian surface, against in-situ measurements, the deliquescence relative humidity (DRH) of calcium, magnesium, and sodium perchlorate, and the ice line (i.e., where saturation w.r.t. ice is reached, $RH_{ice} = 100\%$).

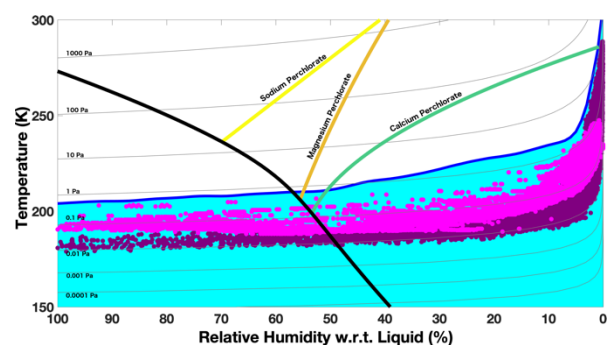


Figure 1: Phase diagram for Mars-relevant deliquescent salts along with the possible combination of conditions as simulated by the MarsWRF GCM (cyan space) and PHX (magenta) and MSL (purple) in-situ measurements. Light gray lines are isobars of constant water vapor pressure.

In order for a brine to be stable on the surface of Mars against freezing and evaporation, its freezing point, which follows the ice line, must be within the possible combination of temperature and relative humidity that can occur on Mars. Should a brine form outside of this phase space, it would quickly evaporate away due to the high vapor pressure associated with its liquid phase. As such, from Fig. 1 we see that Mars-relevant brines are those with freezing temperatures < 210 K.

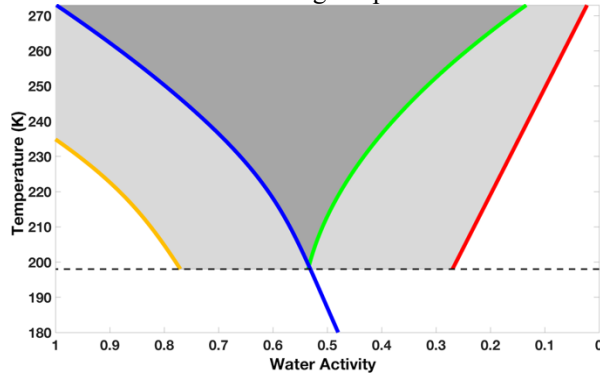


Figure 2: Phase diagram for $\text{Ca}(\text{ClO}_4)_2$ including stable (dark gray) and metastable (light gray) liquid phases. Blue is the ice line, green is DRH, red is ERH, and orange is $RH_{ice} = 145\%$.

In Fig. 1, we also see that calcium perchlorate should more readily lead to brine formation through deliquescence. As such, we further explored its stability on Mars. In order for a salt to deliquesce, the temperature must be above the eutectic and $RH_l > \text{DRH}$. Though thermodynamically solutions should recrystallize once $RH_l < \text{DRH}$, due to a hysteresis effect, efflorescence occurs at a lower relative humidity [4,5], allowing for metastable liquids. Furthermore, experiments under Mars-like conditions have shown that solutions persist even after saturation with respect to water ice is reached [7], up to $RH_{ice} = 145\%$. In Fig. 2, we show the stable and metastability conditions for $\text{Ca}(\text{ClO}_4)_2$.

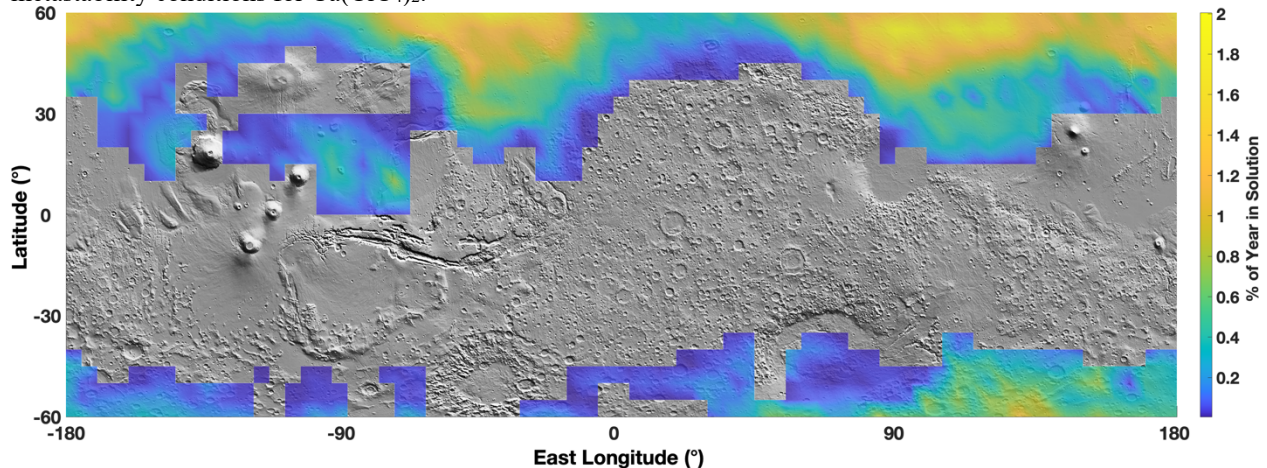


Figure 3: Modeled stable calcium perchlorate brines formed via deliquescence on the surface of Mars. The percent of the year a solution is present is shown in color overlay onto a shaded relief map of Mars.

Given the experimentally-constrained (meta)stable phase space for $\text{Ca}(\text{ClO}_4)_2$, we used the model outputs from MarsWRF to investigate where, when, and for how long such solutions could form via deliquescence (Fig. 3). $\text{Ca}(\text{ClO}_4)_2$ brines can form over some 40% of the Martian surface. These brines are most likely at high northern latitudes, where they are (meta)stable for up to 2% of the year. Although $\text{Ca}(\text{ClO}_4)_2$ brines may persist for at most half a sol per sol, they may be liquid for at most six consecutive hours. In the northern hemisphere, $\text{Ca}(\text{ClO}_4)_2$ brines occur around $L_s 140^\circ$ while in the southern hemisphere around $L_s 225^\circ$.

We find that the maximum water activity of such brines is 0.8 with a corresponding temperature of 205 K. These conditions are met just before complete freezing. On the other hand, the maximum possible brine temperature is 225 K with an associated $a_w = 0.24$. These conditions are met just prior to efflorescence. As such, although metastability extends the locations where brines may form, they do not simultaneously meet the required conditions for habitability.

Acknowledgements: This research was supported by NASA through the Habitable Worlds Program under Grant No. 80NSSC17K0742.

References: [1] Martínez & Rennó (2013) Spac. Sci. Rev. 175, 29-51. [2] Ulrich (2009) Icarus 201, 127-134. [3] Fischer et al. (2016) Astrobiology 16, 937-948. [4] Gough et al. (2011) EPSL 312, 371-377. [5] Nuding et al. (2014) Icarus 243, 420-428. [6] Rivera-Valentín et al. (2018) JGR Planets 123. [7] Primm et al. (2017) GCA 212, 211-220. [8] Rennó et al. (2009) JGR Planets 114. [9] Stillman & Grimm (2011) JGR Planets 116. [10] Cull et al. (2010) GRL 37. [11] Chevrier et al. (2009) GRL 36. [12] Chevrier et al. (2020) PSJ 1, 64. [13] Rivera-Valentín et al. (2020) Nat. Astro. 4, 756-761. [14] Rummel et al. (2014) Astrobiology 14, 887-968. [15] Lee et al. (2018) Icarus 311, 23-34.

SPECIAL REGIONS BASED HABITAT SUITABILITY INDEX MODEL FOR BRINE ENVIRONMENTS ON MARS. E. G. Rivera-Valentín¹, A. Méndez², K. L. Lynch¹, A. Soto³; ¹Lunar and Planetary Institute (USRA), Houston, TX 77058, ²Planetary Habitability Laboratory, University of Puerto Rico at Arecibo, Arecibo, PR 00612, ³Southwest Research Institute, Boulder CO 80302.

Introduction: In ecology, habitat suitability index (HSI) models are quantitative ways of representing the potential for an environment to support a selected species or model organism. These indices apply known environment-species relationships, such as temperature tolerances, to predict survival, reproduction, and development, as well as the environment's potential for species recruitment. Additionally, HSIs allow for a consistent way of comparing environments and to examine their suitability over time. Recently, [1] suggested applying such ecological models to planetary science in order to resolve the habitability of extraterrestrial environments. Because the question of habitability does not fundamentally have a binary answer but is rather a spectrum, habitat suitability indices provide an excellent resource to compare extraterrestrial environments and understand their potential to support life.

Given the level of environmental data available from both orbiters, landers, and general circulation models, HSIs can now be used to assess the present-day habitability of the Martian surface. Furthermore, the Martian surface may presently support (meta)stable liquids, specifically brines [2,3]. Such brines may provide the liquid water environment necessary for life, as well as shielding from the martian radiation environment [4]. To date, the Special Regions requirement (water activity $a_w \geq 0.6$ and temperature $T \geq 255$ K) has been adopted to assess the habitability of martian environments [5,6]. Given the surface conditions, though, recent work has shown that expected brine environments would not support terrestrial-like life because the maximum temperature a (meta)stable brine could achieve is 225 K [2].

The environmental conditions required by the Special Regions definition, though, are based on life as we have known it. Indeed, the boundary conditions for life have over time been pushed into more extreme conditions. Since the publication of these requirements, microorganisms have been found living in a hypersaline deep-sea brine that can reach $a_w \sim 0.4$ and $T \sim 290$ K [7], though not in Don Juan Pond in Antarctica where $a_w \sim 0.45$ and $T \sim 237$ K [8].

To assess and compare martian environmental habitability, here we develop an HSI model based on the species-environment relationships used in the Special Regions definition (i.e., water activity and temperature). The developed quantitative metrics are aimed at finding where and when Mars would be, relatively

speaking, the most habitable. Because liquid water is important for life as we know it, the models are particularly applied to potential brine environments, but we also apply them outside of these conditions to gain a general understanding of Martian habitability.

HSI Model: Typically, an HSI varies between zero, for a fully unsuitable environment, to one, for a fully suitable environment [1]; however, given the low temperature and hyperarid conditions experienced on Mars, which are typically below known microbial tolerances [8], our developed suitability index ranges between +1 and -1. The positive HSI boundary is defined by the maximum possible temperature and brine water activity while the negative boundary is defined by the minimum possible temperature and brine water activity. The zero boundary represents the mortality conditions in temperature and water activity. For the purposes of this work, we set this to the Special Regions values, but note that the HSI is developed to allow this boundary to be easily changed.

While temperature is readily obtained for Mars either from in situ or orbital measurements and as model outputs given thermal inertia and albedo, brine water activity is not. Brine water activity, though, is related to the local relative humidity with respect to liquid (RH) at equilibrium by $a_w = (RH/100)$ because at this point the brine is stable against evaporation. This now allows for HSI calculation following two environmental parameters, T and RH . Within this space, we develop our HSI as a measure of the shortest distance to the mortality boundary. In Figure 1, we plot the developed HSI model over the range of Mars-relevant temperatures and relative humidity.

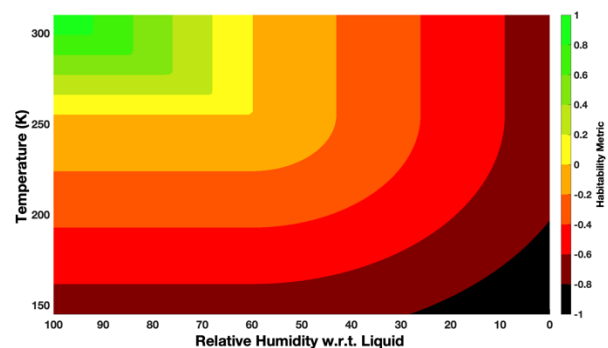


Figure 1: The proposed habitat suitability index model based on the temperature and relative humidity mortality point used to define Special Regions on Mars.

To conduct global HSI calculations, we used the modeled surface temperature and water mixing ratio, which we then translated to RH_i , from the MarsWRF general circulation model [9]. We also used in situ measurements from the Phoenix (PHX) lander and the Mars Science Laboratory (MSL) rover. For environmental context, in Figure 2, we plot PHX and MSL data bounded by the maximum and minimum combination of temperature and relative humidity that is predicted by MarsWRF to occur on the surface of Mars. Additionally, we include data from weather research stations, assimilated observational and model data, from the Atacama Desert and the Antarctic Dry Valleys, which are often used as Mars analogs on Earth because of their arid environments.

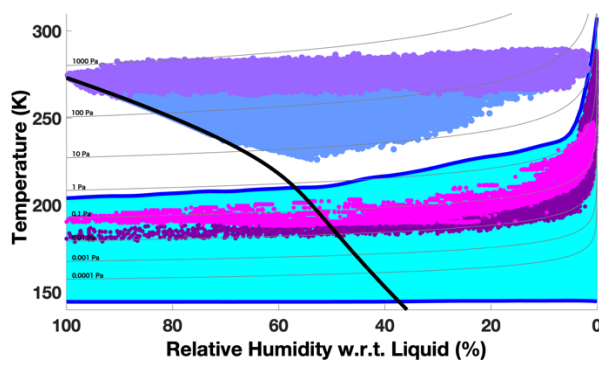


Figure 2: Temperature and relative humidity measurements from PHX (magenta) and MSL (purple) compared with the Atacama Desert (lavender) and the Antarctic Dry Valleys (light blue). For context, the possible combinations of conditions as predicted by MarsWRF is shown by the cyan space bounded in blue by the maximum and minimum combination. The light gray lines are of constant water vapor pressure and the solid black line is the ice line ($RH_{ice} = 100\%$).

Results: In Figure 3, we show the hourly calculated HSI using data from PHX and MSL, as well as the Atacama Desert and Antarctic Dry Valley for one year. As can be seen in Figure 2, due to the hyperarid conditions on Mars, relative humidity is strongly correlated with temperature such that low temperatures are associated with high humidity at night and high temperatures are associated with low humidity during the day. The latter association manifests in Figure 3 as a clustering around a value of -0.7. The terrestrial sites are free of this clustering, even at the drier site of Antarctica. Furthermore, both Earth sites exhibit seasons where $HSI > 1$ (i.e., habitable), while the highest value for Mars is only -0.32. Such values occur only briefly during a single day rather than a season.

At the conference, we shall present global results and discuss implications for relative habitability across the Martian surface, as well as temporal dependencies.

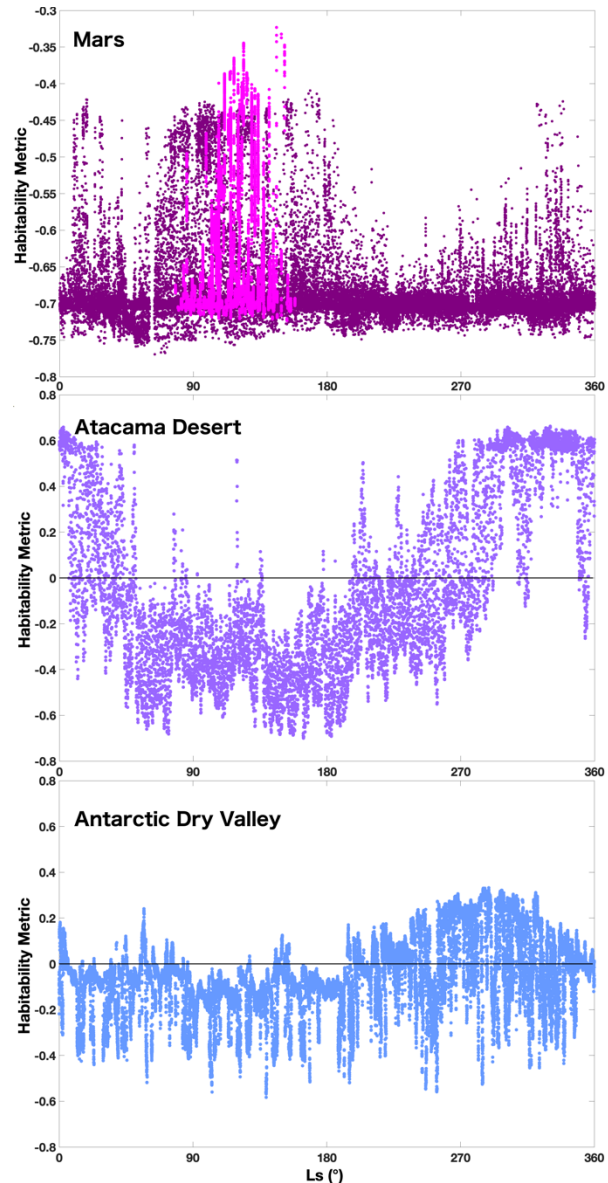


Figure 3: Calculated HSI using in-situ PHX and MSL measurements for Mars, as well as data representative of the Atacama Desert and Antarctic Dry Valley as a function of time (Ls, heliocentric longitude). Colors follow from Fig. 2.

Acknowledgements: This research was supported by NASA through the Habitable Worlds Program under Grant No. 80NSSC17K0742.

References: [1] Méndez, A. et al. (2021) *Astrobiology* 21,10. [2] Rivera-Valentín, E. G. et al. (2021) *Nat. Astro.* 4, 756 – 761. [3] Chevrier, V. F. et al. (2021) *PSJ* 1, 64. [4] Diaz, B. & Schulze-Makuch, D. (2006) *Astrobiology* 6, 332 – 347. [5] Kminek, G. et al. (2010) *Adv. Space. Res.* 46, 811 – 829. [6] Rummel, J. D. et al. (2014) *Astrobiology* 14, 887 – 968. [7] Steinle, L. et al. (2018) *ISME Journal* 12, 1414 – 1426. [8] Merino, N. et al. (2019) *Front. in Microbio.* 10:780. [9] Richardson, M. I. et al. (2007) *JGR Planets* 112, E09001.

Raman spectroscopy: quantitative analyses of modern brines on Mars A. J. Rodriguez¹; M. E. Elwood Mad-den¹; D. P. Mason² University of Oklahoma, School of Geosciences, ²University of New Mexico

Introduction: The Raman spectrometers onboard the Perseverance and Rosalind Franklin rovers have the ability to identify polyatomic ions present in saline solutions [1–3]. Since salts are ubiquitous on Mars, they will likely be detected by the rovers. Furthermore, since salts lower the freezing point and vapor pressure of liquid water, they may enable deliquescence or melting of salt-brine mixtures at temperatures and pressures near the equator of Mars [4–6].

This work aims to provide a reference Raman spectral library of aqueous solutions. By comparing the relative intensity of peaks observed in the Raman spectra, we can both compare the relative concentrations of multiple salts, and estimate the absolute concentration of each salt by comparing to known water peaks. This is part of an ongoing project that will create a spectral library within the Planetary Database System.

Methodology: Six salts were added to 18.2 MΩ H₂O (UPW) until saturated : NaCl, NaClO₄, Na₂SO₄, MgCl₂, MgSO₄, CaCl₂. Serial dilutions (0.0001–2 mol/kg) of 13 salt standards (Na₂CO₃, NaHCO₃, NaNO₃, NH₄Cl, H₃PO₄, Na₂HPO₄, NaH₂PO₄, Na₂SO₄, NaHSO₄, NaCl, NaClO₃, NaClO₄, NaF) were also prepared. We mixed the diluted salt standards with each endmember brine at a 1:3 ratio within wells on a ceramic painter's palette and immediately analyzed the solution with a Renishaw InVia Raman Spectrometer using both 532nm and 785nm lasers. Each spectra was collected for 100 s, then we removed the background noise normalized the spectra. Curve fitting was performed using the WiRE 4.2 software and the peak intensity ratios for the solute salt standards, salts within the matrix brine, and water were calculated using the peak heights and areas. Using the peak ratios, we constructed calibration curves, conducted linear regressions, and produced equations that can be used to calculate solute concentrations based on the observed spectra.

Results: Of the salts chosen as near-saturated brines, three have an ionic characteristic which produces a Raman signature, NaClO₄, Na₂SO₄, and MgSO₄. Of these brines, NaClO₄ produces such an intense peak that only NaNO₃ has a Raman peak intensity capable for calibration curves (fig. 1). Otherwise, the salts that produce a Raman peak is strong enough to allow us in creating calibration curves with a strong certainty. The salts Na₂SO₄ and NaHSO₄ reacted in the CaCl₂ brine to produce identifiable amounts of gypsum, thereby altering the concentrations of the ions where we

cannot say with certainty the final concentration of the ions in solution.

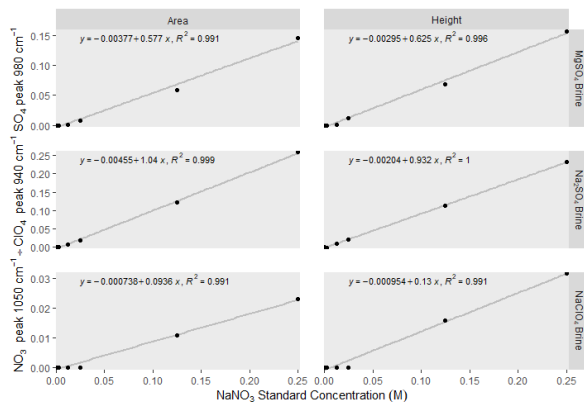


Figure 1. Raman calibration curves for NaNO₃ serial dilution versus near saturated endmember brines MgSO₄, Na₂SO₄, and NaClO₄. Raman spectra collected using a 532nm laser.

The spectra collected shows a clear line of regression when comparing the more dilute solute peak height and area with the water peak height and area at 1640 cm⁻¹ as well as to the brine peaks (fig. 2). Additionally, the goodness of fit is similar to that of the ClO₄⁻ peak at 940 cm⁻¹ compared to the water peak in the UPW solution (fig. 3).

Discussion: This project shows that anions producing a clear Raman peak such as NO₃⁻ or NaClO₄⁻ can be identified in a mixed solution. The concentration of these salts has a direct effect on the relative intensity on the peak height and area of the curves produced, and this change can be used in conjunction with the peak produced from water or the endmember brine to measure the concentration of the anion in solution, even within a near-saturated brine matrix.

The ratio trend observed in figure three gives evidence that the Raman peak intensity is not altered or shows evidence of any chemical bonding that would cause the peak intensity to be suppressed at higher concentrations. The trend in ratios is strong enough to say that as long as there is no thermodynamic motivation for the ions to react (such as Na₂SO₄ + CaCl₂ forming gypsum), the ions in the solution will show up in the Raman spectra relative to water as if they were not present. This gives us confidence that as long as

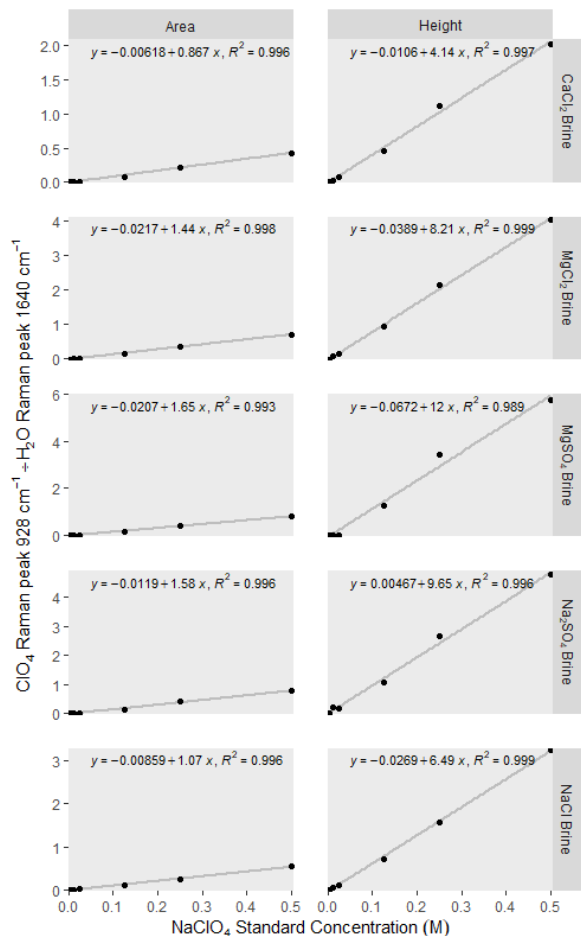


Figure 2. Raman peak ratios of the ClO₄⁻ peak at 928 cm⁻¹ against the water peak at 1640 cm⁻¹ from within the endmember brines CaCl₂, MgCl₂, MgSO₄, Na₂SO₄, and NaCl. Raman spectra collected using a 532nm laser

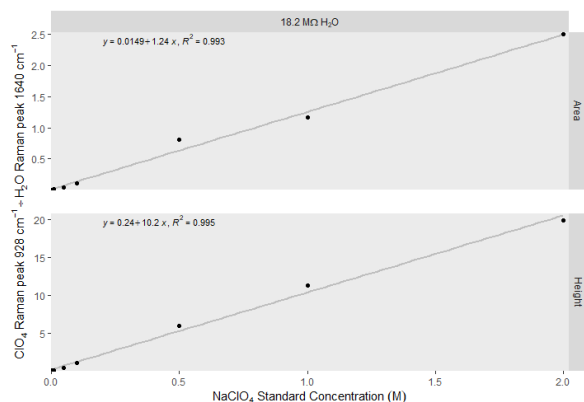


Figure 3. Raman peak ratios of the ClO₄⁻ peak at 928 cm⁻¹ against the water peak at 1640 cm⁻¹ in UPW. Raman spectra collected using a 532nm laser.

both the anion and water peak are detectable, the concentration can be calculated from the peak of water, even if the solution observed is nearly saturated with a salt. Indeed, if we are confident that one of the salts is at saturation, we can also use that peak to provide a second reference by which to measure concentration of the less concentrated solute and provide further confidence in the calculated concentrations.

This procedure does have its limits. Salts that do not include a polyatomic ion will not produce a Raman peak and will go undetected. However the presence of these salts in solution does not significantly affect the peak ratios of detectable salts or the water peak at 1640 cm⁻¹. Other methods will be needed to detect these ions.

Conclusion: This research shows how Raman spectroscopy can be used to identify and calculate the concentration of a polyatomic solutes if liquid water is detected within the sampling area. Such a discovery would give support for the theory of transient liquid water on the Martian surface as well as provide insight into environmental conditions affecting habitability.

Acknowledgements: This project was funded by NASA PDART grant 80NSSC18K0512. N. Wood helped with data processing.

References: [1] Dable B.K. (2006) *Appl Spectrosc.*, 60, 773-780 [2] McGraw L.E (2018) *ACS Earth Space Chem.*, 2, 1068-1074 [3] Israel E.J. (1997) *Geophys Res Planets*, 102, 28705-28716 [4] Haberle R.M. (2017) *Cambridge Uni Press* [5] Squyres S.W. (2006) *Sci.*, 313, 1403-1407 [6] Clancy R.T. (2000) *Geophys Res Planets*, 105, 9553-9571

BACTERIAL SURVIVAL AND GROWTH IN DENSE BRINES, DELIQUESCENT LIQUIDS, AND CRYSTAL FLUID INCLUSIONS. M. A. Schneegurt¹, H. Z. Zbeeb¹, R. M. Cesur, MD Joad¹, H. H. Zayed¹, I. M. Ansari, A. Mahdi¹, T. M. Luhring¹, F. Chen², and B. C. Clark³, ¹Department of Biological Sciences, Wichita State University, 1845 Fairmount Street, Wichita, Kansas 67260, USA, mark.schneegurt@wichita.edu, ²Jet Propulsion Laboratory, 4800 Oak Grove Dr., Pasadena, CA 91109, USA, ³Space Science Institute, 4765 Walnut St., Boulder, CO 80301, USA.

Life in brine: Liquid water on cold arid worlds needs to be salty, relying on high solute concentrations to depress the freezing point of water. Life requires liquid water, so growth tolerance to dense brines broadens the range of potentially habitable regions and periods [1]. Sulfate and chloride salts are important constituents of Mars regolith, with Ca, Fe, Mg, and Na counterions [2], while brine pockets and oceans on icy worlds may have similar salts. Significant concentrations of (per)chlorate salts are present on Mars with eutectic temperatures as low as $-69\text{ }^{\circ}\text{C}$ for $\text{Mg}(\text{ClO}_4)_2$. Icy worlds may maintain liquid water with high concentrations of ammonia.

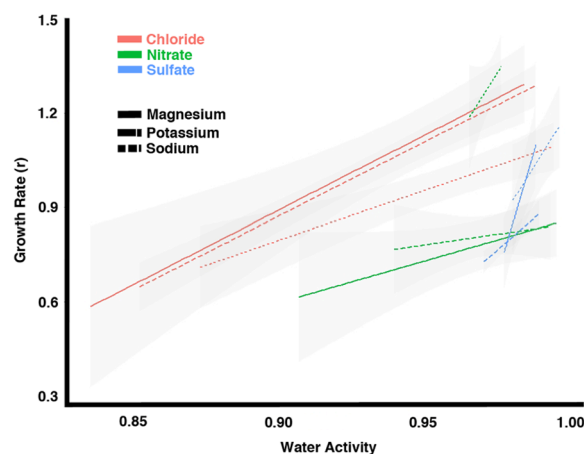
Microbial tolerances to NaCl and carbonates have been studied far more than other salts. No single quality of these salts or ions appears to determine which will inhibit microbial growth, although it is clear that water activity (a_w) and ionic strength are important. Here we have measured growth in a series of salts, testing an iterative matrix of ions with different physical qualities.

When brines dissipate on arid worlds, the evaporites formed can entrap microbial cells within fluid inclusions and between crystals. Microbes tolerant to saturated brines may survive for extended periods in these liquid refugia. As more humid conditions occur, hygroscopic evaporites can deliquesce, creating liquid brines. This process may occur on Mars, particularly for (per)chlorate salts.

Bacterial isolates from analogue sites: Our bacteria were isolated from natural environments rich in NaCl (Great Salt Plains, OK) or MgSO_4 (Hot Lake, WA) [3]. The collections include *Bacillus*, *Halomonas*, *Marinococcus*, *Nesterenkonia*, *Planococcus*, and *Virgibacillus* isolates that grow at $\geq 10\%$ NaCl (1.7 M), $\geq 50\%$ (~ 2.0 M) MgSO_4 , and $>20\%$ (~ 2.0 M) Na chlorate [3]. Salt Plains (SP) medium was supplemented with various salts at increasing concentrations to saturation.

Tolerance to an iterative matrix of ion pairs: Over 4000 time-series were fit to logistic growth curves of 18 salinotolerant bacteria to estimate the intrinsic rate of population increase (r) and maximum culture density (K) in the presence of an iterative matrix of all combinations ($N = 1051$) of 3 cations (Mg, K, Na) and 3 anions (Cl, NO_3 , SO_4) and their physical qualities. Lower a_w led to lower growth rates ($P < 2.2\text{e-}16$) across all salts. Further, r was affected

by salt-specific responses from ion pairing (anion \times cation interaction, $P < 2.2\text{e-}16$). Responses appear to cluster by anion ($P < 9.1\text{e-}15$). No 3-way interactions were significant with a_w .



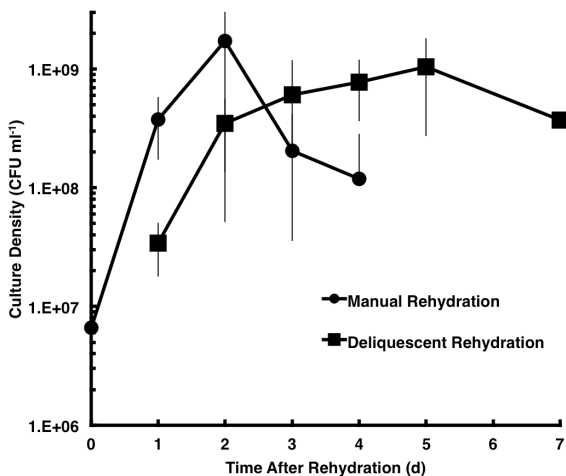
Effect of water activity on the growth rates of 18 salinotolerant bacteria over a range of permissible concentrations for salts (to saturation) in an iterative matrix of ion pairs

Degree of saturation and ionic strength similarly gave significant correlations between r and ion-pair interactions ($P = 0.007$). Models showed 2-way interactions of ionic strength with anions ($P = 0.0008$) and cations with anions ($P < 0.0001$), but not for ionic strength with cations ($P = 0.15$). Degree of saturation had a more complex 3-way interaction with anions and cations ($P < 0.003$), indicating that the effects of degree of saturation on r were salt-specific. Ions and salts affect bacterial growth differentially across gradients of solution qualities with no single physical quality adequately accounting for the observed solute-specific effects on bacterial growth.

Tolerance to ammonia: Icy ocean worlds at the low cryogenic temperatures ($-100\text{ }^{\circ}\text{C}$) may rely on eutectic ammonia-water mixtures (34 wt% NH_4^+) to remain liquid, since all brines freeze below $-80\text{ }^{\circ}\text{C}$. Substantial tolerance to $(\text{NH}_4)_2\text{SO}_4$ at $\sim 53\%$ w/v (11 wt% NH_4^+) was observed in soils and for salinotolerant microbial isolates.

Growth in Deliquescent Liquids: Salinotolerant bacteria grown in brines of MgSO_4 , NaCl, and NaClO_3 were vacuum-desiccated in small cups, which were

then incubated in sealed containers with a pool of matching brine at the bottom. The evaporites rehydrated by humidity, deliquesced to liquid and microbial growth was monitored. Bacteria survived desiccation and renewed robust growth once rehydrated by manual addition of water or by humidity alone, as shown here for *Halomonas* in 2 M MgSO_4 . Cells readily survived several cycles of drying and deliquescent rewetting, exhibiting growth during wet phases of the cycles. Similar results were obtained using SP medium supplemented with 10% NaCl or 20% NaClO_3 . Note that the eutectic conditions are 17 wt% at -4°C , 27 wt% at -21°C , and 39 wt% at -23°C for MgSO_4 , NaCl, and NaClO_3 , respectively.

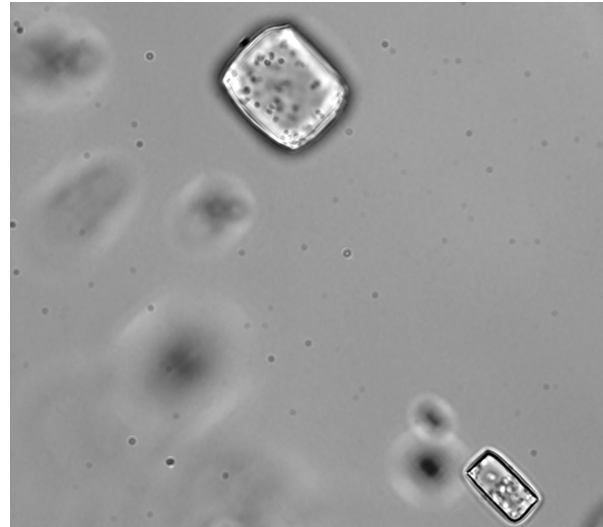


Growth of *Halomonas* sp. str. HL12 after manual and deliquescent rehydration of desiccated evaporites of cultures grown in the presence of 2 M MgSO_4

Entrapment in salt crystals: Primary crystals ($\sim 1\text{-mm}^3$) of NaCl were formed by air-drying from *Halomonas* cultures grown in 10% NaCl that was diluted 10-fold with a saturated NaCl solution. Cells entrapped in fluid inclusions were readily observed microscopically. Viable cells were culturable from individual crystals that were surface-sterilized. These crystals deliquesce and create brines suitable for microbial proliferation. Similar results were obtained for *Marinococcus* and with MgSO_4 evaporites.

Last refugia for life: The four most plausible wet environments to harbor extant life on Mars are caves, evaporites, ices, and the subsurface [4]; each of these involve salt brines, precipitates, efflorescences, and/or evaporite minerals. As climate change causes worlds to aridify, successful microbes might adapt to the scarcity of water and its increasing salinity. The last habitable water may be within evaporite minerals, eventually leaving only the steadfast brines within salt crystal inclusions [5]. Since evaporite minerals can be hygroscopic, should conditions become more humid,

evaporite minerals may deliquesce to brines, the first habitable wet environments. Further, entrapped microbes are protected during dispersion in the wind and crystals may deposit in locations humid enough for deliquescent brine to form.



Micrograph of *Halomonas* cells within fluid inclusions of a NaCl crystal

Acknowledgements: We appreciate the technical assistance of Amer Al Soudi, Meris Carte, J. Alden Consolver, Casper Fredsgaard, Robert Goldstein, William Hendry, Shannon Howell, Tyler Nolan, Alexander Ratcliffe, Nayan Shrestha, Andrew Swindle, and Ali Taleb.

Funding: Supported by Wichita State University and awards from NASA, Research Opportunities in Space and Earth Science (ROSES), Planetary Protection Research (09-PPR09-0004 and 14-PPR14-2-0002) and Kansas INBRE NIGMS NIH (P20 GM103418).

References: [1] Rummel JD *et al.* (2014) *Astrobiology* 14:887; [2] Clark BC *et al.* (2005) *Earth Planet Sci Lett* 240:73, Clark BC & Kounaves SP (2016) *Int J Astrobiol* 15:311; Thomas NH *et al.* (2019) *Geophys Res Lett* 46:10754; [3] Caton TM *et al.* (2004) *Microb Ecol* 48:449, Crisler JD *et al.* (2012) *Astrobiology* 12:98, Kilmer BR *et al.* (2014) *Int J Astrobiol* 13:69, Al Soudi AF *et al.* (2017) *Int J Astrobiol* 16:229, Wilks JM *et al.* (2019) *Int J Astrobiol* 18:502; [4] Carrier BL *et al.* (2020) *Astrobiology* 20:785; [5] Rothschild LJ *et al.* (1994) *J Phycol* 30:431; Vreeland RH *et al.* (1998) *Extremophiles* 2:321

INITIAL RESULTS SUGGEST THAT SHORT-LIVED FLOWS MOBILIZED BY BRINES, IMMEDIATELY FOLLOWING AN IMPACT, FORMED CURVILINEAR GULLIES, LOBATE DEPOSITS AND PITTED TERRAIN ON VESTA AND CERES. J. E. C. Scully¹, S. R. Baker^{1,2}, M. J. Poston³, E. M. Carey¹, J. C. Castillo-Rogez¹ and C. A. Raymond¹. ¹Jet Propulsion Laboratory, California Institute of Technology, Pasadena, CA, USA (jennifer.e.scully@jpl.nasa.gov), ²California Institute of Technology, Pasadena, CA, USA, ³Southwest Research Institute, San Antonio, TX, USA.

Introduction: Prior to the Dawn mission, Vesta was thought to be depleted in volatiles while Ceres was predicted to be volatile rich [1]. Ceres was confirmed to have a volatile-rich crust and low density, likely heavily hydrated, rocky mantle [e.g. 2-4]. Unexpectedly, the discovery of pitted terrain [5], curvilinear gullies and lobate deposits [6] in vestan impact craters indicated that Vesta might contain a significant amount of volatiles, at least on a local scale.

[6] hypothesize that localized deposits of subsurface water ice were heated by impacts, releasing liquid water onto the walls of newly formed impact craters. This liquid water would be unstable, but [6] propose is was transiently present for a sufficient time to form curvilinear gullies and lobate deposits via a debris-flow-like process, in a timescale on the order of tens of minutes. Vaporization of the liquid water could also lead to pitted terrain formation [6]. Similar geomorphological features to those described in [6] have also been observed on Ceres [7]. We evaluate this hypothesis via laboratory experiments and geomorphological analyses.

Laboratory experiments – set-up: We investigate the behavior of liquid water/brine under vestan/cerean conditions immediately following an impact. We use the modeled transient atmospheric pressures of $\sim 10^{-4}$ - 10^{-5} torr [8], and we use heat tape to keep the antechamber at a consistent temperature, slightly above ambient ($\sim 25^\circ\text{C}$). This consistent temperature reduces potential complications in interpretation caused by changes in ambient temperature, and is representative of the hotter than average temperatures expected in the impact crater shortly after formation. We perform the experiments in the JPL Extraterrestrial Materials Simulation Laboratory (EMSiL)/Ice Physics Lab.

Our set-up consists of: (i) a 2.65 cubic-foot cryogenic vacuum chamber (main chamber), (ii) an antechamber and (iii) a large valve that connects the main chamber to the antechamber (Figure 1). The valve allows us to isolate the internal pressure of the antechamber from the main chamber. We place the sample container in the base of the antechamber, on top of a mass balance. Samples consist of (a) pure water, (b) brine, and (c) pure water or brine mixed with glass beads, to simulate the debris-flow-like material that is hypothesized to form the curvilinear gullies and lobate deposits.

We output data to LabView: (i) pressure, (ii) temperature of the antechamber/sample, and (iii) mass of

the sample. We also record video through the top view-port of the antechamber. Three thermocouples are taped to the inside of the sample container, which report temperatures from the same depth in the sample container in each experiment. Pressure gauges monitor the antechamber and main chamber pressures.

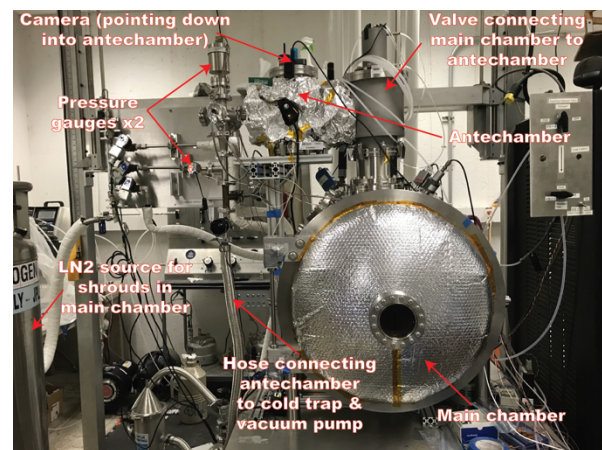


Figure 1. The main components of the experimental set-up are labelled.

Laboratory experiments – procedure: We reduce the main chamber down to 10^{-4} - 10^{-5} torr by both active pumping and cryogenic cold trapping on the shrouds in the main chamber. This effectively eliminates interparticle collisions on the size scale of our apparatus (mean-free-path greater than the distance between chamber walls) and simulates the transient atmospheric pressures expected on Vesta's/Ceres' surfaces shortly following an impact into a volatile-rich target [8].

We slightly decrease the pressure in the antechamber to degas the sample, so that dissolved atmospheric gases will not complicate our observations. We note that on Vesta and/or Ceres, dissolved gases may exist, and may inhibit or slow freezing, thus making our experiments a conservative case. The liquid water/brine in the sample container is stable at the pressures (~ 18 torr) and temperatures ($\sim 25^\circ\text{C}$) in the antechamber prior to initiation of the experiment. This simulates the stability of liquid water beneath the surfaces of Vesta/Ceres, after it was released from localized deposits of subsurface water ice by heating during the crater-forming impacts.

By opening the valve, we suddenly expose the liquid water/brine to pressures of 10^{-4} - 10^{-5} torr, simulating the

sudden release of the liquid(s) onto the crater walls. The liquid water/brine is not stable because conditions are near or below the triple point. We measure the time it takes for the liquid water/brine to evaporate/freeze, to test if liquid would be present long enough to form the curvilinear gullies and lobate deposits, before vaporization of liquid that seeped into the crater floor formed the pitted terrain. We test whether liquid longevity is affected by composition and the presence or absence of particles of varying sizes.

Laboratory experiments – initial results:

Pure water. The water begins the experiment in the liquid form. Once the valve to the main chamber is opened, the liquid water is at or below triple point conditions. Thus, it rapidly evaporates/boils and the liquid rapidly changes state to a solid and a gas. No liquid remains ~4 seconds after the valve is opened: water ice remains in the sample container/antechamber and vapor has migrated to the cold shrouds in the main chamber.

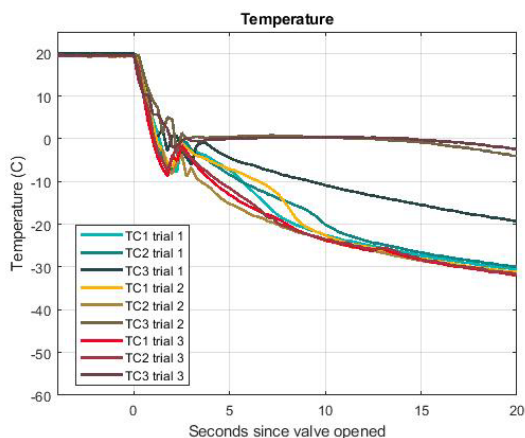


Figure 2. Temperature data (three thermocouples: TC1–3) from three repeat pure water experiments. Discontinuities at 0–5 seconds are due to sample freezing.

Pure water or brine mixed with glass beads. Liquid water or brine is mixed with glass beads (~20% liquid and ~80% beads). For both pure water and brine mixed with glass beads, the behavior is very similar: once the valve to the main chamber is opened, rapid evaporation/freezing occurs, so that no liquid remains ~4 seconds after the valve is opened. The rapid freezing is likely because the glass beads act as nucleation sites. Glass bead size does not significantly change the results.

Brine. To date, we have used NaCl brines at the eutectic concentration. Once the valve to the main chamber is opened, there is rapid evaporation/freezing of the top of the liquid sample. However, in contrast to the pure water, freezing does not progress down throughout the sample: a solid lid forms on top of the brine, which remains liquid below. The solid lid initially appears to

be water ice. The underlying brine periodically breaches the solid lid, and freezes on the surface to become an opaque white solid. This opaque white solid appears brighter than the material that appears to be water ice, and is probably a mixture of water ice and NaCl. No underlying liquid brine appeared to remain after at least 55 minutes.

Laboratory experiments – initial conclusions and future work: A brine forming curvilinear gullies and lobate deposits is plausible on Ceres, because there are numerous salts available [e.g. 9] to mix with impact-melted water. We plan to investigate the possibility that water/rock interactions preceding the impacts could also produce limited amounts of salts and brines on Vesta.

For Ceres, we plan to test brines made from other observed salts (e.g. Na₂CO₃ and NH₄Cl). We are also developing a method to agitate the samples, which will be more analogous to the proposed debris-flow-like process. We hypothesize that agitating the sample will prolong the presence of the liquid water/brine, in contrast to the current static samples.

Geomorphological analyses: We investigate whether there are additional geomorphological indicators for the presence of volatiles. We have made mosaics of ten Vestan impact craters and of ten Cerean impact craters in which curvilinear gullies, lobate deposits, pitted terrain and/or other geomorphological indicators for the presence of volatiles have been definitively or tentatively identified [5-7,10]. We are currently searching for curvilinear gullies and lobate deposits on Ceres. We are also searching for geomorphological indicators for the presence of volatiles on both Vesta and Ceres, including: channels, fractures whose formation is associated with volatiles, pits possibly formed by sublimation, mounds/domes formed in a pingo-like process and lobate landslides/ejecta interpreted to be rich in water ice [features summarized in 10].

Acknowledgments: This work is funded by NASA ROSES DDAP: grant 16-DDAP16_2-0016. Part of this work is being carried out at the Jet Propulsion Laboratory, California Institute of Technology, under contract to NASA. Government sponsorship acknowledged.

References: [1] Russell, C.T. and Raymond, C.A. (2011) *SSR*, 163, 3-23. [2] Combe, J.-P., et al. (2016) *Science*, 353 (6303). [3] Fu, R.R., et al. (2017) *EPSL*, 476, 153-164. [4] Schmidt, B.E., et al. (2017) *Nat. Geo.*, 10, 338-343. [5] Denevi, B.W., et al. (2012) *Science*, 338, 246-249. [6] Scully, J.E.C., et al. (2015) *EPSL*, 411, 151-163. [7] Sizemore, H.G., et al. (2017) *GRL*, 44, 6570–6578. [8] Magni, G. (2014) *9th EPSC*, #599. [9] De Sanctis, M.C., et al. (2016) *Nature*, 536, 54–57. [10] Sizemore, H.G., et al. (2019) *JGR:P*, 124, 1650-1689.

BRINES REACTING WITH ROCK: HOW BRINE COMPOSITION AFFECTS HYDROGEN GENERATION DURING SERPENTINIZATION. S. Sevgen^{1,2}, A. Suttle³, S.M. Som². ¹Institute of Marine Sciences, Middle East Technical University, 33731, Erdemli, Mersin, Turkey (serhat@bmsis.org), ²Blue Marble Space Institute of Science, Seattle, WA, 98154, ³The Queen's College, The University of Oxford, High Street, Oxford, OX1 4AW

Introduction: Serpentinization is a geochemical process resulting from the aqueous alteration of ultramafic rocks. A common byproduct of serpentinization is the generation of biologically available hydrogen, which is a basal energy source for life. Therefore, understanding the conditions controlling hydrogen generation during serpentinization (e.g. silica activity, temperature, pH, rock composition and water/rock ratio) has been an important effort [1, 2, 3, 4]. Additionally, serpentine type minerals are not restricted only to Earth and have been discovered on Mars [5]. Therefore, present day serpentinization may be occurring on Mars and possibly in Ocean Worlds of our Solar System (e.g. Europa and Enceladus) [6]. However, the geochemistry resulting from brines reacting with rocks on these planetary bodies is poorly constrained. In this work, we computationally explore the effects of salinity on hydrogen generation during serpentinization.

Using the computer code EQ3/6, we evaporated seawater to create a series of brines with different water activities (aw). Then, we used reaction path modeling to examine the generation of hydrogen as a result of serpentinization of a harzburgite rock because harzburgites are the common ultramafic rocks that undergo serpentinization on Earth.

Our preliminary results indicate that water activity strongly affected the ultimate degree of hydrogen generation, especially above 200 °C, with hydrogen concentrations decreasing with decreasing water activity. We observed a sharp transition in hydrogen concentration below aw = 0.7, however there was still ~25% of maximum dissolved hydrogen present at activities as low as 0.3 compared to hydrogen generation during serpentinization with seawater.

Different hypotheses explain this concentration shift. Iron likely plays an important role because partitioning of iron into different phases (e.g. magnetite, serpentine, brucite) has crucial consequences for hydrogen generation during serpentinization [7, 8]. However, our model results indicate that a fraction of iron is captured in FeCl₂ and thus prevents Fe²⁺ from oxidating into Fe³⁺. At water activities smaller than 0.7, we observed that FeCl₂ forms, in exceeding 475 mM at 350 °C. Furthermore, FeCl₂'s concentration follows a positive trend with decreasing water activity. At seawater and brines with water activities closer to seawater values, we did not observe FeCl₂ formation.

Considering the potential of serpentinization with various brine compositions across diverse planetary bodies such as on Mars, Jupiter's moon Europa and Saturn's moon Enceladus, our computational models provide additional insight on the habitability on these systems, given that salts provides a sink for ferrous iron, thus limiting high-temperature hydrogen generation during serpentinization.

Acknowledgments: We would like to thank to Ocean Across Space and Time project which is part of the Network for Life Detection (NfoLD), funded by NASA's Astrobiology Program,

References: [1] Frost and Beard (2007) *J. Petrol.* 48, 1351–1368. [2] McCollom and Bach (2009) *Geochimica et Cosmochimica Acta*, 73, 856–875. [3] Klein et al. (2013) *Lithos*, 178, 55–69. [4] McCollom et al. (2016) *Phil. Trans. R. Soc. A*, 378:20180428. [5] Ehlmann et al. (2010) *Geophysical Research Letters*, 37, L06201. [6] Holm et al. (2015) *Astrobiology*, 15, 7, 587–600. [7] Klein et al. (2009) *Geochimica et Cosmochimica Acta*, 73, 6868–6893. [8] McCollom et al. (2020) *Geochimica et Cosmochimica Acta* 282, 55–75.

Gamma-CaSO₄ with Abnormally High Stability from Hyperarid Region on Earth and from Mars Erbin Shi^{1,2}, Alian Wang¹, Huafang Li³, Ryan Ogliore⁴, Zongcheng Ling¹, Shandong Key Laboratory of Optical Astronomy and Solar-Terrestrial Environment, School of Space Science and Physics, Institute of Space Sciences, Shandong University, Weihai, Shandong, 264209, China. ²Department of Earth & Planetary Sciences and McDonnell Center for the Space Sciences Washington University in St. Louis, MO, 63130, USA; ³The Institute of Materials Science & Engineering, Washington University in St. Louis, MO, 63130, USA. ⁴Department of Physics and McDonnell Center for the Space Sciences Washington University in St. Louis, MO, 63130, USA; (shierbin1990@gmail.com)

Introduction: The ordinary gamma phase of anhydrous calcium sulfate (γ -CaSO₄) is not stable in the laboratory, even at low relative humidity (RH). When being exposed to air, it absorbs atmospheric H₂O immediately and converts to bassanite (CaSO₄·0.5H₂O) within a few seconds [1-4]. The structure of γ -CaSO₄ is very similar to that of bassanite, both have continuous tunnels along the c-axis ([001]). The cross-sections of their tunnels, evaluated by the distances between the corner oxygens of (SO₄) tetrahedra and (CaO₆) octahedra that form the wall of a tunnel, are between 4 to 5.5 Å in both structures. The only difference is that the tunnels in bassanite are partially filled with H₂O, while the tunnels in γ -CaSO₄ are empty. Because of their structural similarity, it is very difficult to distinguish them using XRD technology, but quite straightforward using Raman spectroscopy, by H₂O peak of bassanite (at 3555 cm⁻¹), and by ν_1 peak positions (1026 cm⁻¹ vs. 1015 cm⁻¹).

However, γ -CaSO₄ was found stable in the soil or salt samples from Atacama Desert (Chile), White Sands (US), Da Langtan of Qinghai-Tibet Plateau (China), and in Martian meteorite MIL03346, even after those samples were kept in ambient lab-conditions for years [5-8].

Why γ -CaSO₄ from hyperarid regions on Earth or Mars show unusual stability? Two issues need to be understood: (1) what is the reason that caused this unusual stability, structural or chemical? (2) is there a relationship between these structural or chemical characters to the hyperarid environment?

To answer these questions, we re-examined an Atacama soil that contains about 20% of γ -CaSO₄ and the γ -CaSO₄ in Martian meteorite MIL03346,168 using multiple micro-analysis technologies.

Experiments: Three grains of γ -CaSO₄ were picked from Atacama soil using its unique Raman ν_1 peak at 1026 cm⁻¹. Then these single grains were ground, placed on a copper grid, and coated with carbon. These grains were measured firstly using transmission electron microscope-energy dispersive spectrometer (TEM-EDX) for their chemical characters, then using transmission electron microscope-selected area electron diffraction (TEM-

SAED) system for their structural characters. For the γ -CaSO₄ in Martian meteorite MIL03346,168 (found in veins), we first cut off a few micro-pieces using Focus Ion Beam technology (FIB), and then run the same measurements as on Atacama γ -CaSO₄, electron energy loss spectroscopy (EELS) in TEM/STEM, and nanoscale secondary ion mass spectrometry (NanoSIMS). All instruments used in this study are at Washington University in St. Louis.

Results and discussion: Fig. 1a shows the SAED pattern from a grain of Atacama γ -CaSO₄, and in Fig. 1c shows the SAED from a γ -CaSO₄ phase in a FIB-cut micro-pieces of MIL03346, 168. The d spacings in the structures of two samples were calculated based on the measurements of 1/2d or 1/d in these patterns. The overall uncertainty for this type of measurements and calculations is 2%. We selected to show the differences between d spacings of two phases, i.e., to compare the $d_{\text{meas}} = (d_{\text{meas-}\gamma\text{-CaSO}_4} - d_{\text{std-bassanite}})$ and the $d_{\text{std}} = (d_{\text{std-}\gamma\text{-CaSO}_4} - d_{\text{std-bassanite}})$, which were plotted as an orange line and a blue line respectively in Fig. 1b and 1d.

As shown in Fig. 1b, the orange line has a trend of variation very similar to that of the blue line, which indicates that the measured Atacama γ -CaSO₄ sample (grain A) has a structure very similar to that of standard γ -CaSO₄. In addition, another two grains of Atacama γ -CaSO₄ have same results as grain A. It means all three grains of Atacama γ -CaSO₄ have structures similar to that of standard γ -CaSO₄. The TEM-SAED pattern from the Martian γ -CaSO₄ phase in a FIB-cut micro-pieces from a vein in MIL03346, 168 was shown in Fig. 1c. The measurements and calculations similar to Fig. 1a, 1b were used. Obviously, the trend of variation in orange line is very similar to that of blue line. It suggests that the Martian γ -CaSO₄ phase in FIB-cut micro-piece has a structure similar to that of standard γ -CaSO₄. Moreover, after the FIB and TEM-SAED measurements, the FIB-cut micro-piece was re-checked using Raman spectroscopy, the characteristic Raman peak 1026 cm⁻¹ of γ -CaSO₄ was found, thus confirmed the finding of TEM-SAED.

From that, the TEM-SAED results on Atacama γ -CaSO₄ and Martian γ -CaSO₄ support that they all have structure very similar to that

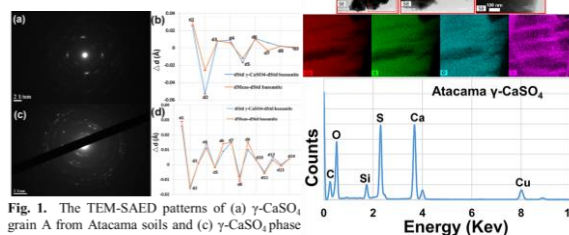


Fig. 1. The TEM-SAED patterns of (a) γ -CaSO₄ grain A from Atacama soils and (c) γ -CaSO₄ phase in a FIB-cut micro-pieces from a vein in MIL03346, 168. (b) Atacama γ -CaSO₄ grain A, and (d) Martian γ -CaSO₄ phase in a FIB-cut micro-pieces.

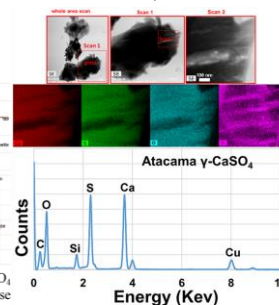


Fig. 2. Top row: Three-step "zone-in" EDX mapping on Atacama γ -CaSO₄ (Grain A), from Whole Area Scan, to Scan 1, to Scan 2. Bottom row: EDS spectra of γ -CaSO₄ from Atacama soil sample corresponding to the element mapping of Scan 2 (grain A);

of standard γ -CaSO₄. It means that the major reason for the abnormal stability of these γ -CaSO₄ is not the structural changes. At least, their structural changes are not large enough to be detectable by TEM-SAED technology.

TEM-EDS mapping and EDS spectra obtained from the three grains (A, B, C) of Atacama γ -CaSO₄ show that they are not pure γ -CaSO₄. For example, a three-step “zoom-in” EDS elementary mapping was made on the grain A of Atacama γ -CaSO₄. Further zoomed into Scan 2 (Fig 2), Si is the only impurity in Atacama γ -CaSO₄. The EDS mapping revealed that Si is quasi-homogeneously distributed in the matrix of Atacama γ -CaSO₄, co-existing with Ca, S, and O.

The TEM-EDS mapping and EDS spectra of γ -CaSO₄ phase in FIB-cut micro-pieces also revealed a different chemical feature (Fig. 3). In addition to Si, this Martian γ -CaSO₄ also contains P as an impurity. Both Si and P are quasi-homogeneously distributed in the matrix, co-exist with Ca, S, and O. Using EELS and NanoSIMS analysis, the existences of Si and P within the Martian γ -CaSO₄ were furtherly confirmed.

The Raman spectra of Atacama γ -CaSO₄ and Martian γ -CaSO₄ in Fig. 4 (a, b) revealed many additional peaks in the range of 100-600 cm⁻¹ that do not belong to γ -CaSO₄ or any sulfates. Many of them are in the spectral region of Si-O_b vibrations. The positions of additional peaks in Fig. 4a and 4b do not match with any crystalline SiO₂ or other known silicates. Being the only chemical impurity in Atacama γ -CaSO₄, Si atoms could only bond with oxygen atoms in SO₄ tetrahedra or in CaO₆ octahedra, to form Si-O_b-S or Si-O_b-Ca bonds.

To combine the fact the γ -CaSO₄ originated from the hyperacid region on Earth and on Mars can maintain an extraordinary stability in humid environment with the finding of quasi-homogeneous distribution of Si in Atacama γ -CaSO₄ (Si & P in Martian γ -CaSO₄) and Si-O_b-(S or Ca) bonding suggested by Raman spectroscopy, we would suggest that the tunnels in these γ -CaSO₄ phases were filled-up by impurities (Si and P), which have prevented the entrance of atmospheric H₂O from humid air afterward.

A synthesized calcium sulfate, hemimethanolate CaSO₄·0.5CH₃OH, is a great example, in which the methanol molecule CH₃OH enter the structural tunnels [4]. In addition, this CH₃OH to H₂O substitution changed the crystal morphology, from a hexagon column (of bassanite) to a shape of cauliflower (of CaSO₄·0.5CH₃OH), but interestingly did not change much of its structure parameters from a standard

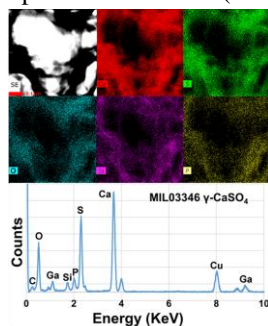


Fig. 3. SE image, EDS mapping, and EDS spectrum of a $1 \times 1 \mu\text{m}$ area of γ -CaSO₄ phase in FIB-cut micro-pieces.

γ -CaSO₄ structure [4]. Similarly, in the two studied impure γ -CaSO₄ samples formed at hyperarid region on Earth and Mars, we observed the crystal morphology change, almost non-detectable structural changes, enriched Si impurity (Si & P in Martian γ -CaSO₄), and Si-O_b vibrational peaks.

Moreover, in the Raman spectra of γ -CaSO₄ from MIL03346,168 (Fig. 4b), a weak but sharp peak appeared at 980 cm⁻¹ (at the left-wing of 1026 cm⁻¹ peak), which does not exist in the spectrum of Atacama γ -CaSO₄ (Fig. 4a). This peak position is suggestive of a P-O vibrational peak, near the ν_1 peak (961 cm⁻¹) in apatite (Ca₅(PO₄)₃(OH, Cl, F)). Similar to the cases of Si atoms or Si-O bonds or CH₃OH molecules, the structural tunnels in γ -CaSO₄ structure also would be able to tolerant the entrance of P atoms or bonded P-O.

Conclusions: In this study, we used multiple microanalysis to characterize the chemical and structural properties of two such γ -CaSO₄: from an Atacama soil and from veins in Martian meteorite MIL03346,168. We found the abnormally high stability of those γ -CaSO₄ from hyperarid environments was due to the chemical impurities, with non-detectable structural distortion. Silicon was determined quasi-homogeneously distributed in Atacama γ -CaSO₄, and silicon plus phosphorus in martian γ -CaSO₄. These impurities filled the structural tunnels, blocked the entrance of atmospheric H₂O, and thus maintained the abnormally high stability of these γ -CaSO₄. In future, the geological process of the impurities enters the γ -CaSO₄ will be discussed and advance to know the geology history of Mars.

Acknowledgments: Erbin Shi thanks the China Scholarship Council (CSC No. 210806220274) and the Natural Science Foundation of Shandong Province (ZR2019MD008) to support his joint-training Ph.D. study at Washington University in St. Louis. Alian Wang thanks the special support 94351A from WUSTL_MCSS to support a continuous collaboration with scientists and students from the Shandong University of China.

References: [1] Chio C.H., et al. (2004) AM, 89,390-5. [2] Prasad P.S., Chaitanya V.K., Prasad K.S., D.N. Rao. (2005) AM, 90, 672-8. [3] Tang Y., et al. (2019) ACS omega, 4, 7636-42. [4] Voigtländer, H., et al. (2003) Host-Guest-Systems Based on Nanoporous Crystals, 280-305. [5] E.B. Shi, A. Wang (2020) GeoRaman XIV Conference. [6] Wei J., et al. (2015) JRS, 46, 810-2. [7] Ling Z. and Wang A. (2015) JGR, 120, 1141-59. [8] Wang, A., et al. (2015) PSS, 112, 23-34.

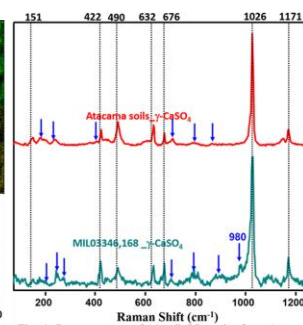


Fig. 4. Raman spectra of (a) γ -CaSO₄ grains from Atacama soil, and (b) from a spot in the γ -CaSO₄ phase in a FIB-cut micro-piece of Martian meteorite MIL03346,168.

SOILS INCREASE THE STABILITY OF MAGNESIUM PERCHLORATE BRINES ON MARS. A. O. Shumway¹, D. C. Catling¹, and J. D. Toner¹, ¹Department of Earth and Space Sciences, University of Washington, Seattle, WA 98195, shumway@uw.edu

Introduction: Water shapes the geochemistry, morphology, and habitability of Mars' surface. Understanding water on Mars is also crucial for mission planning because *in situ* resource utilization and planetary protection depend on accurately quantifying the availability of water on the surface. However, liquid water is rare on Mars due to low temperature, pressure, and relative humidity (RH). Despite these extreme conditions, water can form on Mars through the processes of deliquescence and adsorption. Deliquescence occurs when salts absorb atmospheric water vapor, dissolve, and form brines. By contrast, adsorption occurs when water vapor adheres to grains of soil and forms thin films of water. Both of these processes likely occur simultaneously on Mars to form adsorbed brines (mixtures of brine and soil). Once formed, adsorbed brines are more stable than pure water because salts and soils reduce the freezing point and evaporation rates of solution[1, 2]. On Mars, brines likely exist within the soil matrix; however, relatively few studies have characterized soil-brine mixtures at Mars-relevant conditions.

We bridge this knowledge gap by studying the formation and stability of magnesium perchlorate ($\text{Mg}(\text{ClO}_4)_2$) brines in Martian soil simulant at temperatures, RH conditions, and salt concentrations relevant to Mars. Specifically, we measure (1) water activity (a_w)—essentially, the availability of water in a solution—and (2) freezing point depression in soil-brine samples. We then compare soil-brine mixtures to well-characterized pure brines (i.e. brines without soil) to understand how soils affect the stability and potential habitability of realistic Martian brines.

Martian Soil-Brine Sample Preparation: Our experiments study mixtures of $\text{Mg}(\text{ClO}_4)_2$ brine and Mojave Mars Simulant (MMS) soil. We use $\text{Mg}(\text{ClO}_4)_2$ because of its abundance in Martian soil (~0.6 wt. %)[3] and tendency to form brines through deliquescence[1]. We use MMS for soil because it physically and chemically resembles actual Martian regolith. Briefly, MMS is weathered basalt that is crushed to a grain size of 0.5 to 1.27 mm[4].

We prepare our soil-brine mixtures by pipetting the desired amount of $\text{Mg}(\text{ClO}_4)_2$ solution into ~0.5 g of MMS. Then, we add excess water to ensure the salt is evenly distributed throughout the soil. We repeat this to study samples at salt contents 0% (no salt), 1%, 2%, and 5% by weight.

Methods: To understand how brines realistically behave on Mars, we measure a_w and both infer and measure the freezing temperature of brines in soil between RH of 0% and 100%. Essentially, a_w measures the chemical and biological availability of water in a solution and defines a lower limit for habitability (no life is known to grow at $a_w < 0.6$)[5]. We measure a_w using the isopiestic method[6], by which unknown thermodynamic properties of a sample are determined through comparison with a well-characterized reference solution. The sample ($\text{Mg}(\text{ClO}_4)_2$ -MMS mixture) and reference (H_2SO_4) are placed in a closed chamber where the RH is controlled by the reference solution. The chamber remains in a 25°C temperature bath for 2-3 days. Meanwhile, water vapor exchanges between the sample and reference until the system reaches equilibrium. By taking the masses of sample and reference both before and after equilibration, we measure the water uptake, brine concentration, and a_w of the sample. We then estimate the freezing point of $\text{Mg}(\text{ClO}_4)_2$ brine using the measured a_w and a modified form of the Gibbs-Helmholtz equation[2, 7].

Next, we directly measure the freezing temperature of those soil-brine samples using a differential scanning calorimeter (DSC). Briefly, a DSC detects phase transitions (e.g. melting, freezing) by measuring heat flow through a sample as temperature changes. When the sample changes phase, the DSC detects the characteristic release or absorption of heat associated with that particular phase change.

However, it is difficult to accurately measure the freezing temperature of $\text{Mg}(\text{ClO}_4)_2$ because perchlorates are prone to supercooling, a metastable state where solutions remain liquid below their freezing temperature[8]. To avoid supercooling, we instead probe for our sample's melting temperature, which is equal to the freezing temperature. We first cool the soil-brine sample down to -150°C, then warm it to 20°C at a rate of 5°C/min. As the sample slowly warms, we identify the melting temperature from an endothermic peak in the heat flow.

Results: *Water activity (a_w):* Through the isopiestic method, we find that soils depress the a_w of brines at all concentrations. Figure 1 compares the a_w measured in soil-brine mixtures (circles) to the a_w calculated via the Pitzer equations for a pure solution of $\text{Mg}(\text{ClO}_4)_2$ (black line)[2, 9]. Soils likely reduce a_w because water binds to the surface of soil particles through adsorption, which reduces the availability of water in a solution.

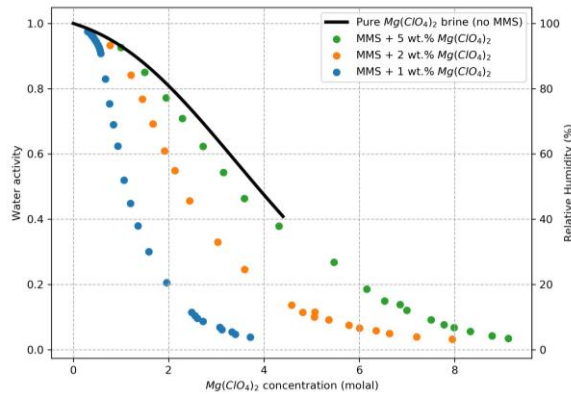


Fig. 1 Water activity in soil-brine samples (circles) is significantly reduced compared to pure brine (black line) at all concentrations for samples equilibrated at 25°C. The curve for the pure brine terminates at 4.4 molal, the saturation point of $\text{Mg}(\text{ClO}_4)_2$ at 25°C.

Freezing point: According to the Gibbs-Helmholtz equation, a reduced a_w indicates a corresponding drop in freezing point for $\text{Mg}(\text{ClO}_4)_2$ in soil. Our calculations predict that soils significantly depress freezing point compared to pure brines (Fig. 2). Under extremely dry conditions ($\text{RH} < 40\%$), we predict freezing points lower than the coldest temperatures on Mars. However, these freezing point predictions are limited because they do not account for other phase changes (i.e. aqueous glass formation, salt precipitation) that are likely to occur in thin-film brines at low temperature and high salt concentration. To experimentally verify the predicted freezing temperatures, we measure phase transitions directly through calorimetry experiments. In this presentation, we will present a phase diagram that compares soil-brine mixtures to pure $\text{Mg}(\text{ClO}_4)_2$ brine.

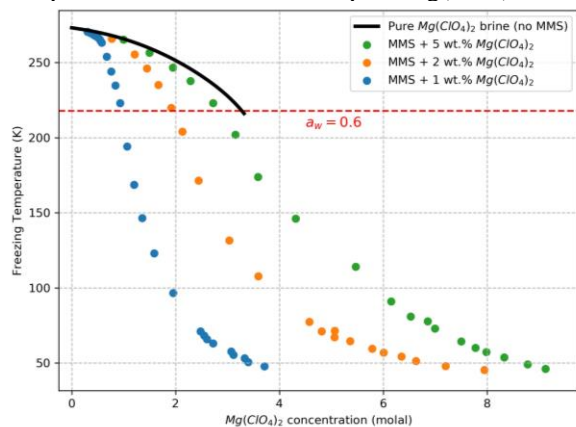


Fig. 2 Freezing temperatures are predicted using a_w values for pure brine (black line) and soil-brine mixtures (circles). The freezing point curve for pure $\text{Mg}(\text{ClO}_4)_2$ terminates at the eutectic temperature (~ 216 K)[10]. The dashed red line represents the lower limit for habitability for terrestrial life ($a_w = 0.6$)[5].

Implications for Water on Mars: The depressed freezing temperatures we measure in soil-brine mixtures indicate that stable liquid water could exist on Mars under more extreme conditions than previously thought possible. Certain relatively dry samples ($\text{RH} < 40\%$) exhibit no signs of freezing or melting over the full range of temperatures (-150 to 20°C), meaning that those samples did not freeze even at Mars' coldest temperatures. This suggests that under some dry conditions, thin films of adsorbed brine could persist year-round. Brines that remain stable for longer periods of time would likely increase ongoing geochemical alteration of the Martian surface.

Though brines in soil can remain liquid for longer, low a_w means that less water is available for chemical or biological processes. This finding is particularly important for assessing habitability because life as we know it requires $a_w > 0.6$ [5]. As a result, areas of Mars where $a_w > 0.6$ are designated “special regions,” which merit additional planetary protection measures that affect mission planning[5]. In Fig. 2, $a_w = 0.6$ is indicated by the dashed red line; any samples below that line are not considered habitable.

Conclusion: We measured water activity and freezing point for $\text{Mg}(\text{ClO}_4)_2$ brines in Martian soil simulant at Mars-relevant conditions. We find that soils reduce the water activity and freezing temperatures of $\text{Mg}(\text{ClO}_4)_2$ brine at salt abundances similar to those measured on Mars. These results suggest that brines could exist in Martian soil for longer portions of the year, but that low water activities make it unlikely for those brines to be habitable.

Acknowledgments: Supported by NASA Solar System Workings grant #80NSSC21K0149.

References: [1] Gough R. V. et al. (2011) *Earth Planet Sc Lett*, 312, 371-377. [2] Chevrier V. F. et al. (2009) *Geophys Res Lett*, 36. [3] Hecht M. H. et al. (2009) *Science*, 325, 64-67. [4] Peters G. H. et al. (2008) *Icarus*, 197, 470-479. [5] Rummel J. D. et al. (2014) *Astrobiology*, 14, 887-968. [6] Rard J. A. and Platford R. F. (1991) Experimental Methods: Isopiestic. In *Activity Coefficients in Electrolyte Solutions*, 209-277. [7] Stokes R. (1991) Thermodynamics of Solutions. In *Activity Coefficients in Electrolyte Solutions*, 2nd ed.; Pitzer, K. S., Ed. CRC Press, 1-28. [8] Toner J. D. et al. (2014) *Icarus*, 233, 36-47. [9] Pitzer K. S. (1991) Ion Interaction Approach: Theory and Data Correlation. In *Activity Coefficients in Electrolyte Solutions*, CRC Press, 75-153. [10] Stillman D. E. and Grimm R. E. (2011) *J. Geophys. Res.*, 116, E09005.

ALTERATION OF COMMON REGOLITH ANALOGUES AND PRECIPITATION PRODUCTS FROM RAPIDLY DEHYDRATED FERRIC SULFATE SATURATED BRINES IN THE PRESENCE AND ABSENCE OF NaCl – A STORY OF AMORPHOUS MARS. E. C. Sklute¹, A. E. Geist², B. Koretke², J. F. King², R. J. Hopkins³, A. D. Rogers³, R. Clark¹, and M. D. Dyar², ¹Planetary Science Institute, 1700 E. Fort Lowell Rd. Tucson, AZ 85719, ecsklute@psi.edu, ²Mount Holyoke College, 50 College St. South Hadley, MA 01075, ³Stony Brook University, 255 ESS Bldg. Stony Brook, NY 11794.

Introduction: In cold and dry climates, like Antarctica or Mars, both the mobile moisture budget and the aqueous geochemistry are likely restricted to the surface hydration layer of individual mineral grains [1], although larger aqueous deposits may accumulate when locally buffered relative humidity [2,3] and/or fluid chemistry form or consolidate a concentrated brine [4]. In arid environments, salt migration, separation, and accumulation are thought to be primarily liquid film transport processes, which are highly dependent upon the solubility and deliquescent properties of the salt. The salt distribution, in turn, is the driving force behind weathering [5]. The brine evolution and regolith alteration that occurs along the path of salt migration will proceed based on the local relative humidity and the individual and solution dependent solubility of ionic phases [1,5]. Thus, the weathering of dry Antarctic, and presumably Martian soils, will depend on the short- and long-term stability and reactivity of saturated brines and common regolith materials at temperatures and pressures relevant to the system in question.

A fundamental understanding of static interactions and stabilities is required before more complicated migration and alteration experiments can be undertaken. For many phases, like the magnesium and sodium sulfates, sodium chloride, sodium nitrate, and other phases common to arid Earth environments, these data are available [1,5], but for compositions not common to Earth (but possible on other planets), this fundamental information is lacking. One such class of brines is those comprised of or containing concentrated ferric sulfate. These brines could remain liquid across much of the Martian surface and subsurface [6]. Furthermore, when dehydrated rapidly at low relative humidities or low pressures, they form amorphous phases [7], and thus are possible candidates for the amorphous regolith components prevalent on Mars. As such, these brines may play an important role in the hydration budget and surface geochemistry of The Red Planet.

The reactivity of the brine and the long-term stability of its precipitation products naturally depends on brine composition as well as the mineralogy of the regolith. Here we investigate the short- and long-term evolution of the precipitation products of five regolith analogues: basaltic glass, nontronite, hematite, gypsum, and magnesite, mixed with ferric sulfate (+/- NaCl) that

are hydrated to ferric sulfate deliquescence at high relative humidity and then dehydrated and stored and low and moderate relative humidities. This simulates the relative humidity (RH) induced formation of a ferric sulfate brine in the presence of common regoliths, the dehydration of that brine and salts in the low RH of the Martian atmosphere, and then the stable storage of those phases in locally buffered soil environments.

Methods: Mixtures of 0.250 g of each regolith analogue was mixed with 0.250 g of mikasaite alone or in addition to 0.250 g of NaCl. Each mixture was placed in an individual air tight container buffered to 92% RH with DDI water. After the mixture deliquesced (7-10 days for samples $\geq 4^{\circ}\text{C}$, each mixture was transferred to an individual air tight container buffered either to 11% RH with LiCl or 33% RH with MgCl_2 . Multiple samples were made for each experimental condition and sample evolution was monitored by optical photograph, x-ray diffraction (XRD; Rigaku Smartlab II, Bragg-Brentano geometry, 0.02° step size, $0.3^{\circ}/\text{min}$, 10-80 2θ), Fourier transform infrared attenuated total reflectance spectroscopy (FTIR ATR; Bruker Alpha, 4 cm^{-1} resolution, 128 scans), Raman spectroscopy (Bruker Bravo, (785/852.3 nm laser; 30 1000s integrations), and visible near infrared spectroscopy (VNIR; ASD Fieldspec 4 Max; Ocean Optics HL-2000-HP light source; 30° input 0° emission; Spectralon reference, 300 1s integrations). Not all solutions dehydrate at the same rate. Repeat experiments have shown that the majority of the changes occur during or close to the time of dehydration. Analyses for individual compositions occur at different time points along the early stages of the experiment to accommodate different dehydration and transformation rates. Long term (~640 day) time points are analyzed for comparison. Sample are currently aging to intermediate time points.

Results: Differences in stability against both rehydration and mechanical manipulation change by regolith analogue and brine composition. Samples composed of nontronite and ferric sulfate without NaCl are the most difficult to break down into powders. The addition of NaCl almost always increases resistance to rehydration and makes the sample easier to physically manipulate (**Fig 1**). It appears that the ferric sulfate can form a continuous glassy solid that, when still slightly

hydrated, ‘glues’ the regolith together. Only under the driest of conditions, does this material become brittle.

Samples dehydrate at different rates depending upon their composition. All samples containing NaCl dehydrate faster than those without NaCl. In almost all cases, the sample appears completely different in texture and color than samples without NaCl (**Fig 1**).

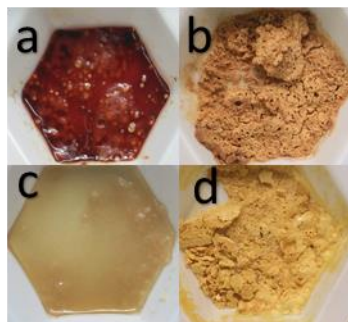


Fig 1. Magnesite and ferric sulfate (a) with NaCl (b) gypsum and ferric sulfate (c) with NaCl (d). Samples imaged after dehydration at 11% RH and RT for 31 days.

Samples stored at low temperatures have very different physical properties, even though their spectral properties are in many cases similar. For instance, magnesite stored at 11% or 33% RH at room temperature or 11% at -20 °C are some of the fastest dehydrating samples and those that are most resistant to rehydration. Magnesite stored at 33% RH and -20 °C, however, is still pliable and damp after 650 days, although a phase has precipitated out of the brine.

VNIR and MIR data for gypsum mixtures with ferric sulfate, with and without NaCl, are shown in **Fig 2-3**. The XRD data for gypsum containing samples have peaks that correspond to NaCl and hexahydrate. There is no appreciable XRD signature for phases containing iron or iron sulfates in the mixtures, indicating that these phases remain amorphous at the resolution of XRD throughout the course of the experiment. This scenario is common to most of the mixtures investigated, and is particularly prominent for samples where the regolith is poorly crystalline (basalt and nontronite).

Conclusions: The low relative humidity samples are remarkably stable, even at room temperature. Most samples maintain some or all of their amorphous character for the entire (>641) day experiment. Rapid changes do occur as the samples are dehydrating. Certain mixtures stored at moderate relative humidities do change with time.

Acknowledgments: This work is supported by NSF grant #1819209

References: [1] Keys J. R. (1980) *PhD Thesis, Victoria University of Wellington*. [2] Wang A. et al. (2008) *JGR*, 113, E12S40. [3] Wang A., J. J. Freeman, and B. L. Jolliff (2009) *JGR*, 114, E04010. [4] Bishop, J. L. et al. (2021) *Sci. Adv.*, 7, eabe4459. [5] Doornkamp J. C. and H. A. M. Ibrahim (1990) *PPG: Earth and Environ*, 14, 335-348. [5] Goodie A. S. and R. U. Cooke

(1984) *Geoforum*, 15, 563-582. [6] Chevrier V. F. and T. S. Altheide (2008) *GRL*, 35, L22101. [7] Sklute E. C. et al. (2018) *Icarus*, 302, 285-295.

Check out the work at <https://lionsandlamms.com>.

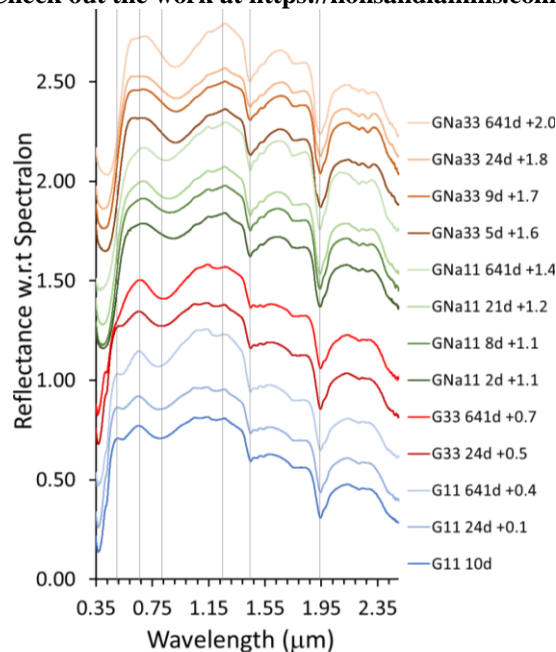


Fig 2. VNIR spectra of gypsum - ferric sulfate - (+NaCl) mixtures aged at room temperature in either 11% or 33% RH. Number of days (d) aged and offset applied to data are indicated in the legend.

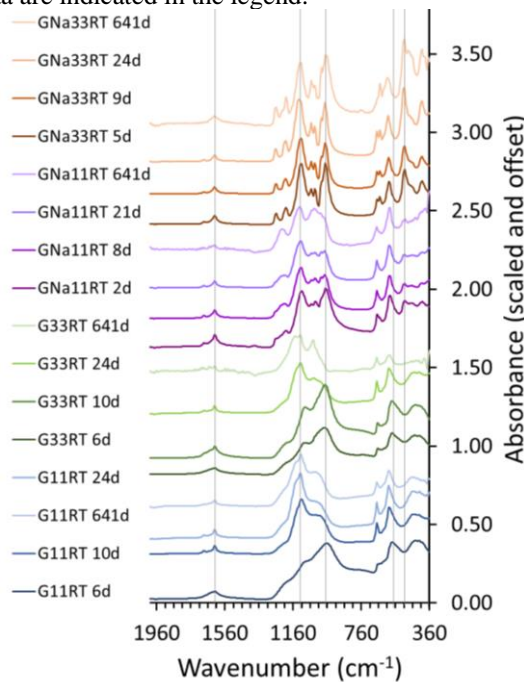


Fig 3. MIR ATR spectra of gypsum - ferric sulfate - (+NaCl) mixtures aged at room temperature in either 11% or 33% RH. Number of days (d) aged indicated in the legend.

EXPERIMENTAL INVESTIGATION OF THE NEAR-SURFACE MARTIAN WATER CYCLE WITH A SALTY REGOLITH: IMPLICATIONS FOR BRINE FORMATION. R. A. Slank¹, E. G. Rivera-Valentín², and V. F. Chevrier¹; ¹Arkansas Center for Space and Planetary Science, University of Arkansas, Fayetteville, AR (rslank@uark.edu), ²Lunar and Planetary Institute (USRA), Houston, TX.

Introduction: Recent work has shown that the present-day conditions on Mars may allow for stable brines on the surface and shallow subsurface, though only for a small fraction of the year [1]. A potential formation pathway for brines is deliquescence, the transition from a solid salt crystal into an aqueous solution when exposed to a humid atmosphere. Some experiments, though, suggest that under the Mars-relevant pairing of temperature and relative humidity, the kinetics of deliquescence may be too slow to form brines [2]. Furthermore, salts in the regolith would be competing for water vapor in a hyperarid environment against other processes, such as adsorption [1, 3], and salt hydration [4]. Such dynamics of water vapor through atmosphere-regolith interactions, particularly at short timescales (day to year), remains largely unexplored. Furthermore, experimental work thus far has focused on defining the phase space for Mars-relevant brines [5], but not much work has been done to explore the stability of brines under Mars-like conditions [2].

To explore potential brine formation under Mars-like conditions, we conducted a series of experiments focused on investigating atmosphere-regolith interactions, particularly water vapor transfer between the atmosphere and a layer of JSC Mars-1 regolith simulant with varying concentrations of $\text{Ca}(\text{ClO}_4)_2$ (0-10 wt.%) at a range of temperature of -23°C to 5°C . Our simulation chamber replicates well the Martian pressure, temperature, and atmospheric composition. Such experiments are vital to understanding how the water vapor diurnal and seasonal cycle may allow for the formation of liquid water on the surface of present-day Mars.

Methodology: We conducted fourteen experiments in the Ares Mars simulation chamber at the University of Arkansas under two temperature regimes. The first was a set cooled with liquid nitrogen, traveling through coiled copper tubing around the sample petri dish, along with a chiller helping to maintain the temperature in the chamber. Those experiments ranged from -23°C to -12°C . Liquid nitrogen was manually let into the chamber to maintain a specific temperature. The second set of experiments were cooled with just the chiller system. Those experiments ranged from 3°C to 5°C . A lithium chloride humidity buffer was placed in the chamber, near the sample, creating stable humidity in the chamber. The buffer has a humidity of $11.2\% \pm 0.5$

at 0°C . While none of our samples were at 0°C , the humidity was fairly close to this average with the chiller temperature-controlled experiments. Experiments were run at a pressure of ~ 6 mbar.

To test for competing effects, our sample consisted of regolith mixed with 1 to 10wt% calcium perchlorate. We also had two control samples, one just regolith and another just salt. The regolith and salt were both prepared to be as water free as possible, including baking and time in a desiccator. Once they were desiccated they were moved to a freezer to cool to -25°C . The calcium perchlorate was weighed and then evenly mixed within the regolith. Although there was a short exposure to the atmosphere while the sample was removed from the desiccator and placed in the chamber, the chamber was filled with CO_2 to help prevent water contamination. The entire exposure time was less than 120 seconds.

Results and Discussion: In Fig. 1, we plot the temperature and humidity conditions throughout each experiment on the phase diagram of calcium perchlorate. As can be seen, four experiments were within conditions that would permit the deliquescence of calcium perchlorate, one experiment was on the DRH boundary, and two experiments should not have achieved deliquescence. In Figure 2, we show the measured sample mass over time and the relative humidity (RH) gradient between the sample and the atmosphere.

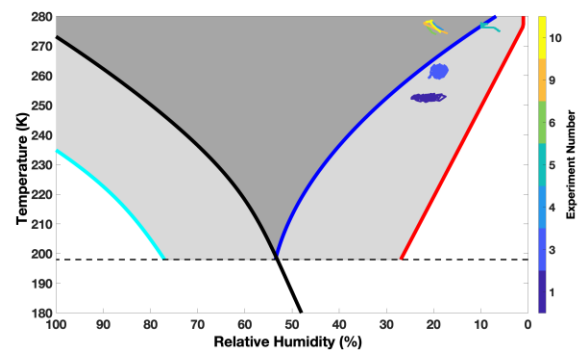


Figure 1: Temperature and humidity conditions of each experiment on the phase diagram of calcium perchlorate. Experiments 1 and 3 should not deliquesce, experiment 5 is on the DRH boundary, and experiments 4, 6, 9, and 10 should deliquesce. However, just because they should deliquesce does not mean we saw evidence that they did deliquesce.

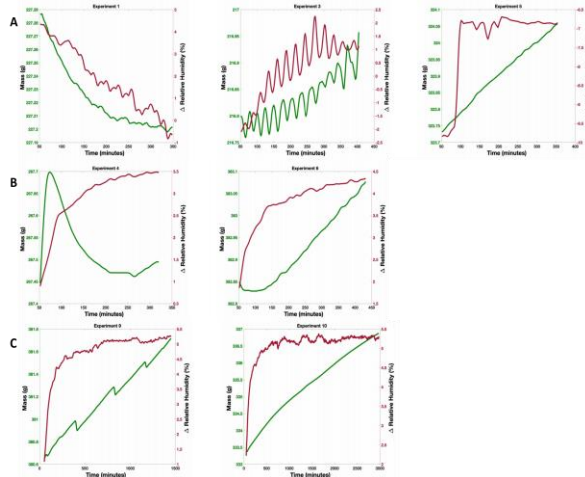


Figure 2: Mass vs time vs change in relative humidity (RH) A: experiments that should not deliquesce. B: experiments that should deliquesce. C: Longer experiments that should deliquesce.

For the three experiments that should not have deliquesced, we note that when the RH gradient was negative, sample mass would steadily increase, and while it was positive, sample mass would steadily decrease. We interpret this to be a signature of adsorption (mass gain) and desorption (mass loss) driven by the humidity gradient.

Typically, visible wetness on regolith grains can be used to identify the occurrence of deliquescence; however, we did not observe visible wetness during the four experiments that experienced the appropriate conditions for deliquescence. Nevertheless, as can be seen in Fig. 2, all four experiments experienced a sample mass increase over time. Furthermore, this occurred during a positive humidity gradient. This is in contrast to the non-deliquescence experiments where a positive humidity gradient led to sample mass loss.

This does not mean that water is not being absorbed into the salt. Mass increase is a great way to help identify water uptake by deliquescence or adsorption. Of the six experiments with increased mass, five of them were experiments conducted in the warmer conditions. (Fig. 1; Fig. 2). Three of the experiments had visible wetness shortly after the experiment, when removed from the simulation chamber and left in a terrestrial environment. This leads us to believe that water was being absorbed into the regolith and/or salt but did not fully deliquesce. This is especially true with the longer run time, where more water was able to be absorbed increasing the mass by 1.14 and 3.71g respectively.

Conclusion: Although there were no obvious visible signs of regolith wetness at the surface in the

experiments, there were four experiments that had parameters in favor of deliquescence. Those four experiments also had a mass increase from adsorption of water into the regolith and possible deliquescence, that did not deliquesce enough to visibly wetten the regolith around the salt during the experiment. There were also three instances of deliquescence occurring shortly after the experiment had concluded. We infer this to imply be that the salt was close to saturation. That said, there was deliquescence in the controlled experiment of calcium perchlorate. This may imply that when deliquescence is in competition with adsorption, the regolith adsorption of water vapor may prevent salt deliquescence, at least under the conditions studied here. This is supported by deliquescence occurring during the control and not during the experiment, as well as why deliquescence occurred shortly after the end of some of the experiments.

The kinetics of adsorption and deliquescence are experimentally not well constrained under Mars-relevant combinations of temperature and humidity. Although our experiments may suggest that adsorption may act as a more effective water vapor sink than salt deliquescence, more experiments are needed to understand the dependence of these processes over a broader range of environmental conditions (e.g., temperature and/or humidity). Additional experiments are being conducted at cooler temperatures, to better characterize the potential of deliquescence at various humidities under ideal Martian conditions. Exposing complex subtleties in diffusion, adsorption/desorption cycles, and deliquescence processes on Mars, specifically the limits to which liquid formation is possible, has important implications for liquid stability and habitability near the surface, liquid brines, future missions to Mars, and the continuing search for liquid water.

Acknowledgments: This grant is funded by NASA Habitable Worlds Program award #80NSSC20K0227.

References: [1] Rivera-Valentín, E.G. et al., (2020), *Nat Astron* 4, 756–761. [2] Fisher, E. et al. (2016) *Astrobiology*, 16(12), pp.937-948. [3] Rivera-Valentín, E.G. et al., (2020), *BAAS* 53(4). [4] Gough, R. V. et al., (2014), *Earth Planet. Sci. Lett.* 393(0), 73-82. [5] Fisher, E., et al. (2014) *Geophysical research letters*, 41(13), pp.4456-4462.

AGAR GELATION SPECTROPHOTOMETRIC ASSAY OF CHAO- AND KOSMO-TROPICITY OF INORGANIC SALTS, AND IMPLICATIONS FOR LIFE IN TERRESTRIAL AND MARTIAN BRINES.

S. M. Smith and S. R. Poulson, Dept. Geol. Sci. & Eng. MS-172, Univ. Nevada-Reno, Reno, NV 89557, USA. saramsmith@nevada.unr.edu, poulson@unr.edu.

Introduction: The presence of solutes in aqueous solution has a general effect on microbial behavior, as the ionic strength of a solution impacts the activity of water in the solution. However, there is also a specific effect associated with the presence of solutes upon microbial behavior, which can be considered to be either chaotropic (inhibiting microbial activity) or kosmotropic (facilitating microbial activity) [1]. These chao- vs. kosmo-tropic effects have been studied by performing microbial culture experiments in the presence of various solutes [e.g. 2-5], but have also been quantified using an empirical agar gelation spectrophotometric assay technique [2, 4-7], which has the advantage that it can produce a quantified, universal scale of chao- vs. kosmo-tropic activity (CKA). A large number of pure solutes have been assayed previously, although assays of solute mixtures are relatively uncommon. Moreover, assays of some pure salts pertinent to hyper-arid terrestrial and Martian environments are currently unavailable (e.g. alkali metal nitrates, bicarbonates, perchlorates).

This study has performed agar gelation spectrophotometric assays to quantify CKA values for various pure inorganic salts, as well as binary, ternary and quaternary mixtures of inorganic salts. In addition to quantifying CKA values for solutions relevant to possible terrestrial and Martian brines, this study attempts to identify if the chao-/kosmo-tropic effects of a salt mixture follows conservative behavior (i.e. simple additive/subtractive combination of the chao-/kosmo-tropic effects of the component pure salts). Recommendations for future CKA experimental procedures are also provided.

Methods: Gelation experiments were performed with a procedure similar to that used previously [6]. Experiments used extra pure reagent-grade agar, gel strength 600-700 g/cm³ (Nacalai Tesque, Kyoto, Japan, code 01028-85, lot # M0G2724) at a concentration of 1.5% w/v. All inorganic salts were of ACS grade or better. Ca-salts were not used as CaCl₂ has a specific interaction with agar [6], and Ca-rich brines are relatively rare in nature due to the low solubility of Ca-carbonate and Ca-sulfate salts. Agar/salt solutions were prepared at salt concentrations up to concentrations that induced agar precipitation, as determined visually. Spectrophotometric assays were performed at a wavelength of 500 nm using optical glass cuvettes (Fisher Scientific, cat. #14-958-120) in

an Evolution 260 Bio UV-vis spectrophotometer equipped with an 8-cell Peltier system with thermoelectric temperature control. Initial solution temperature for experiments was set approx. 7°C above the anticipated gel point, and then decreased at a rate of 0.5°C/2.5 mins., with absorbance readings taken every 2.5 mins. Gel point was identified at the temperature when the absorbance value was measured at 0.03 absorbance units greater than the initial absorbance value at gel point +7°C. Gel point ΔT = solution gel point T – agar-only gel point (41.5°C). All experiments were performed in replicate. Calculation of CKA values used a gel solution heat capacity of 4.15 kJ/kg.°C [2, 6].

Results: All pure salts showed a linear effect of gel point ΔT vs. salt concentration ($R^2 > 0.98$), except for NaHCO₃ and MgCl₂. Values of CKA for a 1°C change of gel point are plotted in Fig. 1.

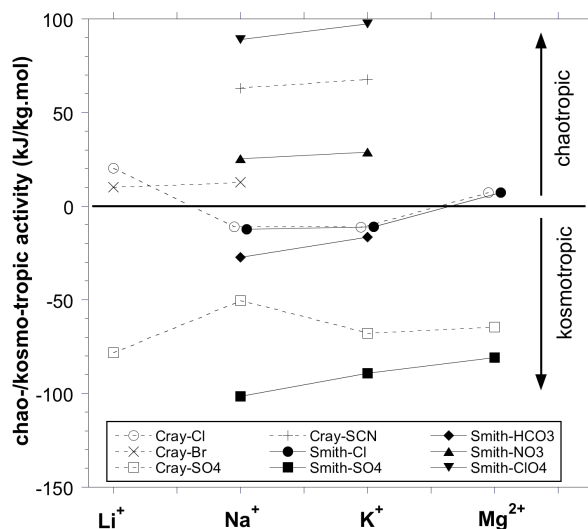


Figure 1. Values of chao-/kosmo-tropic activities for a 1°C change of gel point for pure salts. Data from this study, [6], and [7] for MgCl₂.

Figure 1 shows generally good agreement between results of this study and previous studies [4-6]. Perchlorate salts were previously considered to be very chaotropic [8], and Fig. 1 confirms this to be correct. Nitrate salts are also chaotropic, while bicarbonate salts are kosmotropic. In general, K-salts are

consistently more chaotropic (or less kosmotropic) than the corresponding Na-salts.

Values of gel point ΔT vs. salt concentration (M) were calculated for each individual salt in salt mixtures, and these values of ΔT were combined conservatively (i.e. simple additive/subtractive behavior), to generate a calculated ΔT . Values of Measured ΔT – Calculated ΔT vs. Calculated ΔT for all salt mixtures are plotted in Fig. 2. Figure 2 shows that Measured ΔT - Calculated $\Delta T = 0 \pm 2$ °C for most salt mixtures, i.e. that salt mixtures generally show conservative chao-/kosmo-tropic behavior for mixing of their component salts. There does not appear to be any systematic explanation for the mixtures that show larger values of Measured ΔT – Calculated ΔT , although such mixtures tend to have significant concentrations of $MgCl_2$.

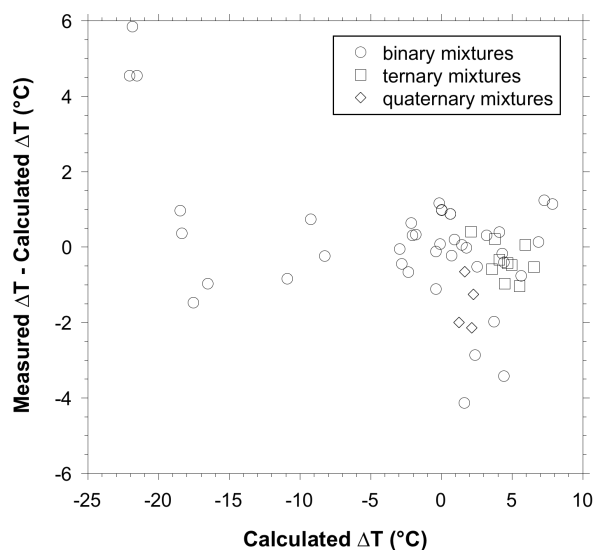


Figure 2. Measured ΔT – Calculated ΔT vs. Calculated ΔT for gel points of salt mixtures (55 experiments).

Discussion: The values of CKA for nitrates, perchlorates, and bicarbonates are generally consistent with the relative order of anions in the Hofmeister series [9]. The chaotropic nature of nitrate and perchlorate salts is particularly relevant to microbial habitability in hyper-arid terrestrial environments such as the Atacama Desert, Chile [10], but also in locations such as Gale Crater, Mars [11]. However, the common co-occurrence of kosmotropic bicarbonate and sulfate salts may help to ameliorate the chaotropic effects of nitrate and perchlorate salts.

Chao-/kosmo-tropic behavior of salt mixtures. The generally conservative chao-/kosmo-tropic behavior of salt mixtures enables prediction of the CKA value of a

range of naturally-occurring brine compositions with a reasonable degree of confidence, and may allow for a more targeted approach to search for possible past or present microbial life in hyper-saline environments on Earth and on Mars. However, future work to determine CKA behavior for more salt mixtures (esp. quaternary mixtures) would be valuable, as would further study of the non-conservative CKA behavior observed for some salt mixtures.

Recommendations for future agar gelation assays.

Agar gelation assays are a valuable experimental technique to measure CKA values, but standardization of an analytical methodology would facilitate comparison of measurements between different studies. Recommendations include: use of a consistent brand and chemical specifications for the agar gel (different brands and specifications of agar gel may provide different experimental results); the use of optical glass cuvettes (with better thermal conductivity than plastic cuvettes); and a standard thermal program when performing spectrophotometric measurements (i.e. initial starting temperature, cooling rate).

Conclusions: The chao-/kosmo-tropic activity (CKA) of various pure salts and salt mixtures have been performed using an agar gel spectrophotometric assay technique. Standardization of agar gelation assay procedures would facilitate comparison between results of future agar gelation assay studies. Results show that nitrates are chaotropic, perchlorates are very chaotropic, while bicarbonates are kosmotropic. Measured values of CKA for salt mixtures indicate that CKA behavior is generally conservative with respect to the salt mixture components. Results enable the prediction of CKA values for a range of natural brine compositions, and have implications for the feasibility of microbial life in hyper-arid environments on Earth and on Mars.

Acknowledgments: Research supported by NASA Cooperative Agreement Number 80NSSC18M0027.

References: [1] Ball P. and Hallsworth J. E. (2015) *Phys. Chem. Chem. Phys.*, 17, 8297-8305. [2] Hallsworth J. E. (2003) *Env. Microbiol.*, 5, 1270-1280. [3] Stevens A.H. and Cockrell C.S. (2020) *Front. Microbiol.*, 11, #1478. [4] Crisler J.D. et al. (2012) *Astrobiol.*, 12, 98-106. [5] Fox-Powell M. G. (2016) *Astrobiol.*, 16, 427-442. [6] Cray J. A. et al. (2013) *Env. Microbiol.*, 15, 287-296. [7] Yakimov et al. (2015) *Env. Microbiol.*, 17, 364-382. [8] Ascittuo E.K. et al. (2010) *Biophys. J.*, 98, 186-196. [9] Marcus Y. (2015) *Ions in Solution and Their Solvation*, Wiley. [10] Lybrand R. A. et al. (2016) *Chem. Geol.*, 442, 174-186. [11] Stern J. C. et al. (2017) *Geophys. Res. Lett.*, 44, 2643-2651.

SEARCHING FOR LIFE IN SALTS: FREEZING/GEOCHEMICAL MODELING TO INVESTIGATE STABILITY AND MICROBIAL HABITABILITY OF MODERN MARTIAN BRINES.

S. M. Smith and S. R. Poulson, Dept. Geol. Sci. & Eng. MS-172, Univ. Nevada-Reno, Reno, NV 89557, USA. saramsmith@nevada.unr.edu, poulson@unr.edu.

Introduction: Liquid water is typically unstable at the surface of Mars due to the combination of low temperatures and pressures. However, present-day surface conditions are close to the triple point of water and the presence of dissolved salts on the Martian surface may allow metastable brines to persist for periods of time [1-3]. Polyhydrated sulfates, chlorides, perchlorates, and carbonates have been detected by various Mars missions and the presence of these salts will substantially depress the eutectic temperature of aqueous solutions and allow liquid water to become stable in modern Martian environmental conditions [4-10]. The presence of water is considered the most important prerequisite for life, so understanding how brines form and evolve on Mars could help us understand the microbial habitability of Mars [11].

Brine characteristics that might limit habitability include: activity of ions (a_i); activity of water (a_w); salt precipitation parageneses; ionic strength (I); pH; eutectic temperature (T_E); and the chaotropic vs. kosmotropic effects of salts. The mechanisms which induce chaotropic and kosmotropic effects are not fully understood, but chaotropic agents are thought to induce stress on cells and disrupt the structure of macromolecules, whereas kosmotropic agents facilitate water-water interactions to stabilize macromolecules [12]. The lower limit of a_w to allow microbial activity is often considered as $a_w = 0.611$ [13-14]. However, recent evidence has indicated that the limit for biochemical reactions in certain xerophiles could be as low as $a_w = 0.565$ and potentially as low as $a_w = 0.4$ in rare sulfate reducers [15-16].

Martian brines have been studied using laboratory experiments and geochemical modeling, but studies of brines in equilibrium with Mars evaporite minerals are uncommon. We modeled freezing trajectories of water chemistries in equilibrium with potential Martian mineral assemblages to explore: 1) how modern Martian environmental conditions affect brine evolution; and 2) the stability and habitability of evolved brine compositions to determine if microbial life could potentially exist on Mars.

Methods: Water geochemistry modeling was performed with Geochemist's Workbench using Pitzer parameters, and a fixed P_{CO_2} of 6 mbar [17], representing the modern Martian atmosphere. Various mineral assemblages identified at Valles Marineris (VM), the southern highlands (SH), and Meridiani

Planum (MP) [4-10] were considered, with combinations of different Ca-Mg-Na-K sulfates, chlorides, and carbonates, and commonly include halite, gypsum/anhydrite, and/or epsomite.

Brine freezing trajectories were performed using the program FREZCHEM [19] starting with 1 kg of water, an initial pH 5-8, with an initial temperature of 298.15 K, 293.15 K, or 274.15 K and decreasing to T_E . Both equilibrium (EQ) and fractional (FX) crystallization methods were used to model freezing, such that EQ modeling allows precipitated minerals to re-equilibrate with the brine, but FX modeling does not. Initial pH conditions were established based on calculations in equilibrium with values of P_{CO_2} in the Martian atmosphere, and with or without the presence of carbonates (calcite).

Brine	Initial Temp (K)	Initial pH	pH		I		a_w	T_E
			start	end	start	end		
MP1-FX	298	5	4.70	0.94	1.97	3.72	0.96	269
MP1-FX	298	7	7.99	9.56	1.96	5.20	0.92	265
MP3-FX	298	8	8.40	9.77	0.75	9.96	0.87	259
SH1-FX	298	5	3.65	-1.76	5.84	8.82	0.56	212
SH1-EQ	298	5	3.65	-0.80	5.84	5.70	0.78	247
SH1-FX	298	8	7.89	7.03	5.85	6.27	0.79	249
SH1-EQ	298	8	8.65	7.50	5.91	6.14	0.79	249
SH4-FX	298	8	8.54	9.65	5.85	12.60	0.66	231
SH6-FX	274	8	8.27	8.75	5.14	9.10	0.70	237
SH8-FX	298	8	7.89	9.76	7.67	14.33	0.66	229
VM4-FX	298	7	7.00	8.48	4.81	5.38	0.80	251
VM5-FX	274	8	8.08	9.78	5.56	14.19	0.65	229
VM6-FX	293	8	8.46	2.32	5.38	9.44	0.70	237

Table 1. Result summary of brine freezing trajectories for pH, ionic strength (I), activity of water (a_w), and eutectic temperature in K (T_E).

Results: Modeling results are summarized in Table 1. All brines have final $a_w \geq 0.65$, except for Ca-Cl brine SH1-pH5-FX with final $a_w = 0.56$. Evolution of a_w as freezing progresses for all brines with final $a_w \leq 0.7$ are plotted in Fig. 1. Brines SH1-pH5-EQ, SH1-pH8-EQ/FX, SH6-pH8-FX, VM4-pH8-FX, and VM6-pH8-FX developed final values of a_w between 0.7 - 0.8. Three brines (SH4-pH8-FX, SH8-pH8-FX and VM5-pH8-FX) evolved into concentrated Mg-Cl brines with $a_w \leq 0.66$. The final values of I range from 3.72 - 14.33 mol/L. Brines MP1-pH5-FX and SH1-pH5-EQ/FX reached a final pH < 1 and brine VM6-FX-pH8

was the only brine with an initial pH 7-8 that had a final pH < 3. The eutectic temperatures of the final brines range from 212 - 269 K.

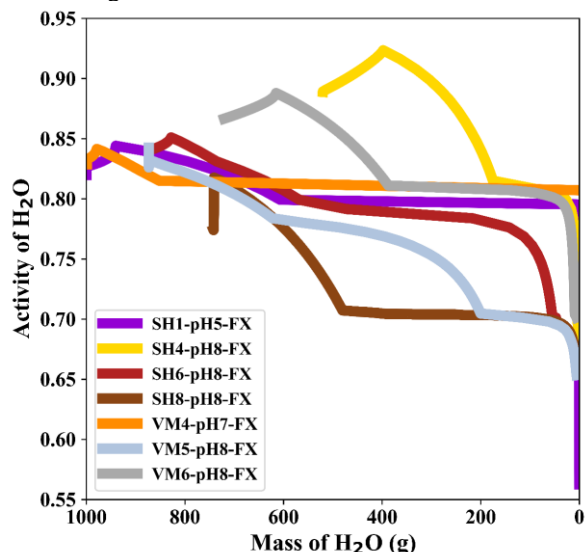


Figure 1. Freezing trajectories for activity of water (a_w) for brines with final $a_w \leq 0.7$.

Discussion: A “Special Region” is an area where organisms could propagate, with a temperature ≥ 255 K (lowest observed T for cell division) and $a_w > 0.6$ [2], although chaotropic substances may lower this T [20]. With the exception of the Ca-Cl brine SH1-pH5-FX ($a_w = 0.56$), all brines developed $a_w > 0.64$ (Table 1), and could potentially support microbial activity. However, brines with $a_w \geq 0.7$ and $T_E \geq 237$ K may only exist as aqueous solutions for seconds to minutes on Mars [3]. The lower T_E of brines with lower values of a_w may exist as aqueous solutions for a few hours up to a full Martian day [3], and may allow for microbial habitability. Many of the final pH values are not exceptionally acidic, and should allow for microbial activity [21]. A combination of low a_w , low pH, high I, and the presence of chaotropes (such as Ca-Mg-chlorides, perchlorates, and/or nitrates [22]) in some brines may have a substantial negative synergistic effect, which will depress microbial habitability. However, these negative effects may be offset by the presence of kosmotropic solutes such as NaCl, KCl, or Na-K-Mg sulfates [23].

In addition to the effect of lowering the values of T_E , chloride solutions may also increase the survivability of halo- and cryo-tolerant species of bacteria at cooler temperatures and during freeze/thaw cycles [24]. Recent findings also describe a more abundant and complex microbial community than those found in less salty brines nearby in a natural, cold, chloride rich brine found at the Boulder Clay

(Northern Victoria Valley, Antarctica) [25]. Results of this study indicated concentrated chloride brines on Mars may be good microbial habitats for these types of bacteria in particular, and could potentially serve as prime candidates for Special Regions on Mars. However, future work to determine the sustained habitability of these brines with their combined extreme characteristics under Martian conditions would be valuable. Continued efforts should also be made to explore water chemistries in equilibrium with perchlorate assemblages and to further investigate chao/kosmotropic effects on microbial habitability in various salt mixtures.

Conclusions: The habitability of various potential Martian brines have been evaluated using the modeling program FREZCHEM, and our results indicate that some brines may be stable for at least short periods on the modern Martian surface while maintaining characteristics (especially water activity, pH, and eutectic temperatures) that could allow for microbial activity. Microbial habitability may be either hindered by the presence of chaotropic solutes, and/or facilitated by the presence of kosmotropic solutes.

Acknowledgments: Research supported by NASA-EPSCoR grant #80NSSC18M0027, sub-awards 18-52 and 18-53.

References: [1] Martínez G. M. and Renno N. O. (2013) *Space Sci. Rev.*, 175, 29–51. [2] Rivera-Valentín E. G. et al. (2020) *Nat Astron.*, 4, 756–761. [3] Chevrier V. F. et al. (2020) *Planet. Sci. J.*, 1, 64-76. [4] Gendrin A. et al. (2005) *Science*, 307, 1587–91. [5] [6] Chevrier V. F. and Mathé P. E. (2007) *Planet. Space Sci.*, 55, 289–314. [7] Hecht M. H. et al. (2009) *Science*, 325, 64–67. [8] Ehlmann B. L. and Edwards C. S. (2014) *Annu. Rev. Earth Planet. Sci.*, 42, 291–315. [9] Ojha L. et al. (2015) *Nat. Geosci.*, 8, 829-832. [10] Clark B. C. and Kounaves S. P. (2016) *Int. J. Astrobiol.*, 15, 311–318. [11] Altheide T. et al. (2009). *Earth and Planetary Science Letters*, 282, 69–78. [12] Zhang Y. and Cremer P. S. (2006) *Curr. Opin. Chem. Biol.*, 10, 658–663. [13] Fox-Powell M. G. et al. (2016) *Astrobiol.*, 16, 427–42. [14] Stevenson A. et al. (2015) *Environ. Microbiol.*, 17, 257-277. [15] Stevenson A. et al. (2017). *Environ. Microbiol.*, 19, 687–697. [16] Steinle L. et al. (2018) *ISME J*, 12, 1414–1426. [17] Bethke C. M. (2018) *The Geochemist’s Workbench, Release 12*. [19] Marion G. M. et al. (2010) *Comput. Geosci.*, 36, 10–15. [20] Rummel J. D. et al. (2014) *Astrobiol.*, 14, 887-968. [21] Jin Q. and Kirk M. F. (2018) *Front. Environ. Sci.*, 6: 21. [22] Smith S. M. and Poulson S. R. (2021) *Modern Brines*, Abstract #6017. [23] Cray J. A. et al. (2013) *Env. Microbiol.*, 15, 287-296. [24] Heinz J. et al. (2018) *Astrobiol.*, 18, 1171-1180. [25] Azzaro M. et al. (2021) *Hydrobiologia*, 848, 1837–1857.

STABILITY OF SURFICIAL BRINES ON MARS DURING RECENT ORBITAL CYCLES. A. Soto¹, E. G. Rivera-Valentín², and V. Chevrier³; ¹Southwest Research Institute, Boulder, CO, USA; ²Lunar and Planetary Institute (USRA), Houston, TX; ³University of Arkansas, Fayetteville, AR.

Introduction: Recent work has shown that meta-stable brines can form and persist on the surface and in the shallow sub-surface of Mars for up to six consecutive hours for a few percent of the Martian year [1]. However, the maximum temperature such brines are stable is 225 K, which is far too low to sustain life [1][2]. Given that Mars has undergone significant orbital cycles, though, brine formation, persistence, and habitability may be different over the last few million years. This is because variations in obliquity and eccentricity change the distribution of ice at the surface and in the subsurface, which affects the brine (meta)stability [3]. Therefore, here we investigate how the Martian climate response to varying orbital configurations may have controlled the distribution and habitability of brines in Mars’ modern history.

To investigate the possible liquid brine and habitability conditions during recent geologic history, we have applied the analyses of [1] and [3] to climate model simulations for obliquity and eccentricity that sample the range of values experienced by Mars in the last 10 million years. Here we discuss the preliminary results from this work and how this history of liquid brine distribution informs the history of recent habitability on Mars.

Recent Orbital Cycles: Over the past 10 million years, the obliquity of Mars has oscillated with a period of about 120,000 years and the eccentricity has oscillated with a period of 95,000 to 99,000 years [4][5]. In that time, the Martian obliquity ranged from ~15° to ~35° while the eccentricity varied from just below 0.03 to as high as 0.11 [4][5]. Obliquity variations can change the distribution of surface brines by changing the annual average distribution of insolation. At lower obliquities (less than 20°), less insolation reaches the polar regions, therefore the bulk of radiative energy is delivered to the tropics and extratropics. At higher obliquities (greater than 40°), the annual peak insolation occurs in the polar region and the equatorial region becomes the preferred residence of water and carbon dioxide ice.

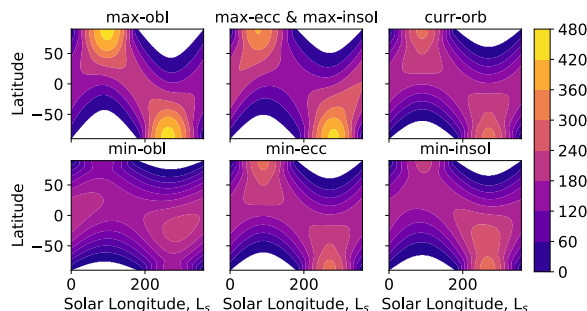


Figure 1. The latitude and solar longitude dependent insolation at the top of the Martian atmosphere for each of the simulated scenarios. The polar regions received much more insolation during periods of maximum obliquity (max-obl), maximum eccentricity (max-ecc), and when the annual mean insolation is at a maximum (max-insol). Additionally, there is a strong north-south asymmetry in the distribution of insolation.

Selection of Recent Martian Climates to Simulate:

We used the annually- and globally averaged insolation to choose the specific orbital conditions for our modeling. Since simulating every obliquity cycle over the last 10 million years is computationally unfeasible, we used the insolation history as a guide in selecting orbital conditions that sampled the range of possible recent Martian climates. Table 1 shows the orbital configurations chosen, and Figure 1 shows the latitudinally-distributed insolation as a function of time of year (i.e., solar longitude) for each of the orbital configurations. First, we selected the orbital configuration for the maximum and minimum annually averaged insolation received by Mars. These two configurations reflect the combination of orbital parameters that created possibly the greatest changes in the spatial and temporal distribution of insolation on the Martian surface. The next set of simulations were for the maximum and minimum possible obliquities and eccentricities, individually. These simulations allow us to understand how both orbital properties separately affect brine distribution. Since the maximum insolation occurs when the eccentricity is at a maximum, max-ecc and max-insol are the same.

Description	Simulation Name	Mean Insolation	Eccentricity	Obliquity	Long. of Perihelion
Maximum obliquity.	max-obl	147.648584	0.068675	47.665870°	1.371898°
Minimum obliquity.	min-obl	147.622915	0.066107	14.680017°	130.064686°
Maximum eccentricity.	max-ecc	148.428906	0.123100	39.869903°	157.042589°
Minimum eccentricity.	min-ecc	147.300538	0.002702	29.648553°	54.882691°
Maximum insolation	max-ecc	148.428906	0.123100	39.869903°	157.042589°
Minimum insolation	min-insol	147.300433	0.002424	29.791104°	81.272256°

Table 1. The orbital parameters for the climate simulations.

We focused on obliquity and eccentricity since these two orbital parameters are known to strongly control the forcing of the climate in terrestrial atmospheres. As the obliquity increases, the annually averaged coldest region on the planet moves from being at the poles, to being in the equatorial regions, while the poles receive much more insolation compared to the current insolation (see Figure 2). When the obliquity is greater than roughly 40° , much of the polar ice moves to mainly the equatorial mountains. This shift in ice distribution undoubtedly affects the distribution of potential brines. Additionally, increasing the obliquity will increase the polar insolation leading to increase sublimation of water from the surface, which may generate annually averaged higher atmospheric water content near the surface. This higher water content may allow the near surface atmosphere to reach nearly 100% Rh at higher temperatures, within the stability field of liquid brines.

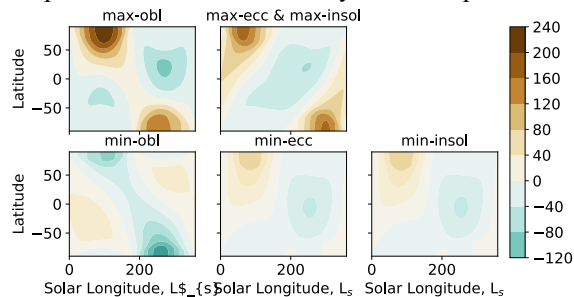


Figure 2. When the current orbit insolation (curr-orb) is subtracted from the other scenarios, clear differences in insolation distribution and duration are revealed.

The eccentricity affects the asymmetry in the length of the seasons, and the combination of the changing longitude of perihelion with the eccentricity determines when the longest season occurs. For example, currently perihelion occurs during the northern summer, therefore the northern hemisphere has a longer summer season where the total accumulated insolation in northern summer is greater than in southern summer. This difference in the accumulated insolation, as shown in Figure 2, per season may affect the duration of brine formation events. The higher eccentricities may increase the atmospheric water content, thereby contributing to the formation of stable liquid brines.

Anticipated results: We will show how liquid brine stability and durations are affected by the various orbital conditions. Our analysis is similar to that done by [1] and by [3]. In Figure 3, which shows an example of the expected results, we see the percent of the year that each region on Mars sustains liquid brine for the minimum insolation simulation (min-insol) as well as the maximum number of hours, for any given sol, for

which the brines are in a liquid state. Similar plots for the minimum obliquity case (min-obl), are shown in Figure 4. The difference in the results is drastic. Although the minimum obliquity case has a higher annual average insolation, the minimum obliquity case generates less liquid brine because of the increased insolation in the extratropics and polar regions. This is just one example of the results that we will present.

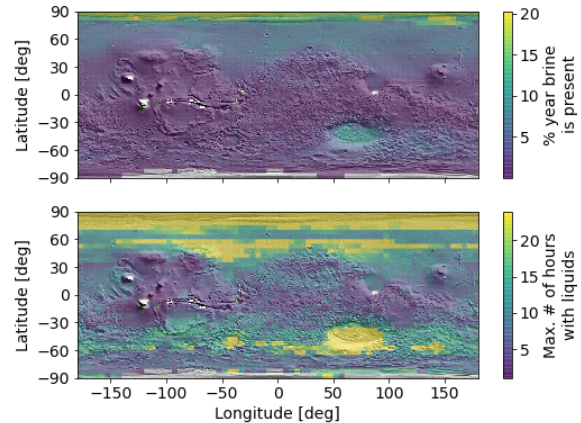


Figure 3. (top) Percent of the year when the brine is in solution for the minimum insolation simulation (min-insol). (bottom) The maximum number of hours in a sol during which there is liquid brine. MOLA shaded relief plotted below the data in each plot.

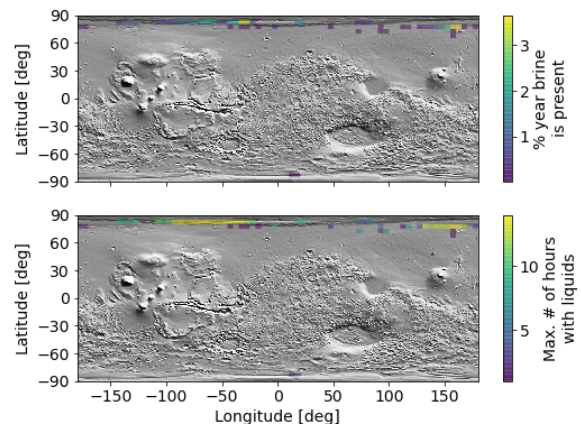


Figure 4. (top) Percent of the year when the brine is in solution for the minimum obliquity simulation (min-obl). (bottom) The maximum number of hours in a sol during which there is liquid brine. MOLA shaded relief plotted below the data in each plot.

References: [1] Rivera-Valentín et al. (2020). *Nature Astronomy*, 4:756–761, doi:10.1038/s41550-020-1080-9. [2] Merino et al. (2019). *Frontiers in Microbiology*, 10, doi:10.3389/fmicb.2019.00780. [3] Chevrier, V. F., et al. (2020). *PSJ*, 1(3):64, doi:10.3847/PSJ/abbc14. [4] Laskar et al. (2002). *Nature*, 419:375–377. [5] Laskar et al. (2004). *Icarus*, 170:343–364, doi:10.1016/j.icarus.2004.04.005.

PERCHLORATE AND CHLORIDE BRINES AS THE CAUSE OF THE MARSIS BRIGHT BASAL REFLECTIONS: LABORATORY MEASUREMENTS. D.E. Stillman¹, E. Pettinelli², K.M. Primm³, G. Caprarelli⁴, E. Mattei², S.E. Lauro², and B. Cosciotti². ¹Southwest Research Institute (dstillman@boulder.swri.edu), ²Mathematics and Physics Department, Roma Tre University, ³ Planetary Space Institute, ⁴Centre for Astrophysics, University of Southern Queensland, Australia.

Introduction: Temperature on Mars are generally too low for water to be liquid. Salts can act as an antifreeze by lowering the freezing point greatly. Thus, an increasing body of research is focused on the study of the physical and chemical properties of saline solutions at planetary conditions [1-3] and the detection of extraterrestrial brines. In parallel to geophysical and geochemical investigation of terrestrial analogs and other world brines, exobiologists have suggested that hypersaline waters may offer conditions of habitability in extreme environments, where we would not normally expect to find life [4]. The presence and distribution of salts on the Martian surface point strongly to a major role for hypersaline aqueous solutions in relation to geochemical cycles, and as possible agents of geomorphic evolution on Mars [5]. What makes Mars particularly enticing, is that its hyper-arid conditions and thin atmosphere conjure very difficult conditions for the formation and persistence of liquid aqueous solutions. Yet, radar sounder data acquired over the region of Ultimi Scopuli, part of the South Polar Layered Deposits (SPLD), have recently been interpreted to indicate the presence of briny bodies of liquid water at the base of the SPLD [6-7]. Understanding the peculiar physical conditions and mechanisms that may have led to the formation and persistence of briny waters in this region, and their electromagnetic properties, will greatly advance our knowledge of Martian geological and climatic evolution, of the potential for extreme habitable environments. In this work, we present and interpret the preliminary results of our permittivity experiments on chloride and perchlorate solutions at temperatures consistent with the Martian surface and subsurface.

Stability of Martian brines: Saline solutions are two-component salt-water mixtures characterized by a eutectic concentration corresponding to the lowest freezing temperature of the system. The eutectic temperatures of salt-water solutions relevant to Mars have been shown to range from 222 K (CaCl₂) to 198 K (Ca-perchlorate) for values of water activities $a_{wt} \leq 0.62$ [8]. Toner et al. [1] studied the metastability of brines below their eutectic temperature and found that magnesium perchlorate did not freeze, speculating a transition into a glass at 123 K. During warming, Stillman et al. [9] and Toner et al [1] have found that the eutectic temperature of magnesium perchlorate was almost 10 K warmer, then the theoretical eutectic

temperature [8]. Additionally, Primm et al. [3] found that the eutectic temperature of magnesium chloride changed depending on the temperature of the brine was before freezing again.

Methodology: Pre-mixed brine samples were poured into a three-electrode sample holder with an attached Teflon cup. The sample holder was then placed in an ultra-low freezer. Previously published electrical property measurements of CaCl₂, 44wt% Mg(ClO₄)₂, and mixtures with sand [9-12] were made while warming the sample to reduce the effects of metastable brines. However, metastability can last for days, if not much longer in laboratory environments [3]. Thus, when measuring 100mM Mg(ClO₄)₂ sample we preformed measurements while cooling as well.

Results: Our ultra-low freezer could not completely freeze our 100mM Mg(ClO₄)₂ sample, therefore we had to use a liquid nitrogen fed cold plate to freeze the sample. It eventually froze between -87°C and -81°C which is 14 and 20°C below the stable eutectic temperature of magnesium perchlorate ($T_e = -67^\circ\text{C}$ [8]). **Figs 1 & 2** shows the interpreted phase, temperature history, and evolution of the electrical properties (permittivity and conductivity) as the brine freezes, then warms back up. The (1), (2), and (3) labels in **Fig. 2** are to show the temperature trajectory since the temperatures shown on the left. These numbered labels also show that (1) and (2) are brine when cooling the temperature and (3) shows when the solution freezes.

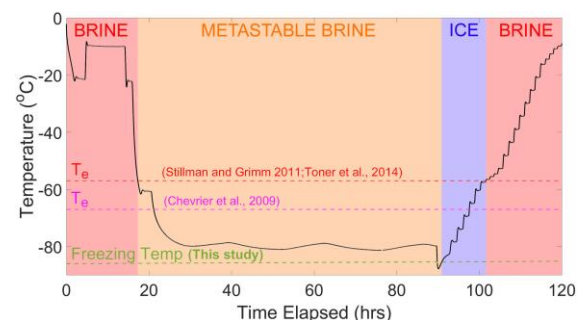


Fig. 1 Temperature history of the 100mM Mg(ClO₄)₂ sample with the previous measured and theoretical eutectic temperatures. Note uncertainty of the freezing temperature is large -87°C and -81°C, but will be better constrained in future measurements. Note this sample stayed a metastable brine for more than 70 hours.

We then plotted the data for different chloride and perchlorate solutions in terms of apparent permittivity

versus temperature (Fig. 3) during warming. It is important to note that MARSIS data do not allow to separately compute separately the real and imaginary parts of complex permittivity, but only the apparent permittivity which is a real single quantity that accounts for both polarization and conductive processes [7]. The results suggest that at eutectic concentrations the apparent permittivity is well above MARSIS value, whereas for low concentrations (100mM) reach such value at higher temperature are required. Nevertheless, solutions >300mM will likely reach the MARSIS threshold above their eutectic temperatures.

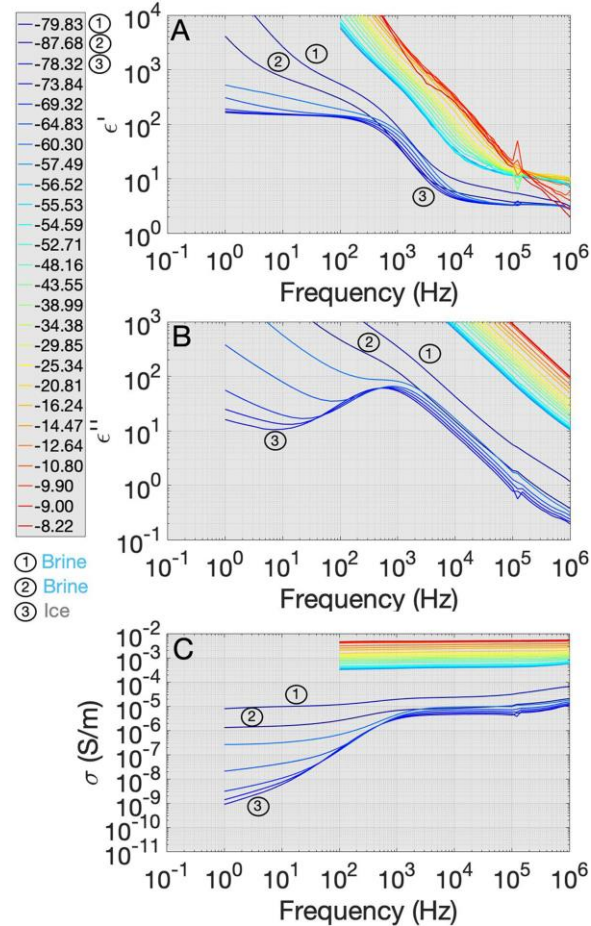


Fig. 2 Electrical properties of 100mM $Mg(ClO_4)_2$ sample measured during freezing (1 and 2) and melting (3). (A) Real part of relative permittivity, (B) Imaginary part of relative permittivity, and (C) Conductivity. The displayed experimental temperature trajectory starts out at temperature (1) $-79.83^\circ C$, cools to temperature (2) $-87.68^\circ C$, and warms back to $-78.32^\circ C$ and then follows the temperature order in the column to the left of (A) and (B). (1) and (2) shows a highly conductive sample possessing liquid vein networks that indicate the sample is partially liquid [10,11]. Once the brine is frozen the sample becomes more than 4 orders of magnitude less conductive.

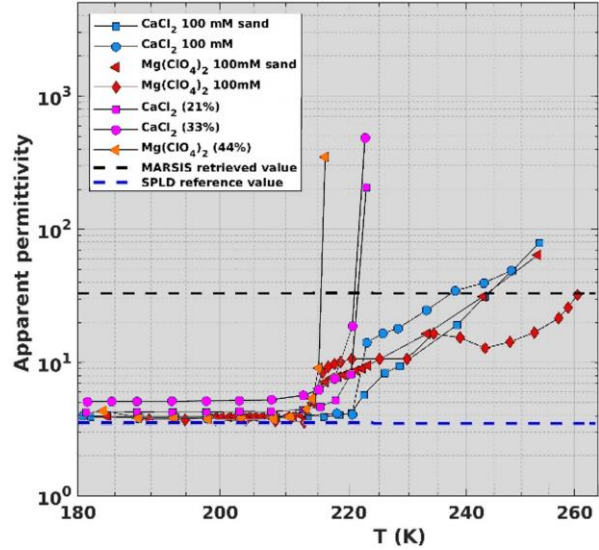


Fig. 3 The apparent permittivity of the frozen solutions is compared with a threshold value $\epsilon_a=33$ (dashed black line), which is the median of the distribution of the apparent permittivity values retrieved from MARSIS data (4MHz) in the brightest area at Ultimi Scopuli.

Conclusions: Our work demonstrates that liquid brines exhibit a very strong dielectric response at temperatures consistent with those of the Martian surface and subsurface. Significantly, our laboratory results also show that salty solutions need not be super-concentrated for the experimental system to register high values of permittivity. This supports interpretation of bright radar reflections from the base of Ultimi Scopuli as caused by saline waters. Because of the metastable properties of perchlorate solutions, if salts under the SPLD were brines in the past (i.e., during a past obliquity cycle), then they might still be liquid, if the basal temperature was not dropped below our measured freezing temperature of 186-192 K. This appears plausible without the need for high geothermal gradients [13]. We note that the lower metastability temperature of Ca-perchlorate (no discussed here) may open up the possibility to even colder conditions.

References: [1] Toner J. D. et al. (2014) *Icarus*, 233, 36-47. [2] Primm K. M. et al. (2017) *Geochim. Cosmochim. Acta*, 212, 211-220. [3] Primm K.M. et al. (2020) *Icarus*, 342, 113342. [4] Stamenković V. et al. (2018) *Nature Geosci.*, 11, 905-909. [5] Bishop J. L. et al. (2021) *Sci. Adv.*, 7, eabe4459. [6] Orosei R. et al. (2018) *Science*, 361, 490-493. [7] Lauro S. E. et al. (2021) *Nat. Astron.*, 5, 63-70. [8] Chevrier V. F. et al. (2020) *Planet. Sci. J.*, 1, 64 (12 pp.). [9] Stillman and Grimm (2011) *JGR* 116, E09005. [10] Grimm et al. (2008) *JPCB*, 112, 15382-15390. [11] Stillman et al. (2010) *JPCB*, 114, 6075-6073. [12] Stillman and Grimm (2011) *JGR*, 116, E03001. [13] Sori M. M. and Bramson A. M. (2019) *Geophys. Res. Lett.*, 46, 1222-1231.

IRON-SULFUR BRINES AS HYPOTHETICAL ECOSYSTEM ANALOGUES OF EARLY MARS AND

ICY WORLDS. M. V. Tarasashvili^{1,2,3}, marika.tarasashvili@btu.edu.ge; N. G. Aleksidze[†], N. G. Dobarjginidze¹, dobo78@gmail.com; N. G. Gharibashvili^{1,4}, Tusa.ghari@gmail.com. ¹Georgian Space Research Agency, 4 Vasil Petriashvili Street, 0179, Tbilisi, Georgia; ²Business and Technology University, 82 Ilia Chavchavadze Avenue, 0162, Tbilisi, Georgia; ³Javakishvili Tbilisi State University; 1, Ilia Chavchavadze Avenue, 0179 Tbilisi, Georgia; ⁴Spase Farms Ltd, 14 Merab kostava Street, 0108, Tbilisi, Georgia.

Introduction: Some experimental studies have shown that types of brines can form and persist from the equator to high latitudes on the surface of Mars [1, 2], also the ability of organisms to actively metabolize and grow in high salt water at low temperature at partial exposure to the unshielded solar short radiation triggered the theoretical basis for investigating habitability in icy ocean worlds [3, 4], however the problem remains disputable, which underlines an importance of the further scientific discussions regarding brines as biomarkers and/or biosignatures.

Material and Methods: For the preliminary assessment of the brines and their potential habitability, an analogue environment has been investigated (Fig. 1).



Figure 1. Tsagveri brines are very rich in microbial communities, which can potentially serve as an analogues for the spectroscopic investigations of possible habitability of the likelihood systems on Mars and Icy Worlds.

Chemistry and microbiology of Tsagveri brines: Extremophiles have been obtained from the iron-rich slopes of Tsagveri (41° 47' 54" N, 43° 28' 57" E), Georgia, known for its icy volcanic springs (0°C – 4°C, pH~4.4; bivalent Iron 12-18mg/L) containing high concentrations of Iron and Sulfur compounds; Concentration of other ions in mg/L is: Mg²⁺ (34-120), Ca²⁺ (36-112), Na⁺ (750-1150), SO₄²⁻ (70-244), HCO₃⁻ (2400-4400), Cl⁻ (42-95).

Major species identified were: *Acidithiobacillus ferroxidans*, *Thiobacillus ferroxidans*, *Gallionella*, *Spirillum desulfuricans*, *Sporovibrio desulfuricans*, *Shewanella oneidensis*, *Beggiatoa*, *Thiorthrix*, *Ferri-bacterium*; *Rhodferax ferrireducens* and some others. Interestingly, these extremophiles have been reported to be able to survive in simulated conditions of Mars [5].

Brines as biosignatures: Colored patterns visible on Fig. 1. also provides the insights for the validity of spectroscopic investigation of the brines as of possible analogues of extraterrestrial environment suitable for the origin and development of life;

Spectra have been obtained from the clear silicagel saturated by bacterial colonies and control [6], frozen at -43°C (Martian permafrost, Icy moon surface).

Obtained results: In vivo absorption maximums for various extremophiles inoculated within clear silicagel were as follows: 1. B chl a, 850–910nm, purple sulfur bacteria; 2. B chl a, 350, 805–810nm, all green bacteria; 3. B chl b, 1020–1035nm, all purple-red bacteria; 4. B chl c, 745–760nm, purple-red non-sulfur bacteria; 5. B chl d, 725–745nm, green sulfur bacteria; 6. B chl e, 715–725nm, brown iron and sulfur bacteria; 7. B chl g, 320-550nm, heliobacteria and some iron bacteria.

By comparing obtained absorption spectra to that of inorganic background mineral signature, significant differences have been found; The data not only have the potential to reveal the environment in which the organic matter was generated, but could potentially indicate specific domains of life and therefore serve as biosignatures and serve as statistical standards for the instruments and methods developed for the analysis of brine-analogue environments in Solar system and beyond.

References: [1] Rivera-Valentín, Edgard G. et al. (2020) *Nature astronomy*, (4), 756-761. [2] Fischer, E. et al (2016), *Astrobiology*, 16(12), 937–948; [3] Domagal-Goldman, Shawn D et al. *Astrobiology* (2016) 16(8), 561-653; [4] Stevens A.H. et al (2018) *Astrobiology*, 19(1), 87–98; [5] Aleksidze et. al., (2018), *IJSRT*, 3(12), 688-692. [6] Mukbaniani et al, (2016) *IJA*, 15(2), 155-160.

STABILITY DIAGRAM OF AQUEOUS CHLORATE SOLUTIONS UNDER MARTIAN RELEVANT TEMPERATURES AND RELATIVE HUMIDITIES.

S. Tu¹, J. B. Parise^{1,2}, E. Lars^{1,2}, A. D. Rogers¹,
¹Department of Geosciences, Stony Brook University, Stony Brook, NY, 11790-2100. ²Brookhaven National Lab, National Synchrotron Light Source II, Upton, NY, 11973-5000.

Introduction: Oxy-chlorine salts, mainly chlorates and perchlorates, are proposed to constitute an important fraction of the Martian regolith [1, 2]. Their highly hygroscopic nature [3-5] and the ability to depress the freezing point of water [2, 6] make oxy-chlorine salts a possible repository for liquid brines to be sporadically stable at the Martian surface despite the prevailing cold and dry conditions. Evidence proving the flowing brines across the Martian surface includes the seasonal recurring slope lineae (RSL) [7] and the spheroids on the leg of Phoenix lander [8]. The Curiosity Rover also measured that the changes in the hydration state of perchlorate salts within the subsurface are consistent with an active atmosphere-soil water exchange [9]. To better understand the water cycle on Mars, it is important to figure out the stability field of aqueous oxy-chlorine salt brines against temperature (T) and relative humidity (RH). The stability of aqueous solution is mainly controlled by its water activity (a_w), which is defined as the partial vapor pressure of water in a solution relative to the standard state partial vapor pressure of pure water. The water activity of a saturated salt solution is equal to the deliquescence relative humidity (DRH) of the dry salt [4, 5]. A plenty of experimental and modeling studies have investigated the deliquescence of perchlorate under Martian relevant conditions [3-5]. However, little work has been done on chlorates, especially at subzero temperature. Therefore, in our study, we constructed the T-RH phase diagram of $\text{NaClO}_3/\text{H}_2\text{O}$ and $\text{Mg}(\text{ClO}_3)_2/\text{H}_2\text{O}$ binary system at supercooling temperature range based on their water activity (a_w), while their a_w data were derived from the measured heat capacity data of solutions at varying molalities and temperatures.

Methods:

Sample preparation. Aqueous solutions at various molalities (from ~1m to saturated) were prepared by dissolving NaClO_3 or $\text{Mg}(\text{ClO}_3)_2$ salt into deionized water, respectively. While solid NaClO_3 salt was directly purchased from Sigma-Aldrich[®], solid $\text{Mg}(\text{ClO}_3)_2 \cdot 6\text{H}_2\text{O}$ was synthesized by slowly mixing aqueous $\text{Ba}(\text{ClO}_3)_2 \cdot \text{H}_2\text{O}$ and MgSO_4 solution under constant stirring. After centrifuging the mixture to get rid of the BaSO_4 precipitation, we evaporated the remaining supernatant under vacuum at room

temperature for ~3 days to grow the crystalline $\text{Mg}(\text{ClO}_3)_2 \cdot 6\text{H}_2\text{O}$.

Measurement of Heat Capacity. The specific heat capacity C_{sp} ($\text{J} \cdot \text{K}^{-1} \cdot \text{g}^{-1}$) of chlorate solution was quantitatively measured by a differential scanning calorimeter, Netzsch DSC 200 F3 Mafia[®]. The DSC basically tracks the heat flux (HF) across the sample against that of a reference during a dynamic thermal cycle, while the heat flux is proportional to C_{sp} . Liquid sample at each molality was sealed in an aluminum crucible, and cooled from 298.15K to 173.15K at a constant cooling rate of $10\text{K} \cdot \text{min}^{-1}$ using a liquid nitrogen cooling system. Then a standard run using Al_2O_3 powder with known C_{sp} were conducted under the same thermal cycle to calculate the unknown C_{sp} of samples at various molalities and temperature.

Calculation of water activity. From the measured C_{sp} data, we derived the a_w of each chlorate solution sample as a function of temperature and molality according to the thermodynamic relations given by Toner and Catling (2015) [10] as followed:

$$R \ln a_w = R \ln a_{w,298.15K} + \bar{L}_{1,298.15K} \left(\frac{1}{T} - \frac{1}{298.15} \right) - \int_{298.15}^T \left(\frac{1}{T^2} \int_{298.15}^T (\bar{C}_{p,1} - C_{p,1}^0) dT \right) dT$$

While $\bar{C}_{p,1}$ is derived from our measurements, all the other quantities were taken from the published results [5, 11-13].

Results and conclusion: As mentioned above, the a_w of the saturated solution is equal to the DRH of a salt. Thus, the calculated a_w in this study was applied to build stability diagrams of chlorate salts as a function of temperature and relative humidity (RH) as Fig 1 shows. The red curve indicates the calculated values of DRH of each salt varying with temperatures. When the atmospheric RH > DRH, the crystalline salts start to take up humid and gradually deliquesce into aqueous brines; once RH < DRH, liquid brines recrystallize back to solid phase. For NaClO_3 , the DRH is relatively high, increasing from 73% to 80% with decreasing temperature. In comparison, $\text{Mg}(\text{ClO}_3)_2$ is more deliquescent, with DRH climbing up from 20% at room temperature to 41% at ~200K before hitting the ice line. To trace the deliquescence and

efflorescence behavior of both chlorate salts during a sol on Mars, we overlapped a diurnal cycle of T and RH at a depth of ~3cm below the subsurface of the Phoenix landing site from Nuding et al. (2014) [3] as the green line presents on the diagram. While Na-chlorate never had a chance to deliquesce (Fig 1, upper), Mg-chlorate was found to form a stable aqueous phase early in the morning at 10:00 and persist for a few hours before efflorescence into a crystalline hydrate (Fig 1, lower). Then at 21:00 it deliquesced again and lasted for a few hours until ice was formed. There's a large time window, at least 4 hours, for aqueous phases to exist per day. Given the extreme low eutectic temperature of $Mg(ClO_3)_2$ (at ~204K [2]) and its low DRH values (20% ~ 41% in this study), it serves as a potential candidate to periodically form liquid water on the Martian surface, thus may play an important role in the water cycle on Mars.

428. [4] Gough R. V. et al. (2011) *EPSL* 312, 371-377. [5] Toner J. D. and Catling D. C. (2018) *EPSL* 497, 161-168. [6] Toner J. D. et al. (2015) *GCA* 166, 327-343. [7] Ojha L. et al. (2015) *Nature Geoscience* 8.11, 829-832. [8] Rennó, N. O. et al (2009) *JGR: Planets* 114.E1. [9] Martín-Torres F. J. et al. (2015) *Nature Geoscience* 8.5, 357-361. [10] Toner J. D. and Catling D. C. (2016) *GCA* 181, 164-174. [11] Murphy D. M. and Koop T. (2005) *Q J R Meteorol Soc Q J ROY METEOR SOC* 131.608, 1539-1565. [12] Campbell A. N., and Bhatnagar O. (1971) *Can. J. Chem.* 49.2, 217-224. [13] Simoes M. C. et al. (2017) *J. Chem. Eng. Data J CHEM ENG DATA* 62.7, 2000-2013.

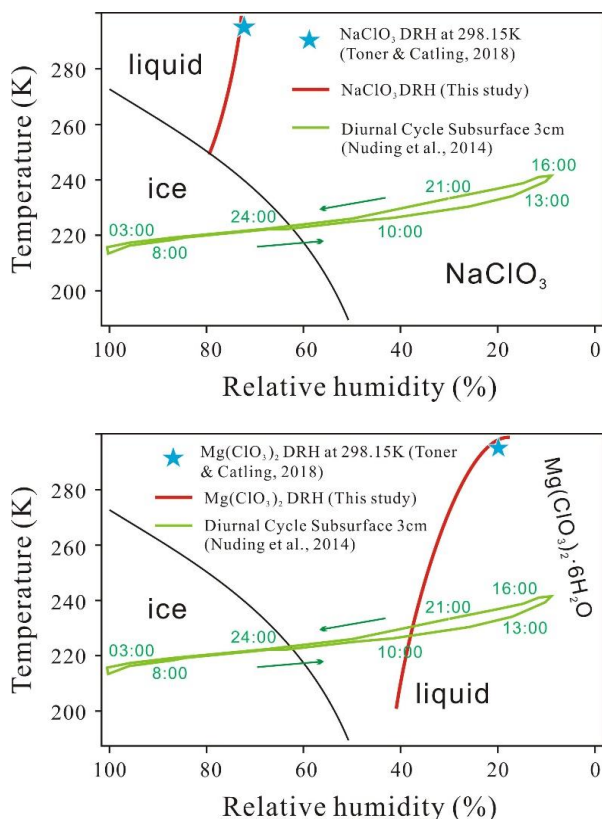


Fig 1. Stability field of $NaClO_3$ (aq) (upper) and $Mg(ClO_3)_2$ (aq) (lower) compared with Martian diurnal cycle of temperature and relative humidity. The Martian diurnal cycle was taken from Nuding et al. (2014)

References: [1] Hecht M. H. et al. (2009) *Science*, 325, 64-67. [2] Hanley J. et al. (2012) *GRL* 39, 8. [3] Nuding D. L. et al. (2014) *Icarus* 243, 420-

THE MINERALOGY AND CATION EXCHANGE OF SEDIMENTS IN DON JUAN POND, ANTARCTICA DRY VALLEY: IMPLICATIONS FOR MARS. V. M. Tu¹, D. W. Ming², and R. S. Sletten³

¹Jacobs JETS, Houston, TX, valerie.m.tu@nasa.gov, ²NASA JSC, Houston, TX, douglas.w.ming@nasa.gov, ³University of Washington, sletten@uw.edu.

Introduction: Located in the McMurdo Dry Valleys of Antarctica (MDV) is among of the saltiest bodies of water of Earth, Don Juan Pond (DJP) [1]. DJP pond waters are unique in that they contain nearly 40% salt by weight including 95% CaCl₂ [1-5] and they never evaporate or freeze entirely due to the high hygroscopicity and low eutectic temperature of the CaCl₂ brine (-52°C) [6]. The source of DJP water is suggested to be due to groundwater upwelling through a weathered dolerite aquifer and/or near-surface runoff, including salt deliquescence in the pond's watershed [7,8], however the source of water is still a topic of study.

During the 2017-2018 field season, we collected soil samples and altered sediments on hillslopes and drainage basins near the pond (Fig. 1). Two drill bores were also acquired in Don Juan Pond sediments in a episodically flooded area of the pond basin. This study's objectives were to characterize the mineralogy of these soils and sediments to determine if there are mineralogical indicators and/or controls for the delivery of salts to DJP and understand the role of salts on Mars on these analog studies.

Materials and Methods:

Study Site. DJP resides within a salt pan DJP approximately 800m long (E-W) and 250m wide (N-S), with a pond depth of ~10-30cm (Fig. 1) [9,10], bound by a rock glacier to the west, small basins to the east, and steep colluvial slopes to the north and south [8]. The mineralogy of the DJP reflects the granitic basement material and the surrounding mountains of Beacon sandstone and Ferrar dolerite (Jurassic-aged dolerite sills) [11]. Two boreholes approximately 1.5 meters deep were extracted from near the water line in DJP sediments (Fig.1), and sampled loose fines were collected at 10 cm intervals. Soil pits were excavated, described, and sampled in the drainage basins that flow into DJP. Several small streams flow out of a rock glacier into the pond and a drainage basin with a small stream channel (dry surface but evidence of subsurface water flow) is evident in the eastern watershed.

Sediments were sampled from several ephemeral lakes in the eastern watershed towards a ridge that separates the DJP and Lake Vida drainage basins. Visual observations suggest that most of the water in the eastern watershed is supplied by snowmelt from the Asgard Mountains. Mineralogy of the core and soil samples was characterized by XRD. Samples were ana-

lyzed in the field with a Terra XRD instrument and in the laboratory with a PANalytical XRD.

Results and Discussion: Mineralogy of pond sediments indicates that salt formation and concentrations are due to evaporation wicking of salts towards the surface. Smectite is common in lake sediments and may provide cation exchange control for salts in DJP.

Salt Mineralogy. Core 1, sampled outside of the "wet" zone, contains higher abundances of gypsum than core 2. Halite abundance are relatively similar between the two boreholes and is concentrated near the surface of the DJP sediments (Fig. 2). Gypsum is also abundant near the surface and decreases with depth until encountering the water table, and then abundances significantly increase (Fig. 2). The concentration of more soluble salts near the surface in DJP sediments indicates that water movement was upwards, most likely by pond water evaporation.

Clay Mineralogy. All borehole sediment samples contained about 5 wt. % smectite (Fig. 3) and abundant smectite (20- 35 wt. %) was present in sediments from ephemeral lakes in the eastern watershed towards the ridge that separates the DJP and Lake Vida drainage basins. No smectite was observed in the soil samples around the pond.

Smectite tends to be the most common authigenic clay mineral and can form at low temperatures and low pressures [12]. We hypothesis that smectite formed in-situ as an alteration product of granitic mica in the glacial till, or weathering of Ferrar dolerite sills and dikes that intrudes the valley walls to the south and north of the pond. The high salt contents of DJP and other pond basins in the vicinity may aid in providing aqueous conditions that enhance the formation of smectite. Generally, synthesis of smectite requires the presence of Mg in solution [12], hence, smectite formation in DJP and other lake sediments with high Ca²⁺ water concentrations may be the result of the alteration of mica under sustained aqueous conditions due to the lowering of the freezing point of H₂O [13].

Antarcticite. An extremely hygroscopic and cryogenic mineral, Antarcticite (CaCl₂·6H₂O), was observed in field XRD measurements at DJP. Antarcticite readily precipitates and dissolves with diurnal changes; evaporation of the pond causes precipitation and then dissolves during freshwater input during the "hotter" times of the day. Deep groundwater models yielded early precipitation of antarcticite, which were hypothe-

sized to limit the concentration of Ca^{2+} [8] however this is inconsistent with the high Ca^{2+} concentrations (5.6 mol kg^{-1}) measured in DJP. Antarticite may play a role in influencing the concentrations of Ca^{2+} , but further investigation is required.

Cation Exchange. Smectite in DJP and adjacent lake sediments may selectively remove Na^+ from the solution and provide a mechanism for enhancing Ca^{2+} in lake waters. [14] reported temperate climate soils showed an affinity for Na^+ with an increase in ionic strength. Salts affect the surface charges of clay particles, and an increase in ionic strength can increase the surface charge of clays, which can act as temporary ion repositories for cation exchange [15]. Also, interlayer charge in smectite and ionic strength of solutions will have a role in the selectivity of Na^+ and Ca^{2+} on exchange sites.

Previous studies have suggested salts were introduced into the pond by groundwater upwelling through a weathered dolerite aquifer and/or via near-surface run-off, including salt deliquescence in the pond's watershed. Here we hypothesize that cation exchange with smectite affects the type of ions delivered to DJP brines. Smectite formation in streams and lakebeds provides an avenue to exchange Ca^{2+} for Na^+ , thereby providing a mechanism to "concentrate" Ca^{2+} in DJP water. Clay mineral ion selectivity experiments by [16] demonstrated that the selectivity of divalent ions over monovalent cations varies considerably with changes to ionic strength, and an increase ionic strength and entropy cause a preference for Ca^{2+} over Na^+ . [17] indicated an increase in the surface concentration of high-charge ions generally increases up to a maximum, and then decreases beyond that. This may be one mechanism responsible for Ca^{2+} in DJP, however, more research is required to determine critical variables such as interlayer charge density, cation exchange capacity, and cation selectivity under various ionic strength systems.

Implications for Mars: DJP is a unique analog site for Mars (chloride deposits) to understand the habitability potential on Mars in these types of environments [2,3]. Mars is a cold, dry environment, and aqueous flows on Mars may be enhanced by CaCl_2 -rich brines [3,18,19].

Cation exchange may have played a role early in Mars history in concentrating and removing salt cations in clay minerals. Smectite and chlorite are the most abundant phyllosilicates on Mars [20], and partial chloritization has been hypothesized as a mechanism for expanded smectite in Gale crater [21, 22] due to cation exchange. High ionic-strength water similar to DJP brines may provide a low-temperature aqueous environment for forming clay minerals on Mars.



Figure 1. Core samples and water drainage into Don Juan Pond.

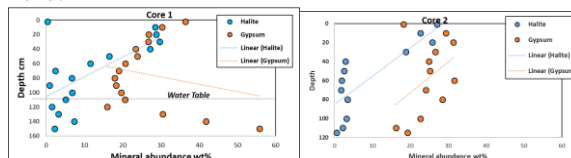


Figure 2. Halite and gypsum mineral abundance trends for DJP core sediments. Halite is concentrated near the surface and decreases with depth. Gypsum decreases with depth to the water table and then increases with depth below the water table.

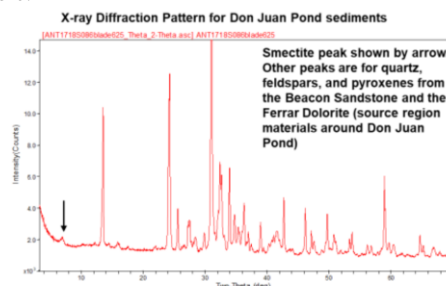


Figure 3. X-ray diffraction pattern for the 80-90cm DJP core sample. The black arrow indicates the 001 basal peak for smectite ($\sim 15 \text{ \AA}$). Other major peaks are quartz, feldspar, and pyroxenes from the Beacon Sandstone and the Ferrar Dolerite from the source region materials around DJP.

Acknowledgments: NASA's Habitable Worlds and ISFM Programs funded this research.

References:

- [1] Meyer, Morrow. et al. (1962) Science 138:1103-1104. [2] Siegel, B.Z. (1979) Nature 280:828-829. [3] Burt & Knauth (2003) J. Geophys. Res. 108:8026. [4] Yamagata, Torii, & Murata (1967) Victoria Land 1963-1965 5:53-75. [5] Wilson (1979) Nature 280:205-208. [6] Marion (1997) Science 9: 92-99. [7] Dickson, et al. (2013) Scientific Reports, 3:1-7. [8] Toner et al. (2017) Earth and Planetary Science Letters 474:190-197. [9] Harris, & Cartwright, (1981) AGU 161-184. [10] Torii, et al. (1977) Antarct. Rec. 58:116-130. [11] McKelvey & Webb (1962) NZ J. Geol. Geophys. 5:143-162. [12] Klopogge, et al. (1999) Clays Clay Min., 47:529-554. [13] Cuzzo, et al. (2020) GCA, 278:244-260. [14] Evangelou & Mars, (2003) Plant and Soil, 250 (2):307-313. [15] Faure (1998) Princ. & App. of GeoChem. [16] McEwen, et al. (2011) Science 333:740-743. [17] McBride (1980) Clays Clay Min., 28(4):255-261. [18] Chevrier, Rivera-Valentin, (2012) Geophys. Res. Lett. 39:1-5. [19] Stillman, et al. (2016) Icarus 265:125-138. [20] Ehlmann, B.L. et al. (2013) Space Sci Reviews, 174:1-4:329-364. [21] Perry & Rampe, (2017) LPSC XLVIII, Abstract #1628. [22] Bristow, et al., (2015)

SALTS & BRINES: ACTIVE INTERGRADIENT IN MODERN-DAY MARTIAN GEOCHEMISTRY.

Alian Wang, Planetary Spectroscopy Team, Department of Earth and Planetary Sciences and the McDonnell Center for the Space Sciences, Washington University in St. Louis, (alianw@levee.wustl.edu).

A systematic study: S, Cl, H, O, C are the most mobile elements on Mars. Current atmosphere-surface interactions can induce the alteration of salts, as well as the transformation of salts to brines.

Following the identification of martian salts by Mars Express, MER, MRO, Phoenix, and MSL, the *Planetary Spectroscopy Team* at Washington University in St. Louis (WUSTL) started a systematic study on the fundamental properties of martian salts, supported by NASA Mars Fundamental Research Program (MFRP), Mission of Opportunity (MoO) for ESA ExoMars-RLS project, and Solar System Working Program (SSW).

Thermodynamics and kinetics are the center of this study, i.e., the stability fields of salts (sulfates, chlorides, oxychlorine salts), the pathways of phase transformations, and the rates of reactions under the current environmental conditions at Mars surface and in shallow subsurface. Among various salt-affecting processes during the different periods on Mars, our emphasis has been the post-deposition processes, i.e., the phase transformation of salts in modern-day on Mars that directly links to the mission observations.

Our study has been emphasized on two aspects of atmosphere-surface interactions: (1) *dehydration – rehydration - deliquescence* of salts induced by diurnal temperature variation, atmospheric global circulation, and martian obliquity cycle; (2) *heterogeneous electrochemical reactions* induced by the radicals and atoms/molecules at excited states produced in martian dust activities. From this set of studies, the team published 34 papers in peer-reviewed journals.

Methodology: We used mission observations, analog sites study, and laboratory simulations in these studies. Spectroscopy has been our tools. Analog sites (Atacama Desert and Tibet Plateau) provide climatically similar environments, and especially, the long-duration (millions years) for phase equilibrium development that is superior to the limited duration (years) of any laboratory simulation.

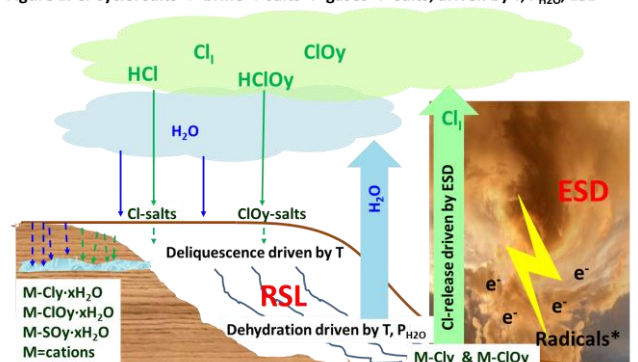
Due to the mobility of S, Cl, H, O, C under Mars conditions, simulation experiments within reasonable temperature window can move fast enough, from which the kinetic information on the reaction rates can be extracted. In addition, we built a Planetary Environmental Chamber with multiple in situ sensors (PEACH), and used it for many experiments. Study of Martian meteorites brought in additional information.

Modern-day salts and brines on Mars: On the basis of mission observations and the results from analog site studies and laboratory simulations, we built up the following understanding which addressing the five big questions about the Modern-day salts and brines on Mars.

1. Two major hydrous sulfates: Monohydrated Mg-sulfate and polyhydrated sulfate are the most common and abundant hydrous sulfates observed thus far on Mars. On the basis of results from three sets of experiments and observations at DLT saline playa in a hyperarid region on the Tibet Plateau [1, 2], we were able to set constraints on the nature and origin of these two major Martian sulfates. Starkeyite ($\text{MgSO}_4 \cdot 4\text{H}_2\text{O}$) is the best candidate for polyhydrated sulfate. $\text{MgSO}_4 \cdot \text{H}_2\text{O}$ in the form of “LH-1w,” generated from dehydration of Mg-sulfates with high degrees of hydration, is the most likely mineral form for the majority of monohydrated Mg-sulfate. Two critical properties of Mg-sulfates are responsible for the coexistence of these two phases with very different degrees of hydration: (1) the meta-stability of a sub-structural unit in starkeyite at relatively low temperatures on Mars, and (2) catalytic effects attributed to co-precipitated species (sulfates, chlorides, oxides, and hydroxides) from chemically complex brines that help overcome the meta-stability of starkeyite. The combination of these two properties controls the coexistence of the LH-1w layer and starkeyite layers at many locations on Mars, which sometimes occur in an interbedded stratigraphy.

2. High RH in salty subsurface: Salty soils (enriched with hydrous sulfates and oxychlorine salts) were dogged out by rovers and lander. At the Martian surface, relative humidity (RH) is controlled by the partial pressure of H_2O ($P_{\text{H}_2\text{O}}$) in the atmosphere, but the salty soils in subsurface can keep a much higher

Figure 1. Cl-cycle: salts → brine → salts → gases → salts, driven by T, $P_{\text{H}_2\text{O}}$, ESD



RH. Our experiments revealed that the RH value maintained by a hydrous salt (in the form of dry grains) in a quasi-closed space approaches its $RH_{\text{buffer}}(T)$ value that is consistent with its deliquescence-phase boundaries defined by stability field experiments. In addition, we demonstrated that the RH values kept by common hydrous chlorides and oxychlorine salts (HyCOS) and hydrous sulfates in enclosures have a general trend as $RH_{\text{sulfates}} > RH_{\text{perchlorates}} > RH_{\text{chlorides}}$ (with same type of cation) in wide T range [3]. This finding supports the color change observed using Pancam of Spirit rover on the excavated hydrous ferric sulfates at Tyrone site. The VNIR spectral changes matches with a dehydration of ferricopiapite to rhomboclase [4], and confirmed again, the salty martian subsurface has high RH that is extremely different from the environment at surface.

3. HyCOS as the source materials for RSL: Our experimental study on dehydration–rehydration–deliquescence of hydrous chlorides and oxychlorine salts (HyCOS) supports a brine-related hypothesis for the recurring slope lineae (RSL) on Mars, in which the subsurface HyCOS are the potential source materials [3]. We found that within the observed RSL T range, $T_{\text{RSL}}(250\text{--}300\text{ K})$, the deliquescence of HyCOS could occur in mid-low RH range that can be provided by co-existing salts. Furthermore, we found a strong temperature dependence of the deliquescence rates for all tested HyCOS, e.g., duration of 1–5 sols for all HyCOS at the high end (300 K) of T_{RSL} , and of 20–70 sols at the low end (250 K) of T_{RSL} . These deliquescence rates are consistent with the observed seasonal behavior of RSL on Mars. To support the recurrence of RSL in consecutive Martian years, we found the rehydration of HyCOS can occur in a few minutes, under Mars relevant P-T-RH conditions, which support the rehydration of remnant HyCOS layers during a local cold season through atmospheric H_2O -to-salt direct interaction. This rehydration would facilitate the recharge of H_2O back into subsurface HyCOS reservoir, to serve as the source material that will form RSL in a subsequent warm season.

4. Cl-cycle enabled by Martian dust activates: Our new ESD (electrostatic discharge) experiments that simulate the effect of martian dust activity on common chlorides suggest that chlorine could cycle on modern-day Mars between atmosphere and surface, driven by heterogeneous electrochemistry induced by dust storms, dust devils, and grain saltation. Two evidences demonstrate the instantaneous release of chlorine from seven common chlorides (Mg, Fe^{2+} , Fe^{3+} , Ca, Na, K, Al) during a medium strength ESD process in a Mars environmental chamber [5]. (1) a direct detection of a plasma emission line at 837.8 nm

of the first excited state of the Cl atom; (2) the characterization of Cl-deposition on the upper electrode using Raman, XRD, SEM, EDX, and XPS. This study is consistent with the most recent TGO observation, the HCl in martian atmosphere, and especially, the variation of its values positively correlated with 2018 global dust storm [6]. Furthermore, the Cl-release from chlorides induced by dust events added the last pieces of puzzles in the recurrence of RSL (Figure 1), i.e., the Cl-bearing gases can help to replenishing the Cl-bearing salts onto martian surface and then into shallow subsurface, thus to maintain the HyCOS reservoir for RSL.

5. Salt -- potential host for biomarker: Three Ca-sulfates, gypsum, bassanite, and anhydrite ($\beta\text{-CaSO}_4$) were identified on Mar, by CheMin on Curiosity rover [7]. The 4th Ca-sulfate, $\gamma\text{-CaSO}_4$, was found widely distributed and enriched in Martian meteorite and in the soils of hyperarid region on Earth (Atacama Desert and Tibet Plateau). Ordinary $\gamma\text{-CaSO}_4$ is metastable but those in Martian meteorite and from hyperarid regions show an abnormally high stability. Using multiple microanalysis, we found these abnormal $\gamma\text{-CaSO}_4$ phases are chemically impure, with Si and Si+P entering its structural tunnels along the C-axis, which blocked the entrance of atmospheric H_2O , and kept its abnormally high stability in ambient conditions [8]. Similarly, CH_3OH was found to fill the tunnels of $\text{CaSO}_4 \cdot 0.5\text{CH}_3\text{OH}$ in another study [9]. Because $\gamma\text{-CaSO}_4$ and bassanite have very similar structures with their XRD lines heavily overlapped, thus cannot be distinguished by CheMin. We would suggest some martian bassanite could be $\gamma\text{-CaSO}_4$ actually. Its structural tunnels would allow ions and ionic groups to fill. Thus this porous mineral has the potential to host biomarkers. The ID of $\gamma\text{-CaSO}_4$ can be achieved by Raman system on Perseverance and ExoMars rover.

Conclusion: Our study indicates that salts and brines are extremely active intergradient in modern-day Martian geochemistry. The Cl-cycle between surface and atmosphere (Figure 1), driven by T, $P_{\text{H}_2\text{O}}$, circulation and dust-induced electrochemistry, may impact Martian isotope geochemistry as well.

Acknowledgements: NASA MFRP NNX07AQ34G and NNX10AM89G, MoO contract #1295053, ASTEP NNX09AE80A, MatISSE NNX13AM22G, SSW 80NSSC17K0776, and ICEE-2 NNH18ZDA001N. Special supports by WUSTL and MCSS, the contributions made by the members of the Planetary Spectroscopy Team in past 15 years, and the collaborations with planetary scientists in US and internationally.

References: [1] Wang et al. (2016), *JGR*; [2] Wang et al., (2018) *Astrobiology*; [3] Wang et al., (2019) *Icarus*; [4] Wang et al. (2011), *JGR*; [5] Wang et al., (2020), *JGR*; [6] Olsen et al (2021), *A & A*; [7] Vaniman et al. (2018) *Am. Min.*; [8] Shi et al., (2021) *LPSC*; [9] Voigtländer et al (2003), *Host-Guest-Systems Based Nanoporous Crystal*.

EVALUATION OF BRINE CONCENTRATION EFFICACIES FOR NUCLEIC ACID PRESERVATION.

M. L. Winzler^{1,2}, S. M. Per²⁻⁴, C.S. Cockell⁵, S. Pailing⁶. ¹Biological Sciences, California State University, Long Beach, Long Beach, CA, 90815, USA (Meghan.Winzler@student.csulb.edu); ²NASA Jet Propulsion Laboratory, California Institute of Technology, 4800 Oak Grove Drive, Pasadena, CA, 91109, USA; ³Mineral Sciences, Los Angeles Natural History Museum, 900 W Exposition Blvd, Los Angeles, CA 90007, USA; ⁴Blue Marble Space Institute of Science, 600 1st Avenue, 1st Floor, Seattle, Washington 98104; ⁵School of Physics and Astronomy, University of Edinburgh, Edinburgh, Scotland, EH9 3FD, UK; ⁶Department of Physics and Astronomy, University of Sheffield, Hounsfield Road, Sheffield, S3 7RH, UK.

Introduction & Motivation: Brine environments on Earth maintain thriving halophilic microbial communities and offer UV radiation protection and long-term desiccation prevention to halophilic microorganisms through enclosed brine fluids in evaporite minerals or fossilized stromatolites [1] The evaporite salt minerals in these hypersaline environments, created through billions of years of wetting and drying events, is uniquely responsible for life preservation in brine environments in geologically old mineralogy.

Modern Mars and Europa contain signs of evaporites and the characteristic wetting and drying events, signifying that these brine environments may have the same preservation potential to harbor extant life as on Earth.

In-situ experimentation on evaporitic sites on both Mars and Europa for extant life has the highest potential for detecting life in these planetary environments. The standardization and optimization of the scientific methodology utilized for planetary life-detection missions are fundamental to producing accurate measurements that evaluate planetary extant life while mitigating mission logistics. Microbiological life-detection methods, especially in low biomass environments as Mars and Europa are expected to be, traditionally concentrate samples to achieve ample DNA for DNA sequencing and then quantify the DNA present.

The purpose of this paper is to establish the efficacy of concentrating brine for nucleic acid extraction with three planetary analogue field sites: two hypersaline brines (Searles Lake and Boulby Mine) and one alkaline lake (Mono Lake). This research will guide specific parameters to aid the optimization of sample concentration and DNA quantification machinery onboard landed missions for potential microbial sample quantification and identification. Moreover, future onboard sample concentration efficiency will increase for landed missions, thus increasing overall potential yield for extant life in planetary brine environments.

Methodology & Laboratory Processes: After sampling at each of these sites, quantification of DNA before concentration was conducted. Samples will be

concentrated and remeasured (post-concentration) for changes in bulk DNA quantification measurements.

Fluorometer Measurements: We utilized the Qubit 4 Fluorometer to quantify the DNA in the samples. Due to the low biomass of the samples, the dsDNA HS (high sensitivity) kit was used in these experiments. DNA quantification was measured in both ng/ml and ng/μl.

Planetary Analogue Field Sites: *Searles Lake:* Searles Lake is a dry, evaporitic saline lake located in the Mojave Desert in Searles Valley, California, USA. Due to the abundance of rare materials and evaporite minerals, Searles Lake has mining operations that extract sodium- and potassium-rich minerals (namely trona, hanksite, and halite) from its subsurface brines for industrial use. This lake experienced at least four extreme drying events throughout its history, creating a potentially hospitable environment for evaporite minerals to form. In these drying events, the salts become pigmented from photobiological responses [2] reminiscent of the haloarchaeal communities that inhabited the lake during each drying event. The oldest geologically dated subsurface brine in our sampling is ~1.1 million years old from the mid-Pleistocene.

Boulby Mine: Located near Loftus, North Yorkshire England, the Boulby Mine is an industrial salt mine charged with mining polyhalite, polysulphate, and potash for use as agricultural fertilizers. It is the second deepest mine in Europe, at depth of 4,600 ft. The deepest part of the mine is geologically dated to be 253 million years (Permian age) and of the Zechstein Formation, derived from the Zechstein Sea [3]. The sites sampled in the Boulby Mine were 327-18X/C, 29X/C, “White Crust”, and Bentham Baths.

Mono Lake: Mono Lake is a terminal saline soda lake in Mono County, California, USA. Situated at the north end of the Mono-Inyo Craters' volcanic chain, it is both geologically active from heat produced by lava flow and microbiologically active with thermophilic organisms. Two thermal sites were sampled at Pahoa Island: near the geologically active site and downstream of the site.

Pre-concentration Analysis: Quantifiable DNA was found in almost all the pre-concentrated samples and was relatively consistent within each site. Reported

below are partial datasets from total observations. In both the Searles Lake and Boulby Mine samples, a trend seems to be absent in terms of depth and DNA quantification measurements (Table 1). This is particularly interesting, as the expectation was that as the depth increased, microbial DNA density would as well. In the Mono Lake samples, only the samples stored in the freezer contained quantifiable DNA, despite bio-visual cues otherwise in the shelf samples (Table 1). This indicates a measurement anomaly within the data set, and investigative measures will be conducted to determine the cause.

A) Boulby Mine Pre-Concentration Bulk DNA Per Site		
Site (All Permian)	DNA (ng/ml)	DNA (ng/μl)
328 18 x/c	85.6	0.0833
	84.5	0.0836
White Crust	71.8	0.0892
	99.4	0.0835
Bentham Baths	61.7	0.077
	75.9	0.0751
29 x/c	68.0	0.0849
	105.0	0.104

B) Searles Lake Brine Pre-Concentration Bulk DNA		
Depth (m)	DNA (ng/ml)	DNA (ng/μl)
Surface	432.0	0.434
149- 149.6	337.0	0.327

C) Searles Lake Resuspended Salts Pre-Concentration Bulk DNA		
Depth (m)	DNA (ng/ml)	DNA (ng/μl)
Surface	86.4	0.0869
29.5	91.9	0.0887
103	109	0.104
144.7	114	0.114

D) Mono Lake Pre-Concentration Bulk DNA (ng/ml)		
Temperature Stored	Green	Red
Shelf (Room temperature)	Too Low	Too Low
Fridge (4 °C)	Too Low	Too Low
Freezer (-20 °C)	6	30

Table 1. Selected Pre-Concentration Reads for Bulk DNA. (a) Boulby Mine partial pre-concentration DNA. (b) Searles Lake partial pre-concentration DNA quantification in the brine and (c) in the resuspend salt minerals from transects in relation to depth of sample. (d) Mono Lake pre-concentration DNA quantification. Samples were incubated for about four years at room temperature, 4 °C, or -20 °C.

Preservation of Nucleic Acids in Brines: As microorganisms may become entombed in evaporitic salt mineral fluid inclusions, the biomolecules associated may be preserved as well. Biomolecules (nucleic acids, carotenoids, etc.) serve as excellent biomarkers in brine environments and as a signifier for halophilic life, extant or extinct, in hypersaline planetary environments [4].

Considerations of Biomass Loss: By design, the side of the pore filters used in the concentration process will dictate the total biomass, nucleic acids, and intact cells, that are contracted. Any biomolecule volume that is concentrated after the pores are filled will be lost to the filtrate. While this is unavoidable due to conservative estimates of planetary analogue brines, future robotic missions could utilize the filtrate for further sample analyses.

Ocean Worlds Sample Extraction: Future landed missions to Europa will likely involve producing ice melt from crustal regions for in-situ and onboard sample analyses [5]. These brines will come from heated ice samples that, if containing any biomass, would need to be heated slowly to reduce the risk of osmotic shock to cellular structures such that onboard geobiological analyses can take place. The decision to concentrate any samples, due to short duration commanding windows and mission timeline, will likely lead to an umbrella sampling procedure that would include brine concentration. While appropriate, determining the efficiency of such cryobrine concentrations would be critical for understanding total biomass per volume.

Summary & Future Work: These samples are from low biomass environments, so the presence of quantifiable DNA challenges our dependency on concentration to quantify DNA and provides an opportunity to witness the efficiency of concentration in these settings. In turn, an evaluation of the efficacy of concentration for DNA quantification will aid future in-situ experimentation and quantification of potential extant life present in planetary brine environments.

For future directions, these samples will be concentrated and measured for their DNA quantities. In this, we will be able to evaluate potential changes in diversity between the pre-and post- concentrated samples and determine if the act of concentrating modifies the diversity present in the samples.

References: [1] Carrier, B. L. et al. (2020) *Astrobiology* 20:785-814 DOI: 10.1089/ast.2020.2237. [2] Perl, S. M. et al. *Great Salt Lake Biology* (2020) DOI: 10.1007/978-3-030-40352-2_16 [3] Cockell et al. *Astrobiology* 20(7):864-877(2020) DOI: 10.1089/ast.2019.2053 [4] Perl, S. M. et al. (2021) *Astrobiology* v21, 7 DOI: 10.1089/ast.2020.2318. [5] Bedrossian M. et al. (2017) *Astrobiology* 17:913–925 DOI: 10.1089/ast.2016.1616.

A FRAMEWORK FOR MODELING THE DISTRIBUTION OF BRINE AND SALT IN AN ICE SHELL.

N. S. Wolfenbarger¹, M. G. Fox-Powell², J. J. Buffo³, K. M. Soderlund¹, and D. D. Blankenship¹, ¹Institute for Geophysics, University of Texas at Austin, J.J. Pickle Research Campus, Bldg. 196; 10100 Burnet Road (R2200), Austin, TX 78758 (nwolfenb@utexas.edu), ²AstrobiologyOU, The Open University, Walton Hall, Milton Keynes, UK, ³Thayer School of Engineering, Dartmouth College, Hanover, NH 03755

Introduction: The presence of liquid water has long guided the search for life beyond Earth. Once thought to be confined to the “Goldilocks zone”, vast saltwater oceans have been inferred to exist beneath the thick ice shells of moons in the Jovian and Saturnian systems [1]. Although these sub-ice oceans represent the most compelling potential habitats in the outer solar system, their overlying ice shells pose a challenge to life detection missions aiming to directly sample them.

Salts entrained from the ocean during the formation and thickening of these ice shells would allow liquid water to remain stable within the ice shell interior as brine well below the pure ice pressure-melting temperature. These brine pockets could represent an oasis for life trapped within the ice and serve as a more accessible target for future missions. Furthermore, the volume fraction of brine, solid salt, and ice in the ice shell governs bulk thermophysical properties (e.g., density, thermal conductivity, specific heat capacity, viscosity), which modulate processes of surface-ice-ocean exchange, as well as dielectric properties (e.g., electrical conductivity, relative permittivity), which influence signal reflection and attenuation for future ice-penetrating radar and electromagnetic investigations. As such, development of a modeling framework for the distribution of brine and solid salts in impure water ice represents a crucial step in the search for and characterization of potential habitats beyond Earth.

Methods: We present a framework for modeling the volume fraction of ice, brine, and solid salts in an ice shell of bulk salinity, S , inspired by models developed for terrestrial sea ice [2]. Whereas previous methods have used experiments to obtain properties of the solution as a function of temperature, we employ the opensource aqueous geochemistry program FREZCHEM which supports the extension of this approach to impure water ice of any composition [3].

Impure ice is a multiphase, multicomponent system made up of solid ice, solid salts, liquid water, dissolved salts (ions), and trapped gases. The amount of brine stable in ice is governed by the bulk salinity of the ice, the temperature, and the composition of the salts. Through knowledge of the solution properties as a function of temperature (e.g., brine density, brine salinity, relative amounts of salt in brine vs. solid salt),

the brine volume fraction as a function of bulk ice salinity and temperature can be obtained. These properties are defined for a particular solution composition as a function of temperature between the pure ice pressure-melting temperature (0 °C for 1 atm) and the eutectic temperature. As such, only a single FREZCHEM simulation for a relatively dilute solution of a given composition across the relevant temperature domain is necessary to derive the phase behavior functions (Fig. 1). Note that we model equilibrium crystallization and as such the bulk composition of the system does not change. At temperatures below the eutectic, where brine is not thermodynamically stable, the volume fraction of solid salt is a simple function of the mass fraction and density of salt and pure ice. The pure ice density is modeled using the Gibbs potential function released by the International Association for the Properties of Water and Steam (IAPWS).

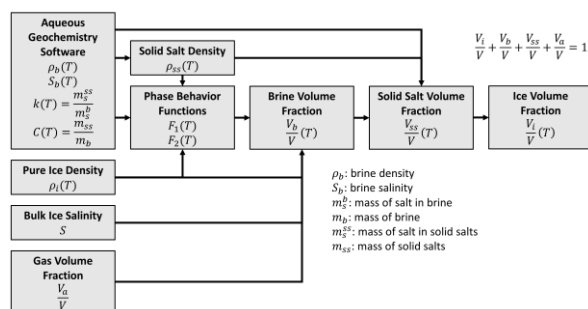


Figure 1. Framework for modeling the volume fraction of ice, brine, and solid salts.

We validate our proposed framework using terrestrial sea ice, with a composition represented by standard mean ocean water [4]. Figure 2 presents a comparison of the brine volume fraction estimated for sea ice using our model and the contemporary standard [5]. The models agree with each other across their defined domains, although our model predicts a slightly lower brine volume fraction at temperatures below -22.9 °C, where hydrohalite begins to precipitate. Both models are consistent with the “rule of fives”, which states that at a bulk salinity of 5 ppt, the brine volume fraction of sea ice is 5% at -5 °C [6]. Two notable limitations of [5] are: (i) the data used to derive the model phase behavior reflects a non-equilibrium freezing pathway for seawater (Ringer-

Nelson-Thompson) [7] and (ii) the model is not defined below $-30\text{ }^{\circ}\text{C}$. Our model reflects the equilibrium freezing pathway for seawater (Gitterman) and extends to the predicted eutectic temperature of $-36.2\text{ }^{\circ}\text{C}$ [8].

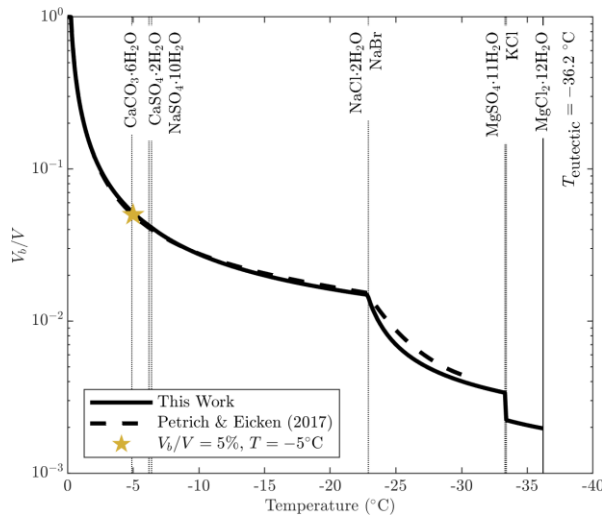


Figure 2. Validation of our brine volume fraction model for sea ice of 5 ppt bulk salinity, neglecting the presence of gases. The solid line represents our model derived using FREZCHEM v13.3 whereas the dashed line represents the model of [5].

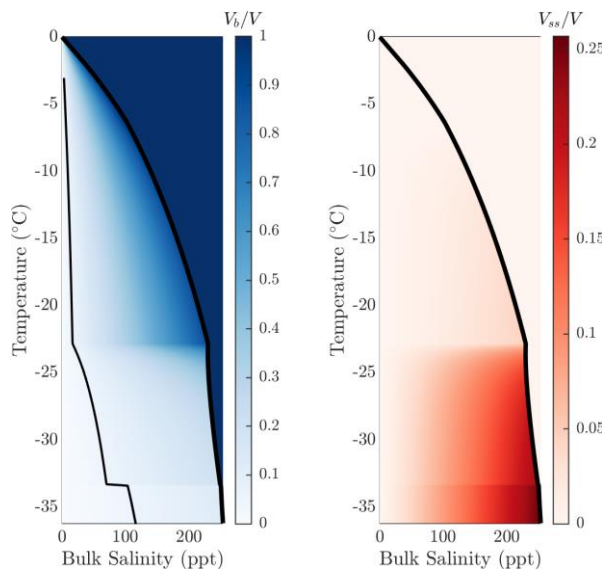


Figure 3. Brine (V_b/V) and solid salt (V_{ss}/V) volume fraction for sea ice. The thick black line depicts the liquidus and the thin black line depicts where the brine volume fraction is 5%, corresponding to an apparent percolation threshold in columnar sea ice [6].

Figure 3 illustrates the brine and solid salt volume fractions for terrestrial sea ice over a temperature range spanning from the pressure-melting temperature to the eutectic temperature and a bulk salinity range spanning from pure water to the eutectic composition.

A limitation of the proposed approach is that the pressure is assumed to be fixed (i.e., the pressure dependence of phase behavior is not modeled). This is not an appropriate assumption for modeling the stability of brine where ice shells exceed a certain thickness, and the influence of overburden pressure is no longer negligible. One atmosphere of pressure corresponds to ~ 100 meters of ice at Europa, which could represent $<1\%$ of the potential ice shell thickness. To account for the influence of pressure, multiple FREZCHEM runs over a range of pressures are needed to obtain surfaces, as opposed to curves, for the phase behavior functions.

Discussion: We will apply our proposed framework to Europa’s ice shell. We will prescribe a bulk composition based on spectroscopic observations of the surface which suggest Na, Cl, Mg, and SO_4 are likely the dominant impurities [9]. We will consider binary end-member cases for bulk ice shell composition (e.g., NaCl, MgSO_4) before exploring permutations of these species to represent more complex sulfate-dominated and chloride-dominated systems. We will first assume a pressure of one atmosphere to model an ice shell of arbitrary thickness, then we will account for the influence of pressure to examine the vertical extent of brine for a range of ice shell thicknesses and an assumed temperature profile.

Because the presence of water alone is not sufficient to evaluate habitability, selected metrics will be used to further evaluate the distribution of potential habitats. The water activity, ionic strength, and SO_4/Cl ratio will be plotted for Earth seawater and the sulfate-dominated and chloride-dominated European ice shells to evaluate the suitability of these briny, in-ice environments as potential habitats. We evaluate Earth seawater as validation since sea ice represents a known in-ice habitat on Earth.

References: [1] Lunine J. I. (2017) *Acta Astronaut.*, 131, 123–130. [2] Cox G. F. N. and Weeks W. F. (1983) *J. Glaciol.*, 29, 306–316. [3] Marion G. M. et al. (2010) *Comput Geosci*, 36, 10–15. [4] Millero F. J. et al. (2008) *Deep Sea Res. Part I Oceanogr. Res. Pap.*, 55, 50–72. [5] Petrich C. and Eicken H. (2017) *Sea Ice*, 1–41. [6] Golden K. M. et al. (1998) *Science*, 282, 2238–2241. [7] Marion G. M. et al. (1999) *Cold Reg Sci Technol*, 29, 259–266. [8] Vancoppenolle M. et al. (2019) *JGR: Oceans*, 124, 615–634. [9] Trumbo et al. (2019) *Sci. Adv.*, 5, eaaw7123.

ENVIRONMENTAL FUNCTIONS OF PURPLE SULFUR BACTERIA IN THE GREAT SALT LAKE, UTAH, UNDER CHANGING CLIMATIC CONDITIONS J. Xu¹, B. Baxter² ¹Earth, Environmental and Resource Sciences, the University of Texas at El Paso, 500 W. University Ave., El Paso, TX 79968, ²The Great Salt Lake Institute, Westminster College, Salt Lake City, UT 84105

Abstract: The Great Salt Lake (GSL) is a shallow, terminal lake that exhibits a maximum and a mean depth of ~9.0 m and 4.3 m, respectively. The construction of a rock and gravel railroad causeway in the late 1950s segregated the lake into north and south arms (Figure 1), and the restricted flow of water between these two “arms” resulted in the development of a salinity gradient [1][2]. The north arm salinity is typically at saturation (~5 M, 270–300 g/L TDS), whereas the salinity in the south arm surface brine is substantially lower (~ 2.5 M, 140–150 g/L TDS) due to freshwater inputs via three rivers [2].

GSL is also sulfur-rich and its sediments were reported to contain high contents of heavy metals and metalloids. It was previously shown that concentrations of sulfate in GSL could reach up to 7% of the total salt [3]. Such high concentrations of sulfate support an active community of sulfate reducers (SRB) that produce sulfide at high rates within GSL sediments [4]. Dissolved sulfide may accumulate to up to ~ 4 mM at certain sites whereas drop below 2 μ M at others [5], indicative of significant variations in sulfide oxidation and removal mechanisms across the lake. The intense solar radiation in the area of GSL can penetrate through the relatively shallow water depths and reach the lake bottom microbial communities, likely making the photosynthesis-driven primary production a most critical player in sustaining bacterial sulfate-reduction, which is closely tied to the sequestration of metals and metalloids. In comparison to the reductive part of the sulfur cycle, less is known about the microbial communities driving sulfide-/sulfur-oxidation. It is known that anoxygenic photosynthetic bacteria that belong to purple sulfur bacteria exist in significant abundances in the microbial communities isolated from water columns and sediments of GSL [6][7]. Purple sulfur bacteria thrive in anoxic sulfidic environments where sunlight can penetrate, and have caused blooms in some of the reservoirs in western Texas during past dry years. Scientific data regarding how these purple sulfur bacterial blooms form and their environmental effects remain elusive, however. The continuing changing climatic conditions (e.g., the drought condition that has been affecting most regions of the US West) may favor the growth of such halophilic, anoxygenic photosynthetic sulfur-oxidizers through expanding euxinic conditions within certain areas of GSL. Thus, there is an urgent need to scrutinize the

population dynamics as well as environmental roles and functions of these anoxygenic photosynthetic bacteria in face of fast changing climatic conditions, especially how such groups may contribute to balancing the overall microbial ecosystems and affect the metal cycles in GSL. Obtaining relevant knowledge will help to better predict the evolution of GSL and to formulate corresponding management plans. The current fragile condition of GSL in terms of continual freshwater loss and salinity increase may also have implication for understanding the ancient conditions on Mars and search of life in those niches.



Figure 1. Satellite image of the Great Salt Lake and proposed sampling sites for water columns and sediments. The railroad causeway that separates the lake into south and north arms and the proposed field sites are indicated.

The focus of our current study is on the mechanisms of interaction among anoxygenic photosynthetic sulfur-oxidizers (especially purple sulfur bacteria), sulfate-reducers, dissolved metal species, and metal sulfide precipitates within GSL under various salinities. We will quantify the rates of microbial sulfate-reduction and oxidation at six sites of GSL (indicated in Figure 1)

through measuring the expression of marker gene *dsrA* and gene combination *dsrA* + *pufL/M*, respectively, in the isolated microbial biomass from water samples at various depths and lake bottom sediment. We will also measure the field parameters including the water pH, conductivity, sulfide and sulfate concentrations, and dissolved oxygen levels, and characterize the aqueous geochemistry of the sediment pore water and quantify the metal and metal sulfide content of the sediment. Our key hypothesis is that the expansion of anoxygenic photosynthetic sulfide- and sulfur-oxidizers are critical for sustaining a healthy microbial community within the GSL in face of reduced fresh water input and increased salinity. We note that we are only at an early phase of carrying out this work.

References: [1] Cannon, J.S., Cannon, M.A. (2002) The Southern Pacific Railroad trestle - past and present. In: Gwynn JW (ed) *Great Salt Lake: an overview of change. Special Publication of the Department of Natural Resources, Salt Lake City, UT*, 283–294. [2] Baxter, B.K., Litchfield, C.D., Sowers, K., Griffith, J.D., DasSarma, P.A., DasSarma, S. (2005) *Microbial diversity of Great Salt Lake*. In: Gunde-Cimerman N, Oren A, Plemenitaš A (eds) *Adaptation to life at high salt concentrations in archaea, bacteria, and eukarya. Cellular origin, life in extreme habitats and astrobiology*, 9th edn. Springer, Dordrecht, 9-25. [3] Wurtsbaugh, W.A., Gardberg, J., Izdepski, C. (2011) *Sci Total Environ*, 409: 4425–4434. [4] Brandt, K.K., Vester, F., Jensen, A.N., Ingvorsen, K. (2001) *Microb Ecol*, 41: 1–11. [5] Boyd, E.S., Yu, R., Barkay, T., Hamilton, T.L., Baxter, B.K., Naftz, D.L., Marvin-DiPasquale, M. (2017) *Sci Total Environ*, 581: 495–506. [6] Meuser, J.E., Baxter, B.K., Spear, J.R., Peters, J.W., Posewitz, M.C., Boyd, E.S. (2013) *Microb Ecol*, 66: 268–280. [7] Lindsay, M.R., Johnson, R.E., Baxter, B.K., Boyd, E.S. (2019) *Ecology*, 100: e02611

POTENTIAL BIOAVAILABILITY OF CRYSTALLIZATION WATER IN SULFATE MINERALS UNDER WATER-RESTRICTED CONDITIONS – A CASE STUDY OF GYPSUM INTERDUNES IN THE TULAROSA BASIN, NEW MEXICO J. Xu¹, B. N. Lajoie^{1, #}, B. Brunner¹, H. Afrin², R. Langford¹, and O. Fernandez Delgado³, E. Cantando⁴, G. Arnold⁵ ¹Earth, Environmental and Resource Sciences, the University of Texas at El Paso, 500 W. University Ave., El Paso, TX 79968, ²Environmental Science and Engineering Program, the University of Texas at El Paso, 500 W. University Ave., El Paso, TX 79968, ³Department of Chemistry, the University of Texas at El Paso, 500 W. University Ave., El Paso, TX 79968, ⁴Virginia Tech National Center for Earth and Environmental Nanotechnology (NanoEarth), Blacksburg, VA 24061, ⁵Medical Professional Institution, the University of Texas at El Paso, 500 W. University Ave., El Paso, TX 79968. Correspondence should be sent to: jxu2@utep.edu

Abstract: The formation of gypsum sand dunes in the Tularosa Basin, New Mexico, was closely related to a “water-loss” history of paleo salt lakes, thereby representing the end-member of a certain type of modern brine environments. As these gypsum sand dunes only persist in dry and water-restricted conditions, they are considered generally harsh and extreme environments for life. Different from silicates (of which most terrestrial sand dunes are composed), however, gypsum is a hydrate mineral, which contains ~ 21% of water in its crystal structure. This simple but intriguing fact has urged us to examine the habitability of gypsum-dominated environments (which are largely arid to hyper-arid and results of continuous water loss) from a different angle. Here we report the findings of our field work based on the gypsum sand dunes and interdune basins in the Tularosa Basin, NM. In this work, we have conducted systematic measurement and sampling at five sites, followed by geochemical, mineralogical, and microbiological analyses of the collected samples. The focal point of this work is to understand “if microbial life may capitalize on the structural water in gypsum under water-restricted conditions”. The results of this work may provide new insight into our current understanding the life limits on Earth and into the search of life in extraterrestrial environments.

The samples of the five sites showed high variations in microbial abundances and community structures, which are also dependent on the sample depth within each site (Fig. 1a). The niches with the highest bio-abundance are exclusively confined within the surface layers of gypsum sediments. These niches also contain relatively high abundances of sulfate-reducing communities based on *dsrA* quantification (Fig. 1b) and measurements of S isotopic fractions in the enriched samples. Additionally, the samples with significantly higher bio-abundances have less weight loss when heated from 65-200°C in the thermal gravity analysis (i.e., indicative of the water content in the sediment mineral structures) (Fig. 1c), and are enriched in both

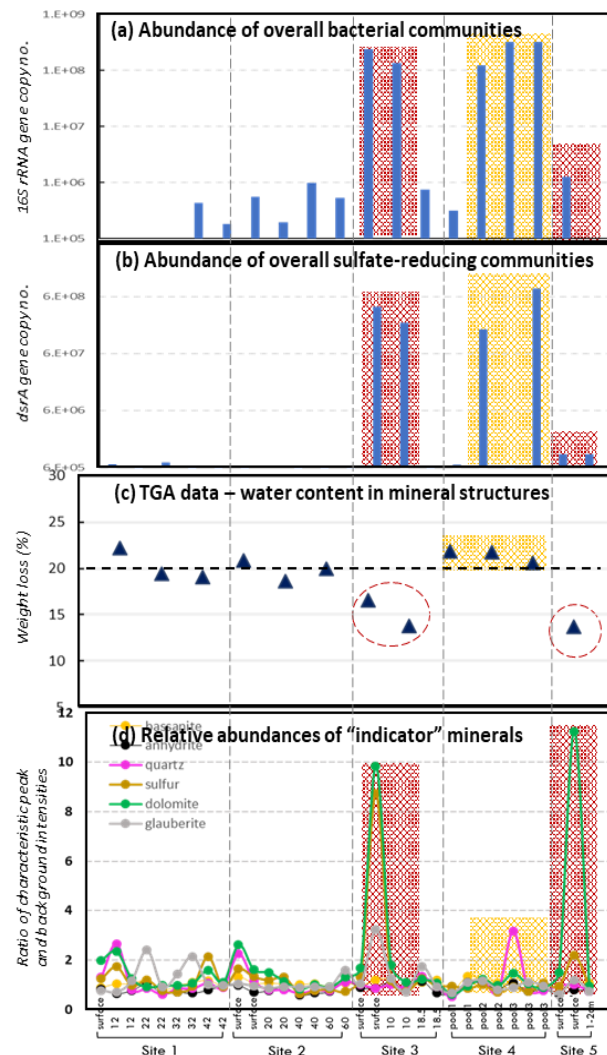


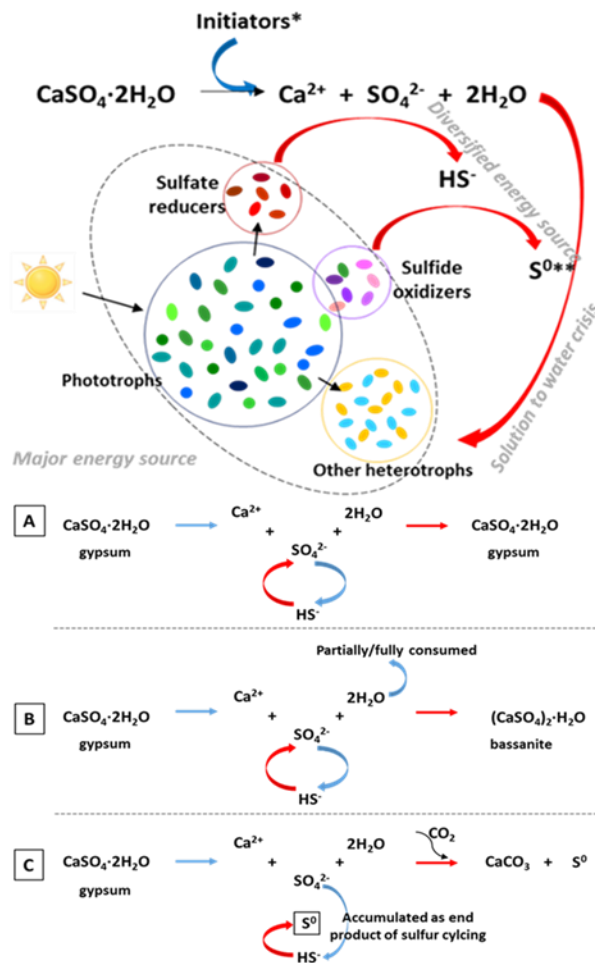
Figure 1. Integrated microbiological and mineralogical data of the interdune basin samples from five sites within the White Sands National Monument, the Tularosa Basin, New Mexico.

dolomite and native sulfur (Fig. 1d) (except those in the vicinity of ephemeral ponds, site 4, which were formed during the unusually wet season of 2019). Collectively, evidence pointing to different survival and growth mechanisms of associated bacterial communities was

identified in the constantly dry interdune sediments (sites 3 and 5) versus the ephemeral pond sediment (site 4) (both composed of > 95% of gypsum), indirectly supporting the hypothesized role of sulfate hydrate minerals being an alternative water source in water-restricted geochemical settings. Based on the results of this study, a specific pathway was proposed leading to the possible release of gypsum structural water (Fig. 2).

Acknowledgments: This study is funded the

work uses shared facilities at the Virginia Tech National Center for Earth and Environmental Nanotechnology Infrastructure (NanoEarth), a member of the National Nanotechnology Coordinated Infrastructure (NNCI) network, supported by NSF (NNCI 1542100). NanoEarth is housed at Virginia Tech's Institute for Critical Technology and Applied Sciences (ICTAS).



National Aeronautics and Space Administration (NASA) under contract number 80NSSC18K0175. This